Spring 5-6-2017

Aberrant Glycosylation In Pancreatic Cancer Progression

Seema Chugh
University of Nebraska Medical Center

ABERRANT GLYCOSYLATION IN PANCREATIC CANCER PROGRESSION

By

SEEMA CHUGH

A DISSERTATION

Presented to the Faculty of

The University of Nebraska Graduate College

In Partial Fulfillment of Requirements

For the Degree of Doctor of Philosophy

Department of Biochemistry and Molecular Biology

Graduate Program

Under the Supervision of Professor Surinder K. Batra

University of Nebraska Medical Center

Omaha, Nebraska

April, 2017

Aberrant glycosylation in pancreatic cancer progression

Seema Chugh, Ph.D.

University of Nebraska, 2017

Advisor: Surinder K Batra, Ph.D.

Aberrant changes in O-glycosylation patterns underlie pancreatic ductal adenocarcinoma (PDAC) progression and metastasis. Glycosylation is a post-translational modification in which carbohydrate moieties are attached to the protein substrate. My dissertation is focused on mucin-type O-glycosylation, which is the predominant form of O-glycosylation and is regulated by a myriad of glycosyltransferases.

PDAC is one of the most lethal diseases and the mechanistic involvement of aberrant O-glycosylation in its progression and metastasis is unknown. The aberrant glycosylation refers to the appearance of unusual carbohydrate structures such as truncated carbohydrate antigens, often referred to as tumor-associated carbohydrate antigens.

In this dissertation, my goal was to investigate the role of aberrant glycosylation in pancreatic cancer progression. Aberrant glycosylation is attributed to dysfunction in expression/activity of glycosyltransferases. Prior published studies and our preliminary studies indicate loss of expression of O-glycosyltransferases-GALNT3 and C1GALT1 in PDAC. GALNT3 (N-acetylgalactosaminyltransferase 3) is a member of GALNT superfamily of enzymes that initiates mucin-type O-glycosylation. The second step of mucin-type O-glycosylation is catalyzed by C1GALT1 (Core-1 β-3 galactosyltransferase). My thesis is primarily focused on deciphering the mechanistic role of the first enzyme (GALNT3) and a second enzyme (C1GALT1) of mucin-type O-glycosylation in PDAC progression and metastasis.

My results show that GALNT3 is differentially expressed during pancreatic cancer progression. Decreased/loss of expression of GALNT3 was seen in poorly differentiated

PDAC as compared to well-differentiated PDAC. This instigated further examination of the functional role of GALNT3 in pancreatic cancer. I performed GALNT3 knockdown studies in four different pancreatic cancer cell lines, and the knockdown cells had altered EGFR and Her2 glycosylation, increased growth, and metastasis.

Apart from GALNT3, which catalyze the first step of O-glycosylation, I have also studied the role of a second enzyme, C1GALT1, in PDAC. C1GALT1 expression studies indicate loss of this glycosyltransferase in a subset of PDAC patients. Further, the expression was dramatically decreased in poorly differentiated PDAC as compared to well-differentiated PDAC. To study the functional implications of the loss of C1GALT1 in PDAC, I performed CRISPR/Cas9-mediated C1GALT1 knockout in two different PDAC cancer cell lines. Knockout of C1GALT1 in PDAC cells lead to aberrant MUC16 glycosylation, increased tumorigenicity and metastasis.

To further elaborate on the functional role of C1galt1, I have developed the *Kras^{G12D}; Trp53$^{R172H/+}$; C1galt1$^{loxP/loxP}$; Pdx1-Cre* (KPCC) mouse model, by crossing *C1galt1$^{loxP/loxP}$* mice with *Kras^{G12D}; Pdx1-Cre and Trp53$^{R172H/+}$*mice. Knockout of C1galt1 along with Kras and p53 mutations (KPCC mice) significantly decreased overall survival as compared to KPC mice that have Kras and p53 mutations. Early tumors and metastasis were seen for KPCC mice as compared to KPC mice.

In conclusion, I have experimentally shown that the loss of GALNT3 and C1GALT1 in PDAC results in aberrant glycosylation that contributes towards PDAC progression and metastasis.

TABLE OF CONTENTS

LIST OF FIGURES

LIST OF TABLES

ABBREVIATIONS

vWF-D	Willebrand factor D domain
GalNAc-Ts/GALNTs	UDP-GalNAc: polypeptide GalNAc-transferases/ polypeptide N-acetylgalactosaminyl transferases
TAA	Tumor associated antigens
Dol-P	Dolichol phosphate
Dol-P-P-GlcNAc	Dolichol pyrophosphate N-acetyl glucosamine
DAPGT1	UDP-N-acetylglucosamine-dolichyl-phosphate N-acetylglucosaminephosphotransferase
Man	Mannose
Glc	Glucose
GalNAc	N-Acetylgalactosamine
OST	Oligosaccharyl transferase
GalNAc	N-acetylgalactosamine
Cosmc	Core 1 β3-Gal-T-specific molecular chaperone
C2GnT	Core 2 beta-1, 6-N-acetylglucosaminyltransferase
NK cells	Natural killer cells
MSLN	Mesothelin
Siglecs	Sialic acid-binding immunoglobulin-type lectins
ADCC	Antibody dependent cell cytotoxicity

CTL	Cytotoxic T lymphocytes
BGN	Benzyl-N-acetyl-α-galactosaminide
CSCs	Cancer stem cells
MGAT1	α-1, 3-Mannosyl-glycoprotein 2-beta-*N*-acetylglucosaminyltransferase
GPL	Glycerophospholipids and
SL	Sphingolipids
GalT2	β-1,-galactosyltransferase
CALP	calsenilin like protein
HIF	hypoxia induced factor
FUT	fucosyltransferases
UGT1	UDP-galactose transporter-1 expression
Neu5Gc	*N*-glycolyl neuraminic acid
IBD	Inflammatory Bowel Disease
PLA	proximity ligation assay
TLR2	toll like receptor 2
Tn	Thomsen-nouvelle antigen
STn	Sialylated Tn carbohydrate antigen
TF/T	Thomsen–Friedenreich
ST	Sialylated T carbohydrate antigen

SLex/SLe^{x}	Sialyl-Lewis^{x}
SLea/SLe^{a}	Sialyl-Lewis^{a}
PDAC	Pancreatic ductal adenocarcinoma
TACA	Tumor-associated carbohydrate antigens
Cosmc	core 1 β3-Gal-T-specific molecular chaperone
HPNE	human nestin-positive normal pancreatic epithelial cells
C1GALT1	Core 1 β1, 3-Galactosyltransferase
ST6GalNAc-1	ST6 N-Acetylgalactosaminide Alpha-2,6-Sialyltransferase 1
KPC	Kras^{G12D}; Trp53$^{R172H/+}$: Pdx-Cre
KPCC	Kras^{G12D}; Trp53$^{R172H/+}$; C1galt1$^{loxP/loxP}$; Pdx1-Cre

ACKNOWLEDGEMENTS

This journey of pancreatic cancer glycobiology would not have been possible without the constant motivation from my mentor, Dr. Surinder K Batra. He has been the best mentor and extremely supportive throughout these 5 years. I have learned a lot from him both personally and professionally. I am also thankful to him for always being readily available for discussing work in spite of keeping a busy schedule. I thank him for showing great faith in me and allowing me to think independently.

I sincerely thank my graduate committee members namely Dr. Michael Hollingsworth, Dr. Rakesh Singh, Dr. Joyce Solheim, and Dr. Maneesh Jain for their constructive critiques and useful suggestions over the years.

I would like to also acknowledge our collaborators, Dr. Lijun Xia (University of Oklahoma Health Sciences Center) for providing us *C1galt1*$^{loxP/loxP}$ mice and Dr. Sriram Neelamegham and Xinheng Yu (State University of New York) for providing us the C1GALT1 CRISPR construct and helping us with mass spectrometry studies. Further, I would like to thank Dr. Dhundy Bastola and Ishwor Thapa (University of Nebraska at Omaha) for helping us with RNA-seq data analysis.

I would like to specifically thank Dr. Moorthy P Ponnusamy for teaching me basic research skills and for being extremely generous with his time and knowledge. The discussions with him on my experiments and results were some of the best learning experiences of my Ph.D. work. I would also like to thank Dr. Satyanarayana Rachagani for teaching and helping me in animal work. Further, I would like to thank Dr. Maneesh Jain for their useful suggestions in the lab meetings and committee meetings.

I express my sincere thanks to past and present lab members: Dr. Muzaffar Macha, Dr. Sushil Kumar, Dr. Sukhwinder Kaur, Dr. Wasim Nasser, Dr. Siddharth Mahapatra, Dr. Imayavaramban Lakshmanan, Dr. Parathasarathy Seshacharyulu, Dr.

Javed Siddiqui, Dr. Sakthivel Muniyan, Dr. Raghupathy Vengoji, Dr. Ramesh Pothuraju, Dr. Wade Junker, Dr. Abhijit Aithal, Dr. Shailendra K. Gautham, Dr. Prakash Kshiragar, Dr. Srikanth Barkeer, Dr. Chihiro Hayashi, Dr. Rakesh Bhatia, Dr. Sanjeev Choudhary, Dr. Dhanya Haridas, Dr. Arokiapriyanka Vaz, Dr. Parama Dey, Dr. Srushtidhar Das, Dr. Suhasini Joshi, Dr. Priya Pai, Dr. Shiv Ram Krishn, Dr. Eric Cruz, Rama Nimmakayala, Andrew Cannon, Rahat Jahan, Kasturi Banerjee, Saswati Karmakar, Garima Kaushik, Pranita Atri, Koelina Ganguly, Christopher Thompson, Suprit Gupta, Catherine Orzechowski and Kavita Mallya. In particular, I thank Dr. Srikanth Barkeer, Rama Nimmakayala and Dr. Ramesh Pothuraju for helping me in some of my experiments.

On the personal front, I thank Kavita Mallya for her friendship, kindness, and hospitality. I also thank the BMB staff members; Karen Hankins, Amy Dodson, Jeanette Gardner, Coleen Johnson and April Busch.

No words can thank my parents; my father, Late Shri Ashok Kumar and my mother, Sunita Rani for always prioritizing my education and for being a great motivational support. I thank my brother, Haripankaj Chugh, my younger sister Reemanshi Chugh and my sister in law, Nidhi Chugh for the emotional support they gave me, to carry out my thesis with great ease. I would also like to thank my paternal and maternal grandparents. I want to especially thank all my friends; Divya Kaushal, Chitrangda Srivastava, Rajni Kumari, Pankaj Bhagirath, Simarjeet Negi, Pooja Teotia, Raghubendra Dagur, Nupur Aggarwal, Sagar Bhayana, Sugandha Saxena, Ranjana Kanchan, Pranita Atri, Shashank Srivastava, Stuti goyal, and Kirti Goyal. They had always been with me during the highs and lows I faced while undertaking current investigation and always motivated me to work with my full potential.

Last but not the least, I would like to thank God Almighty for giving me the knowledge and strength to undertake this research work efficiently.

Dedicated

to

My Father

CHAPTER 1A

Introduction

The material covered in this chapter is the subject of 1 published review article

1. Chugh S, Gnanapragassam VS, Jain M, Rachagani S, Ponnusamy MP, Batra SK. *Pathobiological Implications of Mucin Glycans in Cancer: Sweet Poison and Novel Targets* Biochim Biophys Acta. 2015; 1856(2):211-25.

Pathobiological Implications of Mucin Glycans in Cancer: Sweet Poison and Novel Targets

Seema Chugh [a], Vinayaga S. Gnanapragassam[a], Maneesh Jain[a,b], Satyanarayana Rachagani[a], Moorthy P. Ponnusamy[a, b] and Surinder K. Batra[a,b,c*]

[a] *Department of Biochemistry and Molecular Biology, University of Nebraska Medical Center, Omaha, NE 68198-5870, USA*

[b] *Fred and Pamela Buffett Cancer Center, Eppley Institute for Research in Cancer and Allied Diseases, University of Nebraska Medical Center, Omaha, NE 68198-5870, USA*

[c] *Department of Pathology and Microbiology, University of Nebraska Medical Center, Omaha, NE 68198-5870, USA*

Funding: This work was supported, in part, by the grants from National Institutes of Health (UO1 CA111294, P50 CA127297, U54 CA163120, RO1 CA183459, RO1 CA195586, K22 CA175260 and P20 GM103480)

*__Corresponding Author:__ Surinder K. Batra, Ph.D. (sbatra@unmc.edu)

1. Synopsis

Mucins are large glycoproteins, which are expressed on epithelia as a protective barrier against various harsh insults mediated by toxins and pathogenic microbes. They are classified primarily as secreted and membrane-bound forms, and both mucin types are involved in various pathophysiological functions such as inflammation and cancer. High molecular weight of these proteins is attributed to their large polypeptide backbone extensively embraced by glycans. These glycan moieties on mucins modulate their function and hence play an important role in various physiological functions. Deregulation of glycosylation machinery results in altered mucin glycosylation during cellular transformation, and aberrant glycan structures play an active role to support malignancy. This review describes the functional implications and pathobiological significance of altered glycosylation of mucins in cancer. Further, the article delineates various factors such as glycosyltransferases and tumor microenvironment that contribute to dysregulation of mucin glycosylation during cancer. Finally, the scope of mucin glycan epitopes as potential diagnostic and therapeutic targets is discussed.

1. Introduction

Mucins are a family of high molecular weight glycosylated proteins with complex molecular organization. So far, twenty-one mucin genes have been identified and based on their structural organization, they are mainly classified as secreted and membrane-associated forms [1, 2]. Both of these mucin classes are involved in epithelial cell homeostasis by acting as a protective shield against severe environmental insults [3]. MUC2, MUC5AC, MUC5B, MUC6, MUC7 and MUC19 are secretory mucins, which lack transmembrane domains and have a common von Willebrand factor D domain (vWF-D) and C terminus cysteine knot domain that are required for their oligomerization [4]. The transmembrane mucins constitute another important class of mucins, which includes mucins like MUC1, MUC3, MUC4, MUC12, MUC16 and MUC17. These are anchored on the cell surface via their transmembrane domains and are involved in various signaling pathways through their short cytoplasmic tails [5].

Intricacy in the structure of these secretory and membrane proteins is imparted by their large polypeptide chain and various post translational modifications such as glycosylation, sulfation and phosphorylation [6-8]. Glycosylation is one of the major post translational modifications that defines these mucins and impacts their function. Mucins can be *O*-glycosylated or *N*-glycosylated. Both forms of glycosylation occur in distinct subcellular compartments, and differ by the amino acid involved and covalent attachment of the carbohydrates [9]. *N*-glycosylation of mucins is initiated in the endoplasmic reticulum (ER) by the action of UDP-GlcNAc phosphotransferases, whereas mucin type *O*-glycosylation occurs in the golgi and is mediated by a family of enzymes known as UDP-GalNAc: polypeptide GalNAc-transferases (GalNAc-Ts/GALNTs) [10, 11]. *O*-glycosylation is the major post-translational modification on mucins and occurs predominantly in the central tandem repeat domain that is common to all the mucins and is rich in proline, serine and threonine (PTS) residues [12]. The extent of *O*-glycosylation on mucins is determined

by the length and the number of PTS repeats, that are distinct to each mucin and variable in the same mucin due to gene polymorphism [12].

Carbohydrate structures on mucin polypeptides dictate their biochemical and biophysical characteristics and determine their biological functions. For instance, mucin glycans act as a steric barrier, which excludes large molecules and blocks adhesion in a non-specific manner [6, 13]. Some of the glycan structures are also involved in mediating cellular interactions like that with leukocytes [14]. Here, we discuss the pathobiological significance of altered mucin glycosylation in cancer. Importantly, we have focused on how several oligosaccharide structures displayed by this class of biomolecules are involved in cancer progression. We have also discussed regulation of mucin glycosylation by several factors such as glycosyltransferases and tumor microenvironment. Nonetheless, with the recognition of these carbohydrate structures as tumor associated antigens (TAA), their potential involvement in diagnostics and therapeutics is discussed.

2. Mucin glycosylation

Glycosylation is the principal post translational modification that is the hallmark of these mucins. Mucins undergo both O and N-linked glycosylation, depending on the amino acid which is attached to the glycans. Both forms of glycosylation occur in distinct cellular regions and contribute to the biochemical, biophysical and functional properties of mucins [9].

2.1. N-linked glycosylation

Protein *N*-glycosylation is initiated by the transfer of N-acetyl glucosamine phosphate (GlcNAc-P) to the polyisoprenol lipid precursor, dolichol phosphate (Dol-P), that results in the formation of dolichol pyrophosphate N-acetyl glucosamine (Dol-P-P-GlcNAc) (**Figure 1.1**). This occurs on the cytoplasmic face of the ER and is mediated by the action of UDP-N-acetylglucosamine-dolichyl-phosphate N-acetylglucosamine-

phosphotransferase (DAPGT1/GPT). Following this, another molecule of GlcNAc and five mannose (Man) residues are transferred sequentially by specific glycosyltransferases to generate $Man_5GlcNAc_2$-P-P-Dol. Subsequently, the dolichol-linked glycan precursor translocates to the ER lumen by the action of flippase. Further, transfer of four mannose and three glucose (Glc) glycans from Dol-P-Man and Dol-P-Glc, respectively, completes the synthesis of *N* glycan precursor $Glc_3Man_9GlcNAc_2$-P-P-Dol, which is then transferred *en bloc* by oligosaccharyl transferase (OST) to the asparagine residue, in one of the prominent *N* glycosylation sites of the nascent protein (Asp-X-Ser/Thr). A series of enzymatic processing reactions inside the ER trim this fourteen sugar *N*-glycan structure, following which the nascent glycoprotein is transported to the Golgi by COPII-coated vesicles. [15, 16]. In cis Golgi, further processing involves the removal of mannose residues by means of mannosidases. The processed protein is then transferred to the medial Golgi, where hybrid and complex type *N*-glycans are added. *N*-glycan structures are further elongated by the addition of several repeats of LacNAc (-3Galβ1-4GlcNAcβ1-)$_n$. Finally, these elongated structures are capped by the addition of residues like sialic acid, N-acetylglucosamine and fucose [10].

The number of *N*-glycosylation sites varies among mucin family members. For example, MUC1 has 5 potential *N*-glycosylation sites whereas MUC4 has more than 10 putative N-glycosylation sites [17, 18]. *N*-glycosylation in mucins contributes to protein stability, folding and trafficking. In MUC2, *N*-glycosylation has been demonstrated to be critical for dimerization and ensures its correct folding inside ER [19]. Additionally, *N*-glycosylation has been shown to play an important role in the surface localization of MUC17 [20].

2.2. O-linked glycosylation

Although more complex and less understood than N-linked glycosylation, *O*-glycosylation is the major post-translational modification that occurs on mucins (**Figure**

1.2). *O*-glycan chains attached to mucin polypeptide (apomucin) involves various monosaccharides such as *N*-acetylgalactosamine, galactose, *N*-acetylglucosamine, sialic acid and fucose. Arrangement of these sugars on mucins adds to structural diversity of oligosaccharide structures (as outlined in **figure 1.2**), that dictates their biophysical and functional characteristics. *O*-glycosylation of mucins is a multistep process and begins after the glycoproteins are exported to the Golgi by vesicle-mediated transport [9 and 21].

Assembly of *O*-glycans is initiated with the addition of the first sugar, N-acetylgalactosamine (GalNAc), to the serine/threonine amino acid in the PTS region by the activity of a superfamily of enzymes known GalNAc-Ts [22]. The first *O*-glycan formed by this family of enzymes is known as Tn antigen [23]. Based on the *in vitro* studies carried out earlier in 1990s, it has been established that efficient transfer of GalNAc occurs mainly to the threonine residue [24]. Till now, twenty GalNAcTs genes have been identified, which catalyze the initiation of mucin type *O*-glycosylation. Despite the functional redundancy among these GALNTs, varied substrate specificity and tissue specific expression of these enzymes have been reported [22]. The distinguishing feature of this class of glycosyltransferases is their lectin domain, which helps them in binding existing GalNAc residues on mucins. This increases their catalytic efficiency and allows them to complete the initiation of glycosylation before elongation of GalNAc residues begins. [25].

GalNAc (Tn) is then processed by the activity of various glycosyltransferases that add distinct glycans. For instance, sialyl transferases add sialic acid to yield Sialyl-Tn (STn). Alternatively, the glycan chain can be elongated by various glycosyltransferases to give rise to various core structures. Till date, eight core structures have been recognized. Biosynthesis of core 1 structure begins by addition of galactose sugar to GalNAc by T-synthase/Core 1 synthase (C1GALT1) that gives rise to a disaccharide structure known as Core 1/T antigen. The key molecule regulating activity of Core 1 synthase is an ER chaperone molecule Cosmc (core 1 β3-Gal-T-specific molecular chaperone) [26].

Mutations in Cosmc protein lead to the inactivation of Core 1 synthase, which is associated with Tn syndrome [27]. Core 1 is a critical glycan structure necessary for the formation of the core 2 glycan. Formation of core 2 glycan is catalyzed by core 2 beta-1, 6-N-acetylglucosaminyltransferase (C2GnT), which adds N-acetylglucosamine to T antigen. Besides elongation to core 2 glycan, T antigen can also be modified by sialylation to sialyl T antigen.

The first sugar, GalNAc can also be elongated to form core 3 and core 4 structures. The resulting core structure depends on the relative activity of glycosyltransferases. These *O*-glycans can also be extended by addition of several residues of poly-N-acetyllactosamine. Further, these oligosaccharide chains can be terminally glycosylated by sialylation, fucosylation or sulfation. Terminal glycosylation often results in the formation of several carbohydrate epitopes such as Le^x, Le^a, SLe^x, SLe^a, which are commonly expressed by carcinoma mucins (**Figure 1.2**) **.**

Mucin type *O*-glycans have been shown to contribute to viscoelastic properties of mucus and also protect apomucin backbone from attack by proteases. Additionally, a diverse array of glycans on mucins lining different intestinal regions also dictates their interactions with the gut microbiome [28]. This may also explain the specific colonization of microbiota in intestine. Peripheral oligosaccharide structures on mucins such as Le^x, SLe^x serve as ligands for bacterial fimbrial adhesins, thereby trapping them and preventing them to infect the underlying epithelia [29].

3. Role of mucin and its aberrant glycosylation in cancer

3.1. Role of mucins in cancer pathogenesis

Aberrant expression of mucins is observed in various malignancies, wherein they play an essential role in cancer pathogenesis [1, 30]. For example, MUC1 is involved in breast cancer pathogenesis as it affects several signaling pathways that influence disease

aggressiveness. The C terminal subunit of MUC1 acts as an oncoprotein, and through its interaction with various receptor tyrosine kinases such as EGFR and ErbB2, MUC1-CT activates PI3K-Akt and MEK-ERK pathways in breast cancer. Further, this transmembrane mucin is also found to be overexpressed in ovarian cancer and various gastrointestinal malignancies including pancreatic cancer [31, 32]. Similarly, MUC4-another transmembrane mucin-is implicated in the pathobiology of various cancers, including pancreatic, breast, lung and cervical cancers. Several studies from our lab have very well established the involvement of MUC4 in various aspects of cancer progression like metastasis, evasion of apoptosis and induction of drug resistance [33-35]. MUC4 has been shown to promote breast and pancreatic cancer metastasis [33, 34]. Interestingly, in the case of ovarian cancer, MUC4 also plays a role in cancer stem cell maintenance via stabilization of HER2 [36]. MUC4 has also been shown to interact with and stabilize HER2 in pancreatic cancer cells, but whether or not this interaction is involved in cancer stem cells needs to be explored [37].

The largest transmembrane mucin identified till date is MUC16, which is also known as CA-125 and exhibits pro-tumorigenic and pro-metastatic properties [38]. MUC16 is deregulated in ovarian cancer where it plays an important role in metastasis and protects the tumor cells from cytotoxic responses from natural killer cells (NK cells) [39] and [40]. Further, studies from our lab have also indicated the involvement of MUC16 in pancreatic cancer progression and in breast cancer proliferation [41, 42]. In pancreatic cancer cells, MUC16 has been reported to interact with GPI-linked protein, Mesothelin (MSLN), which leads to activation of MMP-7, an extracellular matrix remodeling enzyme, thereby resulting in enhanced pancreatic cancer cell motility and invasion [43]**.** In addition to MUC16, aberrant expression of MUC13 is also observed in many epithelial cancers but has not been significantly explored [44].

Along with transmembrane mucins, expression of secreted mucins is also dysregulated in various malignancies. MUC5AC is one of most studied secretory mucins and has been demonstrated to be upregulated in various cancers including colorectal and pancreatic cancer [45]. Differential expression of MUC5B is also observed in several malignancies such as breast and colorectal cancer [32, 46]. MUC2 is equally important as it has been associated with colorectal cancer and is typically downregulated [47]. Overall, mucins play an important role in the pathobiology of various malignancies.

3.2 Aberrant glycosylation of mucins in cancer

Alterations in the composition and structure of mucin glycans have been observed in various malignancies [48-50]. During carcinogenesis, neo glycan structures emerge on various glycoproteins including mucins. These atypical glycan forms can result from incomplete glycosylation resulting in truncated structures, aberrant extension of glycan chains, or novel carbohydrate patterns [51, 52] (**Figure 1.3**). Mucins with reduced core 1 and core 3 structures along with increased expression of Tn and STn are observed in intestinal, colon and pancreatic cancers [53, 54]. Tn, TF and SLe^x are carbohydrate epitopes commonly observed on MUC1 in cancer [55]. Evidence for the abnormal carbohydrate structures on mucins emerged from earlier studies demonstrating increased expression of TF antigen on mucin in colonic adenocarcinoma and ulcerative colitis as compared to normal colon [56]. Unusual glycan structures formed on these glycoproteins during cancer are involved in cancer biology. The role of these aberrant glycans in cancer cell adhesion, motility, invasion and altering the interaction of cancer cells with other cells such as lymphocytes and endothelial cells has been well documented [53]. Apart from the the pathologic role of these atypical mucin glycans, these aberrant glycan structures also constitute tumor associated carbohydrate antigens (TAA), which are extensively used as diagnostic markers.

4. Pathologic role of mucin glycans in cancer

Accumulating evidence suggest that deregulated expression of mucin glycans significantly influences the function of the mucins in pathological conditions.

4.1. Mucin glycans in mediating cellular interactions

The glycophenotype of cell surface mucins dictates both homotypic and heterotypic cellular interactions. These glycan moieties on mucins serve as ligands for various carbohydrate binding proteins, such as galectins, selectins and Siglecs and mediate diverse biological processes, including cell adhesion, migration, trafficking and inflammation [53]. All of these glycan-binding receptors constitute the lectin family and are expressed by specific subsets of cells such as immune cells and endothelial cells.

4.1.1. Galectins

Cancerous conditions are often accompanied by altered expression of beta galactoside binding lectins known as galectins [57] and [58]. These are soluble lectins with immunomodulatory activity and have been shown to regulate the proliferation and apoptosis of T cells [59]. Various mucins offer binding sugars for galectins. Like it has been shown in our lab, MUC4 interacts with galectin-3 via T antigens on its surface [60]. Further, MUC1 and MUC16 has also been shown to interact with galectin-3 in various cancers [61-63].

4.1.2. Selectins

Selectins are adhesion molecules which recognize galactose-containing carbohydrates on their cognate ligands [64]. Depending on the cell types on which they are expressed, selectins are classified into E-selectin (endothelial cells), L-selectin (Leukocytes) and P-selectin (platelets). These selectins recognize sialylated/sulfated lewis antigens on mucin glycoproteins, which are highly expressed during cancerous conditions [65]. The interaction of selectins with secreted and surface mucins is well depicted in colon cancer cells where they have been shown to induce platelet aggregation

and agglutination of activated PBMCs [66]. This may also explain platelet containing microthrombi generally observed in mucinous cancers [67].

4.1.3. Siglecs (Sialic acid-binding immunoglobulin-type lectins)

Sialic acid binding lectins or Siglecs are expressed by some hematopoietic cells such as macrophages and B cells, and play an important role in modulating the immune response. Siglecs have been demonstrated to interact with mucins. For instance, Siglec-9 expressed on surface of immune cells such as B-cells, monocytes and NK cells has been shown to interact with MUC16 and MUC1 [68, 69].

4.2. Functional consequences of mucin glycotopes-mediated cellular interactions

Interaction of mucin glycans with sugar-binding poteins have been shown to affect several aspects of tumor progression such as tumor growth, escape of immune surveillance and metastasis (**Figure 1.4**).

4.2.1. Mucin glycans in tumor growth

Sialoglyans expressed on mucins have been shown to affect tumor growth. Sialoglycans on MUC1 (SLe^x) mediates its binding to Siglec-9, which is commonly expressed by immune cells. This binding induces recruitment of β-catenin to MUC1-C domain and its translocation to nucleus resulting in increased proliferation of cancer cells [68] (**Figure 1.4a**).

4.2.2 Role of mucin glycans in the evasion from immune surveillance

Although tumor tissues are characterized by infiltration of immune cells, such as macrophages, natural killer cells and cytotoxic T cells, tumor cells effectively escape immune surveillance. This is due to the activation of various immunosuppressive pathways activated by the tumor cells [70]. A considerable body of evidence suggests the involvement of glycan epitopes on cancerous cells in escape of immune surveillance. Elongation of mucin glycans beyond the Tn antigen alters their susceptibility towards NK and CTL-mediated killing [71] (**Figure 1.4b**). This has been shown in breast (T47D) and

pancreatic cancer cells (Capan1), wherein knock out of Cosmc protein (chaperone for core1 synthase) resulted in inhibition of glycan elongation beyond Tn, which consequently increased their sensitivity towards immune attack via NK cell-mediated antibody dependent cell cytotoxicity (ADCC) and cytotoxic T lymphocytes (CTL). Further, reverse correlation was observed between MUC1/MUC16 expression and immune killing, which suggests that upregulated expression of these mucins along with their glycan elongation beyond Tn can possibly be involved in immune evasion [71] .

4.2.3. Mucin glycotope-mediated cancer metastasis

Interaction of mucin glycans with selectins has been implicated in metastasis. Several studies have demonstrated that cancer metastasis involves interaction between carcinoma mucins on cancer cells and P-selectin on platelets [72]. Further, in ovarian cancer, *N*-glycans on MUC16 are implicated in facilitating peritoneal metastasis via their interaction with mesothelin expressed by mesothelial cells lining the peritoneal cavity [73].

Interaction between galectin-3 and MUC4 has been implicated in metastasis where galectin-3 binding results in MUC4 clustering, that exposes adhesion molecules such as integrins which in turn facilitates the attachment of tumor cells with endothelial cells (**Figure 1.4c**) [74]. Similarly, elevated circulating galectin 3 in several cancers has been shown to interact with TF on MUC1 and expose surface ligands for endothelial cells such as CD44. Hence this interaction abrogates the "shield effect" of MUC1 in preventing the adhesion of cancer cells to endothelial cells, thereby resulting in enhanced metastasis (**Figure 1.4c**) [63].

More recently, it has been shown that altered glycans on MUC1 impacts invasion and migration of breast cancer cells by influencing its interaction with CIN85, an adaptor protein involved in invasion and cytoskeletal alterations [75]. This was demonstrated by overexpressing some of glycosyltransferases such as ST6GalNAc1 and ST3Gal1, which are involved in the biosynthesis of carbohydrate antigens, STn and ST respectively.

Increased interaction of CIN85 and MUC1 was observed with increased expression of STn whereas this interaction was not altered with increased expression of ST [76]. This suggests that hypoglycosylated form of MUC1 (MUC1-STn) can promote MUC1's interaction with CIN85 that results in increased migration and invasion.

4.2.4. Role of glycosylation in membrane trafficking of mucins

Most of the aforementioned processes mediated by mucin glycans such as metastasis and tumor growth necessitate the membranous localization of these glycoproteins. Both N- and O- linked oligosaccharides on some of these mucins are identified to contain tremendous information for their apical sorting. This has been well described for MUC1 using Madin Darby Canine Kidney cells (MDCK), with which it was demonstrated that O-glycosylated tandem repeats on MUC1 serve as apical sorting signal [77]. Several studies have suggested the involvement of these O and N glycomoieties in the membrane trafficking of their carrier protein. This was shown using benzyl-N-acetyl-α-galactosaminide (BGN) and tunicamycin, commonly used drugs which interfere with O and *N*-glycan biosynthesis. Incubation of human colorectal adenocarcinoma cells (HT29) with BGN decreases secretion and membrane targeting of MUC1 [78]. Consistent with this study, treatment of endometrial and breast cancer cells with these inhibitors also reduced the expression of MUC1 on their surface [79]. These studies highlight the essential role played by mucin glycosylation in their membrane trafficking. However, the possible role(s) of glycans in apical sorting of other mucins such as MUC4 and MUC16 need to be investigated.

While glycosylation impacts trafficking, altered cellular trafficking can also impact mucin glycosylation. This concept was demonstrated for MUC1, wherein secretory and membrane-shed MUC1 probes displayed altered glycosylation profile. Secreted MUC1 form (MUC1-S) exhibited more of core2 glycan structures whereas membrane-shed form was rich in sialylated core-1 glycan structures [80].

4.2.5 Mucin glycans and cancer stem cells

Recently, mucins have been associated with cancer stem cells (CSCs). Since alterations in mucin glycosylation have been implicated in cancer growth and metastasis, there is a possibility that CSCs have a greater tendency for altered glycosylation of mucins. A few studies have suggested altered glycosylation of mucins in these highly tumorigenic cells. Studies from our lab utilizing ovarian cancer cells ectopically overexpressing MUC4 indicated a slight decrease in the molecular weight of MUC4 in the enriched side-population as compared to non-side population [36]. Altered glycosylation may be a plausible mechanism for such observation but this remains to be investigated. Another study has reported the existence of hypoglycosylated MUC1 in the cancer stem cell population in MCF-7 breast cancer cells [81]. More comprehensive studies are required to decipher the role of mucin glycosylation in development and maintenance of cancer stem cells.

5. Regulation of mucin glycosylation

Given the functional significance of aberrant mucin glycans in cancer, it is important to understand how mucin glycosylation is regulated. Several factors influence the differential expression of mucin glycans during carcinogenesis. These include alterations in glycogene expression, altered localization of the glycosyltransferases, aberrant activity of respective glycosyltransferases/glycosidases, changes in golgi pH, efficiency of the sugar nucleotide transporters, and physiological alterations in the tumor microenvironment such as hypoxia and inflammation [82, 83].

5.1. Mucin glycosyltransferases

The glycogenes consist of either glycosyltransferases (GTs) that are responsible for synthesizing glycan structures, or glycosidases (Gs) that catalyze the release of glycans from glycoproteins and glycolipids. The relative level and activity of GTs and Gs

dictate the glycan profiles of glycoproteins and any imbalance results in aberrant glycosylation [84].

5.1.1 Altered glycogene expression during cancer

Diversity in the expression of GTs and Gs in a cell is manifested in the variety of glycans displayed by mature mucins [85]. In general, cancer-associated glycan expression is regulated by myriad of glycogenes, some of which are transcriptionally repressed while others are induced during malignant transformation [86 and 87]. Genetic and epigenetic silencing mechanisms are involved in the inactivation of many glycogenes during carcinogenesis. For instance, in pancreatic and biliary tract carcinomas, elevated expression of CA19-9 (sialyl Lewis a-SLe^a) on core 1 or core 2 glycan structures has been detected as compared to the normal epithelia, which predominantly express disialyl Lewis A. CA19-9 is associated with mucins, which play significant roles in cancers and specifically pancreatic cancer [88]. This reduced expression of disialyl Lewis A during oncogenic transformation is due to the epigenetic silencing of the glycogene ST6GALNAC6 [89]. Similarly, normal colonic epithelial cells express 6 sulfo-sialyl–Lewis x, which is undetectable in colon cancer cells. Colon cancer cells, in contrast, expresse high levels of sialyl–Lewis x (SLe^x), which is due to epigenetic silencing of diastrophic dysplasia sulfate transporter (DTDST), resulting in insufficient sulfation and increased expression of SLe^x [90]. Additionally in colon cells, activity of core 3 synthase is suppressed by promoter methylation and its ectopic overexpression reduces cancer cell motility, suggesting that cancer cells downregulate this enzyme to enhance their metastatic potential [91]. Further, in gastrointestinal tissues, decreased expression of Sd^a that is expressed in the normal stomach is attributed to CpG island promoter hypermethylation of β4GALNT2. Absence of this glycogene favors the expression of the SLe^x and SLe^a which serve as ligands for selectins and are involved in metastasis. Stable expression of β4GALNT2 glycosyltransferase in colorectal (HT29) and gastric cancer cells

(KATOIII) leads to reduced expression of SLe^x and SLe^a and decreased metastasis [92]. More recently, it has been shown that the O-glycosylation-initiating enzyme GALNT3 is hypomethylated and is overexpressed in epithelial ovarian tumors [93]. Knockdown of this enzyme is associated with increased adhesion and decreased MUC1 stability, which suggest that the involvement of GALNT3 in ovarian cancer progression is possibly via aberrant MUC1 glycosylation [94]. Thus, the epigenetic regulation of the glycogenes significantly contributes to cancer progression and metastasis.

In addition to epigenetic mechanisms, post-transcriptional regulation of GTs has also been reported recently. During the metastasis of melanoma, the expression of the *O*-glycosylation-initiating GalNAc transferase, GALNT7, is down regulated by the increased expression of miR-30b/30d. Knockdown of miR-30b/30d restores GALNT7 expression that results in decreased cellular invasion and the induction of IL-10 (an immunosuppressive cytokine) [95].

5.1.2. Localization of glycosyltransferases in normal and cancer cells

Various glycosylating enzymes are distributed non-uniformly inside golgi, with each compartment expressing unique set of glycosyltransferases. Several factors dictate their golgi localization, some of which are intrinsic structural features of these enzymes. Predominantly, these glycosyltransferases are type II integral proteins which are organized in to N-terminal, cytoplasmic tail, transmembrane and the stem regions (CTS). These regions are involved in directing their golgi localization [96]. Transmembrane domain (TMD) of α-2, 6-sialyl transferase (ST) affects its golgi distribution. Mutagenesis studies have revealed that the length of TMD serves as a sorting signal, and varying the length of TMD alters the golgi retention of this *trans* Golgi enzyme [97]. Compartmental identity of *medial* Golgi enzymes like mannosidase II and MGAT1 (α-1,3-mannosyl-glycoprotein 2-beta-*N*-acetylglucosaminyltransferase) is maintained through their oligomerization mediated by their luminal regions [98]. Differential ratio of

glycerophospholipids (GPL) and sphingolipids (SL) among individual Golgi compartments (SL/GPL being highest in trans golgi and lowest in cis) also account for non-homogenous distribution of these enzymes [96, 99, 100]. For other glycosyltransferases like β-1,-galactosyltransferase (GalT2), β-1, 4-N-acetylgalactosminyltransferase (GalNAcT) and sialyltransferase (SialT2), calcium-binding proteins like calsenilin and calsenilin like protein (CALP) have been shown to influence Golgi localization. GalT2 directly interacts with calsenilin via its cytoplasmic tail and this interaction impacts their mutual subcellular localization, whereas the localization of SialT2 and GalNAcT is mediated through their interaction with GalT2 [101]. Relative position of these glycosyltransferases inside the golgi determines the glycan structure produced by the cells. Aberrant glycosylation in various pathological states can be attributed to anomalous localization of glycosyltransferases.

5.2. Effect of tumor microenvironment on mucin glycosylation

In addition to the aforementioned cell-intrinsic determinants, various factors in the tumor microenvironment such as hypoxia and inflammation can modulate glycans on carcinoma mucins.

5.2.1. Hypoxia-induced glycogene expression

Hypoxic microenvironment prevails in the advancing tumor niche. Hypoxia induces neo-angiogenesis, directs the intracellular metabolism to anaerobic glycolysis and increases the metastatic potential of the cancer cells. Such hypoxic conditions also result in altered glycans structures due to transcriptional deregulation of various glycogenes like sialyl transferase, fucosyltransferase and sugar transporters. Certainly, hypoxia condition induces hypoxia induced factor (HIF) that results in increased expression of SLe^a and SLe^x in colon cancer cells. These selectin ligands were increased due to the increased expression of UDP-galactose transporter-1 expression (UGT1), sialyltransferase (ST3Gal-I), and fucosyltransferases (FUT-7) [102]. Abnormal glycan structures with

increase of *N*-glycosyl sialic acid residues are also prevalent in hypoxic conditions. This is attributed to Sialin, a sialic acid transporter, which is activated under hypoxia and promotes the incorporation of the *N*-glycolyl neuraminic acid (Neu5Gc) in mucin type glycans [103]. Notably, distinct sets of glycans are induced by hypoxia under malignant versus nonmalignant conditions, such as ischemic disorders, suggesting their distinct roles in distinct pathological conditions [86].

5.2.2. Inflammation and altered glycosylation

Inflammation associated with several pathological conditions such as *Helicobacter pylori* infection, inflammatory bowel disease (IBD) and cancer also contributes to changes in glycosylation of many proteins [104-106]. For instance, inflammation is associated with changes on surface glycans of lymphocytes with an increase in sulfated carbohydrate epitopes that mediate transient interactions with selectins on endothelial cells, which facilitates the homing of activated lymphocytes to inflammed sites [107, 108]. Similarly, inflammatory conditions have also been shown to modulate the glycan profile of various mucins on cancer cells [109].

This has been described in research carried out by Brian B. Haab group in Van Ander Research Institute, wherein by stimulating pancreatic cancer cells (Aspc-1, BxPC-3 and SU.86.86) with various inflammatory cytokines such as IFNγ, IL-1α and TNFα, significant changes in mucin glycosylation and their expression were observed. Using immunoprecipitation and antibody microarrays, they demonstrated that TNFα and IFNγ stimulated BxPC-3 cells display elevated CA 19-9 levels on MUC1 and MUC5AC. Elevated levels of terminal GlcNAcβ, GalNAcα, GalNAcβ and lactosamine were observed on MUC16 in MIA PaCa cells [83]. These experiments highlight the impact of inflammation on mucin glycans in cancer. Additional studies are required to determine the underlying mechanisms involving inflammation-mediated glycan changes on mucins.

Interestingly, some of the studies have described the crosstalk between inflammation and glycosylation, wherein they have shown that many glycosylation changes can also contribute to inflammation [110]. Further research to investigate whether such autocrine loop exists between mucin glycosylation and inflammation in cancer will be intriguing.

5.3. Impaired mucin glycosylation with elevated pH

The ability of Golgi to facilitate essential functions such as protein folding, glycosylation, sorting and trafficking relies on its luminal pH. Any aberrations in organelle pH interferes with all these events which results in abnormalities associated with several pathological consequences such as cystic fibrosis and cancer [111, 112]. While altered glycosylation profile of mucins in several cancers is attributed mislocalization of GTs, there is also evidence supporting the involvement of altered golgi pH in aberrant glycosylation. In breast and colorectal cancer cells, increased Golgi pH is associated with expression of T antigen, a core 1 carbohydrate structure usually associated with carcinoma mucins [113]. However the exact mechanism by which these changes occur remains unclear.

6. Diagnostic and prognostic significance of mucin glycans

Early diagnosis is the key for improving the clinical outcome of all malignancies and mandates the development of efficient diagnostic tools. Serum biomarkers are clinically acceptable and more preferred over other diagnostic modalities such as CT scan, MRI and endoscopy due to their non-invasive nature and relatively cost effectiveness. In fact, aberrant mucin glycans have been the basis of several clinically approved serodiagnostic tests for various malignancies [114]. CA-125, used in the diagnosis of ovarian cancer, is an epitope present on MUC16 while CA15-3, an epitope on MUC1, is used to monitor breast cancer [115, 116]. Altered expression of mucin glycans is a hallmark of several malignancies including pancreatic, breast, gastric, colon and lung

cancer [117]. Since these unusual glycan structures are generally not seen in normal tissues, these mucin glycotopes can potentially serve as efficient diagnostic tools. Several glycan epitopes have been approved by the FDA as biomarkers for diagnosis or utilized to monitor response to therapy or disease progression. A well-documented example of such a marker is CA19-9 , which is of clinical utility in various gastrointestinal cancers and is often used for diagnosis of pancreatic cancer [118] .This serological assay detects aberrant changes in SLe^a which is highly expressed on mucins. Similarly, CA72-4 assay is used to detect elevated levels of STn, an another carbohydrate antigen associated with mucins in several epithelial cancers [119].

Due to extremely low abundance during early disease, rapid hepatic clearance and requirement of complexities associated with their characterization, discovery of glycan biomarkers is challenging [120]. As an alternative, a few studies have provided strong hope for the identification of glycan biomarkers by detecting anti-glycotope auto antibodies. During the onset of tumor, the immune system recognizes altered glycan epitopes as neoantigens and elicits humoral response resulting in the generation of auto-antibodies. These auto-antibodies are highly specific and display exclusive affinity toward the host antigen as the disease progresses. These two unique features make the auto-antibodies an effective diagnostic tool for the early detection of cancer, as well as monitoring the disease status. The presence of these autoantibodies towards glycopeptide regions (Tn-MUC1, STn-MUC1) of aberrantly glycosylated MUC1 has been demonstrated in breast, ovarian and prostate cancer [121].

Recently, existence of such auto-antibodies directed toward Tn and STn epitopes, and T antigen on MUC1, MUC4 and other mucins has been demonstrated by seromic profiling of colon cancer patients [122]. Among these auto-antibodies, the IgG type in serum of cancer patients specifically reacted with MUC1 glycopeptides while there was no reactivity with sera from healthy and IBD (Inflammatory Bowel Disease) controls. IgM

type showed reactivity to all the mucins with core 3 glycans. Thus, IgG type autoantibodies are highly specific to MUC1 and can be used to discern between cancerous and IBD patients. Further, their sera samples contained a higher amount of anti-MUC4 IgA type auto-antibodies. The study is also extended to other mucins (MUC2, 6, 7 and 5AC) however, MUC1 and MUC4 carry the most prominent tumor-associated glycan epitopes [122].

More recently, another group made an attempt to detect the combination of mucins and their associated glycans using proximity ligation assay (PLA). Using a set of samples from different types of adenocarcinomas such as colon, lung, breast and ovary, they suggested that this *in situ* technique can detect aberrant mucin glycoforms with better sensitivity and specificity than assays detecting only the O-glycans/mucins [123]. However, further studies with increased cohort size are required to annotate these aberrant glycoforms as cancer biomarkers.

7. Glycans as therapeutic targets

The presence of glycans on various biomolecules underscores their functional importance. Some of these molecules such as mucins are localized on the cell surface and can modulate the cellular functions during physiological and pathological conditions [6]. More specifically, mucin glycans are involved in tumor cell proliferation, invasion, hematogenous metastasis and angiogenesis. Thus, glycans are very attractive targets for cancer therapy.

7.1 .Mucin glycan/glycopeptide vaccines

A major limitation in targeting mucins peptides is posed by the normal homeostatic role played by their secreted and membrane-bound forms. Mucin glycopeptides-based vaccines may offer an added advantage in that the undesired effects on normal epithelial tissues are limited, as there is distinct glycan pattern on mucins of tumor cells as compared

to normal cells. Unusual glycomotifs on mucins are recognized by the immune system but they are poorly immunogenic; therefore administration of synthetic glycans along with carrier protein can be used as anti-cancer vaccines to boost immune response [124]. One such example is the STn-KLH vaccine, which was used in phase III clinical trials of breast cancer patients with metastatic disease and has been shown to induce both humoral and cellular immune responses [125, 126]. Another example of glycan vaccine is multicopy multivalent vaccines, where polymerized Tn carbohydrate antigen is conjugated with gold nanoparticles. *In vivo* experiments on New Zealand white rabbits using this vaccine have demonstrated significant immune responses along with crossreactivity towards Tn antigen on various mucins [127].

A MUC1-based glycopeptide vaccine was designed by linking the glycopeptide antigen sialyl-Tn-MUC1 to tetanus toxoid. This vaccine induced a very strong and selective immune response in mice [128]. Since MUC1 glycopeptide is poorly immunogenic, synthetic vaccines consisting of MUC1 glycopeptide along with T_H (T helper) peptide have also been designed to activate humoral immunity [129]. Similarly, to stimulate the immune response, oligovalent vaccines have been constructed by conjugating MUC1 glycopeptide with toll-like receptor 2 (TLR2) lipopeptide ligands using Click chemistry [130]. More recently, MUC1 tripartite vaccines has been generated using MUC1 glycopeptide, T_H peptide and TLR2/9 agonist and were found to elicit a better immune response [131].

Currently, we are examining the MUC4-associated glycan epitopes and glycan interacting proteins in various cancers. This will lead to the development of novel diagnostic and therapeutic targets. Generating vaccines carrying both N- and O-glycosylated mucin peptides could be an effective therapy against various cancers. It is also important to investigate the possibility of other mucins such as MUC16 as a vaccine candidate, as it is highly overexpressed in pancreatic, breast and ovarian cancers [38]. As

multiple mucins are involved in malignant conditions, multivalent vaccines targeting many mucins could also be of great therapeutic potential.

7.2 Glycosyltransferase inhibitors and glycomimetics as therapeutic agents

Significant studies using individual glycans as therapeutic targets have been performed. The core glycan structures build the *O*-GalNAc glycans and their role has been studied intensively by several investigators. Besides this, the terminal glycans on mucins are also of unique importance due to their primary interactions with other proteins [69]. Sialic acid is the common terminal glycan on mucins. Interestingly a sialic acid molecule alone as a member of an epitope modulates several functions under given conditions and plays a major role in cancer metastasis by aiding the cancer cells in detaching from the primary tumor [132]. Thus the detached cancer cells metastasize by the aid of glycan epitopes, which are expressed on the mucins and other glycoproteins. Also the selectin ligands (e.g. sialylated Lewis antigen) carry α2, 3-linked sialic acid in their terminal regions, further highlighting the importance of this modification on glycans in cancer. The application of sialyltransferases inhibitors, such as soyasaponin, in combination with a cancer drug could be an effective dual-targeted therapy [133]. Several sialyltransferase inhibitors have also been tested; however, very few are potent in inhibiting the enzyme activity.

Glycomimetic drugs have been examined to block selectin interaction with the endogenous glycans [134]. Acetylated derivatives of GlcNAcβ3GalβO-Nap and Galβ4GlcNAcβ1O-Nap have been tested as decoys to disrupt the biosynthesis of natural ligands for selectins. Similarly, the utility of acetylated F-4 GlcNAc as an inhibitor of lectin-mediated ovarian tumor cell adhesion has been evaluated [135]. Recent studies indicate that fluorinated GalNAc metabolically alters glycan structures on mucins. The glycans of leukocyte PSGL-1 are altered, which reduces cell binding to selectins and inhibits the biosynthesis of chondroitin sulfate. Acetylated F-4GalNAc exhibits superior metabolic

inhibitory activity compared to the GalNAcα -OBenzyl inhibitor. Significant efforts have also been invested for synthesizing/isolating natural products to function as competitive inhibitors against their native substrates. Several of these small molecules that mimic the glycan epitope are currently undergoing clinical trials [136]. Much research should be carried out to identify effective glycan targets on mucins that aid in the progression of disease. Their discoveries will provide us the platform for designing systematic studies toward synthesis of therapeutic reagents.

8. Conclusion and perspectives

The glycosylation of mucins not only regulates their stability but also modulates their function. As discussed in this review, mucin glycosylation is altered during neoplastic transformation and cancer progression. This has formed the basis for the use of glycans as prognostic/diagnostic biomarkers. Glycosylation of mucins is influenced by several factors, such as epigenetic regulation and sub-cellular localization of glycosyltransferases and tumor microenvironment. Altered expression of specific glycosyltransferases promotes cancer cell metastasis by various mechanisms. This provides a greater opportunity to screen for the specific inhibitors for these enzymes. The knowledge of specificities of these enzymes and their tissue distribution is important for drug discovery, especially for those enzymes involved in alteration of glycan signature during cancer progression.

Much improvement is required in generating mucin glycopeptide-based vaccines that offers more sensitivity and specificity than the current mucin-based vaccines. Interdisciplinary approaches are urgently required from basic to translational research to enable advancement toward this goal.

Considerable interest in understanding the role of glycans in the versatile functions of the mucins is increasing. Further research is required to identify the functional

glycotopes on mucins that are responsible for cancer progression. To get a deep insight into the involvement of mucin glycans in cancer, animal models with modulated expression of glycosyltransferases such as GALNTs, core1 synthase and sialyltransferase should be developed. This will certainly help in elucidation of the functional significance of mucin glycosylation, not only in cancer but also in other acute and chronic diseases and will lead to the identification of useful prognostic, diagnostic and therapeutic targets.

Figure legends

Figure 1.1 N-glycosylation of mucins: *N*-glycosylation is initiated in the ER by the transfer of GlcNAc from UDP-GlcNAc to lipid molecule known as Dol-P. Further one molecule of UDP-GlcNAc and four molecules of mannose are transferred sequentially on GlcNAc-P-P-Dolichol, resulting in the formation of $Man_5GlcNAc_2$-P-P-Dol. This is followed by the translocation of this oligosaccharide-linked Dolichol to the lumen of ER. Successive addition of four molecules of mannose and three molecules of glucose forms $Glc_3Man_9GlcNAc_2$P-P-Dol, which is transferred *en bloc* by OGT to Asn residue of mucin molecule. *N*-glycans linked onto mucin molecule are further trimmed inside the ER and processed in golgi apparatus (complex *N*-glycan synthesis, elongation and capping) giving rise to mature *N*-glycans linked to mucin molecule.

Figure 1.1

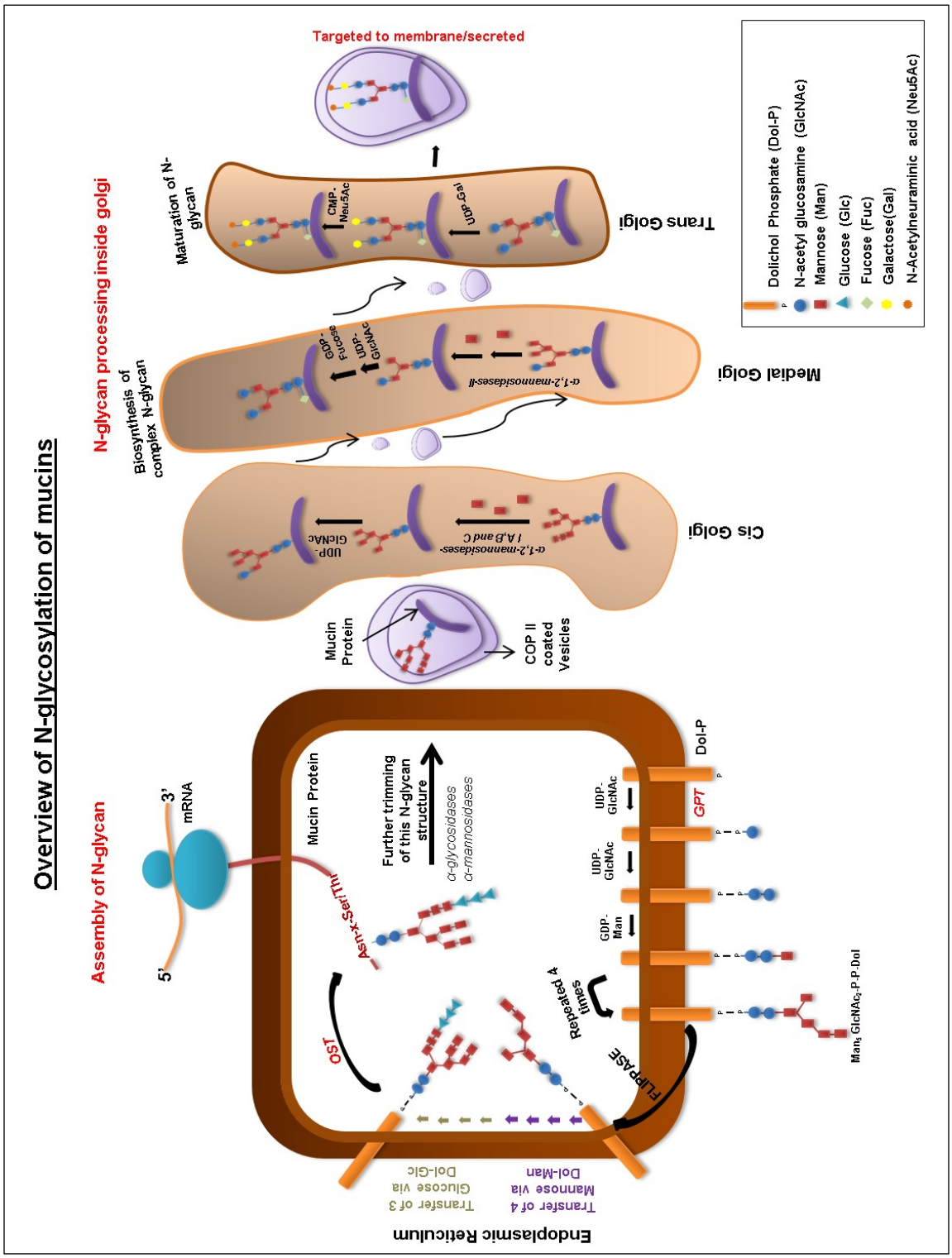
Overview of N-glycosylation of mucins
Assembly of N-glycan
N-glycan processing inside golgi
Endoplasmic Reticulum
Transfer of 4 Mannose via Dol-Man
Transfer of 3 Glucose via Dol-Glc
Dol-P
GPT
UDP-GlcNAc
UDP-GlcNAc
GDP-Man
Repeated 4 times
FLIPPASE
OST
Asn-x-Ser/Thr
Mucin Protein
3'
mRNA
5'
Further trimming of this N-glycan structure
α-glycosidases
α-mannosidases
Mucin Protein
COP II coated Vesicles
Cis Golgi
α-1,2-mannosidases-I A,B and C
UDP-GlcNAc
Medial Golgi
Biosynthesis of complex N-glycan
α-1,2-mannosidases-II
GDP-Fucose
UDP-GlcNAc
Trans Golgi
Maturation of N-glycan
CMP-Neu5Ac
UDP-Gal
Targeted to membrane/secreted
Dolichol Phosphate (Dol-P)
N-acetyl glucosamine (GlcNAc)
Mannose (Man)
Glucose (Glc)
Fucose (Fuc)
Galactose(Gal)
N-Acetylneuraminic acid (Neu5Ac)

Figure 1.2 Overview of mucin type O-glycosylation: *O*-glycosylation is initiated by the activity of ppGalNAcTs, which will attach N-acetylgalactosamine to S/T (highlighted in yellow) residues in the tandem repeat region, resulting in formation of Tn antigen. Tn antigen formed can be extended by activity of core 1 synthase to generate T antigen/core 1 antigen. Alternatively, Tn can be modified by sialyltransferase to sialyl Tn (STn). Core 1 antigen can be further elongated to form core 2 structure. Further, core 2 structure is extended to several structures such as Le^x, SLe^x, Le^a, SLe^a . Tn can also be extended by activity of other glycosyltransferases to form several other core structures (core 3-8)

Figure 1. 2

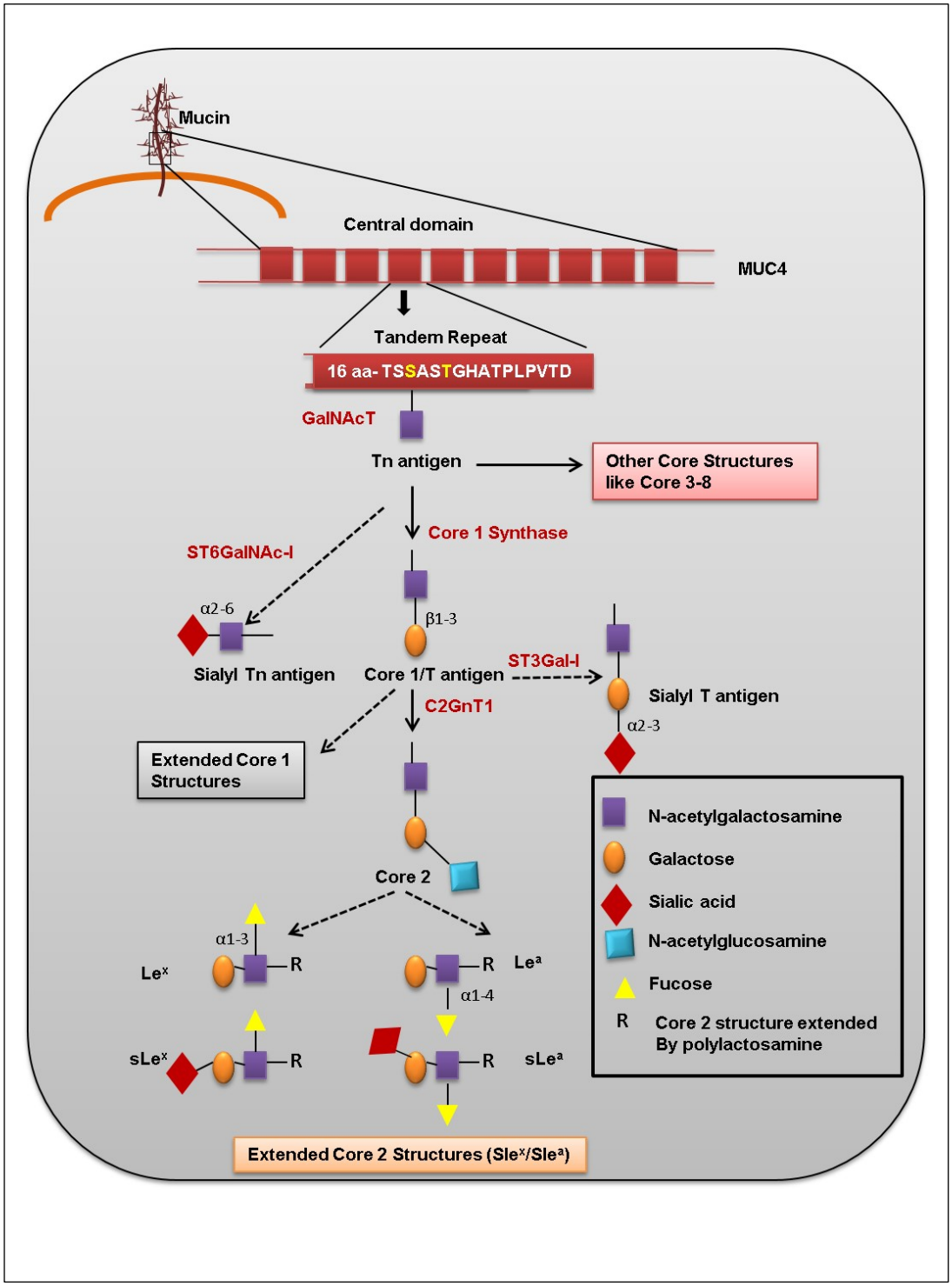
Mucin
Central domain
MUC4
Tandem Repeat
16 aa- TSSASTGHATPLPVTD
GalNAcT
Tn antigen
Other Core Structures like Core 3-8
Core 1 Synthase
ST6GalNAc-I
α2-6
β1-3
Sialyl Tn antigen
Core 1/T antigen
ST3Gal-I
Sialyl T antigen
α2-3
C2GnT1
Extended Core 1 Structures
Core 2
α1-3
Le^x
R
Le^a
α1-4
sLe^x
sLe^a
Extended Core 2 Structures (Sle^x/Sle^a)
N-acetylgalactosamine
Galactose
Sialic acid
N-acetylglucosamine
Fucose
R
Core 2 structure extended By polylactosamine

Figure 1.3 Aberrant glycosylation of mucins during cancerous conditions: Differential glycosylation of mucins occurs in malignant conditions, resulting in truncated glycan structures such as Tn, STn, T, and several core 2 extended structures such as SLe^x and SLe^a. This aberrant glycosylation results from several factors such as altered glycogene expression, mislocalization of glycosyltransferases, abnormal golgi pH and tumor microenvironment.

Figure 1.3

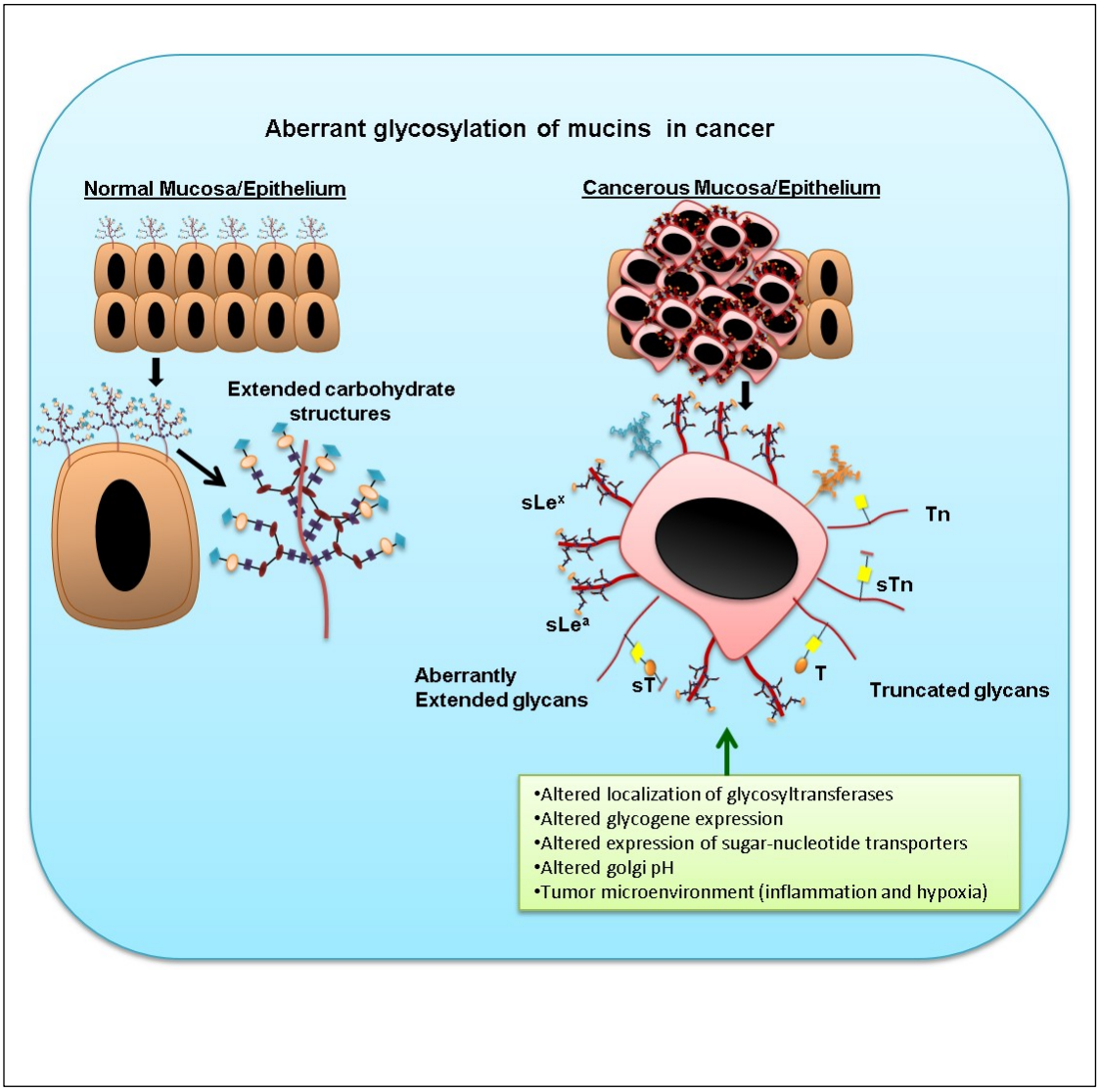
Aberrant glycosylation of mucins in cancer
Normal Mucosa/Epithelium
Cancerous Mucosa/Epithelium
Extended carbohydrate structures
sLe^x
Tn
sTn
sLe^a
Aberrantly Extended glycans
sT
T
Truncated glycans
•Altered localization of glycosyltransferases
•Altered glycogene expression
•Altered expression of sugar-nucleotide transporters
•Altered golgi pH
•Tumor microenvironment (inflammation and hypoxia)

Figure 1.4 A schematic representation of mucin glycans-mediated cellular interactions: a.) Aberrant glycans structures such as SLe^x on MUC1 mediates tumor growth by binding to Siglec-9 on immune cells. This binding induces the translocation of beta-catenin to the nuclei of cancer cells, resulting in cell growth. b.) Extensive glycosylation of MUC16 helps tumor cells in escaping immune attack via NK cells. c.) Interaction between galectin-3 and T antigen on MUC1 prevents anoikis via homotypic aggregation of cancer cells as well as mediates docking of tumor cells to endothelial cells thereby resulting in metastasis

Figure 1.4

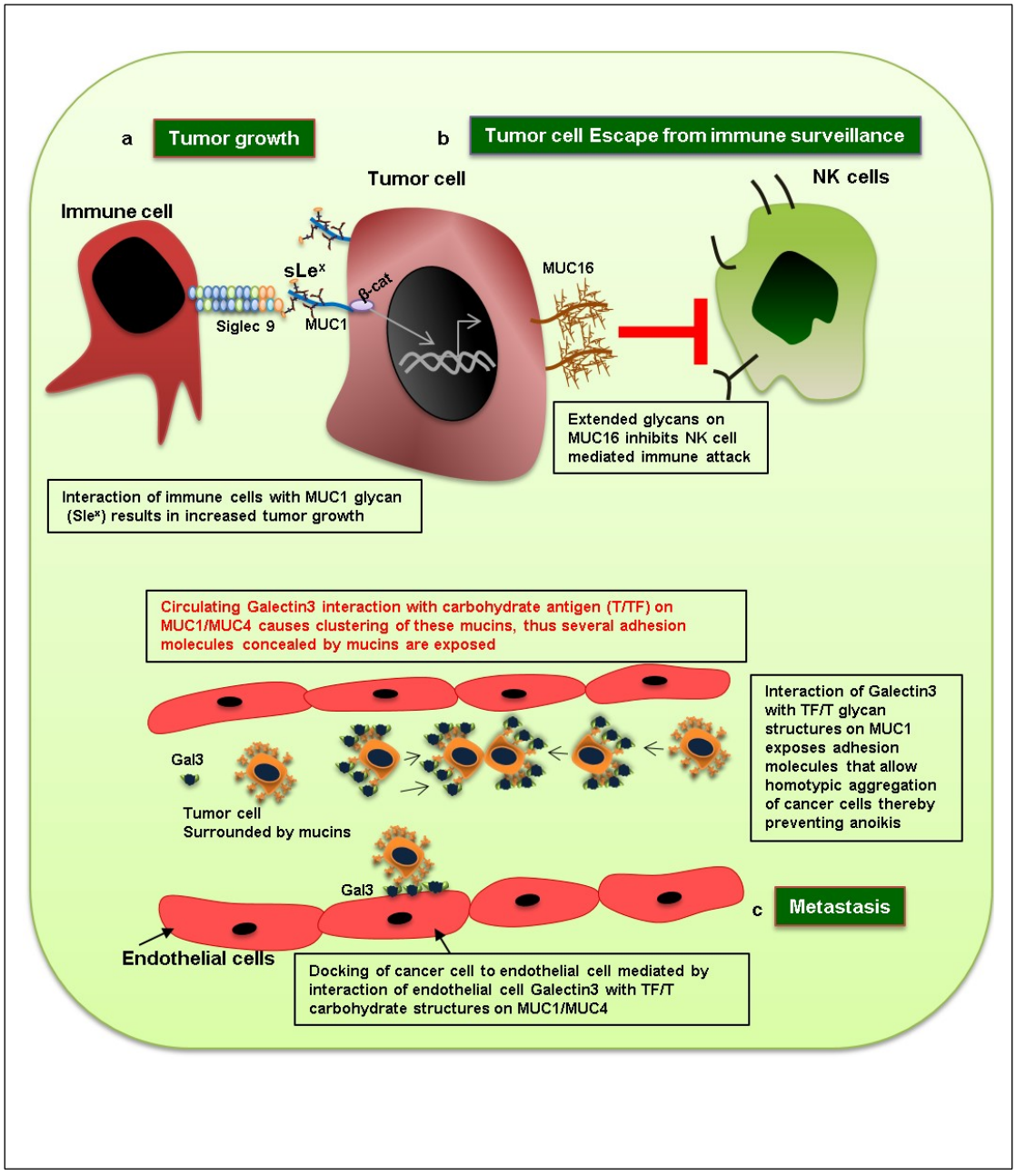
a
Tumor growth
b
Tumor cell Escape from immune surveillance
Tumor cell
NK cells
Immune cell
sLe^x
β-cat
MUC16
Siglec 9
MUC1
Extended glycans on MUC16 inhibits NK cell mediated immune attack
Interaction of immune cells with MUC1 glycan (Sle^x) results in increased tumor growth
Circulating Galectin3 interaction with carbohydrate antigen (T/TF) on MUC1/MUC4 causes clustering of these mucins, thus several adhesion molecules concealed by mucins are exposed
Interaction of Galectin3 with TF/T glycan structures on MUC1 exposes adhesion molecules that allow homotypic aggregation of cancer cells thereby preventing anoikis
Gal3
Tumor cell
Surrounded by mucins
Gal3
c
Metastasis
Endothelial cells
Docking of cancer cell to endothelial cell mediated by interaction of endothelial cell Galectin3 with TF/T carbohydrate structures on MUC1/MUC4

References

[1] D.W. Kufe, Mucins in cancer: function, prognosis and therapy. Nat. Rev. Cancer. 9 (2009) 874-885.

[2] S. Rachagani, M.P. Torres, N. Moniaux, and S.K. Batra, Current status of mucins in the diagnosis and therapy of cancer. Biofactors. 35 (2009) 509-527.

[3] M.E. Johansson, H. Sjovall, and G.C. Hansson, The gastrointestinal mucus system in health and disease. Nat. Rev. Gastroenterol. Hepatol. 10 (2013) 352-361.

[4] J. Perez-Vilar and R.L. Hill, The structure and assembly of secreted mucins. J. Biol. Chem. 274 (1999) 31751-31754.

[5] C.L. Hattrup and S.J. Gendler, Structure and function of the cell surface (tethered) mucins. Annu. Rev. Physiol. 70:431-57. (2008) 431-457.

[6] M.A. Hollingsworth and B.J. Swanson, Mucins in cancer: protection and control of the cell surface. Nat. Rev. Cancer. 4 (2004) 45-60.

[7] P.J. Cullen, Post-translational regulation of signaling mucins. Curr. Opin. Struct. Biol. 21 (2011) 590-596.

[8] B.J. Van Klinken, J.W. Van der Wal, A.W. Einerhand, H.A. Buller, and J. Dekker, Sulphation and secretion of the predominant secretory human colonic mucin MUC2 in ulcerative colitis. Gut. 44 (1999) 387-393.

[9] P. Stanley, Golgi glycosylation. Cold Spring Harb. Perspect. Biol. 3 (2011) a005199.

[10] P. Stanley, H. Schachter, N. Taniguchi, Y.J. Kim, L. Borsig, H.L. Han, N.M. Varki, and A. Varki, N-Glycans Distinct selectin ligands on colon carcinoma mucins can mediate pathological interactions among platelets, leukocytes, and endothelium. Am. J. Pathol. 155 (1999) 461-472.

[11] P. Van den Steen, P.M. Rudd, R.A. Dwek, and G. Opdenakker, Concepts and principles of O-linked glycosylation. Crit Rev. Biochem. Mol. Biol. 33 (1998) 151-208.

[12] M.C. Rose and J.A. Voynow, Respiratory tract mucin genes and mucin glycoproteins in health and disease. Physiol Rev. 86 (2006) 245-278.

[13] S. Kaur, S. Kumar, N. Momi, A.R. Sasson, and S.K. Batra, Mucins in pancreatic cancer and its microenvironment. Nat. Rev. Gastroenterol. Hepatol. 10 (2013) 607-620.

[14] V.A. Resto, M.M. Burdick, N.M. Dagia, S.D. McCammon, S.M. Fennewald, and R. Sackstein, L-selectin-mediated lymphocyte-cancer cell interactions under low fluid shear conditions. J. Biol. Chem. 283 (2008) 15816-15824.

[15] F. Schwarz and M. Aebi, Mechanisms and principles of N-linked protein glycosylation. Curr. Opin. Struct. Biol 21 (2011) 576-582.

[16] L.W. Ruddock and M. Molinari, N-glycan processing in ER quality control. J. Cell Sci. 119 (2006) 4373-4380.

[17] S. Parry, F.G. Hanisch, S.H. Leir, M. Sutton-Smith, H.R. Morris, A. Dell, and A. Harris, N-Glycosylation of the MUC1 mucin in epithelial cells and secretions. Glycobiology 16 (2006) 623-634.

[18] R. Cao, T.T. Wang, G. DeMaria, J.K. Sheehan, and M. Kesimer, Mapping the protein domain structures of the respiratory mucins: a mucin proteome coverage study. J. Proteome. Res. 11 (2012) 4013-4023.

[19] N. Asker, M.A. Axelsson, S.O. Olofsson, and G.C. Hansson, Dimerization of the human MUC2 mucin in the endoplasmic reticulum is followed by a N-glycosylation-dependent transfer of the mono- and dimers to the Golgi apparatus. J. Biol. Chem. 273 (1998) 18857-18863.

[20] J.J. Ho, R.S. Jaituni, S.C. Crawley, S.C. Yang, J.R. Gum, and Y.S. Kim, N-glycosylation is required for the surface localization of MUC17 mucin. Int. J. Oncol. 23 (2003) 585-592.

[21] I. Brockhausen, H. Schachter, P. Stanley, and J.D. Marth, O-GalNAc Glycans Complexity in O-linked oligosaccharide biosynthesis engendered by multiple polypeptide N-acetylgalactosaminyltransferases. Glycobiology. 6 (1996) 701-705.

[22] E.P. Bennett, U. Mandel, H. Clausen, T.A. Gerken, T.A. Fritz, and L.A. Tabak, Control of mucin-type O-glycosylation: a classification of the polypeptide GalNAc-transferase gene family. Glycobiology. 22 (2012) 736-756.

[23] T. Ju, V.I. Otto, and R.D. Cummings, The Tn antigen-structural simplicity and biological complexity. Angew. Chem. Int. Ed Engl. 50 (2011) 1770-1791.

[24] A. Yoshida, M. Suzuki, H. Ikenaga, and M. Takeuchi, Discovery of the shortest sequence motif for high level mucin-type O-glycosylation. J. Biol. Chem. 272 (1997) 16884-16888.

[25] J. Raman, T.A. Fritz, T.A. Gerken, O. Jamison, D. Live, M. Liu, and L.A. Tabak, The catalytic and lectin domains of UDP-GalNAc:polypeptide alpha-N-Acetylgalactosaminyltransferase function in concert to direct glycosylation site selection. J. Biol. Chem. 283 (2008) 22942-22951.

[26] R.P. Aryal, T. Ju, and R.D. Cummings, The endoplasmic reticulum chaperone Cosmc directly promotes in vitro folding of T-synthase. J. Biol. Chem. 285 (2010) 2456-2462.

[27] T. Ju, R.P. Aryal, M.R. Kudelka, Y. Wang, and R.D. Cummings, The Cosmc connection to the Tn antigen in cancer. Cancer Biomark. 14 (2014) 63-81.

[28] S.K. Linden, P. Sutton, N.G. Karlsson, V. Korolik, and M.A. McGuckin, Mucins in the mucosal barrier to infection. Mucosal. Immunol. 1 (2008) 183-197.

[29] A.P. Corfield, Mucins: a biologically relevant glycan barrier in mucosal protection. Biochim. Biophys. Acta 1850 (2015) 236-252.

[30] S. Bafna, S. Kaur, and S.K. Batra, Membrane-bound mucins: the mechanistic basis for alterations in the growth and survival of cancer cells. Oncogene. %20;29 (2010) 2893-2904.

[31] D.W. Kufe, MUC1-C oncoprotein as a target in breast cancer: activation of signaling pathways and therapeutic approaches. Oncogene. 32 (2013) 1073-1081.

[32] P. Mukhopadhyay, S. Chakraborty, M.P. Ponnusamy, I. Lakshmanan, M. Jain, and S.K. Batra, Mucins in the pathogenesis of breast cancer: implications in diagnosis, prognosis and therapy. Biochim. Biophys. Acta. 1815 (2011) 224-240.

[33] P. Mukhopadhyay, I. Lakshmanan, M.P. Ponnusamy, S. Chakraborty, M. Jain, P. Pai, L.M. Smith, S.M. Lele, and S.K. Batra, MUC4 overexpression augments cell migration and metastasis through EGFR family proteins in triple negative breast cancer cells. PLoS. One. 8 (2013) e54455.

[34] S. Rachagani, M.A. Macha, M.P. Ponnusamy, D. Haridas, S. Kaur, M. Jain, and S.K. Batra, MUC4 potentiates invasion and metastasis of pancreatic cancer cells through stabilization of fibroblast growth factor receptor 1. Carcinogenesis 33 (2012) 1953-1964.

[35] S. Bafna, S. Kaur, N. Momi, and S.K. Batra, Pancreatic cancer cells resistance to gemcitabine: the role of MUC4 mucin. Br. J. Cancer. 101 (2009) 1155-1161.

[36] M.P. Ponnusamy, P. Seshacharyulu, A. Vaz, P. Dey, and S.K. Batra, MUC4 stabilizes HER2 expression and maintains the cancer stem cell population in ovarian cancer cells. J. Ovarian. Res. 4 (2011) 7-4.

[37] P. Chaturvedi, A.P. Singh, S. Chakraborty, S.C. Chauhan, S. Bafna, J.L. Meza, P.K. Singh, M.A. Hollingsworth, P.P. Mehta, and S.K. Batra, MUC4 mucin interacts with and stabilizes the HER2 oncoprotein in human pancreatic cancer cells. Cancer Res. 68 (2008) 2065-2070.

[38] D. Haridas, M.P. Ponnusamy, S. Chugh, I. Lakshmanan, P. Seshacharyulu, and S.K. Batra, MUC16: molecular analysis and its functional implications in benign and malignant conditions. FASEB J.2014).

[39] C. Theriault, M. Pinard, M. Comamala, M. Migneault, J. Beaudin, I. Matte, M. Boivin, A. Piche, and C. Rancourt, MUC16 (CA125) regulates epithelial ovarian cancer cell growth, tumorigenesis and metastasis. Gynecol. Oncol. 121 (2011) 434-443.

[40] J.A. Gubbels, M. Felder, S. Horibata, J.A. Belisle, A. Kapur, H. Holden, S. Petrie, M. Migneault, C. Rancourt, J.P. Connor, and M.S. Patankar, MUC16 provides

immune protection by inhibiting synapse formation between NK and ovarian tumor cells. Mol. Cancer. %20;9:11. doi: 10.1186/1476-4598-9-11. (2010) 11-19.

[41] D. Haridas, S. Chakraborty, M.P. Ponnusamy, I. Lakshmanan, S. Rachagani, E. Cruz, S. Kumar, S. Das, S.M. Lele, J.M. Anderson, U.A. Wittel, M.A. Hollingsworth, and S.K. Batra, Pathobiological implications of MUC16 expression in pancreatic cancer. PLoS. One. 6 (2011) e26839.

[42] I. Lakshmanan, M.P. Ponnusamy, S. Das, S. Chakraborty, D. Haridas, P. Mukhopadhyay, S.M. Lele, and S.K. Batra, MUC16 induced rapid G2/M transition via interactions with JAK2 for increased proliferation and anti-apoptosis in breast cancer cells. Oncogene 31 (2012) 805-817.

[43] S.H. Chen, W.C. Hung, P. Wang, C. Paul, and K. Konstantopoulos, Mesothelin binding to CA125/MUC16 promotes pancreatic cancer cell motility and invasion via MMP-7 activation. Sci. Rep. 3 (2013) 1870.

[44] D.M. Maher, B.K. Gupta, S. Nagata, M. Jaggi, and S.C. Chauhan, Mucin 13: structure, function, and potential roles in cancer pathogenesis. Mol. Cancer Res. 9 (2011) 531-537.

[45] H. Hoshi, T. Sawada, M. Uchida, H. Saito, H. Iijima, M. Toda-Agetsuma, T. Wada, S. Yamazoe, H. Tanaka, K. Kimura, A. Kakehashi, M. Wei, K. Hirakawa, and H. Wanibuchi, Tumor-associated MUC5AC stimulates in vivo tumorigenicity of human pancreatic cancer. Int. J. Oncol. 38 (2011) 619-627.

[46] M.D. Walsh, M. Clendenning, E. Williamson, S.A. Pearson, R.J. Walters, B. Nagler, D. Packenas, A.K. Win, J.L. Hopper, M.A. Jenkins, A.M. Haydon, C. Rosty, D.R. English, G.G. Giles, M.A. McGuckin, J.P. Young, and D.D. Buchanan, Expression of MUC2, MUC5AC, MUC5B, and MUC6 mucins in colorectal cancers and their association with the CpG island methylator phenotype. Mod. Pathol. 26 (2013) 1642-1656.

[47] H. Kawashima, Roles of the gel-forming MUC2 mucin and its O-glycosylation in the protection against colitis and colorectal cancer. Biol. Pharm. Bull. 35 (2012) 1637-1641.

[48] S. Pan, R. Chen, Y. Tamura, D.A. Crispin, L.A. Lai, D.H. May, M.W. McIntosh, D.R. Goodlett, and T.A. Brentnall, Quantitative glycoproteomics analysis reveals changes in N-glycosylation level associated with pancreatic ductal adenocarcinoma. J. Proteome. Res. 13 (2014) 1293-1306.

[49] K.O. Lloyd, J. Burchell, V. Kudryashov, B.W. Yin, and J. Taylor-Papadimitriou, Comparison of O-linked carbohydrate chains in MUC-1 mucin from normal breast epithelial cell lines and breast carcinoma cell lines. Demonstration of simpler and fewer glycan chains in tumor cells. J. Biol. Chem. 271 (1996) 33325-33334.

[50] E. Saeland, A.I. Belo, S. Mongera, D. van, I, G.A. Meijer, and K.Y. van, Differential glycosylation of MUC1 and CEACAM5 between normal mucosa and tumour tissue of colon cancer patients. Int. J. Cancer. 131 (2012) 117-128.

[51] I. Brockhausen, Pathways of O-glycan biosynthesis in cancer cells. Biochim. Biophys. Acta. 1473 (1999) 67-95.

[52] S. Hakomori, Glycosylation defining cancer malignancy: new wine in an old bottle. Proc. Natl. Acad. Sci. U. S. A. 99 (2002) 10231-10233.

[53] I. Hauselmann and L. Borsig, Altered Tumor-Cell Glycosylation Promotes Metastasis. Front Oncol. 4:28. eCollection;%2014. (2014) 28.

[54] J. Taylor-Papadimitriou, J. Burchell, D.W. Miles, and M. Dalziel, MUC1 and cancer. Biochim. Biophys. Acta. 1455 (1999) 301-313.

[55] J.M. Burchell, A. Mungul, and J. Taylor-Papadimitriou, O-linked glycosylation in the mammary gland: changes that occur during malignancy. J. Mammary. Gland. Biol. Neoplasia. 6 (2001) 355-364.

[56] B.J. Campbell, I.A. Finnie, E.F. Hounsell, and J.M. Rhodes, Direct demonstration of increased expression of Thomsen-Friedenreich (TF) antigen in colonic adenocarcinoma and ulcerative colitis mucin and its concealment in normal mucin. J. Clin. Invest. 95 (1995) 571-576.

[57] A. Danguy, I. Camby, and R. Kiss, Galectins and cancer. Biochim. Biophys. Acta 1572 (2002) 285-293.

[58] F. van den Brule, S. Califice, and V. Castronovo, Expression of galectins in cancer: a critical review. Glycoconj. J. 19 (2004) 537-542.

[59] G.A. Rabinovich, N. Rubinstein, and M.A. Toscano, Role of galectins in inflammatory and immunomodulatory processes. Biochim. Biophys. Acta 1572 (2002) 274-284.

[60] S. Senapati, P. Chaturvedi, W.G. Chaney, S. Chakraborty, V.S. Gnanapragassam, A.R. Sasson, and S.K. Batra, Novel INTeraction of MUC4 and galectin: potential pathobiological implications for metastasis in lethal pancreatic cancer. Clin. Cancer Res. 17 (2011) 267-274.

[61] P. Argueso, A. Guzman-Aranguez, F. Mantelli, Z. Cao, J. Ricciuto, and N. Panjwani, Association of cell surface mucins with galectin-3 contributes to the ocular surface epithelial barrier. J. Biol. Chem. 284 (2009) 23037-23045.

[62] Q. Zhao, M. Barclay, J. Hilkens, X. Guo, H. Barrow, J.M. Rhodes, and L.G. Yu, Interaction between circulating galectin-3 and cancer-associated MUC1 enhances tumour cell homotypic aggregation and prevents anoikis. Mol. Cancer. 9:154. doi: 10.1186/1476-4598-9-154. (2010) 154-159.

[63] L.G. Yu, N. Andrews, Q. Zhao, D. McKean, J.F. Williams, L.J. Connor, O.V. Gerasimenko, J. Hilkens, J. Hirabayashi, K. Kasai, and J.M. Rhodes, Galectin-3 interaction with Thomsen-Friedenreich disaccharide on cancer-associated MUC1 causes increased cancer cell endothelial adhesion. J. Biol. Chem. 282 (2007) 773-781.

[64] G.S. Kansas, Selectins and their ligands: current concepts and controversies. Blood 88 (1996) 3259-3287.

[65] J.C. Byrd and R.S. Bresalier, Mucins and mucin binding proteins in colorectal cancer. Cancer Metastasis Rev. 23 (2004) 77-99.

[66] Y.J. Kim, L. Borsig, H.L. Han, N.M. Varki, and A. Varki, Distinct selectin ligands on colon carcinoma mucins can mediate pathological interactions among platelets, leukocytes, and endothelium. Am. J. Pathol. 155 (1999) 461-472.

[67] M. Wahrenbrock, L. Borsig, D. Le, N. Varki, and A. Varki, Selectin-mucin interactions as a probable molecular explanation for the association of Trousseau syndrome with mucinous adenocarcinomas. J. Clin. Invest 112 (2003) 853-862.

[68] S. Tanida, K. Akita, A. Ishida, Y. Mori, M. Toda, M. Inoue, M. Ohta, M. Yashiro, T. Sawada, K. Hirakawa, and H. Nakada, Binding of the sialic acid-binding lectin, Siglec-9, to the membrane mucin, MUC1, induces recruitment of beta-catenin and subsequent cell growth. J. Biol. Chem. 288 (2013) 31842-31852.

[69] J.A. Belisle, S. Horibata, G.A. Jennifer, S. Petrie, A. Kapur, S. Andre, H.J. Gabius, C. Rancourt, J. Connor, J.C. Paulson, and M.S. Patankar, Identification of Siglec-9 as the receptor for MUC16 on human NK cells, B cells, and monocytes. Mol. Cancer. 9:118. doi: 10.1186/1476-4598-9-118. (2010) 118-119.

[70] R.T. Costello, J.A. Gastaut, and D. Olive, Tumor escape from immune surveillance. Arch. Immunol. Ther. Exp. (Warsz.) 47 (1999) 83-88.

[71] C.B. Madsen, K. Lavrsen, C. Steentoft, M.B. Vester-Christensen, H. Clausen, H.H. Wandall, and A.E. Pedersen, Glycan elongation beyond the mucin associated Tn antigen protects tumor cells from immune-mediated killing. PLoS. One. 8 (2013) e72413.

[72] L. Borsig, R. Wong, J. Feramisco, D.R. Nadeau, N.M. Varki, and A. Varki, Heparin and cancer revisited: mechanistic connections involving platelets, P-selectin, carcinoma mucins, and tumor metastasis. Proc. Natl. Acad. Sci. U. S. A. 98 (2001) 3352-3357.

[73] J.A. Gubbels, J. Belisle, M. Onda, C. Rancourt, M. Migneault, M. Ho, T.K. Bera, J. Connor, B.K. Sathyanarayana, B. Lee, I. Pastan, and M.S. Patankar, Mesothelin-MUC16 binding is a high affinity, N-glycan dependent interaction that facilitates peritoneal metastasis of ovarian tumors. Mol. Cancer. 5 (2006) 50.

[74] Q. Zhao, X. Guo, G.B. Nash, P.C. Stone, J. Hilkens, J.M. Rhodes, and L.G. Yu, Circulating galectin-3 promotes metastasis by modifying MUC1 localization on cancer cell surface. Cancer Res. 69 (2009) 6799-6806.

[75] S. Havrylov, M.J. Redowicz, and V.L. Buchman, Emerging roles of Ruk/CIN85 in vesicle-mediated transport, adhesion, migration and malignancy. Traffic. 11 (2010) 721-731.

[76] S. Cascio, A.M. Farkas, R.P. Hughey, and O.J. Finn, Altered glycosylation of MUC1 influences its association with CIN85: the role of this novel complex in cancer cell invasion and migration. Oncotarget. 4 (2013) 1686-1697.

[77] C.L. Kinlough, P.A. Poland, S.J. Gendler, P.E. Mattila, D. Mo, O.A. Weisz, and R.P. Hughey, Core-glycosylated mucin-like repeats from MUC1 are an apical targeting signal. J. Biol. Chem. 286 (2011) 39072-39081.

[78] B.A. Potter, R.P. Hughey, and O.A. Weisz, Role of N- and O-glycans in polarized biosynthetic sorting. Am. J. Physiol Cell Physiol. 290 (2006) C1-C10.

[79] A. Paszkiewicz-Gadek, H. Porowska, D. Lemancewicz, S. Wolczynski, and A. Gindzienski, The influence of N- and O-glycosylation inhibitors on the glycosylation profile of cellular membrane proteins and adhesive properties of carcinoma cell lines. Int. J. Mol. Med. 17 (2006) 669-674.

[80] K. Engelmann, C.L. Kinlough, S. Muller, H. Razawi, S.E. Baldus, R.P. Hughey, and F.G. Hanisch, Transmembrane and secreted MUC1 probes show trafficking-dependent changes in O-glycan core profiles. Glycobiology 15 (2005) 1111-1124.

[81] K. Engelmann, H. Shen, and O.J. Finn, MCF7 side population cells with characteristics of cancer stem/progenitor cells express the tumor antigen MUC1. Cancer Res. 68 (2008) 2419-2426.

[82] D.J. Gill, J. Chia, J. Senewiratne, and F. Bard, Regulation of O-glycosylation through Golgi-to-ER relocation of initiation enzymes. J. Cell Biol. 189 (2010) 843-858.

[83] Y.M. Wu, D.D. Nowack, G.S. Omenn, and B.B. Haab, Mucin glycosylation is altered by pro-inflammatory signaling in pancreatic-cancer cells. J. Proteome. Res. 8 (2009) 1876-1886.

[84] J. Rini, J. Esko, and A. Varki, Glycosyltransferases and Glycan-processing Enzymes.2009).

[85] K. Ohtsubo and J.D. Marth, Glycosylation in cellular mechanisms of health and disease. Cell 126 (2006) 855-867.

[86] R. Kannagi, K. Sakuma, K. Miyazaki, K.T. Lim, A. Yusa, J. Yin, and M. Izawa, Altered expression of glycan genes in cancers induced by epigenetic silencing and tumor hypoxia: clues in the ongoing search for new tumor markers. Cancer Sci. 101 (2010) 586-593.

[87] K.A. Maupin, A. Sinha, E. Eugster, J. Miller, J. Ross, V. Paulino, V.G. Keshamouni, N. Tran, M. Berens, C. Webb, and B.B. Haab, Glycogene expression alterations associated with pancreatic cancer epithelial-mesenchymal transition in complementary model systems. PLoS. One. 5 (2010) e13002.

[88] H. Kalthoff, C. Kreiker, W.H. Schmiegel, H. Greten, and H.G. Thiele, Characterization of CA 19-9 bearing mucins as physiological exocrine pancreatic secretion products. Cancer Res. 46 (1986) 3605-3607.

[89] K. Miyazaki, K. Ohmori, M. Izawa, T. Koike, K. Kumamoto, K. Furukawa, T. Ando, M. Kiso, T. Yamaji, Y. Hashimoto, A. Suzuki, A. Yoshida, M. Takeuchi, and R. Kannagi, Loss of disialyl Lewis(a), the ligand for lymphocyte inhibitory receptor sialic acid-binding immunoglobulin-like lectin-7 (Siglec-7) associated with increased sialyl Lewis(a) expression on human colon cancers. Cancer Res. 64 (2004) 4498-4505.

[90] A. Yusa, K. Miyazaki, N. Kimura, M. Izawa, and R. Kannagi, Epigenetic silencing of the sulfate transporter gene DTDST induces sialyl Lewisx expression and accelerates proliferation of colon cancer cells. Cancer Res. 70 (2010) 4064-4073.

[91] T. Iwai, T. Kudo, R. Kawamoto, T. Kubota, A. Togayachi, T. Hiruma, T. Okada, T. Kawamoto, K. Morozumi, and H. Narimatsu, Core 3 synthase is down-regulated in colon carcinoma and profoundly suppresses the metastatic potential of carcinoma cells. Proc. Natl. Acad. Sci. U. S. A. 102 (2005) 4572-4577.

[92] Y.I. Kawamura, R. Kawashima, R. Fukunaga, K. Hirai, N. Toyama-Sorimachi, M. Tokuhara, T. Shimizu, and T. Dohi, Introduction of Sd(a) carbohydrate antigen in gastrointestinal cancer cells eliminates selectin ligands and inhibits metastasis. Cancer Res. 65 (2005) 6220-6227.

[93] M. Keita, Z.Q. Wang, J.F. Pelletier, M. Bachvarova, M. Plante, J. Gregoire, M.C. Renaud, A.M. Mes-Masson, E.R. Paquet, and D. Bachvarov, Global methylation profiling in serous ovarian cancer is indicative for distinct aberrant DNA methylation signatures associated with tumor aggressiveness and disease progression. Gynecol. Oncol. 128 (2013) 356-363.

[94] Z.Q. Wang, M. Bachvarova, C. Morin, M. Plante, J. Gregoire, M.C. Renaud, A. Sebastianelli, and D. Bachvarov, Role of the polypeptide N-acetylgalactosaminyltransferase 3 in ovarian cancer progression: possible implications in abnormal mucin O-glycosylation. Oncotarget. 5 (2014) 544-560.

[95] A. Gaziel-Sovran, M.F. Segura, M.R. Di, M.K. Collins, D. Hanniford, M.E. Vega-Saenz de, J.F. Rakus, J.F. Dankert, S. Shang, R.S. Kerbel, N. Bhardwaj, Y. Shao, F. Darvishian, J. Zavadil, A. Erlebacher, L.K. Mahal, I. Osman, and E. Hernando, miR-30b/30d regulation of GalNAc transferases enhances invasion and immunosuppression during metastasis. Cancer Cell. 20 (2011) 104-118.

[96] L. Tu and D.K. Banfield, Localization of Golgi-resident glycosyltransferases. Cell Mol. Life Sci. 67 (2010) 29-41.

[97] S. Munro, An investigation of the role of transmembrane domains in Golgi protein retention. EMBO J. 14 (1995) 4695-4704.

[98] I.D. Pokrovskaya, R. Willett, R.D. Smith, W. Morelle, T. Kudlyk, and V.V. Lupashin, Conserved oligomeric Golgi complex specifically regulates the maintenance of Golgi glycosylation machinery. Glycobiology. 21 (2011) 1554-1569.

[99] C.L. Jackson, Mechanisms of transport through the Golgi complex. J. Cell Sci. 122 (2009) 443-452.

[100] G.H. Patterson, K. Hirschberg, R.S. Polishchuk, D. Gerlich, R.D. Phair, and J. Lippincott-Schwartz, Transport through the Golgi apparatus by rapid partitioning within a two-phase membrane system. Cell. 133 (2008) 1055-1067.

[101] C.A. Quintero, J. Valdez-Taubas, M.L. Ferrari, S.D. Haedo, and H.J. Maccioni, Calsenilin and CALP interact with the cytoplasmic tail of UDP-Gal:GA2/GM2/GD2 beta-1,3-galactosyltransferase. Biochem. J. 412 (2008) 19-26.

[102] T. Koike, N. Kimura, K. Miyazaki, T. Yabuta, K. Kumamoto, S. Takenoshita, J. Chen, M. Kobayashi, M. Hosokawa, A. Taniguchi, T. Kojima, N. Ishida, M. Kawakita, H. Yamamoto, H. Takematsu, A. Suzuki, Y. Kozutsumi, and R. Kannagi, Hypoxia induces adhesion molecules on cancer cells: A missing link between Warburg effect and induction of selectin-ligand carbohydrates. Proc. Natl. Acad. Sci. U. S. A 101 (2004) 8132-8137.

[103] J. Yin, A. Hashimoto, M. Izawa, K. Miyazaki, G.Y. Chen, H. Takematsu, Y. Kozutsumi, A. Suzuki, K. Furuhata, F.L. Cheng, C.H. Lin, C. Sato, K. Kitajima, and R. Kannagi, Hypoxic culture induces expression of sialin, a sialic acid transporter, and cancer-associated gangliosides containing non-human sialic acid on human cancer cells. Cancer Res. 66 (2006) 2937-2945.

[104] H. Ota, J. Nakayama, M. Momose, M. Hayama, T. Akamatsu, T. Katsuyama, D.Y. Graham, and R.M. Genta, Helicobacter pylori infection produces reversible glycosylation changes to gastric mucins. Virchows Arch. 433 (1998) 419-426.

[105] B.J. Campbell, L.G. Yu, and J.M. Rhodes, Altered glycosylation in inflammatory bowel disease: a possible role in cancer development. Glycoconj. J. 18 (2001) 851-858.

[106] D.H. Dube and C.R. Bertozzi, Glycans in cancer and inflammation--potential for therapeutics and diagnostics. Nat. Rev. Drug Discov. 4 (2005) 477-488.

[107] J. Renkonen, O. Tynninen, P. Hayry, T. Paavonen, and R. Renkonen, Glycosylation might provide endothelial zip codes for organ-specific leukocyte traffic into inflammatory sites. Am. J. Pathol. 161 (2002) 543-550.

[108] J.B. Lowe, Glycan-dependent leukocyte adhesion and recruitment in inflammation. Curr. Opin. Cell Biol. 15 (2003) 531-538.

[109] J.M. Larsson, H. Karlsson, J.G. Crespo, M.E. Johansson, L. Eklund, H. Sjovall, and G.C. Hansson, Altered O-glycosylation profile of MUC2 mucin occurs in active ulcerative colitis and is associated with increased inflammation. Inflamm. Bowel. Dis. 17 (2011) 2299-2307.

[110] L.S. Kreisman and B.A. Cobb, Infection, inflammation and host carbohydrates: a Glyco-Evasion Hypothesis. Glycobiology. 22 (2012) 1019-1030.

[111] J. Barasch, B. Kiss, A. Prince, L. Saiman, D. Gruenert, and Q. al-Awqati, Defective acidification of intracellular organelles in cystic fibrosis. Nature 352 (1991) 70-73.

[112] S. Kellokumpu, R. Sormunen, and I. Kellokumpu, Abnormal glycosylation and altered Golgi structure in colorectal cancer: dependence on intra-Golgi pH. FEBS Lett. 516 (2002) 217-224.

[113] A. Rivinoja, N. Kokkonen, I. Kellokumpu, and S. Kellokumpu, Elevated Golgi pH in breast and colorectal cancer cells correlates with the expression of oncofetal carbohydrate T-antigen. J. Cell Physiol. 208 (2006) 167-174.

[114] F.M. Tuccillo, L.A. de, C. Palmieri, G. Fiume, P. Bonelli, A. Borrelli, P. Tassone, I. Scala, F.M. Buonaguro, I. Quinto, and G. Scala, Aberrant glycosylation as biomarker for cancer: focus on CD43. Biomed. Res. Int. 2014 (2014) 742831.

[115] M. Felder, A. Kapur, J. Gonzalez-Bosquet, S. Horibata, J. Heintz, R. Albrecht, L. Fass, J. Kaur, K. Hu, H. Shojaei, R.J. Whelan, and M.S. Patankar, MUC16 (CA125): tumor biomarker to cancer therapy, a work in progress. Mol. Cancer 13 (2014) 129.

[116] G. Soletormos, D. Nielsen, V. Schioler, H. Mouridsen, and P. Dombernowsky, Monitoring different stages of breast cancer using tumour markers CA 15-3, CEA and TPA. Eur. J. Cancer 40 (2004) 481-486.

[117] E.V. Chandrasekaran, J. Xue, J. Xia, R.D. Locke, S.A. Patil, S. Neelamegham, and K.L. Matta, Characterization of cancer associated mucin type O-glycans using the exchange sialylation properties of mammalian sialyltransferase ST3Gal-II. J. Proteome. Res. 11 (2012) 2609-2618.

[118] F. Safi, W. Schlosser, G. Kolb, and H.G. Beger, Diagnostic value of CA 19-9 in patients with pancreatic cancer and nonspecific gastrointestinal symptoms. J. Gastrointest. Surg. 1 (1997) 106-112.

[119] M. Ychou, J. Duffour, A. Kramar, S. Gourgou, and J. Grenier, Clinical significance and prognostic value of CA72-4 compared with CEA and CA19-9 in patients with gastric cancer. Dis. Markers 16 (2000) 105-110.

[120] M.G. Wahrenbrock and A. Varki, Multiple hepatic receptors cooperate to eliminate secretory mucins aberrantly entering the bloodstream: are circulating cancer mucins the "tip of the iceberg"? Cancer Res. 66 (2006) 2433-2441.

[121] H.H. Wandall, O. Blixt, M.A. Tarp, J.W. Pedersen, E.P. Bennett, U. Mandel, G. Ragupathi, P.O. Livingston, M.A. Hollingsworth, J. Taylor-Papadimitriou, J. Burchell, and H. Clausen, Cancer biomarkers defined by autoantibody signatures to aberrant O-glycopeptide epitopes. Cancer Res. 70 (2010) 1306-1313.

[122] J.W. Pedersen, O. Blixt, E.P. Bennett, M.A. Tarp, I. Dar, U. Mandel, S.S. Poulsen, A.E. Pedersen, S. Rasmussen, P. Jess, H. Clausen, and H.H. Wandall, Seromic profiling of colorectal cancer patients with novel glycopeptide microarray. Int. J. Cancer. 128 (2011) 1860-1871.

[123] R. Pinto, A.S. Carvalho, T. Conze, A. Magalhaes, G. Picco, J.M. Burchell, J. Taylor-Papadimitriou, C.A. Reis, R. Almeida, U. Mandel, H. Clausen, O. Soderberg, and L. David, Identification of new cancer biomarkers based on

aberrant mucin glycoforms by in situ proximity ligation. J. Cell Mol. Med. 16 (2012) 1474-1484.

[124] Z. Guo and Q. Wang, Recent development in carbohydrate-based cancer vaccines. Curr. Opin. Chem. Biol. 13 (2009) 608-617.

[125] N.K. Ibrahim and J.L. Murray, Clinical development of the STn-KLH vaccine (Theratope). Clin. Breast Cancer 3 Suppl 4 (2003) S139-S143.

[126] D. Miles and K. Papazisis, Rationale for the clinical development of STn-KLH (Theratope) and anti-MUC-1 vaccines in breast cancer. Clin. Breast Cancer 3 Suppl 4 (2003) S134-S138.

[127] A.L. Parry, N.A. Clemson, J. Ellis, S.S. Bernhard, B.G. Davis, and N.R. Cameron, 'Multicopy multivalent' glycopolymer-stabilized gold nanoparticles as potential synthetic cancer vaccines. J. Am. Chem. Soc. 135 (2013) 9362-9365.

[128] A. Kaiser, N. Gaidzik, U. Westerlind, D. Kowalczyk, A. Hobel, E. Schmitt, and H. Kunz, A synthetic vaccine consisting of a tumor-associated sialyl-T(N)-MUC1 tandem-repeat glycopeptide and tetanus toxoid: induction of a strong and highly selective immune response. Angew. Chem. Int. Ed Engl. 48 (2009) 7551-7555.

[129] U. Westerlind, A. Hobel, N. Gaidzik, E. Schmitt, and H. Kunz, Synthetic vaccines consisting of tumor-associated MUC1 glycopeptide antigens and a T-cell epitope for the induction of a highly specific humoral immune response. Angew. Chem. Int. Ed Engl. 47 (2008) 7551-7556.

[130] H. Cai, Z.H. Huang, L. Shi, Y.F. Zhao, H. Kunz, and Y.M. Li, Towards a fully synthetic MUC1-based anticancer vaccine: efficient conjugation of glycopeptides with mono-, di-, and tetravalent lipopeptides using click chemistry. Chemistry. 17 (2011) 6396-6406.

[131] A.B. Abdel-Aal, V. Lakshminarayanan, P. Thompson, N. Supekar, J.M. Bradley, M.A. Wolfert, P.A. Cohen, S.J. Gendler, and G.J. Boons, Immune and anticancer responses elicited by fully synthetic aberrantly glycosylated MUC1 tripartite vaccines modified by a TLR2 or TLR9 agonist. Chembiochem. 15 (2014) 1508-1513.

[132] S. Julien, P.A. Videira, and P. Delannoy, Sialyl-tn in cancer: (how) did we miss the target? Biomolecules. 2 (2012) 435-466.

[133] W.W. Chang, C.Y. Yu, T.W. Lin, P.H. Wang, and Y.C. Tsai, Soyasaponin I decreases the expression of alpha2,3-linked sialic acid on the cell surface and suppresses the metastatic potential of B16F10 melanoma cells. Biochem. Biophys. Res. Commun. 341 (2006) 614-619.

[134] B. Ernst and J.L. Magnani, From carbohydrate leads to glycomimetic drugs. Nat. Rev. Drug Discov. 8 (2009) 661-677.

[135] D.D. Marathe, A. Buffone, Jr., E.V. Chandrasekaran, J. Xue, R.D. Locke, M. Nasirikenari, J.T. Lau, K.L. Matta, and S. Neelamegham, Fluorinated per-

acetylated GalNAc metabolically alters glycan structures on leukocyte PSGL-1 and reduces cell binding to selectins. Blood. 115 (2010) 1303-1312.

[136] A.L. Sorensen, C.A. Reis, M.A. Tarp, U. Mandel, K. Ramachandran, V. Sankaranarayanan, T. Schwientek, R. Graham, J. Taylor-Papadimitriou, M.A. Hollingsworth, J. Burchell, and H. Clausen, Chemoenzymatically synthesized multimeric Tn/STn MUC1 glycopeptides elicit cancer-specific anti-MUC1 antibody responses and override tolerance. Glycobiology. 16 (2006) 96-107.

CHAPTER 1B

Dissertation General Hypothesis and Objectives

1. Background and rationale

Several mechanisms that contribute to increased cancer aggressiveness have been identified in recent years. These include genetic and epigenetic modifications, varied translation, altered metabolism and post-translational modifications [1-3]. Among several post-translational modifications underlying cancer progression and metastasis, glycosylation has been recognized to play an important role [4]. Glycosylation involves the addition of carbohydrate residues to the protein substrate. O- and N-glycosylation are the two types of glycosylation, which is based on the amino acid to which carbohydrate residues will be linked. In the case of O-glycosylation, carbohydrates are linked to the hydroxyl group of serine/threonine. N-glycosylation involves attachment of carbohydrates to the amide nitrogen of asparagine[5]. This dissertation is focused on O-glycosylation, specifically mucin-type O-glycosylation.

Mucin-type O-glycosylation occurs in the Golgi and involves the addition of N-acetylgalactosamine (GalNAc) to serine/threonine residues in the protein backbone by the family of enzymes known as UDP-GalNAc: Polypeptide N-acetylgalactosaminyltransferases (GALNTs) [6]. The resultant carbohydrate structure is known as Tn carbohydrate antigen, which can be extended by the addition of galactose to form T carbohydrate (core-1) antigen. This reaction is catalyzed by the activity of Glycoprotein-N-acetylgalactosamine 3-beta-Galactosyltransferase (C1GALT1) [7]. This thesis is primarily focused on deciphering the mechanistic role of the first enzyme (GALNT3) and the second enzyme (C1GALT1) of mucin-type O-glycosylation in PDAC progression.

The first step in the mucin-type O-glycosylation is catalyzed by GALNT family, which comprises 20 enzymes and have distinct substrate specificities despite their functional homology [8]. Differential expression of several GALNT genes has been

observed in several malignancies [9-11]. Prior studies in pancreatic cancer have reported a loss of one of the GALNT members, GALNT3, in poorly differentiated pancreatic cancer [12]. However, there is limiting information on how the loss of GALNT3 impacts PDAC aggressiveness.

Further, studies have also reported dysregulated activity of the second enzyme (C1GALT1) of the biosynthetic pathway in malignant conditions [4]. Upregulated expression of C1GALT1 has been reported in hepatocellular carcinoma and breast cancer and is associated with increased tumor growth [13, 14]. On the contrary, loss of C1galt1 activity in the colon has been shown to induce colitis, which is a major risk factor for colon cancer [15]. In the case of pancreatic cancer, studies conducted by two independent groups have demonstrated that loss of the molecular chaperone, Cosmc (core 1 β3-Gal-T-specific molecular chaperone), which aids in proper folding and function of C1GALT1, potentiates oncogenesis [16, 17]. However, the precise involvement of C1GALT1 in PDAC has not been studied.

2. Hypothesis

Based on the previous studies suggesting loss of expression of O-glycosyltransferases, GALNT3, and C1GALT1 in PDAC, we hypothesized that loss of GALNT3 and C1GALT1 is associated with aberrant O-glycosylation and enhanced disease aggressiveness.

3. Objectives

Aim 1: To investigate the mechanistic role of GALNT3 in PDAC.

Aim 2: To determine the functional implications of knockout of C1GALT1 in PDAC.

Aim 3: To understand the role of C1GALT1 in PDAC progression and metastasis by use of KPCC *(Kras^{G12D}; Trp53$^{R172H/+}$; C1galt1$^{loxP/loxP}$; Pdx1-Cre)* model.

References

[1] K. Gronbaek, C. Hother, P.A. Jones, Epigenetic changes in cancer, APMIS : acta pathologica, microbiologica, et immunologica Scandinavica, 115 (2007) 1039-1059.

[2] K.E. Krueger, S. Srivastava, Posttranslational protein modifications: current implications for cancer detection, prevention, and therapeutics, Mol Cell Proteomics, 5 (2006) 1799-1810.

[3] P.S. Ward, C.B. Thompson, Metabolic reprogramming: a cancer hallmark even warburg did not anticipate, Cancer Cell, 21 (2012) 297-308.

[4] S.S. Pinho, C.A. Reis, Glycosylation in cancer: mechanisms and clinical implications, Nature reviews. Cancer, 15 (2015) 540-555.

[5] P. Van den Steen, P.M. Rudd, R.A. Dwek, G. Opdenakker, Concepts and principles of O-linked glycosylation, Crit Rev Biochem Mol Biol, 33 (1998) 151-208.

[6] D.T. Tran, K.G. Ten Hagen, Mucin-type O-glycosylation during development, J Biol Chem, 288 (2013) 6921-6929.

[7] T. Ju, K. Brewer, A. D'Souza, R.D. Cummings, W.M. Canfield, Cloning and expression of human core 1 beta1,3-galactosyltransferase, J Biol Chem, 277 (2002) 178-186.

[8] E.P. Bennett, U. Mandel, H. Clausen, T.A. Gerken, T.A. Fritz, L.A. Tabak, Control of mucin-type O-glycosylation: a classification of the polypeptide GalNAc-transferase gene family, Glycobiology, 22 (2012) 736-756.

[9] H. Dosaka-Akita, I. Kinoshita, K. Yamazaki, H. Izumi, T. Itoh, H. Katoh, M. Nishimura, K. Matsuo, Y. Yamada, K. Kohno, N-acetylgalactosaminyl transferase-3 is a potential new marker for non-small cell lung cancers, British journal of cancer, 87 (2002) 751-755.

[10] C. Gu, T. Oyama, T. Osaki, J. Li, M. Takenoyama, H. Izumi, K. Sugio, K. Kohno, K. Yasumoto, Low expression of polypeptide GalNAc N-acetylgalactosaminyl transferase-3 in lung adenocarcinoma: impact on poor prognosis and early recurrence, British journal of cancer, 90 (2004) 436-442.

[11] K. Shibao, H. Izumi, Y. Nakayama, R. Ohta, N. Nagata, M. Nomoto, K. Matsuo, Y. Yamada, K. Kitazato, H. Itoh, K. Kohno, Expression of UDP-N-acetyl-alpha-D-galactosamine-polypeptide galNAc N-acetylgalactosaminyl transferase-3 in relation to differentiation and prognosis in patients with colorectal carcinoma, Cancer, 94 (2002) 1939-1946.

[12] S. Yamamoto, S. Nakamori, M. Tsujie, Y. Takahashi, H. Nagano, K. Dono, K. Umeshita, M. Sakon, Y. Tomita, Y. Hoshida, K. Aozasa, K. Kohno, M. Monden, Expression of uridine diphosphate N-acetyl-alpha-D-galactosamine: polypeptide N-acetylgalactosaminyl transferase 3 in adenocarcinoma of the pancreas, Pathobiology, 71 (2004) 12-18.

[13] C.H. Chou, M.J. Huang, C.H. Chen, M.K. Shyu, J. Huang, J.S. Hung, C.S. Huang, M.C. Huang, Up-regulation of C1GALT1 promotes breast cancer cell growth through MUC1-C signaling pathway, Oncotarget, 6 (2015) 6123-6135.

[14] C.H. Liu, R.H. Hu, M.J. Huang, I.R. Lai, C.H. Chen, H.S. Lai, Y.M. Wu, M.C. Huang, C1GALT1 promotes invasive phenotypes of hepatocellular carcinoma cells by modulating integrin beta1 glycosylation and activity, PLoS One, 9 (2014) e94995.

[15] J. Fu, B. Wei, T. Wen, M.E. Johansson, X. Liu, E. Bradford, K.A. Thomsson, S. McGee, L. Mansour, M. Tong, J.M. McDaniel, T.J. Sferra, J.R. Turner, H. Chen, G.C. Hansson, J. Braun, L. Xia, Loss of intestinal core 1-derived O-glycans causes spontaneous colitis in mice, J Clin Invest, 121 (2011) 1657-1666.

[16] B.T. Hofmann, L. Schluter, P. Lange, B. Mercanoglu, F. Ewald, A. Folster, A.S. Picksak, S. Harder, A.T. El Gammal, K. Grupp, C. Gungor, A. Drenckhan, H. Schluter, C. Wagener, J.R. Izbicki, M. Jucker, M. Bockhorn, G. Wolters-Eisfeld, COSMC knockdown mediated aberrant O-glycosylation promotes oncogenic properties in pancreatic cancer, Molecular cancer, 14 (2015) 109.

[17] P. Radhakrishnan, S. Dabelsteen, F.B. Madsen, C. Francavilla, K.L. Kopp, C. Steentoft, S.Y. Vakhrushev, J.V. Olsen, L. Hansen, E.P. Bennett, A. Woetmann, G. Yin, L. Chen, H. Song, M. Bak, R.A. Hlady, S.L. Peters, R. Opavsky, C. Thode, K. Qvortrup, K.T. Schjoldager, H. Clausen, M.A. Hollingsworth, H.H. Wandall, Immature truncated O-glycophenotype of cancer directly induces oncogenic features, Proc Natl Acad Sci U S A, 111 (2014) E4066-4075.

CHAPTER 2

Materials and Methods

1. Tissue Samples from PDAC Patients

After approval of the Institutional Review Board, formalin-fixed paraffin-embedded tissue specimens from pancreatic cancer patients who underwent Whipple surgery (n=30) were retrieved. Additionally, we also obtained tissue arrays (US Biomax -PA 1002a A009 and BIC14011) that were representative of normal pancreatic tissues, chronic pancreatitis, PanIN lesions and PDAC (*i.e.,* well-differentiated, moderately differentiated, and poorly differentiated cancer).

2. Cell lines and cell culture

Human microvascular endothelial cells (HMEC-1) were a kind gift from Dr. Rakesh Singh (University of Nebraska Medical Center) and were maintained in 5% RPMI supplemented with L-glutamine. Human pancreatic ductal adenocarcinoma (PDAC) cell lines CD18/HPAF, BxPC3, Capan-1, SW-1990 and T3M4 were obtained from the American Type Culture Collection (ATCC) and grown in recommended media supplemented with antibiotics (10% DMEM for CD18/HPAF, Capan-1, and T3M4 cells, and 10% RPMI for BxPC3 cells). These PDAC cells were maintained in a humidified, 5% CO_2 atmosphere at 37 °C. hTERT-Human Pancreatic Nestin Expressing cells (HPNE) and oncogenic transformed hTERT -HPNE-E6/E7/St/KRAS cells were a kind gift from Dr. Michel M. Ouellette [1]. All of these cell lines were tested mycoplasma-free before conducting the experiments.

3. Stable GALNT3-knockdown PDAC cells

Stable transfection of GALNT3 was performed by inserting a specific shRNA sequence (*5'-GGTCTGATCACTGCTCGGT-3'*) in the following four PDAC cell types: CD18/HPAF, BxPC3, Capan-1, and T3M4 cells. The Phoenix Packaging cell line was

transfected with scramble control and pSUPER-Retro-sh-GALNT3 using Lipofectamine 2000 (Invitrogen, Carlsbad, CA, USA). Viral particles collected at 48-hours post-transfection were used to infect CD18/HPAF, BxPC3, Capan-1, and T3M4 cells. Stably transfected, pooled populations of GALNT3-knockdown cells were obtained using the antibiotic selection (puromycin, 4 µg/ml). GALNT3 knockdown-cells were maintained in 1 µg/ml puromycin-selection media.

3. CRISPR/Cas9 mediated knockout of C1GALT1 in PDAC cells

Genomic depletion of C1GALT1 was carried out using CRISPR Vector (pX330-U6-Chimeric_BB-CBh-hSpCas9 vector, Addgene) with C1GALT1 specific guide RNA sequence (GCAGATTCTAGCCAACATAA). At 2-3 weeks after transfection, VVA-fluorescein-based FACS sorting was used to obtain C1GALT1 knockout clones. Complete knockout was confirmed by western blotting. Further, the region around guide RNA was PCR amplified and subjected to Sanger sequencing using primers described in Table 2.1.

4. Genetically engineered mouse models. *C1galt1*$^{loxP/loxP}$ was a kind gift from Dr. Lijun Xia at University of Oklahoma Health Sciences Center. KPC *(Kras*^{G12D}*; Trp53*$^{R172H/+}$*: Pdx-Cre)* and KPCC *(Kras*^{G12D}*; Trp53*$^{R172H/+}$*; C1galt1*$^{loxP/loxP}$*; Pdx1-Cre)* were created by breeding of *Kras*^{G12D}*; Pdx1-Cre* and *LSLTrp53*$^{R172H/+}$ with *C1galt1*$^{loxP/\ loxP.}$ Further, intercrossing of their F1 progeny resulted in the generation of KPCC mice along with KPC control littermates. All of the animals were backcrossed 12 times to C57BL/6 before carrying out the breeding. For progression studies, KPC, KPCC, and age-matched controls were euthanized at 3, 5, 10, 15 and 20 weeks of age (five animals/group/time point). Survival studies were also conducted on KPC and KPCC mice (8-10 animals/group). All of the animal studies were performed in accordance with the U.S. Public Health Service "Guidelines for the Care and Use of Laboratory Animals" under an

approved protocol by the University of Nebraska Medical Center Institutional Animal Care and Use Committee (IACUC).

5. DNA isolation and genotyping

Mice at 15-21 days of age were tail clipped and DNA isolation was performed using standard protocols (Maxwell 16 mouse tail DNA purification kit, Promega, Madison, WI, USA). The genotyping of *Kras, p53, Pdx-Cre, C1galt1*$^{loxP/loxP}$ was performed by PCR using the primer sequences mentioned in Table 2.2.

6. Orthotopic tumor mouse models

For orthotopic tumor studies, 0.5x0^6 PDAC cells were injected into the pancreas of 6-8-week old nude mice (6 to 8 animals/group) using conventional procedures. Euthanization of experimental mice cohorts was performed 21-30 days after orthotopic transplantation. Following euthanization, tumor weights and metastatic lesions were recorded.

7. Reagents and Antibodies

Tables 2.1, 2.2, and 2.3 outline a thorough list of primers and antibodies used in the study. Biotinylated VVA (binds Tn carbohydrate antigen) and PNA (binds T carbohydrate antigen) lectins were purchased from Vector Labs.

8. Immunohistochemistry (IHC)

IHC staining was performed on Whipple samples to analyze GALNT3 and C1GALT1 expression using a previously described method [2]. Further GALNT3 staining was also performed on tissue arrays. Apart from patient tissues, IHC staining was also performed on KPC and KPCC mouse tissues Briefly, after deparaffinization and

dehydration of tissue sections, endogenous peroxidase activity in these human tissues was blocked by 3% H_2O_2 for an hour. Further, antigen retrieval is done by incubating these tissues with 0.01 M citrate buffer (pH 6.8). Subsequently, the tissue slides were blocked with horse serum, which was followed by their incubation with anti GALNT3 antibody for 16 hr in a humidified chamber at 4°C. The specificity of the antibody was confirmed by using isotype control. The sections were probed with streptavidin-HRP and counterstained with hematoxylin. Expression of GALNT3 and C1GALT1 was analyzed by a pathologist. An intensity (0 - no staining, 1 – weak staining, 2 – moderate staining, and 3 – strong staining) and percentage of positive cells (range 1–4; 0–25% positive cells, equal score of 1, 26–50%, equal score 2, 51–75%, equal score 3, and 76–100%, equal score 4) were recorded. A composite score, obtained by multiplying the two values, was assigned and it ranged from 0 to12.

9. Immunofluorescence

Confocal analysis of GALNT3 expression was carried out with CD18/HPAF, T3M4, and Panc-1 PDAC cells. All of these PDAC cells were grown in a 12-well plate dish to 60% confluence on autoclaved coverslips for 48 hours. After their fixation with 4% paraformaldehyde (10 minutes), these PDAC cells were permeabilized with 0.2% Triton-X (15 minutes). Blocking was completed using 10% Bovine Serum Albumin (BSA) (Jackson Immunoresearch Labs, Inc., West Grove, PA, USA), which was followed by overnight incubation with a GALNT3 antibody at 4°C. The cells were then washed with phosphate-buffered saline (PBS) for 3 × 5 minutes and incubated in dark for 30 min with FITC-conjugated anti-mouse secondary antibody (Jackson Immunoresearch Labs, Inc.) at room temperature. Cells were washed again (5 × 5 minutes) in PBS and mounted on glass slides in Vectashield mounting medium that contained the nuclear staining dye DAPI

(Vector Laboratories, Burlingame, CA, USA). Additionally, we also performed immunofluorescence staining on mouse tissues using antibodies described in Table 2.3.

10. Histology

Formalin-fixed mouse tumor tissues were paraffin embedded and sectioned. Following sectioning, the tissues were subjected to H and E staining. KPC and KPCC tumor tissues were also stained with Picro-Sirius red and Alcian blue as per the recommended protocols.

11. Real Time –PCR

RNA is collected from PDAC cells using the RNAeasy kit (Qiagen, Valenica, CA, U.S.A.). Specifically, 1 µg of the RNA was converted to cDNA, which was further used for RT-PCR quantification of glycosyltransferases and EMT-related genes.

12. Tumor endothelium cell adhesion assay

Adhesion of cancer cells to activated endothelial cells was examined using CytoSelect™ Tumor-Endothelium adhesion assay kit (Cell Biolabs, San Diego, CA, USA) [3]. In brief, 10,000-20,000 HMEC-1 endothelial cells were cultured on collagen/gelatin coated 96-well plates (Black/Clear Flat Bottom-Corning™) till the formation of a monolayer. GALNT3-scrambled and -knockdown cells (CD18/HPAF and BxPC3) suspension pre-labeled with CytoTracker™ was placed in 96-well plates containing endothelial cells, and incubated at 37˚C for 1 hr. 96-well plates were then washed 3 times to remove non-adherent cells. Cell adhesion of labeled scrambled control and GALNT3-knockdown cells was determined by measuring the fluorescence using the fluorescent plate reader at an excitation wavelength of 480 nm and an emission of 520 nm.

Percentage adhesion is calculated as follows: % cell adhesion = mean fluorescence intensity of experimental wells/mean fluorescence intensity of total cells plated x100%

13. Lectin Pull-down Assay and Immunoprecipitation

Protein lysates (600 µg) collected from scramble control and GALNT3-knockdown cells were incubated with biotinylated VVA (5 µg) and PNA (5 µg) lectins to detect Tn and T carbohydrate antigens, respectively, located on glycoproteins . Proteins bound to these biotinylated lectins were then pulled down using streptavidin agarose (20 µl) as described previously [4]. Pulled-down proteins were then immunoblotted with EGFR and Her2.

Similarly, lysates collected from wild-type control and C1GALT1-knockout PDAC cells were also also pulled down with biotinylated VVA and probed with MUC16 to detect Tn carbohydrate antigen variation on MUC16 in control and knockout cells. Further, Immunoprecipitation of control and C1GALT1 KO lysates were carried out with MUC4 antibody using standard procedures. MUC4-pulled down lysates were then probed with carbohydrate antigens (Tn and STn) to detect carbohydrate antigen variation on MUC4 in control and knockout cells.

14. Colony formation assay

Colony formation assays were performed in scramble control and GALNT3-knockdown cells using standard protocols [5]. Briefly 500 - 1000 cells were seeded in 6-well plates and allowed to adhere overnight, following which media was changed to 1%, and the colony formation efficiencies of the cells were analyzed after 3 - 4 weeks by staining them with crystal violet (0.1%, w/v) in 20 nM 4-morpholinepropanesulfonic acid (Sigma Chemicals).

15. WST-1 assay

Effect of GALNT3 knockdown on cell growth was assessed using WST-1 assay. For this assay, 1000 cells were plated onto 96-well plates and allowed to adhere overnight. On the next day, the media was changed to 1% DMEM, and WST-1 reagent was added to each well. Absorbance was measured at 450/630 nm 3 hours after WST-1 addition. Similarly, readings taken for another three consecutive days [6].

16. Wound healing assay

Cell motility was evaluated in GALNT3-knockdown cells using a wound healing assay as described previously [7]. Additionally, wound healing assay was also conducted on control and C1GALT1 KO PDAC cells. Wound closure was evaluated in scramble control and GALNT3-knockdown cells using Image J software.

17. Western and lectin blots

Western blotting was performed using standard procedures and manufacturer's protocols. Briefly, lysates were collected from PDAC cells 48 fours after plating. The above-listed lysates (40 µg) were probed for several oncogenic signaling proteins and EMT markers using antibodies listed in Table 2.3. After appropriate incubation of the secondary antibody, bands were visualized using enhanced chemiluminescence (ECL) (Thermo Scientific, Waltham, MA, USA). For lectin blotting, 2% BSA (Jackson Immunoresearch Labs) was used for blocking, and streptavidin HRP was applied to visualize bands using an ECL method [8].

18. C1GALT1 enzyme activity assay

Lysates collected from wild-type control cells and C1GALT1 KO cells were incubated with substrate GalNAcα-O-Benzyl and UDP-Gal. Identification of glycan structures synthesized by control and C1GALT1 knockout cells was carried out using LC-MS and MS/MS analysis using well-described methods [9].

19. Fourier transform ion cyclotron resonance mass spectrometry (FT-ICR MS)

Control and C1GALT1 knockout PDAC cells were incubated with media containing 50 μM of the per-acetylated GalNAcα-OBn substrate for 72hrs. Following incubation, the culture supernatants from the GalNAcα-OBn treated PDAC cells were collected. FT-ICR MS was used to analyze glycosylated products synthesized on this substrate and secreted into culture media [9].

20. RNA-seq analysis

Total RNA was collected from control and C1GALT1 KO PDAC cells and submitted to RNA-Seq facility at UNMC. Gene expression analysis identified differentially upregulated and downregulated genes in control and C1GALT1 KO PDAC cells. (log fold change≥3). IPA analysis further identified the pathways affected in control and C1GALT1 KO PDAC cells.

21. Development of murine tumor cell lines and organoids

Mouse tumors were finely minced and then processed for cell lines and organoids development. Cell lines were derived using standard procedures in a previously described method [6]. For organoid development, tissue was digested using special digestion buffer (collagenase).for 4 hrs. Following digestion, bigger tissue chunks were removed through

strainers and the flow-through was collected. After centrifugation, the cell pellet was washed twice and then mixed with Matrigel. A drop of Matrigel (around 30ul) containing tumor cells was then suspended in the center of 24-well plate. After the solidification of Matrigel, mouse-organoid specific media was added. The media was changed after every 3-4 days and the organoids start appearing in 1-2 weeks [10].

22. Statistical Analysis

For IHC, Student's *t*-test was used to determine the statistical significance of variation in GALNT3 composite score among different disease groups. Similarly, for all the functional assays, Student's t-test was used to determine statistical significance. A p-value of less than 0.05 was considered statistically significant. All statistical analysis was performed using GraphPad Prism 7 software.

Table 2.1: List of human primers used in the study

Gene	Primer sequence
GALNT2	F-5'-AAG GAG AAG TCG GTG AAG CA-3' R-5'-TTG AGC GTG AAC TTC CAC TG-3'
GALNT3	F-5'-AAA GCG TTG GTC AGC CTC TA-3' R-5'-AAC GAG ACC TTG AGC AGC AT-3'
GALNT10	F-5'-ACA GCC AGG TAA TGG GTG A-3' R-5'-GAA GAT GGG ATG GCT TTT CA-3'
GALNT11	F-5'-TGC TTA TCA GTG ACC GCT TG-3' R-5'-ACA CTG TGC ACT GTC CGA AG-3'
GALNT12	F-5'-CAT CTT GCA GGA GGA TGG AT-3' R-5'-CTG GCT CCA CAG TCT CCT TC-3'
GALNT13	F-5'-CAT CTA TCC GGA CTC CCA GA-3' R-5'-TCG GTT CGG ATT TCT TTG TC-3'
GALNT14	F-5'-CTG AGA TGC ACA CTG CTG GT-3' R-5'-CAT TTC ACC TTG GGC AAC TT-3'
CDH-1	F-5'-CGA TTC AAA GTG GGC ACA GAT GGT GT-3' R-5'-CTG TAT TCA GCG TGA CTT TGG TGG AAA-3'
CDH-2	F-5'-CCT GAT ATA TGC CCA AGA CAA AGA GA-3' R-5'-CAC TGT GCT TAC TGA ATT GTC TTG GGA-3'
VIM	F-5'-GCA GCT CAA GGG CCA AGG CA-3' R-5'-CCT GCA ATT TCT CCC GGA GGC G-3'
C1GALT1	F-5'-AAA TGG CCT CTA AAT CCT GGC-3' R-5'-GAG TTT TAG CAA TTC CCT TCT C-3'
ST6GALNAC1	F-5'-GGA TAC AGT GGG AAT CTT GAG AC-3' R-5'-GCC ATT TGC CAT CTT GAG AG-3'
ST6GALNAC2	F-5'-AAT GTC GGT GGA GTG TTC AG-3' R-5'-CCT TGA ATC ACT TTA GCA TCT GG-3'

Table 2.2: List of mouse primers used in the study

Gene	Primer sequence
Kras (Genotyping)	K006F-5'-CCT TTA CAA GCG CAC GCA GAC TGT AGA-3' K005R-5'- AGC TAG CCA CCA TGG CTT GAG TAA GTC TGC A-3'
p53 (Genotyping)	F-5'-CAC AAA AAC AGG TTA AAC CCA G-3' F-5'-AGC ACA TAG GAG GCA GAG AC-3'
Pdx-1-Cre (Genotyping)	F-5'-CTG GAC TAC ATC TTG AGT TGC -3' R-5'-GGT GTA CGG TCA GTA AAT TTG -3'
C1galt1 *C1galt1 (Genotyping)*	F-5′-TGG GTT ATG ACA AGT CCT C-3′ R-5′-TCA TGT ATC CCT GCT TCA C-3′ F-5'-TGA CAG CCA GGA ATG GAA CTT G-3' R-5'-GCC TCT TCT CGC AAC AAA ATA CTC-3'
Vimentin	F-5'-CGG CTG CGA GAG AAA TTG C-3' R-5'-CCA CTT TCC GTT CAA GGT CAA G-3'
Keratin-5	F-5′-GAT GCC AGA AAC AAG CTG ACA GA-3′ R-5′-TTC CCC ACT CAG CCT GCA CT-3′
Keratin-7	F-5′-GCA GAG ATT GAC ACC TTG AAG AA-3′ R-5′-TCC TGG TAC TCT CGA AGT TG-3′
Claudin-4	F-5′-TCT GGG GAT GCT TCT CTC AGT-3′ R-5′-AAG TCG CGG ATG ACG TTG TG-3′
Claudin-6	F-5′-TGA CGC TCA TTC CTG TCT G-3′ R-5′-AGA AGA GCA GGC GCA GCA TA-3′

Table 2.3: List of antibodies used in the study

Molecule	Source	Acquired from	WB dilution	IHC dilution	IF dilution
GALNT3	Rabbit	Novus Biologicals	1:500	1:100	1:100
CC49	Mouse	(Sheer *et al.*, 1988)	1:500		
SLex	Mouse	(Ogata *et al.*, 1995)	1:500		
CA19.9	Mouse	ATCC	1:1000		
Cyclin A	Rabbit	Santa Cruze	1:500		
E-cadherin	Mouse	Dr. Keith Johnson, UNMC	1:500		
N-cadherin	Mouse	Dr. Keith Johnson, UNMC	1:500		
Vimentin	Rabbit	Abcam	1:1000	1:400	1:400
ZEB1	Rabbit	Sigma	1:1000		
ZO-1	Rabbit	Cell Signaling	1:1000		
Sox2	Rabbit	Santa Cruze	1:1000		
pHer2	Rabbit	Santa Cruze	1:1000		
Total Her2	Rabbit	Santa Cruze ruze	1:1000		
pEGFR (Y1068)	Rabbit	Cell Signaling	1:1000		
pEGFR (S1046)	Rabbit	Santa Cruze	1:1000		
Total EGFR	Rabbit	Santa Cruze	1:500		
pHer3	Rabbit	Cell Signaling	1:1000		
Total Her3	Rabbit	Cell Signaling	1:1000		
C1GALT1	Mouse	Abcam	1:1000		
C1GALT1	Rabbit	Sigma		1:200	
Alpha-SMA	Rabbit	Abcam		1:400	1:400
α4-Integrin	Rabbit	Cell Signaling	1:1000		
B1-Integrin	Rabbit	Cell Signaling	1:1000		
pFAK-Y925	Rabbit	Cell Signaling	1:1000		
pFAK-Y397	Rabbit	Cell Signaling	1:1000		
Total FAK	Rabbit	Santa Cruze	1:1000		
MUC1	Mouse				
MUC4 (8G7)	Mouse	Generated in our lab	1:1000		
MUC16	Mouse	DAKO (M3520)	1:1000		

References

[1] P.M. Campbell, A.L. Groehler, K.M. Lee, M.M. Ouellette, V. Khazak, C.J. Der, K-Ras promotes growth transformation and invasion of immortalized human pancreatic cells by Raf and phosphatidylinositol 3-kinase signaling, Cancer Res, 67 (2007) 2098-2106.

[2] S. Kaur, N. Momi, S. Chakraborty, D.G. Wagner, A.J. Horn, S.M. Lele, D. Theodorescu, S.K. Batra, Altered expression of transmembrane mucins, MUC1 and MUC4, in bladder cancer: pathological implications in diagnosis, PLoS One, 9 (2014) e92742.

[3] L. Gu, P. Vogiatzi, M. Puhr, A. Dagvadorj, J. Lutz, A. Ryder, S. Addya, P. Fortina, C. Cooper, B. Leiby, A. Dasgupta, T. Hyslop, L. Bubendorf, K. Alanen, T. Mirtti, M.T. Nevalainen, Stat5 promotes metastatic behavior of human prostate cancer cells in vitro and in vivo, Endocr Relat Cancer, 17 (2010) 481-493.

[4] E.C. Seales, G.A. Jurado, A. Singhal, S.L. Bellis, Ras oncogene directs expression of a differentially sialylated, functionally altered beta1 integrin, Oncogene, 22 (2003) 7137-7145.

[5] S. Bafna, A.P. Singh, N. Moniaux, J.D. Eudy, J.L. Meza, S.K. Batra, MUC4, a multifunctional transmembrane glycoprotein, induces oncogenic transformation of NIH3T3 mouse fibroblast cells, Cancer Res, 68 (2008) 9231-9238.

[6] M.P. Torres, S. Rachagani, J.J. Souchek, K. Mallya, S.L. Johansson, S.K. Batra, Novel pancreatic cancer cell lines derived from genetically engineered mouse models of spontaneous pancreatic adenocarcinoma: applications in diagnosis and therapy, PLoS One, 8 (2013) e80580.

[7] P. Seshacharyulu, M.P. Ponnusamy, S. Rachagani, I. Lakshmanan, D. Haridas, Y. Yan, A.K. Ganti, S.K. Batra, Targeting EGF-receptor(s) - STAT1 axis attenuates tumor growth and metastasis through downregulation of MUC4 mucin in human pancreatic cancer, Oncotarget, 6 (2015) 5164-5181.

[8] V.S. Gnanapragassam, M. Jain, S.K. Batra, Analysis of tumor-associated mucin glycotopes by Western transfer methods, Methods Mol Biol, 980 (2013) 331-340.

[9] G. Stolfa, N. Mondal, Y. Zhu, X. Yu, A. Buffone, Jr., S. Neelamegham, Using CRISPR-Cas9 to quantify the contributions of O-glycans, N-glycans and Glycosphingolipids to human leukocyte-endothelium adhesion, Scientific reports, 6 (2016) 30392.

[10] S.F. Boj, C.I. Hwang, L.A. Baker, Chio, II, D.D. Engle, V. Corbo, M. Jager, M. Ponz-Sarvise, H. Tiriac, M.S. Spector, A. Gracanin, T. Oni, K.H. Yu, R. van Boxtel, M. Huch, K.D. Rivera, J.P. Wilson, M.E. Feigin, D. Ohlund, A. Handly-Santana, C.M. Ardito-Abraham, M. Ludwig, E. Elyada, B. Alagesan, G. Biffi, G.N. Yordanov, B. Delcuze, B. Creighton, K. Wright, Y. Park, F.H. Morsink, I.Q. Molenaar, I.H. Borel Rinkes, E. Cuppen, Y. Hao, Y. Jin, I.J. Nijman, C. Iacobuzio-Donahue, S.D. Leach, D.J. Pappin, M. Hammell, D.S. Klimstra, O. Basturk, R.H. Hruban, G.J. Offerhaus, R.G. Vries, H. Clevers, D.A. Tuveson, Organoid models of human and mouse ductal pancreatic cancer, Cell, 160 (2015) 324-338.

CHAPTER 3

Role of GALNT3 loss in pancreatic ductal adenocarcinoma

The material covered in this chapter is the subject of one published research article:

1. Chugh S, Meza J, Sheinin YM, Ponnusamy MP, Batra SK. *Loss of N acetylgalactosaminyltransferase 3 in poorly differentiated pancreatic cancer: augmented aggressiveness and aberrant ErbB family glycosylation.* **Br J Cancer.** 2016 Jun 14; 114(12):1376-86.

Loss of N-acetylgalactosaminyltransferase 3 (GALNT3) in poorly differentiated pancreatic cancer: augmented aggressiveness and aberrant ErbB family glycosylation

Running title: Loss of GALNT3 in pancreatic cancer

Seema Chugh,[1] Jane Meza [2], Yuri M Sheinin [3, 5], Moorthy P. Ponnusamy, [1, 4, 5] and Surinder K. Batra[1, 4, 5, *]

[1]Department of Biochemistry and Molecular Biology, University of Nebraska Medical Center, Omaha, NE 68198-5870, USA

[2]Department of Biostatistics, UNMC College of Public Health, UNMC, Omaha, NE 68198-4375, USA.

[3]Department of Pathology and Microbiology, UNMC, Omaha, NE 68198-5900, USA.

[4]Eppley Institute for Research in Cancer and Allied Diseases, UNMC, Omaha, NE 68198-5950, USA

[5]Fred and Pamela Buffett Cancer Center, UNMC, Omaha, NE 68198, USA

*Correspondence: Surinder K. Batra, Ph.D., Department of Biochemistry and Molecular Biology, Eppley Institute for Research in Cancer and Allied Diseases, University of Nebraska Medical Center, Omaha, Nebraska, 68198-5870, U.S.A. Phone: 402-559-5455, Fax: 402-559-6650, Email: sbatra@unmc.edu

1. Synopsis

Aberrant glycosylation of several proteins underlie pancreatic ductal adenocarcinoma (PDAC) progression and metastasis. O-glycosylation is initiated by a family of enzymes known as polypeptide N-acetylgalactosaminyl transferases (GalNAc-Ts/GALNTs). In this study, we investigated the role of the O-glycosyltransferase GALNT3 in PDAC. Immunohistochemistry staining of GALNT3 was performed on normal, inflammatory and neoplastic pancreatic tissues. Several *in vitro* functional assays such as proliferation, colony formation, migration and tumour–endothelium adhesion assay were conducted in GALNT3 knockdown PDAC cells to investigate its role in disease aggressiveness. Expression of signalling molecules involved in growth and motility was evaluated using western blotting. Effect of GALNT3 knockdown on glycosylation was examined by lectin pull-down assay. N-acetylgalactosaminyl transferase 3 expression is significantly decreased in poorly differentiated PDAC cells and tissues as compared with well/moderately differentiated PDAC. Further, knockdown of GALNT3 resulted in increased expression of poorly differentiated PDAC markers, augmented growth, motility and tumour–endothelium adhesion. Pull-down assay revealed that O-glycans (Tn and T) on EGFR and Her2 were altered in PDAC cells, which was accompanied by their increased phosphorylation. Our study indicates that loss of GALNT3 occurs in poorly differentiated PDAC, which is associated with the increased and altered glycosylation of ErbB family proteins.

2. Background and Rationale

Pancreatic ductal adenocarcinoma (PDAC) is a highly aggressive gastrointestinal malignancy with a very poor survival rate (*i.e.,* around a 8% five-year survival rate) [1]. The lethal nature of this disease is due to its increased metastatic rate, which accounts for the extreme mortality rate among PDAC patients [2, 3]. In order to design and create much-needed targeted treatment modalities for PDAC, it is necessary to understand the gene signatures that contribute to its aggressiveness and high metastases. Several studies report the critical involvement of post-translational modifications on proteins during cancer development and progression [4, 5]. Further, aberrant changes in glycosylation patterns of proteins have been shown to underlie cancer growth and metastases [6, 7]. Proteins can undergo *O*- and *N*-glycosylation, which is determined by the amino acid getting modified by the glycan residues [8]. Mucin type *O*-glycosylation is the most common *O*-glycosylation that is initiated in the Golgi apparatus through a large family of 20 enzymes, known as UDP-GalNAc:Polypeptide N-acetylgalactosaminyltransferases (*i.e.,* GalNAc-Ts/GALNTs) [9]. GalNAcT enzymes catalyze the first step in mucin type *O*-glycosylation, wherein these enzymes add an *N*-acetylgalactosamine sugar residue to the serine/threonine (Ser/Thr) residues on their specific substrates. This addition results in the formation of a Tn carbohydrate antigen [10], which can be either sialylated to form Sialyl-Tn (STn) antigen, or it can be extended to several core carbohydrate structures [11].

Despite of the functional homology, distinct substrate specificity has been reported for GalNAcTs [12]. For instance, during breast cancer, GalNAc-T6 has been shown to play a critical role in glycosylation of Mucin 1 (MUC1) [13]. Another study on hepatocellular carcinoma showed the significant involvement of GalNAc-T2 in glycosylation of the growth factor receptor EGFR [14]. GalNAc-T2 has also been shown to regulate EGFR

glycosylation and activity in oral squamous cell carcinoma. [15]. GalNAc-T3/ GALNT3 enzyme is one of the members of the *O*-glycosylation-initiating GalNAc-T family, which has been shown to be highly expressed in oral squamous cell carcinomas and in ovarian cancer [16, 17]. Conversely, in lung adenocarcinoma and colorectal carcinoma, decreased expression of GALNT3 is reported, which is associated with a poor prognosis [18-20]. Few studies in pancreatic cancer have shown loss of expression of GALNT3 in poorly differentiated pancreatic cancer [21, 22]. However, the role of GALNT3 in pancreatic cancer progression and metastasis has not been explored much.

The present study elucidates a *novel* role the loss of GALNT3 has in PDAC aggressiveness. The results from the present study evidence the association between the loss of *O*-glycosyltransferase GALNT3 and an altered glycosylation of ErbB receptors, accompanied by the increased phosphorylation of these growth factor receptors, leading to increased PDAC aggressiveness. Altogether, our study for the first time showed the pathobiological implications of loss of GALNT3 in poorly differentiated PDAC.

3. Results

A. Differential expression of GALNT3 in PDAC cells

To investigate expression of the N-Acetylgalactosaminyl transferase 3, GALNT3, during PDAC, a panel of PDAC cell lines derived from well, moderate, and poorly differentiated carcinomas was used. GALNT3 protein expression was increased in well and moderately differentiated PDAC cells (CD18/HPAF, Capan-1, SW1990, Colo-357, BxPC3) as shown by western blot analysis, whereas poorly differentiated PDAC cells displayed no expression of GALNT3 (AsPC-1, Panc-1, MIA PaCa-2) (**Figure 3.1A**). To confirm these findings, immunofluorescence staining of GALNT3 expression was performed for certain PDAC cells with varied differentiation status (**Supplementary**

Figure 3.1a). In accordance with western blot data, immunofluorescence studies also demonstrated loss of GALNT3 in poorly differentiated PDAC cells. These results suggest that GALNT3 is differentially expressed in PDAC cells.

B. Increased GALNT3 expression during PDAC progression from PanINs to well/moderately differentiated PDAC, but subsequent loss in poorly differentiated PDAC tissues

To further evaluate the relationship between GALNT3 expression and disease progression, immunohistochemical (IHC) staining of GALNT3 was conducted on commercially availaible tissue arrays comprised of normal pancreatic tissues, samples procured from patients with chronic pancreatitis, pancreatic intraepithelial precursor lesions (PanINs), and PDAC (well differentiated, moderately differentiated and poorly differentiated). IHC staining was also performed on archived PDAC tissues procured via the Whipple procedure. Granular cytoplasmic pattern of staining was observed in tissues positive for GALNT3 expression. Normal pancreatic ducts were negative for GALNT3 expression (weak staining in islets of Langerhans) (**Figure 3.1C)**. Majority of chronic pancreatitis and PanINs samples showed negative staining, though weak staining was observed in few PanINs ducts (**Table 3.1**). Compared to PanIN lesions and chronic pancreatitis, the composite score for GALNT3 increased significantly ($p<0.001$) in the well and moderately differentiated PDAC samples. However, the composite score decreased significantly ($p<0.05$) in poorly differentiated cancer (**Figure 3.1B**). Overall, these results demonstrate that loss of GALNT3 expression occurs primarily during advanced and poorly differentiated PDAC, and not in moderately or well-differentiated PDAC (**Representative picture-Figure 3.1C, Supplementary Figure 3.1c**).

C. GALNT3 knockdown and decreased expression of Tn carbohydrate antigen

To gain insight into the role of GALNT3 in PDAC progression, knockdown of GALNT3 was performed using specific shRNA in the following four different PDAC cell lines: CD18/HPAF, BxPC3, Capan-1, and T3M4. Knockdown was confirmed by western blot analysis and Real-Time PCR (**Figure 3.2A, Supplementary Figure 3.1d**). Since GALNT3 is the first enzyme in the *O*-glycosylation pathway and catalyzes the formation of Tn carbohydrate antigen, we next evaluated the expression of the Tn carbohydrate antigen in GALNT3-knockdown PDAC cells. VVA lectin blot demonstrated a slight decrease in expression of Tn carbohydrate antigen in GALNT3-knockdown PDAC cells (**Figure 3.2B**).

D. Increased expression of poorly differentiated PDAC cell markers with loss of GALNT3

Considering that loss of GALNT3 expression occurred in poorly differentiated PDAC cells and tissues, the expression of poorly differentiated PDAC cell markers was examined in GALNT3-knockdown PDAC cells. However, no defined markers exist to characterize well, moderate, and poorly differentiated forms of PDAC. On the other hand, previous studies show that expression of the protein Sox2 increases in poorly differentiated PDAC cells [30, 31]. Another study showed loss of the carbohydrate antigen sialyl Lewis a (SLe^a /CA19.9) occurred in poorly differentiated PDAC [32]. In turn, the expression of Sox2 and SLe^a was evaluated in GALNT3-knockdown PDAC cells. Data showed increased expression of Sox2 and decreased expression of SLe^a in GALNT3-knockdown PDAC cells (**Figure 3.2C and 3.2D**).

E. Increased PDAC cell growth and proliferation with GALNT3 knockdown

In our results, loss of GALNT3 was observed in the poorly differentiated PDAC and therefore the effect of GALNT3 knockdown on disease aggressiveness was further examined in the study herein. Specifically, *in vitro* assays were used to examine the effect of GALNT3 knockdown on PDAC cell growth and proliferation. WST-1 assay results demonstrated significant increase in proliferation of GALNT3-knockdown CD18/HPAF cells (**Figure 3.3A**). GALNT3 knockdown also increased proliferation of Capan-1 PDAC cells (p-value <0.05, **Supplementary Figure 3.2a**). Further, increased numbers of colonies were observed in GALNT3-knockdown cells compared to scramble control cells (p-value <0.05, **Figure 3.3B & 3.3C; Supplementary Figure. 3.2b**). Additionally, increased proliferation and numbers of colonies in GALNT3-knockdown PC cells were also associated with increased expression of Cyclin-A (**Figure 3.3D**). Overall, these findings suggest that loss of GALNT3 expression leads to increased proliferation and growth of PDAC cells.

F. Increased motility and endothelial cell adhesion of GALNT3 knockdown PDAC cells

To determine the effect that GALNT3 has on cancer cell mobility, wound-healing assays were conducted for GALNT3-knockdown CD18/HPAF and BxPC3 PDAC cells. Notably, compared to scramble control cells, GALNT3 knockdown significantly increased the percentage of wound closure after 24 hours (p-value <0.05, **Figure 3.4A**). To further assess the effect that GALNT3 has on cancer cell mobility, the expression levels of epithelial mesenchymal transition (EMT) proteins involved in increased cell motility (*e.g.,* E-cadherin, N-cadherin, vimentin and ZEB-1) were examined. Interestingly, increased expression was seen for mesenchymal markers (N-cadherin, vimentin and Zeb1), and

decreased expression was seen for epithelial marker (E-cadherin) in GALNT3-knockdown PDAC cells (**Figure 3.4B; Supplementary Figure. 3.2c, e**). Further, GALNT3-knockdown CD18/HPAF PDAC cells also showed EMT-like cell morphology (**Figure 3.5A**).

Next, we evaluated the expression of the terminal carbohydrate epitope, sialylated Lewis x, SLe^x, for which a study by Kawarada *et al.* demonstrated its involvement in metastasis [33]. Data from our study revealed increased expression of SLe^x in GALNT3-knockdown CD18/HPAF and BxPC3 PDAC cells (**Figure 3.5B**). Additionally, GALNT3-knockdown CD18/HPAF and Capan-1 PDAC cells showed increased expression of sialylated Tn carbohydrate antigen (STn) (**Supplementary Figure. 3.2d**). Likewise, prior studies indicate that the negative charge imparted by sialic acid residues allows cancer cells to detach from each other, thus aiding in metastatic dissemination [34, 35]. Increases in SLe^x and STn carbohydrate antigens in GALNT3-knockdown PDAC cells suggest that there is not a complete abrogation of glycosylation in GALNT3-knockdown cells, which is potentially explained by the compensatory action of other GALNTs. For example, increased expressions of few *GALNT* genes were seen in GALNT3-knockdown cells (such as GALNT2, GALNT10 and GALNT11, GALNT12, GALNT13 and GALNT14) (**Supplementary Figure. 3.3a, b**). SLe^x carbohydrate antigen has been shown to facilitate cancer cells to cross the endothelium barrier through its interaction with E-selectin on endothelial cells, therefore to investigate the functional impact of increased SLe^x expression, we examined the adhesion of GALNT3 knockdown PDAC cells to endothelium cells [36, 37]. Interestingly, GALNT3 knockdown CD18/HPAF and BxPC3 cells showed significantly increased adhesion to endothelium cells as compared to scrambled control cells (**Figure 3.5C**). These results suggest that GALNT3 knockdown cells might have increased propensity to metastasize.

G. GALNT3 knockdown and altered expression of several oncogenic signaling proteins

To gain insight into the mechanisms involved in increased aggressiveness of PDAC, we investigated the expression of ErbB proteins associated with increased tumor malignancy. Increased phosphorylation of ErbB family of membrane receptors has been implicated in PDAC growth and motility [28, 38]. Data from the present study showed increased phosphorylation of ErbB family members, including EGFR, Her2, and Her3, in GALNT3-knockdown PDAC cells compared to scrambled control cells (**Figure 3.6A**).

H. GALNT3 knockdown and altered glycosylation of EGFR and Her2

To delineate the specific mechanisms by which increased phosphorylation of ErbB family members occurs the effect of GALNT3 knockdown on *O*-glycosylation modifications on these proteins was investigated. Previous studies evidence the involvement of altered *O*-glycosylation in regulating activation of EGFR [14, 15, 39]. Therefore to examine effect of GALNT3 knockdown on Tn and T carbohydrate antigens associated with EGFR and Her2, cell lysates from scramble control and GALNT3-knockdown cells were pulled down using biotinylated VVA (binds Tn carbohydrate antigen) and PNA lectins (binds T carbohydrate antigen) (**Figure 3.6B**). VVA and PNA pull down lysates were further probed with EGFR and Her2/Neu to examine Tn and T carbohydrate alterations on these receptors. Lectin-pull down assay demonstrated increased Tn and T carbohydrate antigens on EGFR and Her2 in GALNT3-knockdown CD18/HPAF and BxPC3 cells. (**Figure 3.6B**) Increased Tn and T carbohydrate antigens on these growth receptors in GALNT3 knockdown cells suggest the possible involvement of other GALNTs in EGFR glycosylation in aggressive PDAC. Interestingly, we observed upregulation of GALNT2, which has been shown to enhance the invasive potential of oral squamous cell carcinoma

by regulating EGFR glycosylation (**Supplementary Figure. 3.3a, b**) [15]. However, the role of GALNT2 in EGFR glycosylation in PDAC needs to be explored.

4. Discussion

Deregulated *O*-glycosylation of several proteins underlies cancer progression and metastasis. Furthermore, altered expression of glycosyltransferases leads to aberrant glycosylation of proteins, thus affecting their function. However, specific glycosyltransferases related to increased tumor aggressiveness have been unidentified. We identified that the *O*-glycosylation-initiating enzyme, GALNT3 is differentially expressed in PDAC. Using IHC staining, we found that GALNT3 expression decreased dramatically in poorly differentiated PDAC. Furthermore, we have analyzed some of the poorly differentiation markers in GALNT3 knockdown PDAC cells to prove the concept. However, there are no well-defined markers that can filter poorly differentiated PDAC from moderately or well-differentiated PDAC. On the other hand, recent studies on invasive and poorly differentiated PDAC showed increased expression of the transcription factor SOX2 [30, 31]. In turn, we investigated whether loss of GALNT3 leads to increased expression of SOX2, thus serving as a marker for poorly differentiated PDAC cells. Interestingly, GALNT3-knockdown cells showed increased expression of SOX2. Further, we examined the expression of the carbohydrate antigen SLe^a in GALNT3-knockdown PDAC cells. SLe^a, also known as CA-19.9, is a clinically important prognostic marker for PDAC. Still, poorly differentiated PDAC cells have been shown to produce reduced amounts of CA-19.9 as compared to well or moderately differentiated PDAC cells [32]. Expression of the carbohydrate antigen SLe^a was found to be decreased in GALNT3-knockdown PDAC cells as compared to scramble control cells. These results suggest that knockdown of GALNT3 in PDAC cells might lead to the poorly differentiated state. Our findings are consistent with

previous studies also reporting loss of GALNT3 in other poorly differentiated cancers, including thyroid, gastric and colorectal carcinoma [20, 40, 41]. For instance, GALNT3 expression in thyroid carcinoma is indicative of its differentiation status. Notably, poorly differentiated components of papillary thyroid carcinoma were found to be less positive for GALNT3 expression compared to well-differentiated components [41]. Based on these supporting studies, our results strongly suggest that GALNT3 is decreased in poorly differentiated PDAC.

A 2011 study by Li *et al*. investigated the clinical significance of GALNT3 and GALNT6 in PDAC. Their results demonstrated negative staining for GALNT3 expression in poorly differentiated PDAC; however, expression pattern of GALNT3 in different stages of disease progression such as PanINs and chronic pancreatitis was not examined [22]. Further, the functional role of loss of GALNT3 expression in poorly differentiated pancreatic cancer has not been described in this study. Hence, the *objective* of our study was to study the impact of GALNT3 loss on pancreatic cancer pathogenesis.

Several studies report associations between GALNT3 expression and clinicopathological features of cancers. For example, in lung adenocarcinoma, decreased expression of GALNT3 is associated with poorly differentiated tumors, poor survival, and lymph-node metastasis [18, 19]. Similarly, in the case of gastric and colorectal carcinoma, patients with decreased expression of GALNT3 showed poorer survival, whereas patients with strong GALNT3 expression had a good prognosis [20, 40]. Taken together, these studies suggest the loss of GALNT3 expression is associated with the more aggressive forms of cancer. In contrast to these studies, where loss of GALNT3 expression correlates with poor survival, a study in renal cell carcinoma shows that patients with positive GALNT3 cases have poor prognosis [42]. This suggests that the positive/negative correlation of GALNT3 expression with prognosis depends on specific type of tumor.

We next sought to determine the effect of GALNT3 knockdown on the aggressiveness of PDAC cells. Loss of GALNT3 in PDAC cells was accompanied by increased proliferation. Our findings contrast those from a 2011 study by Taniuchi *et al.,* wherein data demonstrated that overexpression of GALNT3 leads to increased PDAC growth [43]. In our study, GALNT3-knockdown cells also displayed increased motility, accompanied by altered expression of EMT markers. Interestingly, our results corroborate previous findings by Kato *et al.* for hepatocellular carcinoma, wherein cells with increased metastatic potential were marked by decreased expression of GALNT3 [44]. Additionally, a 2014 study by Maupin *et al.,* which focused on identifying glycogene alterations in PDAC EMT, also showed down-regulation of GALNT3 in mesenchymal-like PDAC cells [45]. Based on these supporting information, our results suggests that GALNT3 loss leads to aggressiveness of PDAC cells.

Subsequently, we also found increased expression of SLe^x carbohydrate antigen in GALNT3-knockdown PDAC cells, which was associated with increased percentage adhesion of tumor cells to endothelial cells. Further investigations are necessary to identify the proteins carrying increased expression of SLe^x carbohydrate antigen in GALNT3 knockdown PDAC cells These results indicate that GALNT3 knockdown cells have increased tendency for intravasation/extravasation, which is essential for metastasis. In accordance with results from the functional studies, we also investigated molecular alterations for several members of the ErbB family based on previous study that showed the critical involvement of ErbB family members in PDAC growth and motility [46]. Likewise, we observed increased phosphorylation of EGFR, Her2, and Her3 in GALNT3-knockdown PDAC cells. To further delineate the mechanism by which loss of a glycosyltransferase leads to increased phosphorylation of ErbB proteins and increased cancer aggressiveness, lectin pull-down assays were performed to identify glycan

alterations on EGFR and Her2. Recent studies highlight the significant involvement of *O*-glycosylation modifications on EGFR in regulating EGFR-mediated oncogenic signaling. For instance, knockdown of GALNT2 in oral cancer has been shown to be associated with altered glycosylation and decreased activation of EGFR [15]. We identified that loss of GALNT3 in PDAC cells was associated with increased expression of Tn carbohydrate antigens on EGFR and Her2 proteins. Altered glycosylation on these members of the ErbB family of proteins could be a plausible mechanism for their increased activation. Increased expression of carbohydrate antigens on EGFR and Her2 with loss of GALNT3 provides a perspective about compensatory role of other members of GALNT family. The likelihood of such a switch in the expression/activity of GALNTs as disease progresses to an aggressive stage needs to be deciphered.

Importantly, our study shows, *for the first time*, those *O*-glycan modifications exist on Her2. Prior studies have reported the existence of only *N*-glycans on Her2 [47]. Using the NetOGlyc 4.0 Server (http://www.cbs.dtu.dk/services/NetOGlyc/), which predicts mucin-type GalNAc *O*-glycosylation sites in mammalian protein sequences, we found few potential GalNAc *O*-glycosylation sites in the total Her2. This intriguing finding warrants more experimentation to investigate the exact sites of GalNAc *O*-glycosylation and the effect of altered glycosylation on the conformation of members of the ErbB family of proteins and their subsequent interaction with other signaling proteins.

Overall, this study shows *a novel role* of loss of a glycosyltransferase, GALNT3, in PDAC, which is associated with altered glycosylation of ErbB receptors and increased aggressiveness of PDAC (**Figure 3.7**). Understanding the mechanism by which altered glycosylation brought by loss of GALNT3 leads to increased activation of EGFR and Her2, has the potential to pave the path for the development of novel and more effective therapeutic regimens.

Figure legends

Figure 3.1 Differential expression of GALNT3 in PDAC cells and tissues: (A) Western blot analysis of GALNT3 expression in a panel of eight PDAC cell lines demonstrates loss of GALNT3 expression in poorly differentiated PDAC cells (W.D-well differentiated, M.D-moderately differentiated, P.D-poorly differentiated). **(B)** Immunohistochemistry (IHC) staining performed on tissues representing chronic pancreatitis, PanIN lesions and different grades of PDAC revealed progressive increase of composite score of GALNT3 from chronic pancreatitis and PanIN lesions to well differentiated PDAC, however the composite score is decreased in poorly differentiated PDAC. **(C)** Representative images of GALNT3 immunohistochemical staining in pancreatic cancer progression tissues-upper panel represents H&E staining of normal, chronic pancreatitis, PanIN, moderately and poorly differentiated pancreatic cancer tissues, wheras lower panel represents the corresponding GALNT3 staining in these tissues (figure magnification-400X, scale bar represents 50 μm, black arrows indicate ductal regions).

Figure 3.1

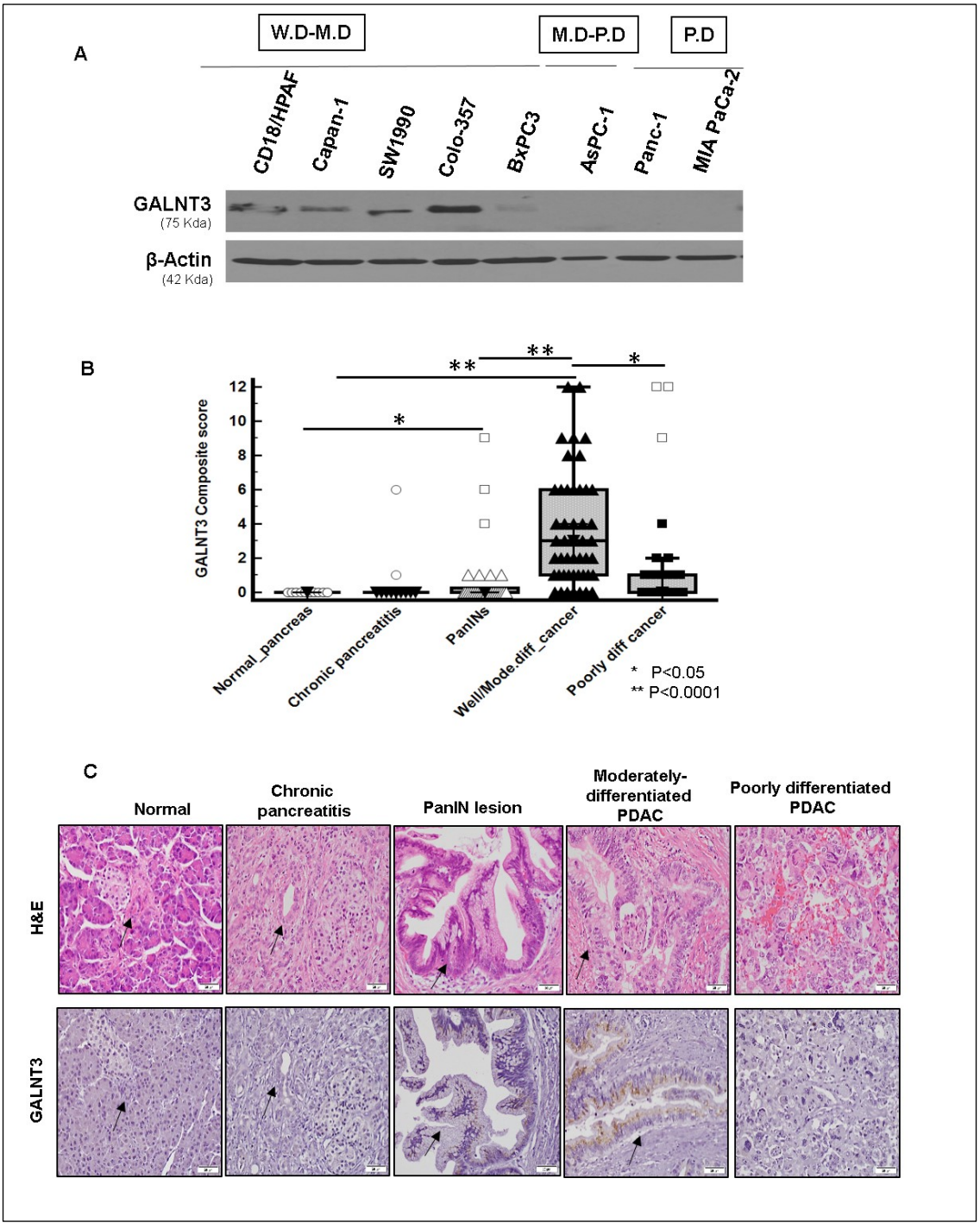
A
W.D-M.D
M.D-P.D
P.D
CD18/HPAF
Capan-1
SW1990
Colo-357
BxPC3
AsPC-1
Panc-1
MIA PaCa-2
GALNT3
(75 Kda)
β-Actin
(42 Kda)
B
GALNT3 Composite score
Normal_pancreas
Chronic pancreatitis
PanINs
Well/Mode.diff_cancer
Poorly diff cancer
* P<0.05
** P<0.0001
C
Normal
Chronic pancreatitis
PanIN lesion
Moderately-differentiated PDAC
Poorly differentiated PDAC
H&E
GALNT3

Figure 3.2 Altered expression of poorly differentiated PDAC cell markers in GALNT3 knockdown cells: (A) Stable knockdown of GALNT3 was carried out using GALNT3 specific shRNA in four different PDAC cells-CD18/HPAF, BxPC3, Capan-1 and T3M4. Beta-actin was used as a loading control. **(B)** VVA lectin blot demonstrates decrease of Tn carbohydrate antigen in GALNT3 knockdown PDAC cells. **(C) and D)** Immunoblot analysis shows altered expression of differentiation markers with increased expression of Sox2 and decreased expression of SLe^a in GALNT3 knockdown PDAC cells.

Figure 3.2

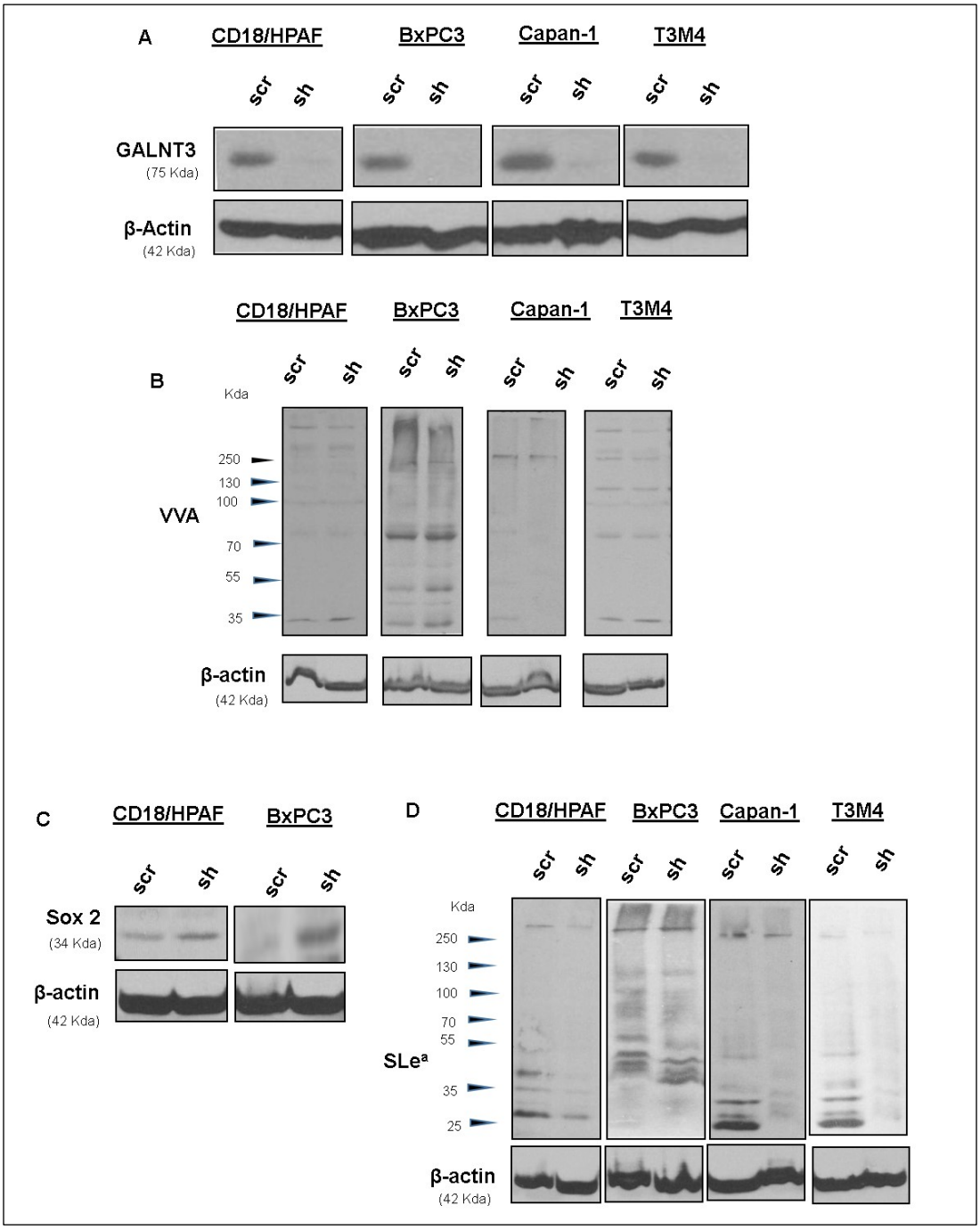
A
CD18/HPAF
BxPC3
Capan-1
T3M4
scr
sh
GALNT3
(75 Kda)
β-Actin
(42 Kda)
B
CD18/HPAF
BxPC3
Capan-1
T3M4
Kda
250
130
100
70
55
35
VVA
β-actin
(42 Kda)
C
CD18/HPAF
BxPC3
Sox 2
(34 Kda)
β-actin
(42 Kda)
D
CD18/HPAF
BxPC3
Capan-1
T3M4
Kda
250
130
100
70
55
35
25
SLeᵃ
β-actin
(42 Kda)

Figure 3.3 Effect of GALNT3 knockdown on growth and proliferation of PDAC cells: **(A)** Bar graph representing significant increase in proliferation of GALNT3 knockdown CD18/HPAF cells ($p < 0.001$) as demonstrated by WST-1 cell proliferation reagent. **(B)** Representative pictures of colony formation assay in CD18/HPAF and BxPC3 cells show significant increase in number of colonies ($p < 0.001$) in GALNT3 knockdown PDAC cells. **(C)** Increased expression of cell cycle regulatory protein Cyclin A in GALNT3 knockdown cells.

Figure 3.3

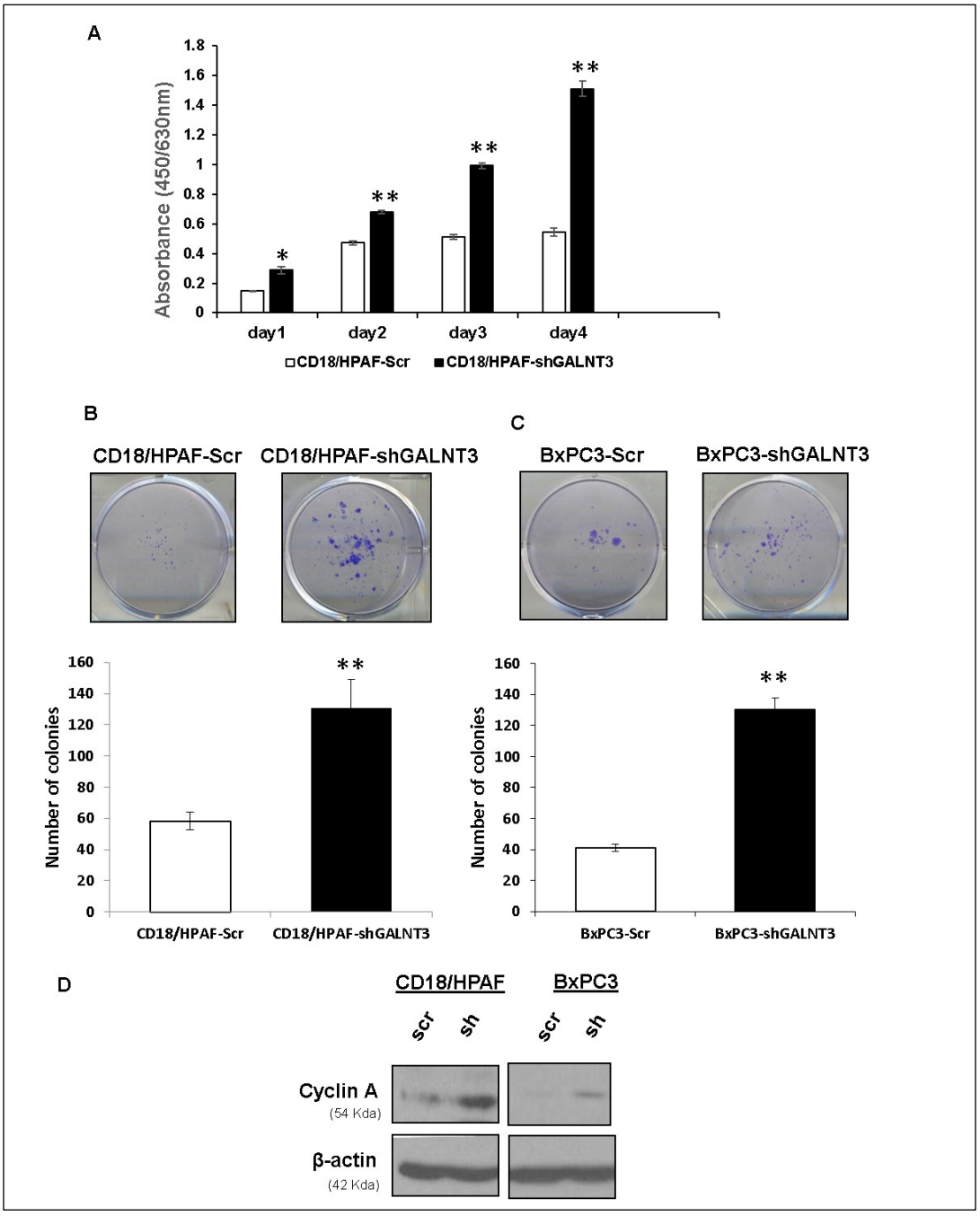
A
Absorbance (450/630nm)
1.8
1.6
1.4
1.2
1
0.8
0.6
0.4
0.2
0
*
**
**
**
day1
day2
day3
day4
CD18/HPAF-Scr
CD18/HPAF-shGALNT3
B
CD18/HPAF-Scr
CD18/HPAF-shGALNT3
C
BxPC3-Scr
BxPC3-shGALNT3
Number of colonies
160
140
120
100
80
60
40
20
0
**
CD18/HPAF-Scr
CD18/HPAF-shGALNT3
Number of colonies
160
140
120
100
80
60
40
20
0
**
BxPC3-Scr
BxPC3-shGALNT3
D
CD18/HPAF
BxPC3
scr
sh
scr
sh
Cyclin A
(54 Kda)
β-actin
(42 Kda)

Figure 3.4 Augmented motility of GALNT3-knockdown PDAC cells: (A) Increased percentage of wound-closure of GALNT3 knockdown cells after 24 hours. Marked areas show places of wound closure in scramble control and GALNT3-knockdown cells. Bar graphs represent a significant increase in the percentage of wound-closure in GALNT3-knockdown CD18/HPAF and BxPC3 cells ($p < 0.05$ for CD18/HPAF, $p < 0.001$ for BxPC3 PDAC cells). **(B)** Altered expression of EMT markers in GALNT3 knockdown PC cells.

Figure 3.4

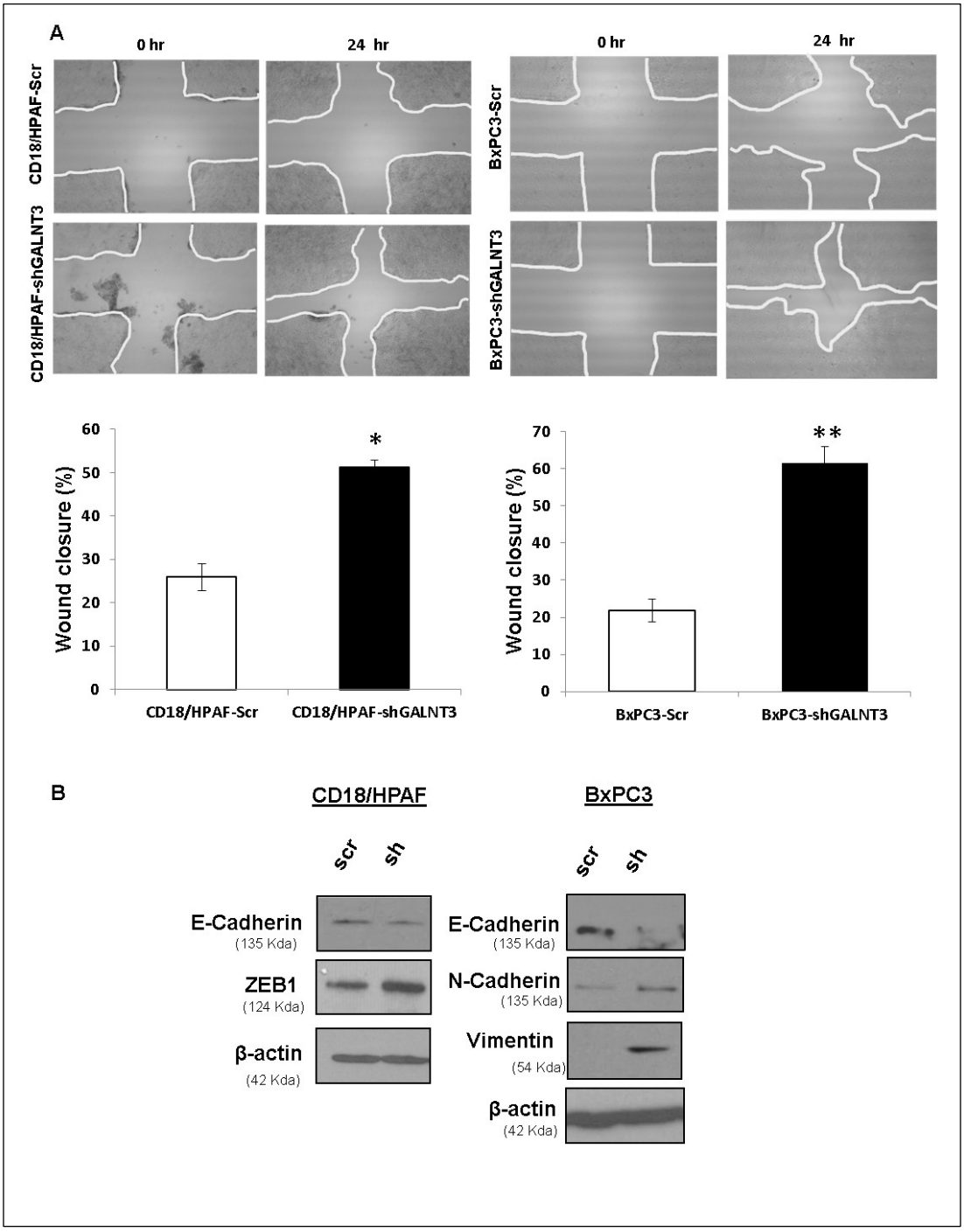
A
0 hr
24 hr
0 hr
24 hr
CD18/HPAF-Scr
CD18/HPAF-shGALNT3
BxPC3-Scr
BxPC3-shGALNT3
Wound closure (%)
60
50
40
30
20
10
0
*
CD18/HPAF-Scr
CD18/HPAF-shGALNT3
Wound closure (%)
70
60
50
40
30
20
10
0
**
BxPC3-Scr
BxPC3-shGALNT3
B
CD18/HPAF
BxPC3
scr
sh
scr
sh
E-Cadherin
(135 Kda)
ZEB1
(124 Kda)
β-actin
(42 Kda)
E-Cadherin
(135 Kda)
N-Cadherin
(135 Kda)
Vimentin
(54 Kda)
β-actin
(42 Kda)

Figure 3.5 Altered morphology and increased adhesion of GALNT3-knockdown cells to endothelium monolayer: (A) EMT-like morphological changes in GALNT3 knockdown CD18/HPAF and BxPC3 PDAC cells. **(B)** Increased expression of metastatic SLe^x carbohydrate epitope in GALNT3-knockdown PDAC cells. **(C)** Bar graphs represent significant increase in percentage adhesion of GALNT3 knockdown cells to endothelial monolayer ($p < 0.001$)**.** Representative immunofluorescent images showing increased adhesion of GALNT3 knockdown cells to endothelium monolayer as compared to scrambled control cells.

Figure 3.5

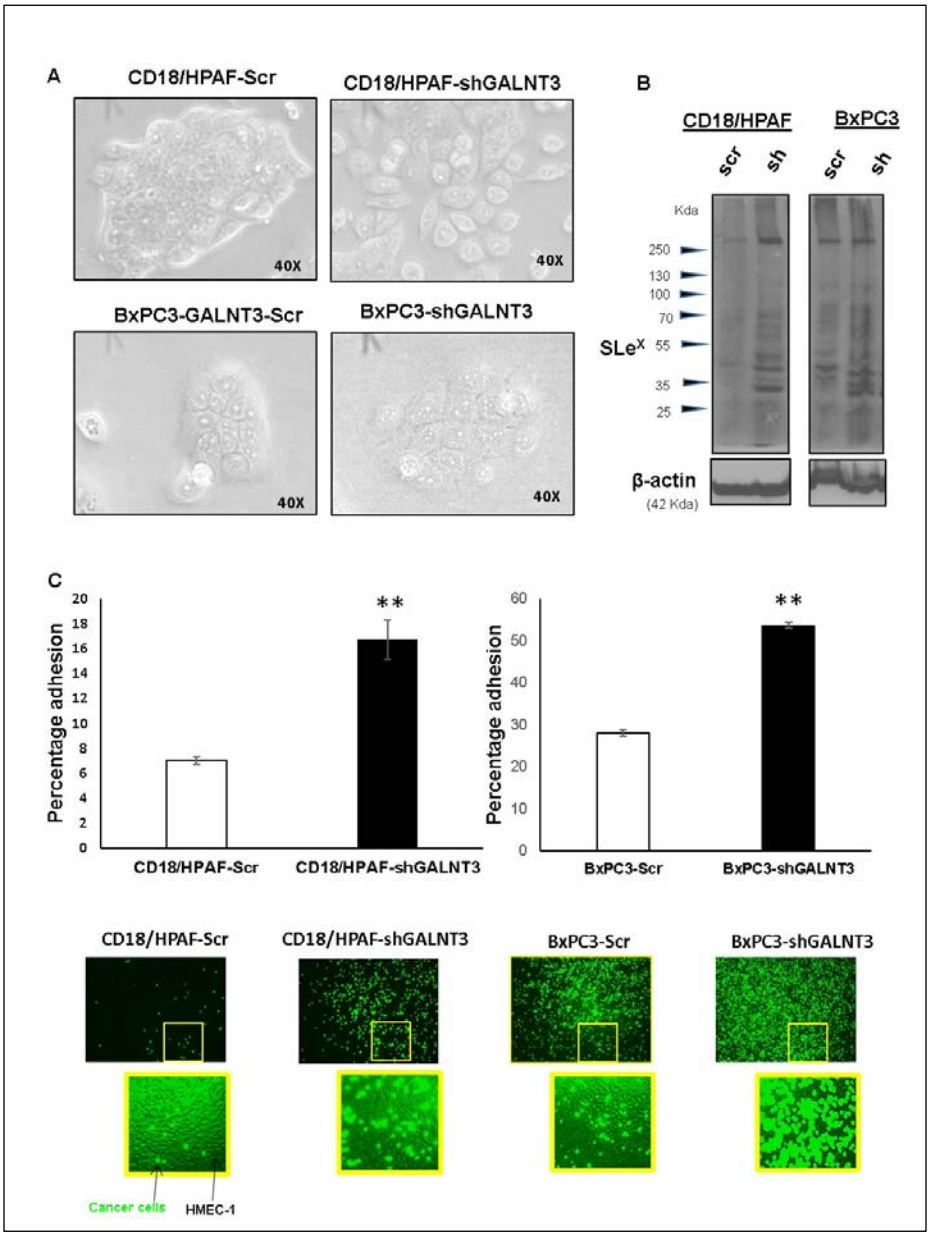
A
CD18/HPAF-Scr
CD18/HPAF-shGALNT3
40X
40X
BxPC3-GALNT3-Scr
BxPC3-shGALNT3
40X
40X
B
CD18/HPAF
BxPC3
scr
sh
scr
sh
Kda
250
130
100
70
SLeX
55
35
25
β-actin
(42 Kda)
C
Percentage adhesion
20
18
16
14
12
10
8
6
4
2
0
**
CD18/HPAF-Scr
CD18/HPAF-shGALNT3
Percentage adhesion
60
50
40
30
20
10
0
**
BxPC3-Scr
BxPC3-shGALNT3
CD18/HPAF-Scr
CD18/HPAF-shGALNT3
BxPC3-Scr
BxPC3-shGALNT3
Cancer cells
HMEC-1

Figure 3.6 Increased phosphorylation and altered glycosylation of members of the ErbB family of proteins in GALNT3-knockdown cells: (A) GALNT3 knockdown PDAC cells were associated with increase in phosphorylated forms of ErbB family of receptors such as EGFR, Her2, and Her3. **(B)** Lysates collected from scrambled control and GALNT3 knockdown cells were used for pull-down assays using biotin-conjugated VVA and PNA lectins. Immunoblotting of pulled down precipitates with biotinylated VVA and PNA lectins revealed effective pull-down of Tn and T carbohydrate antigens respectively. Further immunoblotting of pull-down lysates with anti-EGFR and Her2 antibodies demonstrated increase in Tn carbohydrate antigen association with EGFR and Her2 in GALNT3-knockdown CD18/HPAF and BxPC3 cells compared to scramble control cells. GALNT3 knockdown BxPC3 cells also displayed increased expression of T carbohydrate antigen on EGFR and Her2 as compared to scrambled control cells.

Figure 3.6

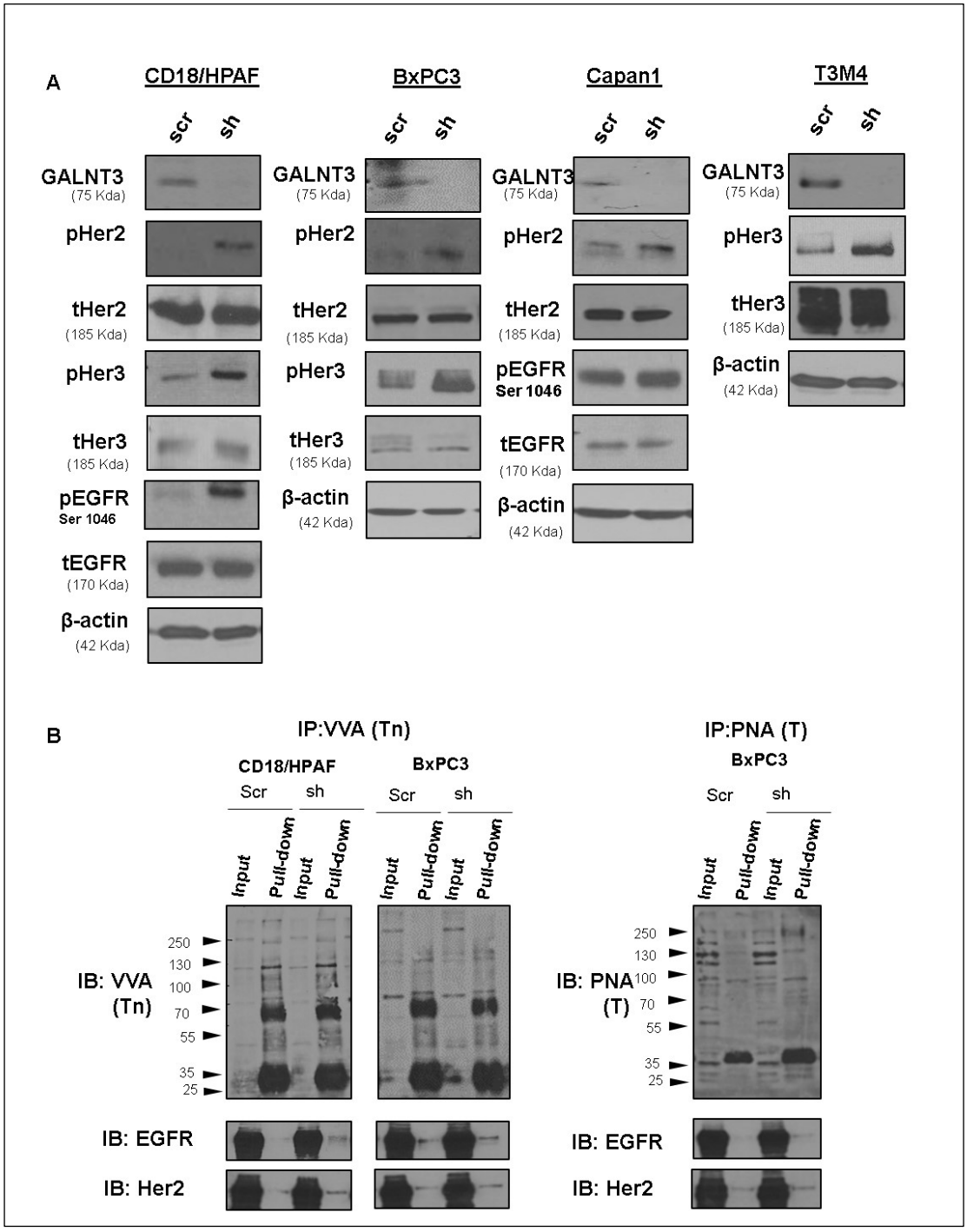
A
CD18/HPAF
BxPC3
Capan1
T3M4
scr
sh
GALNT3 (75 Kda)
pHer2
tHer2 (185 Kda)
pHer3
tHer3 (185 Kda)
pEGFR Ser 1046
tEGFR (170 Kda)
β-actin (42 Kda)
B
IP:VVA (Tn)
IP:PNA (T)
CD18/HPAF
BxPC3
Scr
sh
Input
Pull-down
IB: VVA (Tn)
IB: PNA (T)
250
130
100
70
55
35
25
IB: EGFR
IB: Her2

Figure 3.7 Schematic illustration describing the impact of loss of GALNT3 on PDAC: Reduced expression of GALNT3 was observed in poorly differentiated PDAC tissues as compared to well-differentiated PDAC**.** Therefore, the functional impact of loss of GALNT3 on PDAC cells was studied by stable knockdown of GALNT3 in PDAC cells. **a)** Knockdown of GALNT3 was associated with increased proliferation and motility. **b)** Further, GALNT3 knockdown PDAC cells showed increased adhesion to endothelial cells. **c)** Increased aggressiveness of GALNT3 knockdown PDAC cells was accompanied by increased phosphorylation of ErbB receptors. Altered glycosylation was also observed on ErbB receptors, which suggests the possible involvement of O-glycans in regulating ErbB signaling. Overall, loss of GALNT3 leads to increased aggressiveness of PDAC cells.

Figure 3.7

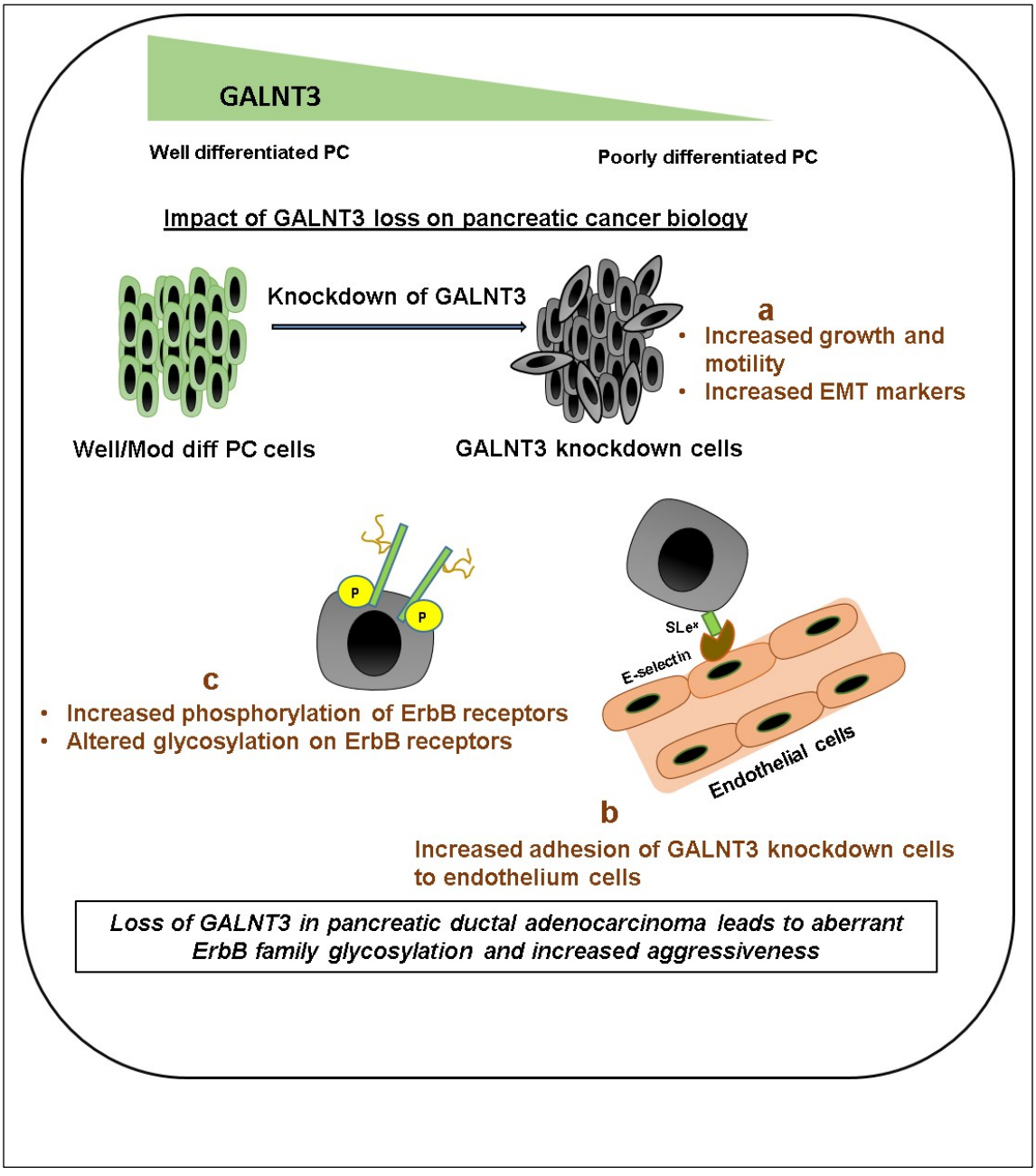
GALNT3
Well differentiated PC
Poorly differentiated PC
Impact of GALNT3 loss on pancreatic cancer biology
Knockdown of GALNT3
a
• Increased growth and motility
• Increased EMT markers
Well/Mod diff PC cells
GALNT3 knockdown cells
P
P
c
• Increased phosphorylation of ErbB receptors
• Altered glycosylation on ErbB receptors
SLex
E-selectin
Endothelial cells
b
Increased adhesion of GALNT3 knockdown cells to endothelium cells
Loss of GALNT3 in pancreatic ductal adenocarcinoma leads to aberrant ErbB family glycosylation and increased aggressiveness

Supplementary Figure legends

Supplementary Figure 3.1: Knockdown of GALNT3 expression in PC cells: (a) Confocal analysis showed loss of GALNT3 expression in poorly differentiated Panc-1 PC cells. **(b)** IHC pictures demonstrating no staining in pancreatic cancer tissue with IgG control whereas GALNT3 antibody showed granular GALNT3 staining confirming the specificity of GALNT3 antibody**. (c)** Low power views of GALNT3 immunohistochemical staining in pancreatic cancer progression tissues-upper panel represents H&E staining of normal, chronic pancreatitis, PanIN, moderately and poorly differentiated pancreatic cancer tissues, whereas lower panel represents the corresponding GALNT3 staining in these tissues (figure magnification-100X, scale bar represents 2000 um). **(d)** Real time validation of GALNT3 knockdown in pancreatic cancer cells- (CD18/HPAF, BxPC3, Capan-1 and T3M4**).**

Supplementary Figure 3.1

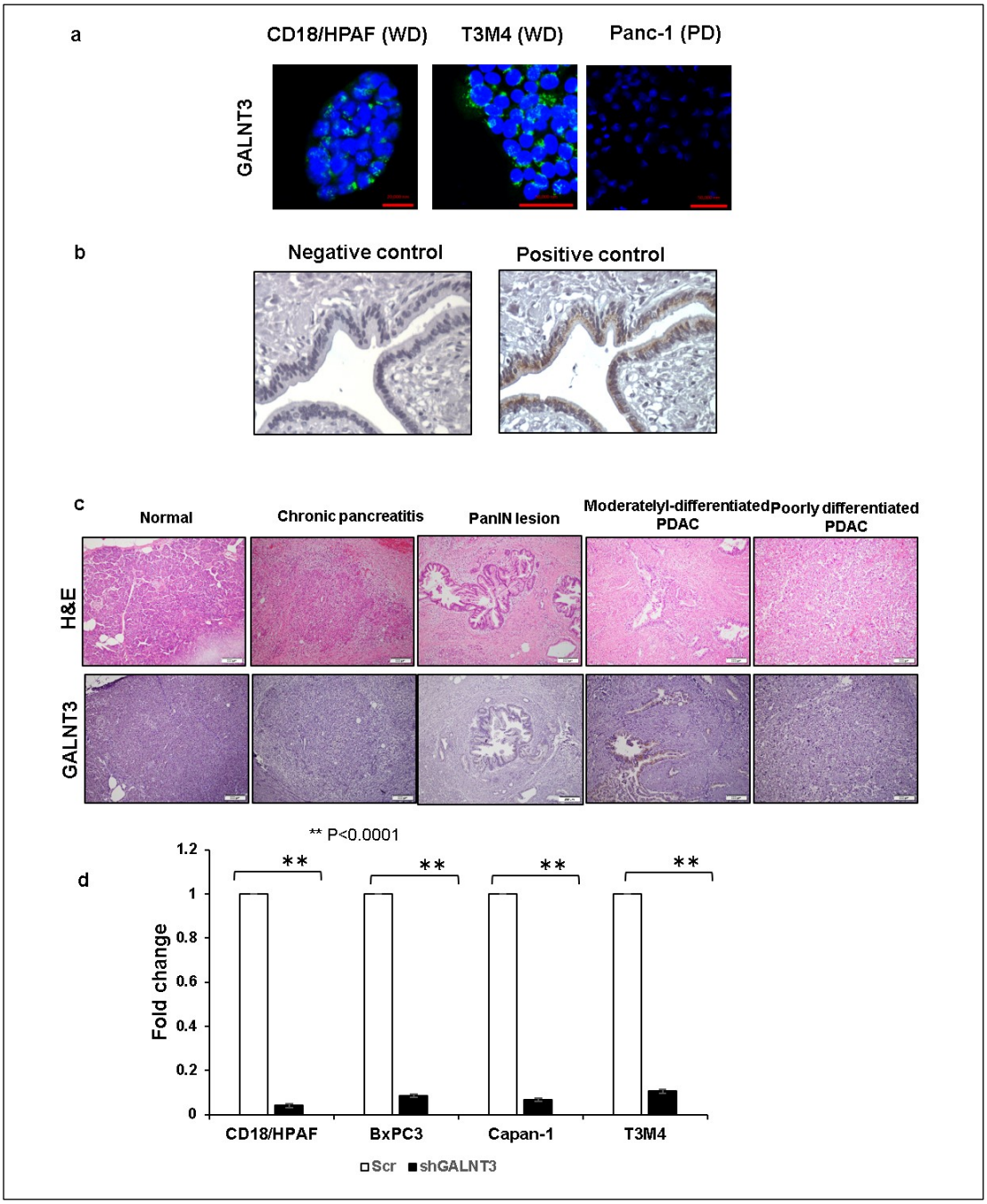

Supplementary Figure 3.2: Aggressive phenotype of GALNT3 knockdown pancreatic cancer cells (a) Bar diagram showing increased proliferation of GALNT3 knockdown Capan1 cells assayed by WST1 reagent. **(b)** Representative picture showing increased number of colonies in GALNT3 knockdown T3M4 cells. Bar plot depicts significant increase in number of colonies in GALNT3 knockdown T3M4 cells as compared to scramble control cells. **(c)** Western blot depicts decreased expression of E-cadherin and increased expression of N-cadherin in GALNT3 knockdown Capan-1 and T3M4 cells as compared to scramble control cells. **(d)** Increased expression of carbohydrate antigen STn in GALNT3-knockdown CD18/HPAF1 and Capan-1 cells. **(e)** Increased mRNA expression of N-cadherin and vimentin in GALNT3 knockdown cells, whereas expression of E-cadherin is decreased.

Supplementary Figure 3.2

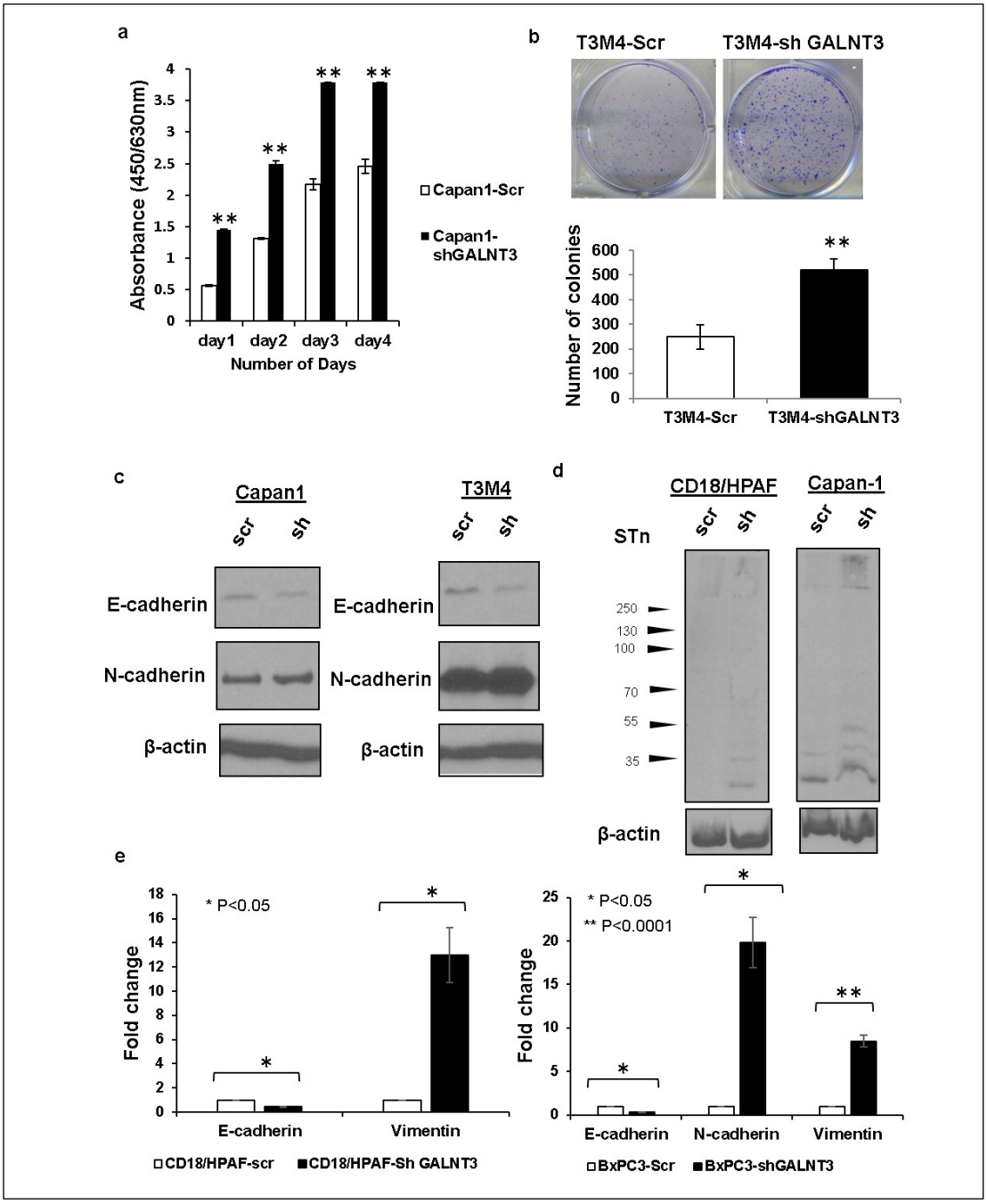

Supplementary Figure 3.3: Compensatory increase of several GALNTs in GALNT3 knockdown pancreatic cancer cells. Real time PCR analysis demonstrates upregulation of several GALNT genes in GALNT3-knockdown PC cells.

Supplementary Figure 3.3

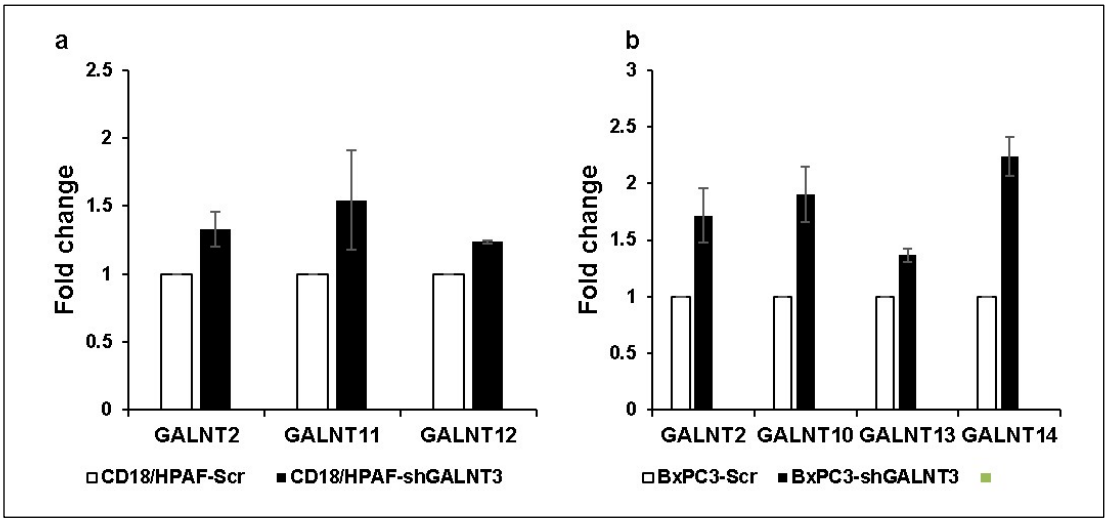

Table 3.1: GALNT3 staining in normal, chronic pancreatitis, PanINs and PDAC.

Group	Number	Staining intensity				Mean composite score
		0 (negative)	1 (weak)	2 (moderate)	3 (strong)	
Normal	10	0	0	0	0	0
Chronic pancreatitis	11	9 (81.8%)	1 (9.01%)	1(9.01 %)	0	0.63
PanINs (1/2/3)	29	22 (75.8%)	5 (17.2%)	1 (3.4%)	1 (3.4%)	0.79
Well/moderate differentiated PDAC	48	7 (14.5%)	16 (33.3%)	19 (39.5%)	6 (12.5%)	3.60
Poor differentiated PDAC	26	15 (57.6%)	6 (23.0%)	2 (7.69%)	3 (11.5%)	1.76

CHAPTER 4

Functional implications of knockout of C1GALT1 in pancreatic ductal adenocarcinoma

1. Synopsis

Aberrant expression/activity of O-glycosyltransferases during malignant conditions often result in impaired O-glycosylation and generation of truncated carbohydrate structures, also known as tumor-associated carbohydrate antigens (TACA) [1]. Abnormal expression of some of these truncated carbohydrate antigens such as Tn, STn is commonly observed in several malignancies including pancreatic ductal adenocarcinoma (PDAC) [2, 3]. Elevated expression of Tn has been attributed to inactive Core 1 β1, 3-Galactosyltransferase (C1GALT1) [4, 5]. C1GALT1 catalyzes the second step of mucin-type O-glycosylation by the addition of galactose to N-acetylgalactosamine (Tn) that forms Core 1 structure, which is usually elongated to several carbohydrate structures [6]. Functional C1GALT1 requires a molecular chaperone, Cosmc for its function [7]. Several studies have reported that loss of Cosmc in PDAC leads to inactive C1GALT1 and increased aggressiveness [8, 9]. However, the precise role of C1GALT1 mediated aberrant glycosylation in PDAC growth and metastasis remains unexplored. We sought to address the functional involvement of loss of C1GALT1 in PDAC aggressiveness by the generation of CRISPR/Cas9 C1GALT1 knockout (KO) PDAC cells. Knockout of C1GALT1 in PDAC cells lead to truncated glycophenotype and increased aggressiveness of PDAC cells. C1GALT1 KO PDAC cells also showed increased tumor growth and metastasis in orthotopic implantation studies. Mechanistic studies identified that knockout of C1GALT1 induced glycosylation changes on MUC16, which could drive increased tumorigenicity and metastasis possibly via increased expression of pAkt and vimentin.

2. Background and Rationale

Mucin-type O-glycosylation is the predominant form of O-glycosylation that involves a cascade of glycosyltransferases [10]. Sequential action of diverse glycosyltransferases that adds specific carbohydrate moieties results in the formation of mature O-glycans. Core-1 β-3 galactosyltransferase (C1GALT1) is one of the O-glycosyltransferases that catalyze the second step of O-glycosylation, wherein it adds galactose residue to first sugar, N-acetylgalactosamine/Tn, resulting in the formation of core-1/T carbohydrate structure [6]. Extension of core-1 carbohydrate structures by other glycosyltransferases results in core-2 carbohydrate structures. Functional C1GALT1 requires a molecular chaperone known as Cosmc (Core 1 β3-galactosyltransferase-specific molecular chaperone), which assists in its correct folding inside ER [7]. Dysfunctional Cosmc results in loss of activity of C1GALT1 and has been linked to several pathological states such as Tn syndrome, IgA nephropathy, and cancer [11]. Inactive C1GALT1 results in incomplete glycosylation and production of truncated Tn (GalNAcα-O-Ser/Thr) carbohydrate structure. Truncated Tn carbohydrate antigen can also be modified by sialylation by α-2, 6-sialyltransferase, ST6GalNAc-1, to form STn [5]. Increased expression of both the truncated carbohydrate antigens, Tn and STn, has been observed in several malignancies including PDAC [2, 12].

Prior studies in PDAC have indicated that loss of Cosmc (core 1 β3-Gal-T-specific molecular chaperone) via promoter hypermethylation leads to increased expression of truncated glycans and increased aggressiveness [8, 9]. However, loss of Cosmc could have other potential effects on PDAC cells. Hence, under cancerous conditions, it is important to understand the specific contribution of C1GALT1 mediated aberrant glycosylation in PDAC. Therefore, using CRISPR/Cas9 approach, we identified that

knockout of C1GALT1 caused aberrant glycosylation and increased tumorigenesis and metastasis. Mechanistic studies indicate that loss of C1GALT1 caused a remarkable increase in Tn on MUC16. Intriguingly, MUC16 is a membrane-bound mucin that originates *de novo* in PDAC and its expression increases progressively in PDAC [13, 14]. The mechanistic role of MUC16 in PDAC growth and metastasis has been well illustrated by our group and other studies [13-15]. Recent studies from our group have illustrated that MUC16 is one of the heavily glycosylated mucins and interacts with galectin-1 and galectin-3 [16]. Notably, mucin interaction to these lectins is facilitated by truncated carbohydrate antigens such as Tn and has been implicated in cancer metastasis [17]. Increased Tn on MUC16 might enhance its interaction with galectin or other carbohydrate binding proteins. Therefore, our studies conclude that loss of C1GALT1 in PDAC drives increase PDAC tumorigenesis and metastasis possibly via aberrant glycosylation on MUC16.

3. Results

A. Loss of expression of C1GALT1 in PDAC patient samples

Real-time PCR analysis was performed using RNA isolated from PDAC tissues to examine the expressional variation of C1GALT1. PCR results demonstrated loss of C1GALT1 in the majority of PDAC samples examined (**Figure 4.1A**). Further, histochemical analysis of C1GALT1 expression was performed in several PDAC samples collected via Whipple procedure. Well and poorly differentiated regions of PDAC were scored independently for C1GALT1 expression. Trace to weak staining was observed in the majority of neoplastic ducts in well-differentiated PDAC tissues. Interestingly, most poorly differentiated PDAC areas stained negative for C1GALT1 (**Figure 4.1B**). The

C1GALT1 histochemical score was significantly reduced in poorly differentiated PDAC samples in comparison to well-differentiated PDAC tissues (**Figure 4.1B**). These results suggest differential expression of C1GALT1 in PDAC, where loss of C1GALT1 expression was observed in poorly differentiated PDAC. Our findings are in accordance with prior studies that have also reported a loss of inactive T-synthase (via Cosmc hypermethylation) in some PDAC samples [9].

B. Decreased expression of C1GALT1 with oncogenic transformation of normal pancreatic epithelial cells

In order to determine whether oncogenic transformation affects C1GALT1 expression, lysates from well characterized immortalized human nestin-positive normal pancreatic epithelial cells (HPNE) and fully transformed HPNE cells (hTERT-HPNE-E6/E7/st-KRAS$^{(G12D)}$) were probed for C1GALT1 using western blotting.[18]. Oncogenic transformation of HPNE cells was associated with decreased expression of C1GALT1 (**Figure 4.2**).

D. Truncated glycan signature with CRISPR/Cas9 KO of C1GALT1 in PDAC cells

To explore the functional role of C1GALT1, knockout of C1GALT1 was carried in authenticated PDAC cells (T3M4, CD18/HPAF, and SW1990 cells) using CRISPR/Cas9-based genome editing. Western blotting demonstrated complete knockout of C1GALT1 in CRISPR/Cas9 KO clones as compared to untransfected control cells (**Figure 4.3A**). Further, Sanger sequencing of T3M4 knockout cells revealed genetic insertion as compared to the wild-type control cells (**Figure 4.3B**).

Deletion of C1GALT1 in the knockout cells was further confirmed by C1GALT1 enzymatic assay using benzyl-α-GalNAc substrate (**Figure 4.4**). Addition of galactose to this substrate (brought by C1GALT1 activity) was completely abolished in KO clones as compared to control cells. Formation of core-1 glycan structures and extended core-1 structures was seen in wild-type control cells. However, KO clones completely lack these structures. Altogether, these results indicate effective knockout of C1GALT1 expression and activity in KO clones as compared to wild-type controls.

We next evaluated the glycosylation profile of C1GALT1 KO PDAC cells. We observed increased expression of Tn and STn in all the KO clones as compared to wild – type control (**Figure 4.5A**). VVA fluorescein staining further confirmed increased expression of Tn and STn carbohydrate antigen (**Figure 4.5B**). Comprehensive analysis of the effect of C1GALT1 on O-glycan biosynthetic pathways was further performed using Fourier transform ion cyclotron resonance mass spectrometry (FT-ICR MS). Here, we looked for secretory O-glycans in the culture supernatants collected from the control and KO clones. Several O-glycan peaks were observed in wild-type control cells, whereas KO cells completely lack these peaks (**Figure 4.6**).

E. Increase of ST6GalNAc-2 in C1GALT1 KO PDAC cells

Since ST6GalNAc-1 has been shown to catalyze the production of STn, we checked if increased production of STn is linked to increased expression of ST6GalNAc-1 (ST6 N-Acetylgalactosaminide Alpha-2,6-Sialyltransferase 1). Surprisingly, we observed decreased expression of ST6GalNAc-1 in KO clones as compared to wild-type control cells (**Figure 4.7A**). Studies have demonstrated that ST6GalNAc-II, another sialyltransferase, can also catalyze STn biosynthesis. We identified marginal increase of

ST6GalNAc-II in KO clones as compared to control cells (**Figure 4.7B**). ST6GalNAc-II might facilitate STn biosynthesis in absence of ST6GalNAc-I. However, this needs to be tested.

F. Loss of C1GALT1 resulted in increased migration of PDAC cells

Knockout of C1GALT1 induced formation of cellular protrusions such as lamellipodia, filopodia, and microspikes as demonstrated by F-actin staining (**Figure 4.8**). Since the formation of these dynamic cytoskeletal structures directs cancer cell migration, the effect of C1GALT1 knockout on cancer cell migration was examined using wound-healing assay (**Figure 4.9**). The wound-healing assay showed a significant increase in cell motility of C1GALT1 KO PDAC cells.

C. Decreased expression of C1GALT1 in highly migratory sublines of PDAC cells

Since knockout of C1GALT1 resulted in increased migration, we next examined if expression of C1GALT1 is modulated in highly migratory PDAC cells. Therefore, we developed an *in vitro* model of migration that comprises less to more migratory PDAC sublines. Serial migration assay was conducted to develop highly migratory sublines of T3M4, BxPC-3 and Colo-357 (**Figure 4.10A**). Briefly, the parental cells (P) were seeded in migration chambers and cells that had migrated after 24 hrs were collected by scraping them with sterile cotton swabs, which were then immersed in media to develop the migratory subline (M1). Subsequently, the M2 subline was developed from the M1 subline by carrying out its migration for 24 hrs. Series of migration assays with a gradual decrease of migration time (12hr, 6hr, and 3hr) resulted in the development of the highly migratory M3, M4 and M5 sublines. Migration potential of parental and these highly migratory T3M4

PDAC sublines was assessed using migration assay. Migration assay demonstrated increased migration of migratory sublines as compared to parental cells (**Figure 4.10B**). Further, altered morphology (increased presence of cellular protrusions) was seen in these migratory sublines as compared to parental cells (**Figure 4.10B**).

Expression of C1GALT1 was examined in the parental and the migratory sublines derived from T3M4, BxPC-3 and Colo-357 using western blotting. Expression of C1GALT1 was decreased in highly migratory M4 and M5 sublines as compared to parental cells in T3M4 and BxPC3 migratory model (**Figure 4.11A**). C1GALT1 expression was also decreased in highly migratory Colo-M1 and Colo-M2 cells as compared to parental cells (**Figure 4.11B**). These findings further suggests that loss of C1GALT1 expression is associated with increased migration.

G. *In vivo* studies using C1GALT1 KO cells showed increased tumorigenicity and metastasis

We next sought to assess the impact of C1GALT1 knockout on tumor growth and metastasis using orthotopic implantation mouse model, wherein wild-type and C1GALT1 KO T3M4 PDAC cells were implanted into the pancreas of nude mice. Mice were euthanized 4 weeks after orthotopic implantation and the formation of tumors and metastatic lesions was examined. Two independent orthotopic implantation studies were performed using two different C1GALT1 clones to explore the involvement of C1GALT1 KO clones on tumorigenicity and metastasis. Our first study utilized GFP and luciferase labeled wild-type and C1GALT1 KO clone-3 PDAC cells. Orthotopic results revealed a significant increase in tumor weight and increased metastasis to distant organs such as liver, lung, diaphragm and peritoneum (**Figure 4.12 A, B**).

To further validate our findings, we used wild-type and C1GALT1 KO clone-4. Orthotopic studies using this clone also demonstrated significant increases in tumor weight and increased metastasis (**Figure 4.13 A, B**). Altogether, *in vivo* orthotopic studies using wild-type and C1GALT1 KO clones indicates that KO of C1GALT1 contributes to increased tumorigenicity and metastasis of PDAC cells.

I. Differential glycosylation of MUC16 in C1GALT1KO PDAC cells

To delineate the molecular mediators that confer increased PDAC aggressiveness in C1GALT1 KO PDAC cells, we examined the expression of mucins. Mucins are the preferential substrates for C1GALT1 owing to the presence of central domain that contains PTS (proline, serine, and threonine) rich repeats. Some of the mucins such as MUC1, MUC4, and MUC16, are also widely recognized to play an important role in PDAC growth and metastasis.[19] We investigated the expression of these aforementioned mucins using western blotting. Western blot results demonstrate a remarkable shift in molecular weight of MUC16 (**Figure 4.14**). The MUC16 band was seen at lower molecular weight position in C1GALT1 KO cells as compared to wild-type cells. However, such a shift was not observed for MUC1 and MUC4.

Since glycosylation also contributes to the molecular weight of protein substrates, we investigated if the observed decrease in molecular weight of MUC16 is due to loss of extended glycan structures on MUC16. As C1GALT1 deficiency leads to loss of extended glycan structures with subsequent increase of truncated glycan structures such as Tn and STn, the presence of Tn glycan on MUC16 was determined using VVA (binds Tn) pull down assay. Lectin pull down assay using T3M4 wild-type and C1GALT1 KO lysates showed increased expression of Tn on MUC16 in C1GALT1 KO lysates as compared to

wild-type cells (**Figure 4.15 A**). These results suggest that loss of C1GALT1 leads to altered glycosylation on MUC16 with increased expression of Tn carbohydrate antigen

We further tested glycosylation alterations on MUC16 in C1GALT1 KO PDAC cells using enzymatic approaches, wherein we utilized glycosidases such as PNGase-F and α-2,3,6,8 neuraminidase (**Figure 4.15 B**). PNGase-F specifically excise N-glycans whereas, α-2,3,6,8 neuraminidase catalyzes the removal of all terminal and branched sialic acid residues. Lysates from wild-type and KO cells were treated with these enzymes and were probed with MUC16. PNGase-F treatment in wild-type and C1GALT1 KO lysates caused molecular shifts in bands that correspond to N-glycosylated MUC16. Similar kind of shifts was seen in wild-type and C1GALT1 KO lysates, suggesting that KO of C1GALT1 didn't alter N-glycosylation of MUC16. On the other hand, cleavage with neuraminidase resulted in increased intensity of MUC16 band in both wild-type and C1GALT1 KO lysates. This can possibly be explained due to increased exposure of epitopes after the release of sialic acid residues that caused increased binding of the MUC16 antibody (raised against the tandem repeat region of MUC16 that represents most of the O-glycosylated region). Hence, increased intensity regions represent a sialylated region of MUC16. Interestingly, the increase in intensity was seen at a lower position in C1GALT1 KO lysates as compared to wild-type lysates. This further suggests that the shift in molecular weight of MUC16 is caused by a decrease in O-glycosylation.

The aforementioned results explain that C1GALT1 KO caused a shift in molecular weight of MUC16 due to altered glycosylation. We also pulled down MUC4 from lysates collected from wild-type and C1GALT1 KO T3M4 cells and probed them with Tn and STn. Interestingly, pulled-down MUC4 from both wild-type and C1GALT1 KO lysates didn't show the presence of truncated glycans (**Figure 4.16**). This suggests that MUC4 in T3M4

PDAC might not possess truncated glycans. This can possibly explain why we didn't observe any shift in molecular weight of MUC4 in C1GALT1 KO cells. However, this doesn't indicate that MUC4 is not glycosylated and predominant glycotopes (could be core-3/4 carbohydrate structures) present on MUC4 in T3M4 PDAC cells need to be explored.

H. Differential upregulation of tumorigenic and metastatic pathways in C1GALT1 KO PDAC cells

To identify how altered glycosylation impacts tumor growth and metastasis, RNA-Seq analysis was conducted on control and C1GALT1 KO PDAC samples that identified pivotal molecular pathways involved in increased aggressiveness of C1GALT1 KO PDAC cells. RNA-Seq results revealed differentially expressed genes (log 2 fold upregulated/downregulated) in the C1GALT1 KO T3M4 cells in comparison with the wild-type (**Figure 4.17**). Significant upregulations of genes involved in migration and tumor growth was observed in C1GALT1 KO PDAC cells as compared to control cells (**Figure 4.17**). IPA analysis of these differentially expressed genes identified upregulation of pAkt pathway in KO cells as compared to control cells (**Figure 4.18**).

Further, using western blotting, we validated increased activation of oncogenic and migratory signaling pathways (as predicted by RNA-seq). We observed increased expression of phosphorylated forms of ErbB signaling proteins such as EGFR and Her2 in knockout clones as compared to wild-type cells. However, the total levels of these signaling proteins remain unchanged (**Figure 4.19A**). We also observed increased expression of α-4 integrin in C1GALT1 KO Clones. All of these signaling proteins have been shown to play an important role in PDAC growth and metastasis. Increased

activation of Akt (downstream effector of ErbB signaling) and FAK-Y925 (downstream effectors of integrin signaling) was also observed (**Figure 4.19A, B**). Furthermore, increased activation of these signaling proteins has been associated with altered expression of EMT markers. Remarkably, increased expression of mesenchymal marker vimentin was seen in C1GALT1 KO PDAC cells, whereas expression of epithelial marker ZO-1 was decreased in C1GALT1 KO PDAC cells.

J. Regulation of C1GALT1 by cytokines in the tumor microenvironment

We next wanted to understand if the C1GALT1 expression is modulated during disease progression as a subset of patients expressed C1GALT1. Since secretory factors in the tumor microenvironment have been shown to regulate glycosylation, we examined the impact of cytokines in the tumor microenvironment on C1GALT1 expression. Suzuki *et al.* demonstrated that IL-4 and IL-6 cytokines decrease C1GALT1 expression, which results in altered IgA1 glycosylation that is implicated in IgA nephropathy. We treated T3M4 PDAC cells with several inflammatory cytokines such as IFN-γ, TNF-α and different doses of IL-4 and IL-6 (25 ng/ml, 50 ng/ml, and 100 ng/ml) (**Figure 4.20**). IFN-γ and TNF-α caused a slight increase of C1GALT1 expression. A lower dose of IL-4 lead to slight increase of C1GALT1 expression, whereas higher doses of IL-4 resulted in decreased expression of C1GALT1. Interestingly, treatment with IL-6 resulted in a dose-dependent decrease of C1GALT1 expression, wherein maximum effect was observed at 100ng/ml.

4. Discussion

Altered expression/activity of O-glycosyltransferases has been observed in several malignancies including PDAC [20]. This results in altered glycophenotype that has been

implicated in tumor growth and metastasis [21]. Not much has been studied about O-glycosyltransferases that are linked with increased PDAC aggressiveness. We observed that O-glycosyltransferase, C1GALT1 is not expressed by some PDAC patients. Further, the C1GALT1 expression is dramatically decreased in poorly differentiated PDAC as compared to well-differentiated PDAC. Our results corroborate with previous studies focused on Cosmc that have also indicated loss of activity of O-glycosyltransferase, C1GALT1, in PDAC. Radhakrishnan et al. have identified hypermethylation of the promoter region of the C1GALT1 chaperone, Cosmc, in PDAC samples, which was associated with loss of C1GALT1 expression and subsequent increase of truncated O-glycans [9].

Apart from patient samples, we also observed decreased expression of C1GALT1 in oncogenic transformed HPNE cells (HPNE-E6/E7/St/KRAS) [18]. These results suggest that loss of C1GALT1 might be associated with increased aggressiveness of PDAC cells. Hence, to explore the functional impact of loss of C1GALT1 on PDAC aggressiveness, CRISPR/Cas9-mediated C1GALT1 knockout was carried out in PDAC cells. Using a C1GALT1 enzymatic assay, we found that KO cells does not synthesize core-1/extended core-1 structures. Since C1GALT1 catalyzes the elongation of Tn carbohydrate antigen to T carbohydrate/core-1 antigen in mucin-type O-glycosylation, we investigated if loss of C1GALT1 results in incomplete O-glycosylation. Lectin blotting and immunofluorescence revealed increased expression of Tn carbohydrate antigen. We also noticed increased expression of STn carbohydrate antigen. These results suggest that abrogation of C1GALT1 activity leads to increased expression of Tn and STn carbohydrate structures, which are commonly observed in cancer and have been implicated in increased growth and motility [2, 12, 22]. For instance, increased expression of STn in gastric cancer cells was associated with increased intraperitoneal metastasis [23]. Further, we noticed that

C1GALT1 KO PDAC cells have altered morphology with increased presence of cytoplasmic protrusions such as lamellipodia, fliopodia and microspikes. Organization of actin filaments into these cytoplasmic protrusions allows cancer cells to migrate, invade and hence successfully metastasize [24, 25]. We found increased migration of C1GALT1 KO cells as compared to control cells. In addition to this, we also observed decreased expression of C1GALT1 in highly migratory PDAC cells as compared to less migratory PDAC cells. Furthermore, orthotopic studies in nude mice demonstrated increased tumorigenicity and metastasis with knockout of C1GALT1. Our data are strongly supported by previous studies that have also linked altered glycosylation with increased metastasis [21, 26].

Given that knockout of C1GALT1 induced aberrant glycosylation, it is important to identify aberrantly glycosylated molecular substrates that drive the observed increase in PDAC aggressiveness. We focused on mucins, which are heavily glycosylated and play an important role in PDAC growth and metastasis [19]. Elevated expression of membrane and secretory mucins is one of the key features of PDAC. For instance, *de novo* expression of MUC4 and MUC16 has been observed in PDAC, wherein it leads to increased growth and metastasis [13, 14, 31]. Recently, using CRISPR/Cas9 knockout of MUC16, our group has recently shown the essential role of MUC16 in PDAC metastasis through activation of FAK signaling [16]. Further, the study also indicated MUC16 as one of the heavily glycosylated mucins, as knockout of MUC16 was associated with decreased expression of Tn and T carbohydrate antigens [16]. Using lectin-pull down and enzymatic assays, we found that knockout of C1GALT1 dramatically altered MUC16 glycosylation. In particular, increased expression of Tn was observed on MUC16.

RNA-seq analysis of C1GALT1 KO cells provided molecular insights into the mechanism involved in increased tumorigenicity and metastasis of C1GALT1 KO PDAC cells. Significant increase in migratory and tumorigenic genes was observed in KO PDAC cells as compared to parental cells. IPA analysis of RNA-seq data identified upregulation of PI3K/Akt pathway that has been implicated in PDAC growth and metastasis [30]. Consistent with these findings, we also observed activation of oncogenic signaling proteins (pEGFR, pHer2, pAkt) and altered expression of EMT markers (pFAK-Y925, α4 integrin, Vimentin and ZO-1) in C1GALT1 KO PDAC cells. Studies from several other groups and our group have illustrated the pivotal role of these signaling pathways in increased PDAC growth and metastasis [28, 29]. We observed a remarkable increase of vimentin expression in C1GALT1 KO cells, which might explain increased migration of C1GALT1 KO cells. Expression of this intermediate filament protein is upregulated during EMT and renders cancer cells with increased motility [27]. We speculate that increased tumorigenicity and metastasis could be attributed to aberrant glycosylation of MUC16, which caused increased activation of growth and metastatic pathways, possibly via increased interaction with growth receptors/signaling proteins. We have recently shown that MUC16 regulates PI3K/Akt signaling [16]. pAkt has been shown to phosphorylate vimentin that prevents its proteolytic degradation and hence mediates increase cancer cell migration [32]. However, the direct involvement of aberrantly glycosylated MUC16 in activation of this putative signaling pathway needs to be explored.

Altogether, our study has established that knockout of C1GALT1 in PDAC leads to increased tumorigenicity and metastasis possibly via altered glycosylation on MUC16 that can potentially activate oncogenic pAkt signaling, resulting in increased expression of vimentin and hence increased growth and metastasis.

Figure legends

Figure 4.1 Loss of expression of C1GALT1 in PDAC: (A) PCR analysis of C1GALT1 in PDAC patients demonstrates loss of C1GALT1 in the majority of PDAC patients examined. **(B**) ***Top Panel***: Scatter dot plot demonstrating significant decrease of C1GALT1 in poorly differentiated PDAC as compared to well differentiated PDAC. ***Bottom panel:*** Representative immunohistochemical pictures showing decreased C1GALT1 staining in poorly-differentiated PDAC as compared to well-differentiated. Weak C1GALT1 staining was also observed in normal pancreas. All the pictures were taken at 40X magnification. **P<0.005; by Mann Whitney test.

Figure 4.1

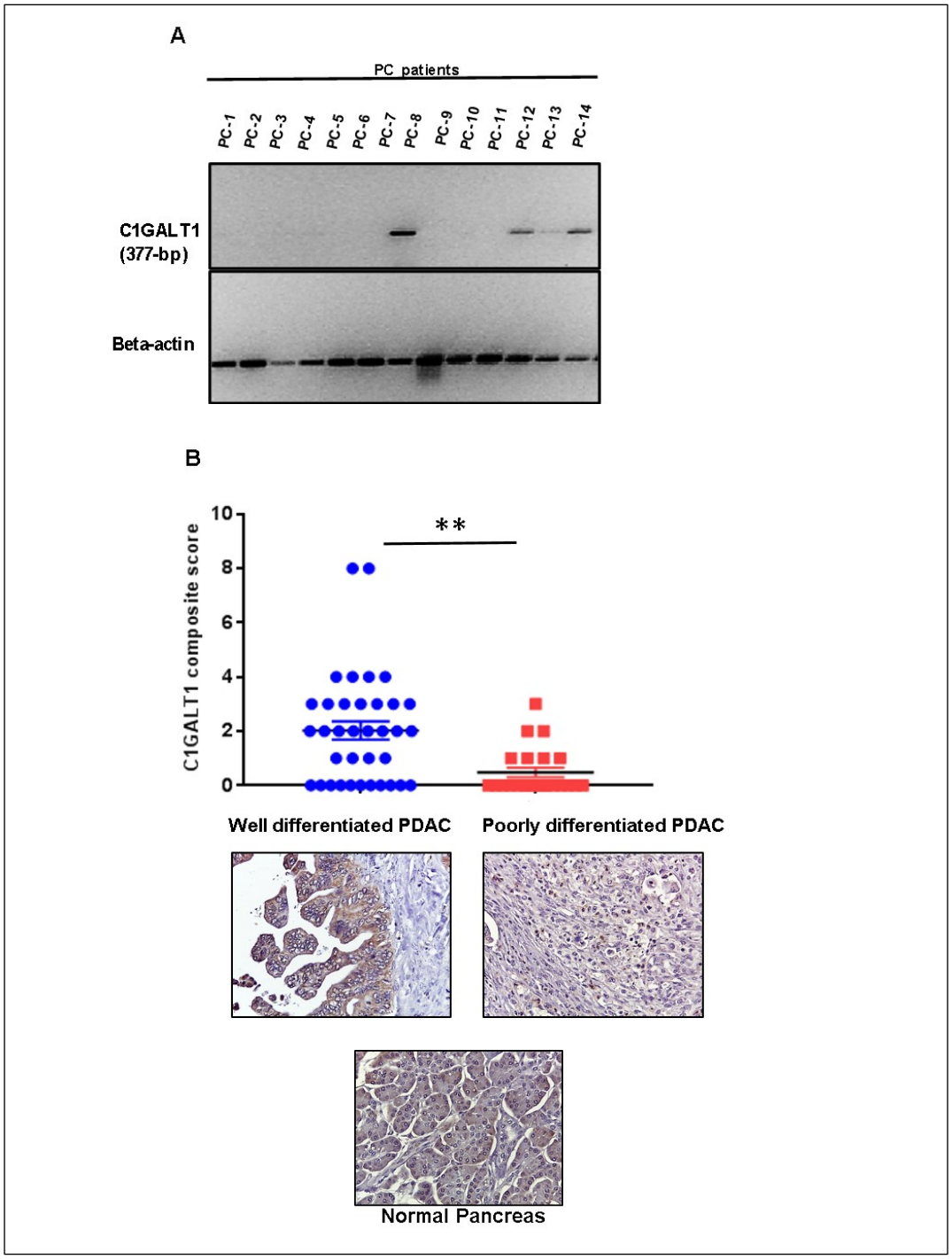
A
PC patients
PC-1
PC-2
PC-3
PC-4
PC-5
PC-6
PC-7
PC-8
PC-9
PC-10
PC-11
PC-12
PC-13
PC-14
C1GALT1
(377-bp)
Beta-actin
B
C1GALT1 composite score
10
8
6
4
2
0
**
Well differentiated PDAC
Poorly differentiated PDAC
Normal Pancreas

Figure 4.2 Decreased C1GALT1 expression in oncogenic transformed HPNE cells: Western blotting demonstrates decreased expression of C1GALT1 in oncogenic transformed HPNE cells (hTERT -HPNE-E6/E7/St/KRAS) as compared to untransformed HPNE (hTERT –HPNE) cells.

Figure 4.2

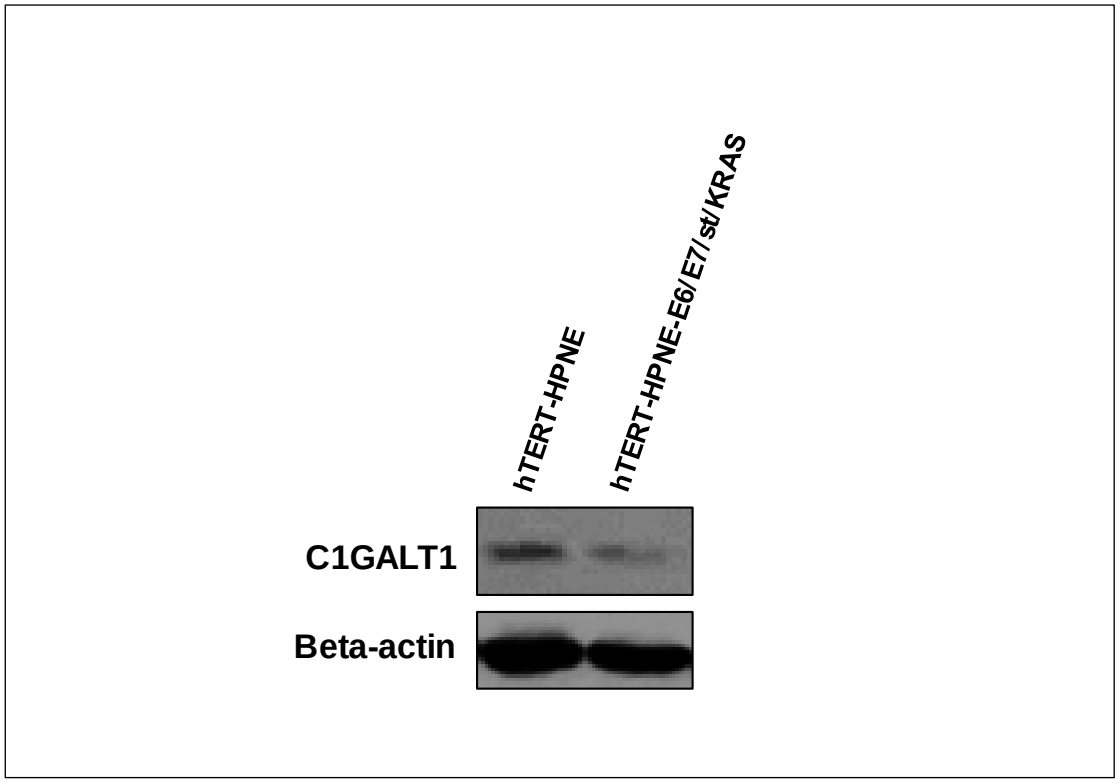

Figure 4.3 CRISPR/Cas9 Knockout of C1GALT1 in PDAC cells: (A) Western blotting demonstrates complete knockout of C1GALT1 in T3M4 and CD18/HPAF PDAC cells **(B)** Sanger sequencing reveals presence of insertion of adenosine nucleotide in guide RNA targeting region of T3M4 knockout PDAC cells as compared to wild type control cells.

Figure 4.3

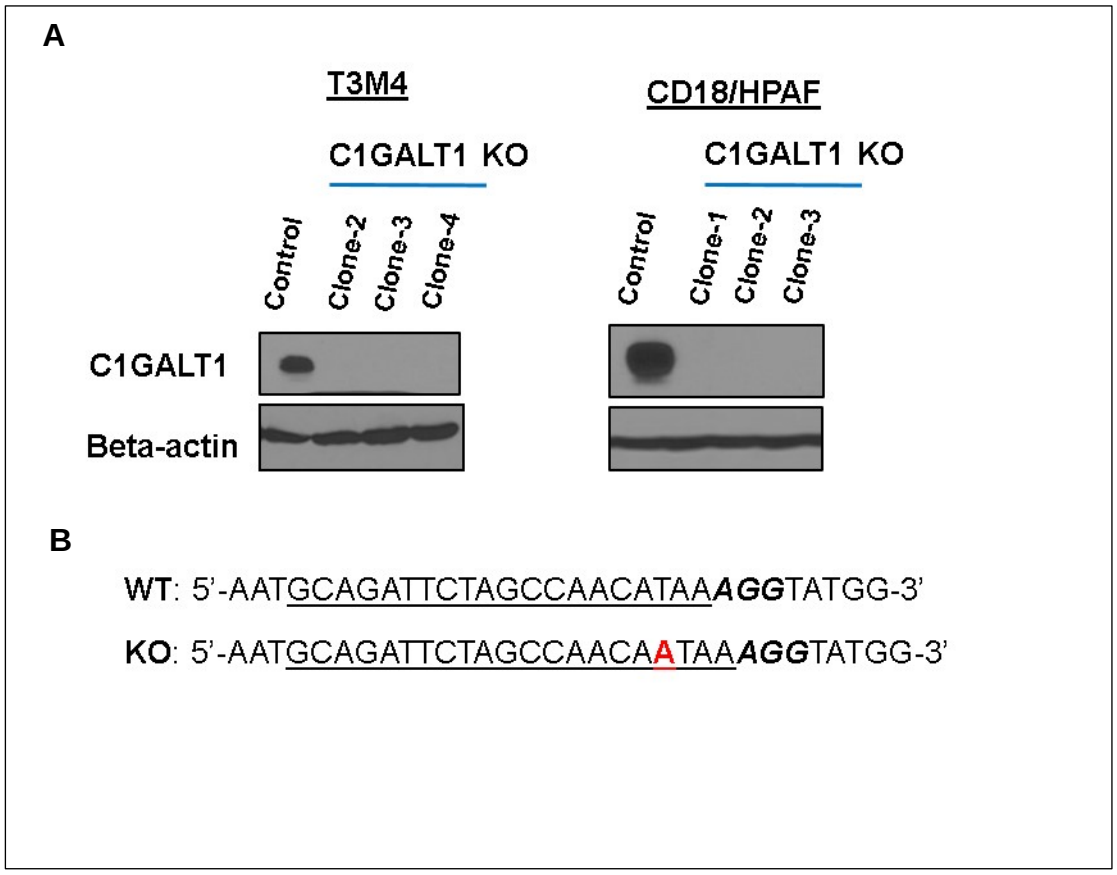
A
T3M4
C1GALT1 KO
Control
Clone-2
Clone-3
Clone-4
CD18/HPAF
C1GALT1 KO
Control
Clone-1
Clone-2
Clone-3
C1GALT1
Beta-actin
B
WT: 5'-AATGCAGATTCTAGCCAACATAAAGGTATGG-3'
KO: 5'-AATGCAGATTCTAGCCAACAATAAAGGTATGG-3'

Figure 4.4 Characterization of T3M4 knockouts: (A) Core1 β1,3GalT enzyme activity was assayed by mixing cell lysates from wild-type T3M4 cells and knockouts with substrate GalNAcα-O-Benzyl in the presence of UDP-Gal. Relative abundance of original substrate (top panel) and product (bottom panel) was quantified based on the area under the curve of the MS1 peak for the corresponding molecule. All structures were validated using MS/MS analysis. **(B)** Core 1 synthase enzyme activity in wild-type T3M4 cells (control) and three different knockouts (Clone 2-4). Absence of Galβ1,3GalNAcα-OBn product in T3M4-KO clones is indicated by asterisk. **(C)** Per-acetylated GalNAcα-OBn was fed to wild-type and C1GALT1 KO cells. Products collected from supernatant were assayed using LC-MS, with structure validation being performed using MS/MS analysis and existing knowledge of biochemistry. All glycans are depicted using Symbol Nomenclature for Glycans. **(D)** Nano-LC separation of various glycosides secreted from wild-type T3M4 cells. Knockout cells lacking Core1 β1,3GalT do not form any of these products.

Figure 4.4

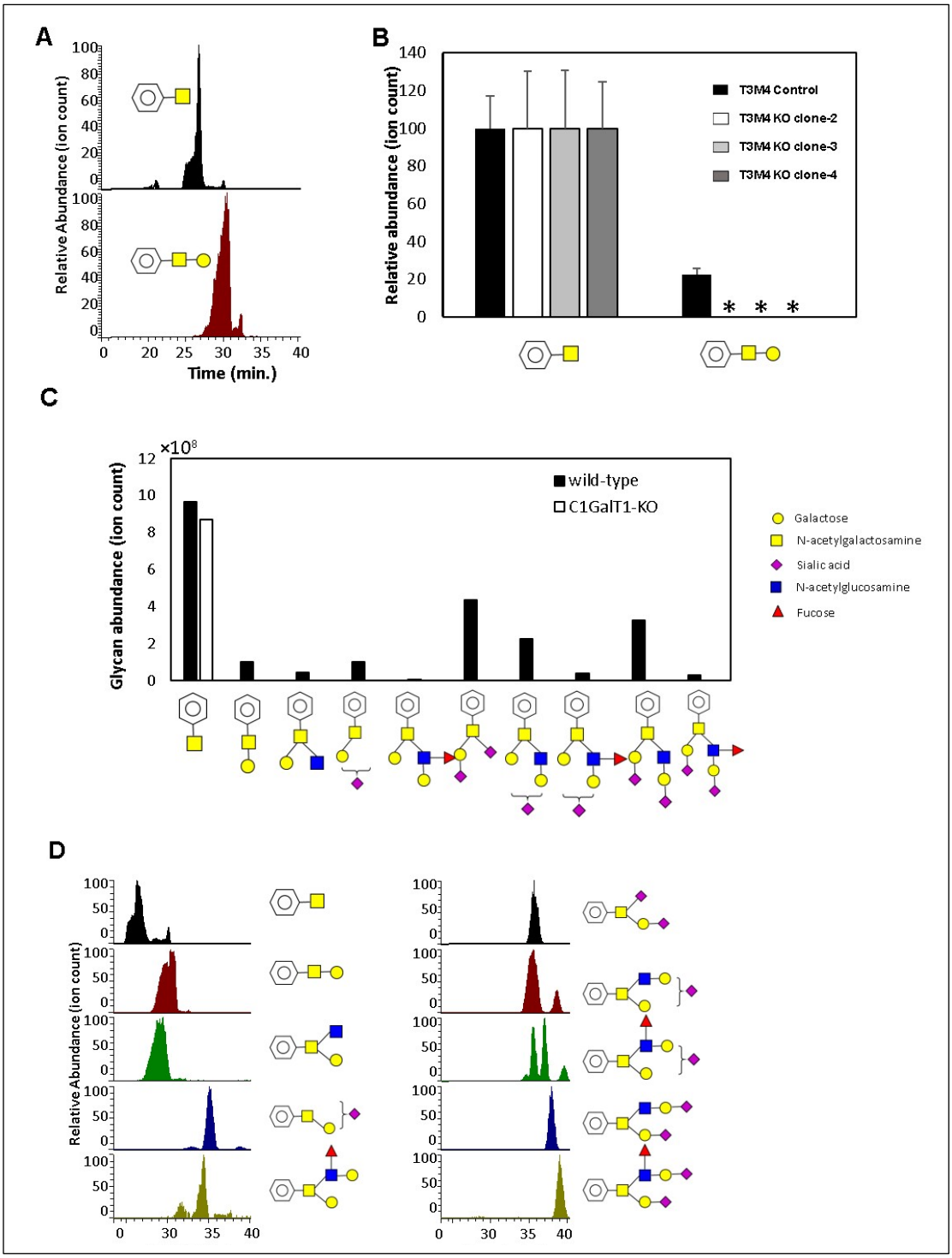
A
Relative Abundance (ion count)
Time (min.)
B
Relative abundance (ion count)
T3M4 Control
T3M4 KO clone-2
T3M4 KO clone-3
T3M4 KO clone-4
C
×10^8
Glycan abundance (ion count)
wild-type
C1GalT1-KO
Galactose
N-acetylgalactosamine
Sialic acid
N-acetylglucosamine
Fucose
D
Relative Abundance (ion count)

Figure 4.5 Aberrant glycosylation of C1GALT1 KO PDAC cells: (A) ***Upper panel:*** Lectin blotting demonstrates increased expression of Tn carbohydrate antigen in C1GALT1 KO clones as compared to control cells. ***Lower panel:*** Western blotting demonstrates increased expression of STn carbohydrate antigen in C1GALT1 KO clones as compared to control cells. **(B)** VVA Fluorescein staining revealed increased expression of Tn carbohydrate antigen in C1GALT1 KO clones as compared to control cells.

Figure 4.5

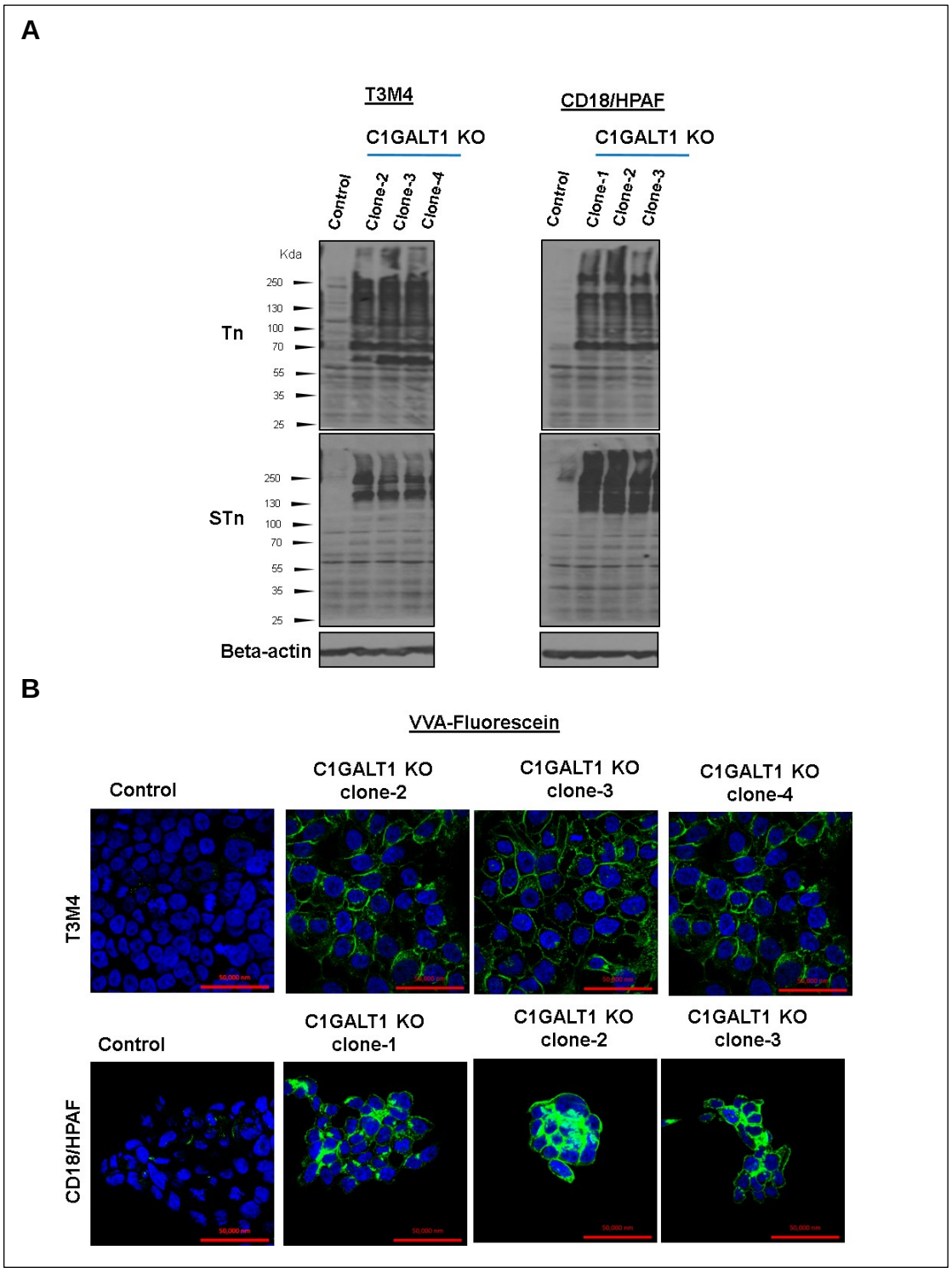
A
T3M4
C1GALT1 KO
Control
Clone-2
Clone-3
Clone-4
CD18/HPAF
C1GALT1 KO
Control
Clone-1
Clone-2
Clone-3
Kda
250
130
100
70
55
35
25
Tn
STn
Beta-actin
B
VVA-Fluorescein
Control
C1GALT1 KO clone-2
C1GALT1 KO clone-3
C1GALT1 KO clone-4
T3M4
Control
C1GALT1 KO clone-1
C1GALT1 KO clone-2
C1GALT1 KO clone-3
CD18/HPAF

Figure 4.6 Mass spectrometry analysis of O-glycan biosynthesis pathway in T3M4 cells: A. T3M4 cells were cultured with 50 μM per-acetylated GalNAcα-OBn for 72h. Glycosylated products synthesized on this substrate and secreted into culture media were analyzed using Fourier transform ion cyclotron resonance mass spectrometry (FT-ICR MS). A number of glycan peaks were observed in the wild-type control (panel ii, top) but not C1GALT1 knockout (panel ii, bottom) cells. Measured and theoretical monoisotopic masses are provided along with isotopic peak distribution for all carbohydrates. **B**. Potential biosynthetic pathway in wild-type T3M4 cells is illustrated based on knowledge of biochemistry and MS data.

Figure 4.6

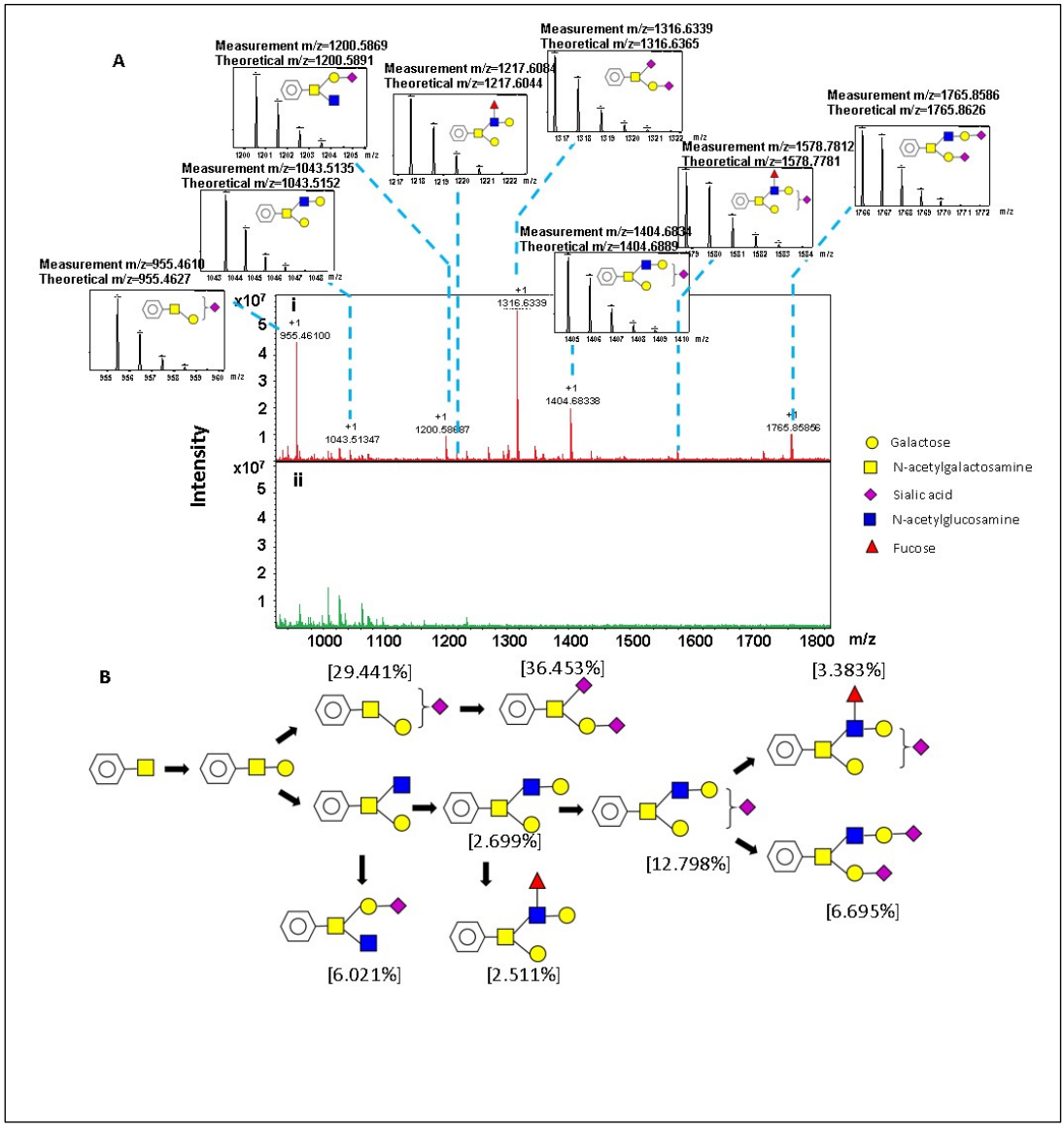
A
Measurement m/z=1200.5869
Theoretical m/z=1200.5891
Measurement m/z=1217.6084
Theoretical m/z=1217.6044
Measurement m/z=1316.6339
Theoretical m/z=1316.6365
Measurement m/z=1765.8586
Theoretical m/z=1765.8626
Measurement m/z=1578.7812
Theoretical m/z=1578.7781
Measurement m/z=1043.5135
Theoretical m/z=1043.5152
Measurement m/z=1404.6834
Theoretical m/z=1404.6889
Measurement m/z=955.4610
Theoretical m/z=955.4627
x10^7
i
955.46100
1316.6339
1404.68338
1200.58687
1043.51347
1765.85856
Intensity
x10^7
ii
1000 1100 1200 1300 1400 1500 1600 1700 1800 m/z
Galactose
N-acetylgalactosamine
Sialic acid
N-acetylglucosamine
Fucose
B
[29.441%]
[36.453%]
[3.383%]
[2.699%]
[12.798%]
[6.695%]
[6.021%]
[2.511%]

Figure 4.7 Altered expression of sialyltransferases in C1GALT1 KO PDAC cells: (A) RT-PCR analysis demonstrates a significant decrease in ST6GALNAC1 expression in C1GALT1 KO T3M4 PDAC cells as compared to control cells. **(B)** RT-PCR analysis demonstrates a significant increase in ST6GALNAC2 expression in C1GALT1 KO T3M4 PDAC cells as compared to control cells. *P<0.05, **P<0.005; by unpaired two-sided Student's t-test.

Figure 4.7

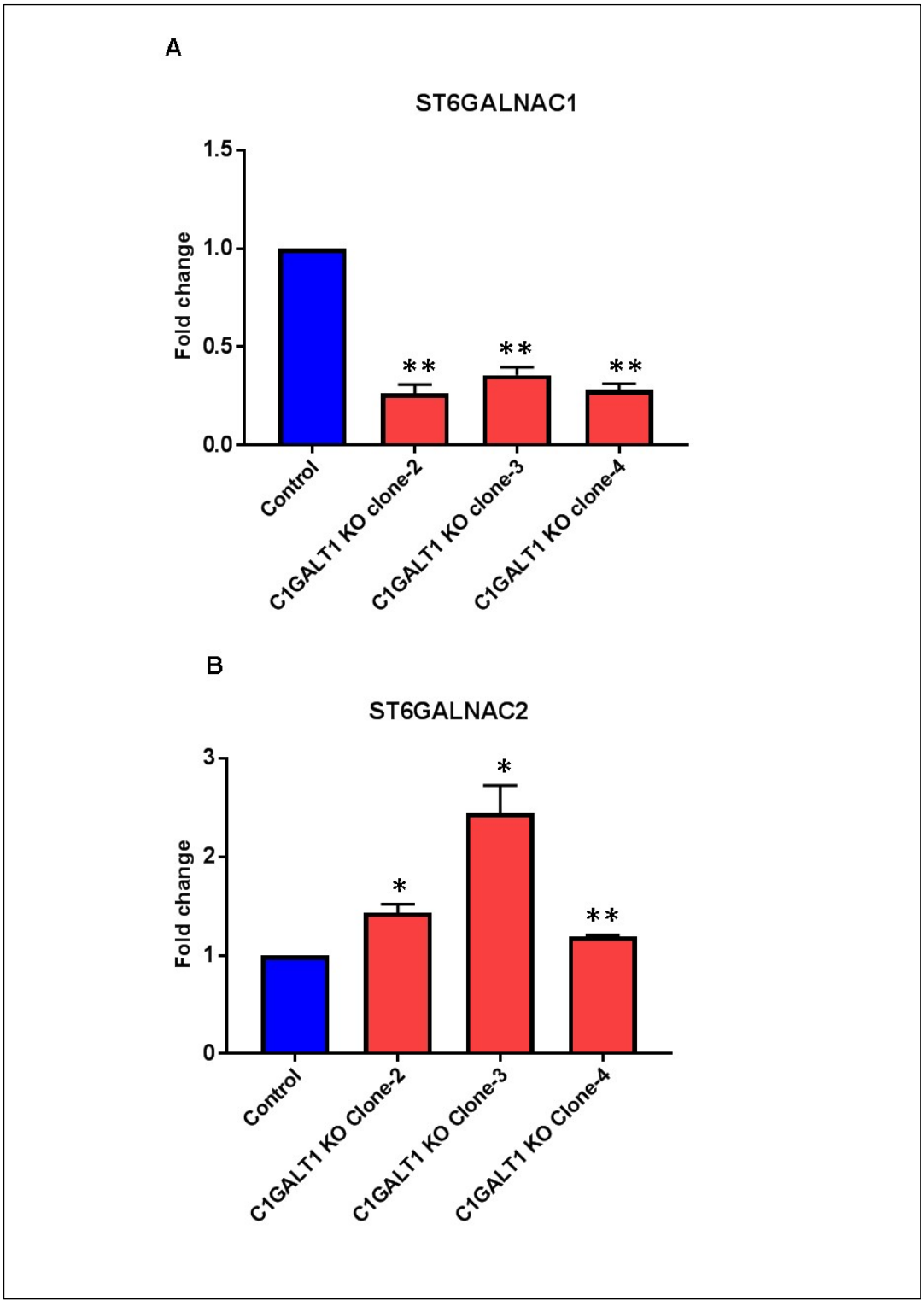
A
ST6GALNAC1
Fold change
1.5
1.0
0.5
0.0
**
**
**
Control
C1GALT1 KO clone-2
C1GALT1 KO clone-3
C1GALT1 KO clone-4
B
ST6GALNAC2
Fold change
3
2
1
0
*
*
**
Control
C1GALT1 KO Clone-2
C1GALT1 KO Clone-3
C1GALT1 KO Clone-4

Figure 4.8 Altered morphology of C1GALT1 KO PDAC cells: F-actin staining demonstrates altered morphology with increased presence of cellular protrusions (marked by arrows) in C1GALT1 KO T3M4 PDAC cells as compared to control cells.

Figure 4.8

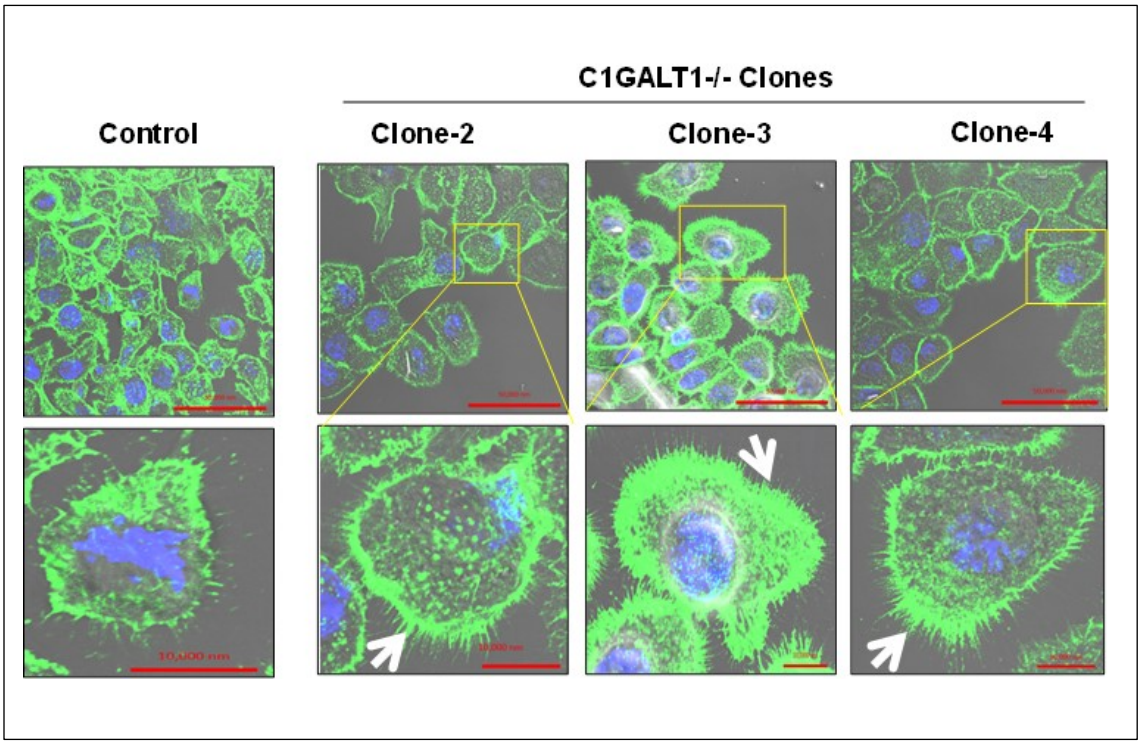

Figure 4.9 Increased migration of C1GALT1 KO PDAC cells: (A) Representative pictures from wound-healing assay after 24 hrs. showing increased migration of C1GALT1 KO T3M4 PDAC cells as compared to control cells **(B)** Quantification of wound-healing assay shows significant increase of wound closure in C1GALT1 KO T3M4 PDAC clones as compared to control cells. *P<0.05, **P<0.005; by unpaired two-sided Student's t-test.

Figure 4.9

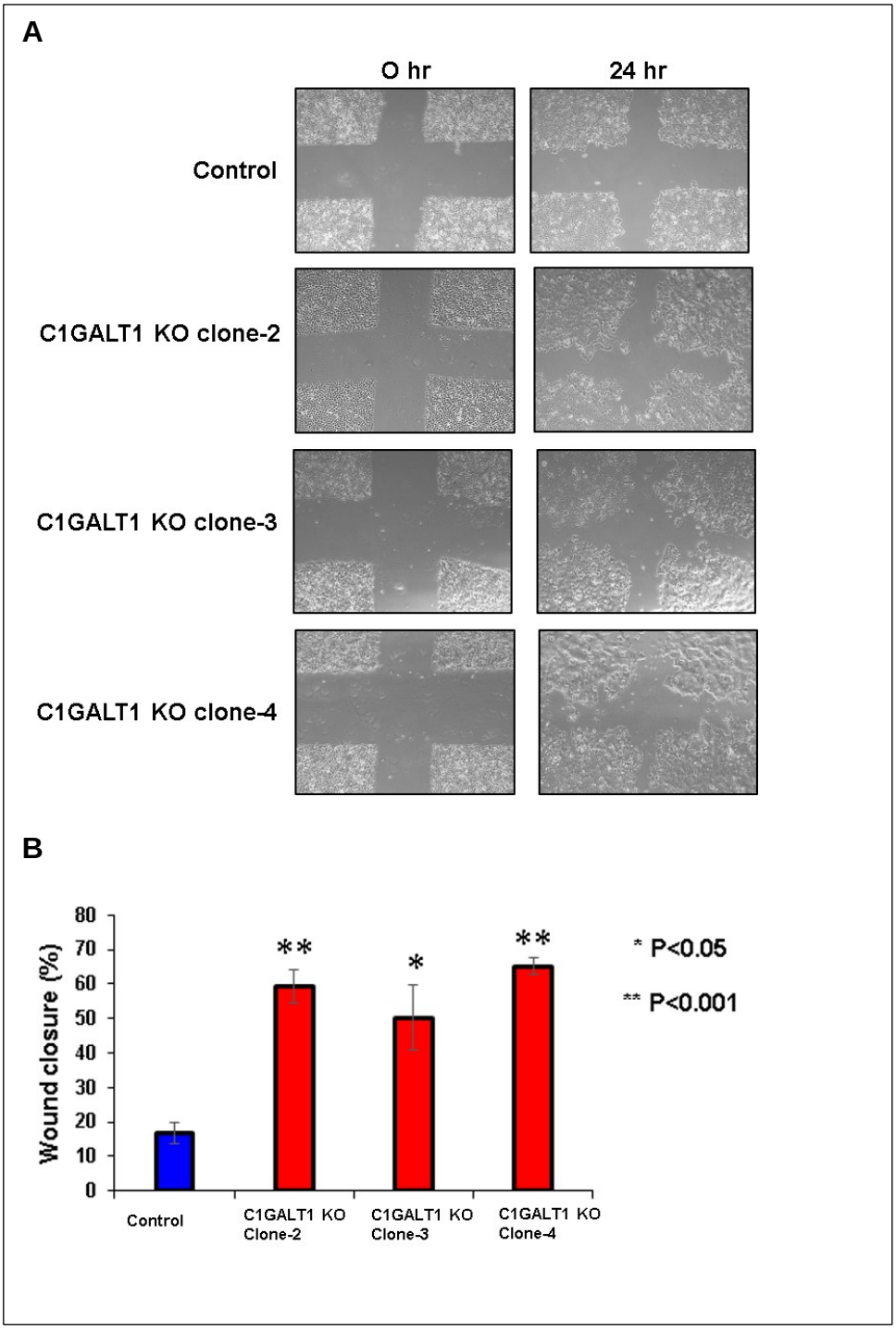
A
O hr
24 hr
Control
C1GALT1 KO clone-2
C1GALT1 KO clone-3
C1GALT1 KO clone-4
B
Wound closure (%)
80
70
60
50
40
30
20
10
0
**
*
**
Control
C1GALT1 KO Clone-2
C1GALT1 KO Clone-3
C1GALT1 KO Clone-4
* P<0.05
** P<0.001

Figure 4.10 Development of migratory model of PDAC: (A) Migration assay was conducted using parental PDAC cells for 24hrs and the migratory subline M1 was developed using cells that have migrated. Further, M1 subline PDAC cells was seeded in migration chamber to develop M2 subline. Similarly, series of migration assays with migratory sublines with progressive decrease in incubation time lead to the development of highly migratory M3, M4 and M5 sublines. **(B)** Representative picture from migration assay demonstrating high migration of migratory sublines as compared to parental cells. Further, actin staining demonstrates altered morphology of migratory sublines as compared to parental cells.

Figure 4.10

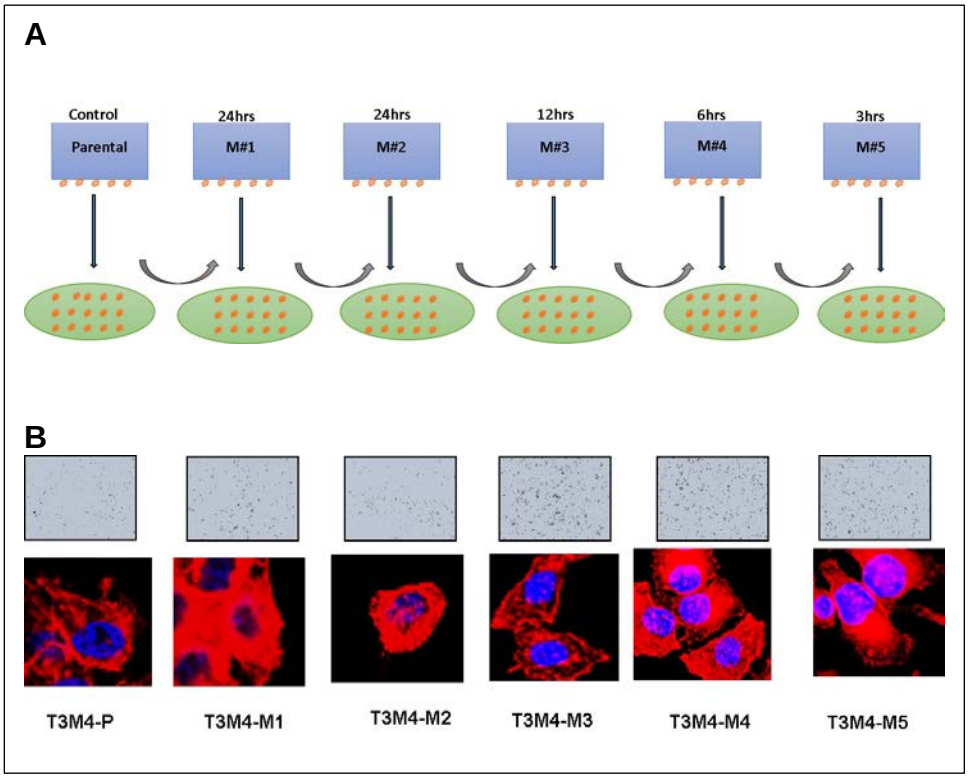
A
Control
Parental
24hrs
M#1
24hrs
M#2
12hrs
M#3
6hrs
M#4
3hrs
M#5
B
T3M4-P
T3M4-M1
T3M4-M2
T3M4-M3
T3M4-M4
T3M4-M5

Figure 4.11 Decreased expression of C1GALT1 in highly migratory PDAC sublines: **A.** ***Left Panel:*** Western blotting demonstrating decreased expression of C1GALT1 in highly migratory T3M4-M4 and T3M4-M5 PDAC cells as compared to parental cells. Further, all the migratory sublines showed increased expression of N-cadherin and vimentin as compared to parental cells. ***Right Panel:*** Western blotting demonstrating decreased expression of C1GALT1 in highly migratory BxPC3-M4 and BxPC3-M5 PDAC cells in comparison with parental cells. **B.** C1GALT1 immunoblotting demonstrating decreased expression of C1GALT1 in highly migratory Colo-M1 and Colo-M2 sublines as compared to parental cells. Further, these migratory sublines showed increased expression of vimentin as compared to parental cells.

Figure 4.11

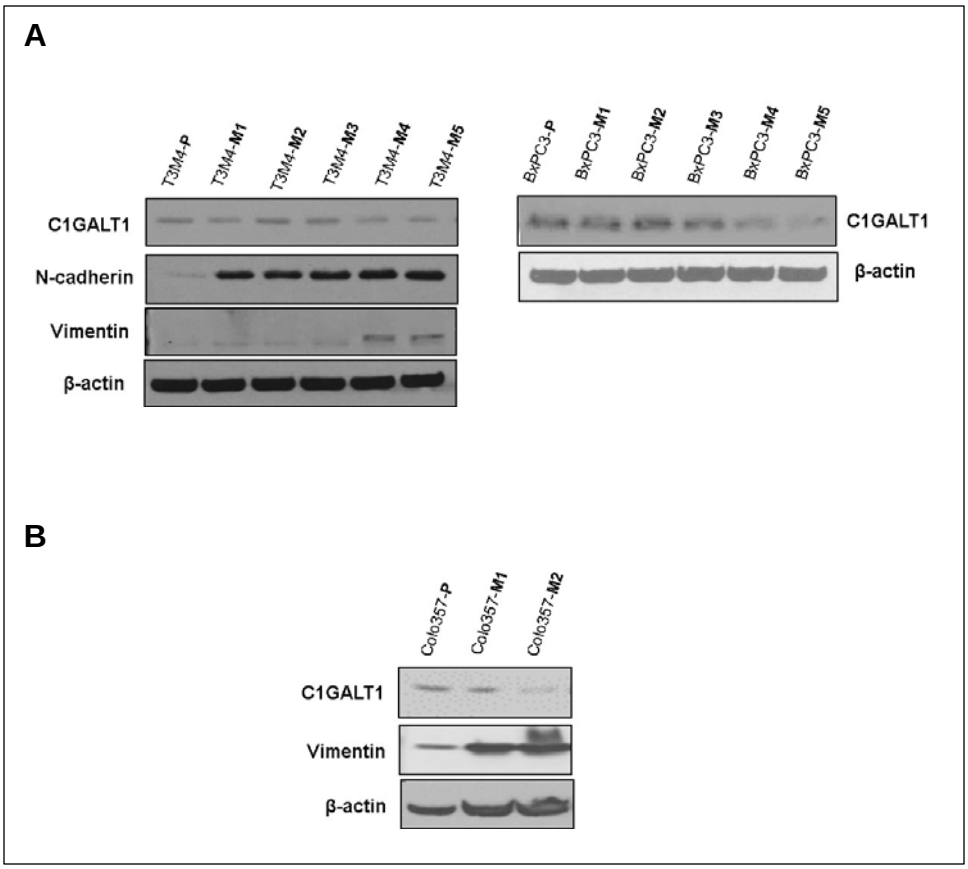
A
T3M4-P
T3M4-M1
T3M4-M2
T3M4-M3
T3M4-M4
T3M4-M5
C1GALT1
N-cadherin
Vimentin
β-actin
BxPC3-P
BxPC3-M1
BxPC3-M2
BxPC3-M3
BxPC3-M4
BxPC3-M5
C1GALT1
β-actin
B
Colo357-P
Colo357-M1
Colo357-M2
C1GALT1
Vimentin
β-actin

Figure 4.12 Impact of GFP and luciferase labelled C1GALT1 KO clone-3 on tumor growth and metastasis: (A) ***Left panel:*** Orthotopic implanation of GFP and luciferase labelled control and KO-clone 3 T3M4 PDAC cells in nude mice revealed significant increase in tumor weights with knockout of C1GALT1. ***Right panel:*** Representative pictures of bioluminescence imaging and pancreatic tumors from control and C1GALT1 KO mice cohort. **(B)** ***Left panel:*** Bar diagram showing significant increase in diaphragm metastasis with orthotopic implantation of C1GALT1 KO-3 as compared to control cells. ***Right panel:*** Representative pictures of GFP positivity in metastatic lesions to kidney, spleen, ovary, diaphragm and testis. Error bars represent mean ± s.e.m ,*P<0.05 by Mann Whitney test.

Figure 4.12

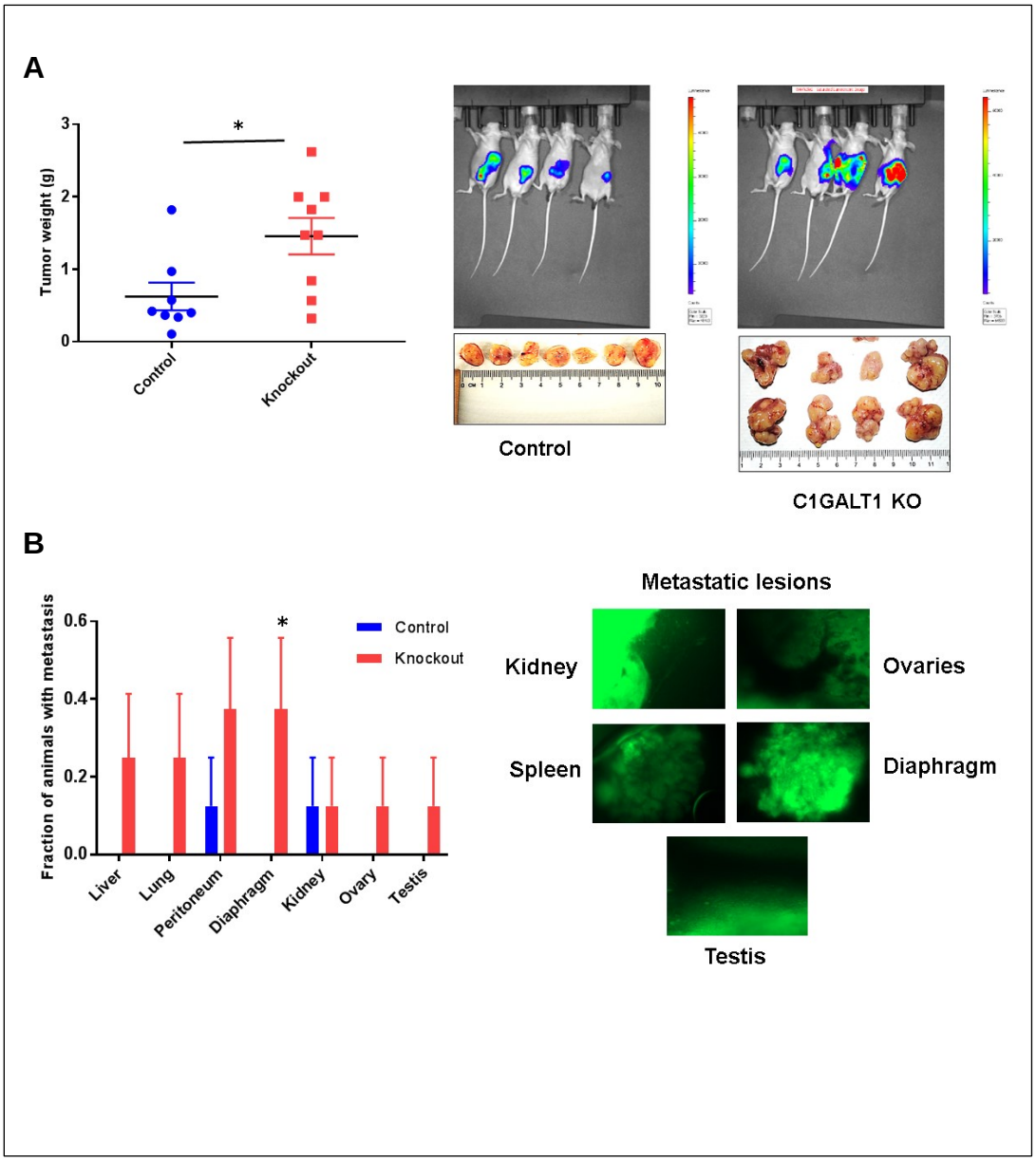
A
Tumor weight (g)
3
2
1
0
*
Control
Knockout
Control
C1GALT1 KO
B
Fraction of animals with metastasis
0.6
0.4
0.2
0.0
*
Control
Knockout
Liver
Lung
Peritoneum
Diaphragm
Kidney
Ovary
Testis
Metastatic lesions
Kidney
Ovaries
Spleen
Diaphragm
Testis

Figure 4.13 Impact of C1GALT1 KO clone-4 on tumor growth and metastasis: (A) Orthotopic implantation of control and KO-clone 4 T3M4 PDAC cells in nude mice revealed significant increase in tumor weights with knockout of C1GALT1. **(B)** Bar diagram showing significant increase in kidney metastasis with orthotopic implantation of C1GALT1 KO-4 as compared to control cells. Error bars represent mean ± s.e.m *P<0.05 by Mann Whitney test.

Figure 4.13

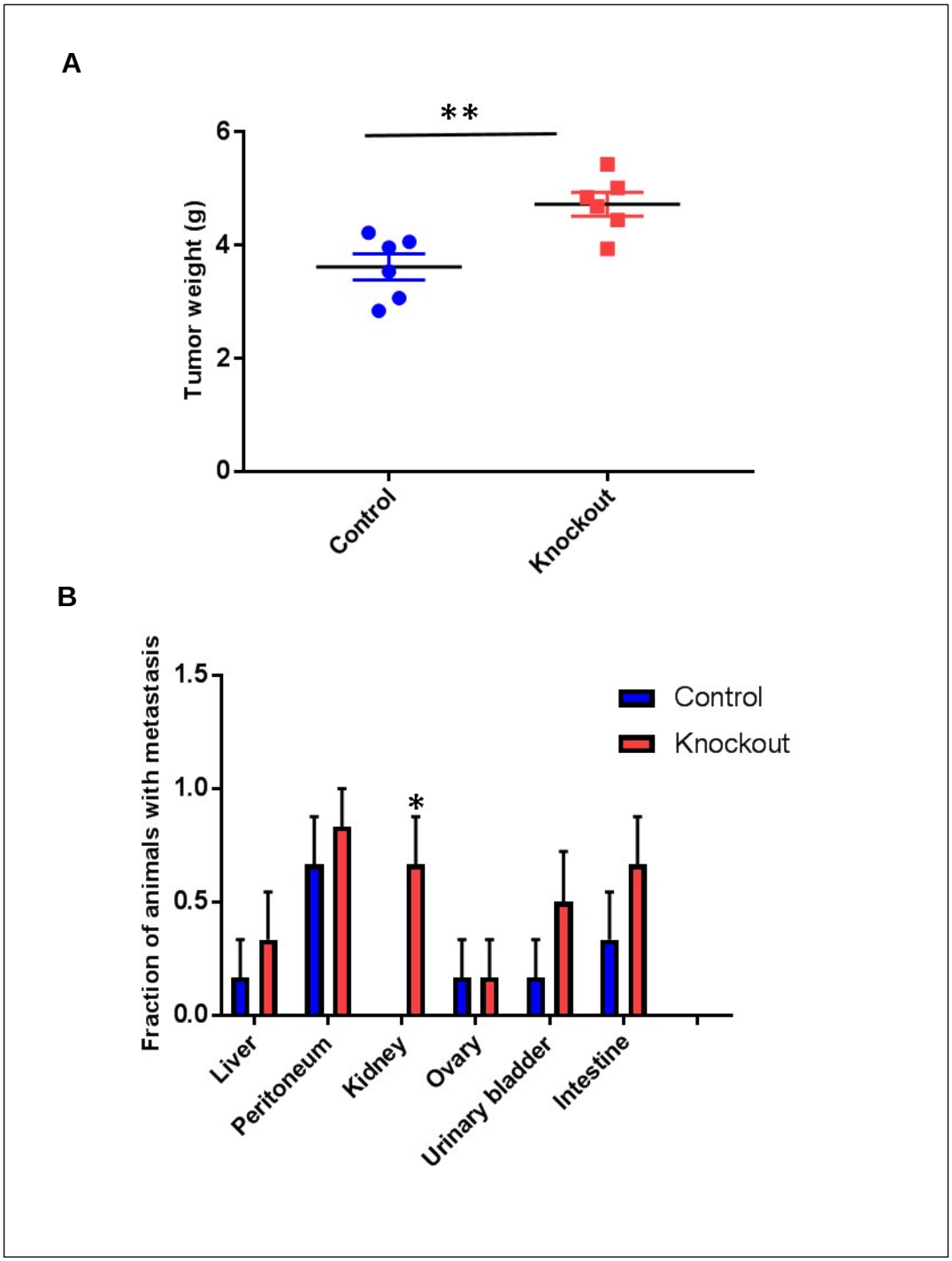
A
**
Tumor weight (g)
6
4
2
0
Control
Knockout
B
Fraction of animals with metastasis
1.5
1.0
0.5
0.0
*
Control
Knockout
Liver
Peritoneum
Kidney
Ovary
Urinary bladder
Intestine

Figure 4.14 Expression of Mucins in C1GALT1 KO PDAC cells: Western blotting demonstrates molecular shift in the MUC16 band in C1GALT1 KO PDAC cells as compared to control cells. Further, the expression of MUC4 and MUC1 is dramatically reduced in C1GALT1 KO PDAC cells as compared to control cells (indicated by arrows).

Figure 4.14

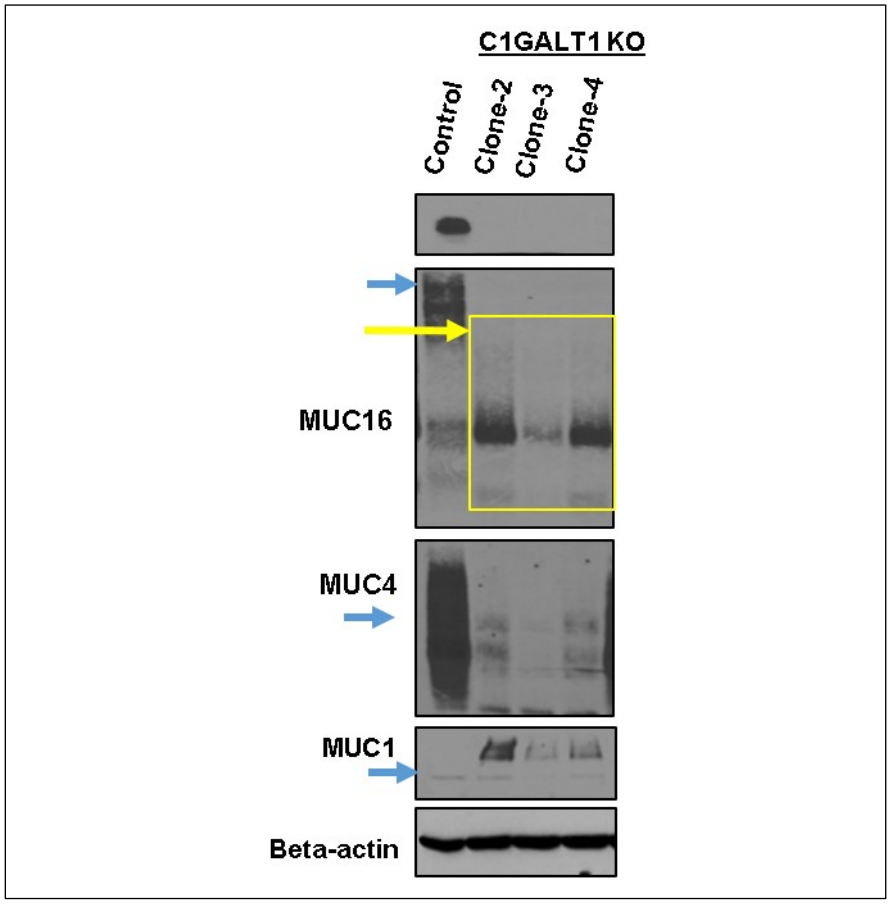
C1GALT1 KO
Control
Clone-2
Clone-3
Clone-4
MUC16
MUC4
MUC1
Beta-actin

Figure 4.15 Aberrant MUC16 glycosylation in C1GALT1 KO PDAC cells: (A) ***Upper Panel*****:** Lectin blotting demonstrates effective pull-down of Tn carbohydrate antigen in control and C1GALT1 KO T3M4 cells by VVA pull down assay. ***Bottom Panel*****:** Immunoblotting of VVA pulled down control and C1GALT1 KO lysates with MUC16 demonstrates significant increase of Tn associated with MUC16 in C1GALT1 KO PDAC cells **(B)** Treatment of control and C1GALT1 KO lysates with PNGase-F and neuraminidase identified N-glycosylated and sialylated regions of MUC16 in control and KO cells. (Arrows indicate MUC16 band)

Figure 4.15

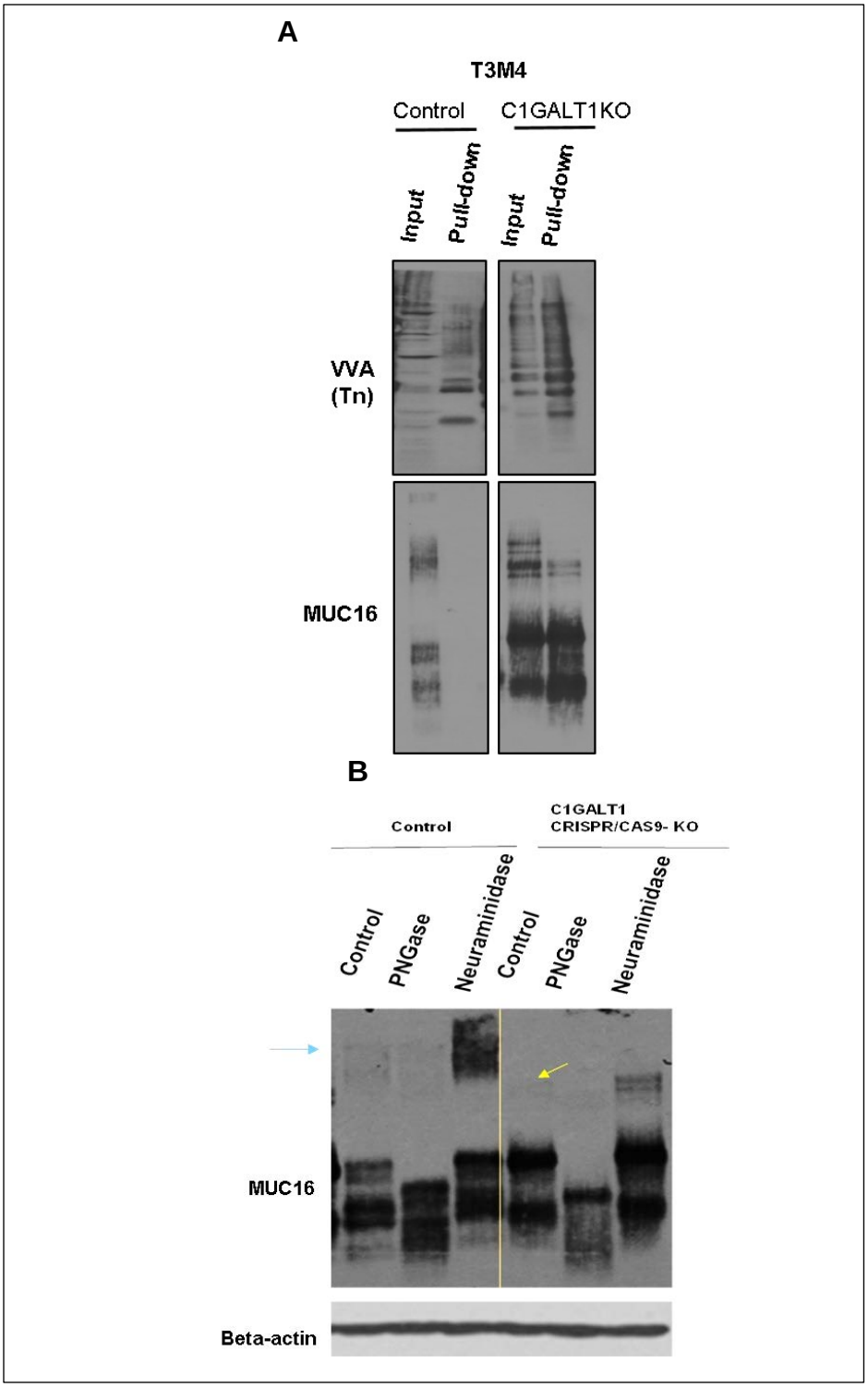
A
T3M4
Control
C1GALT1KO
Input
Pull-down
Input
Pull-down
VVA
(Tn)
MUC16
B
Control
C1GALT1
CRISPR/CAS9- KO
Control
PNGase
Neuraminidase
Control
PNGase
Neuraminidase
MUC16
Beta-actin

Figure 4.16 Impact of C1GALT1 KO on MUC4 glycosylation: (A) ***Left Panel:*** Western blotting demonstrates effective pull-down of MUC4 in control and C1GALT1 KO clones-2 and 3. ***Middle panel:*** Immunoblotting of MUC4-pulled down control and KO lysates with STn showed that STn is not present on MUC4 in control and C1GALT1 knockout clones. ***Right panel:*** Lectin blotting of MUC4-pulled down control and KO lysates with VVA/Tn showed that Tn is not present on MUC4 in control and C1GALT1 knockout clones.

Figure 4.16

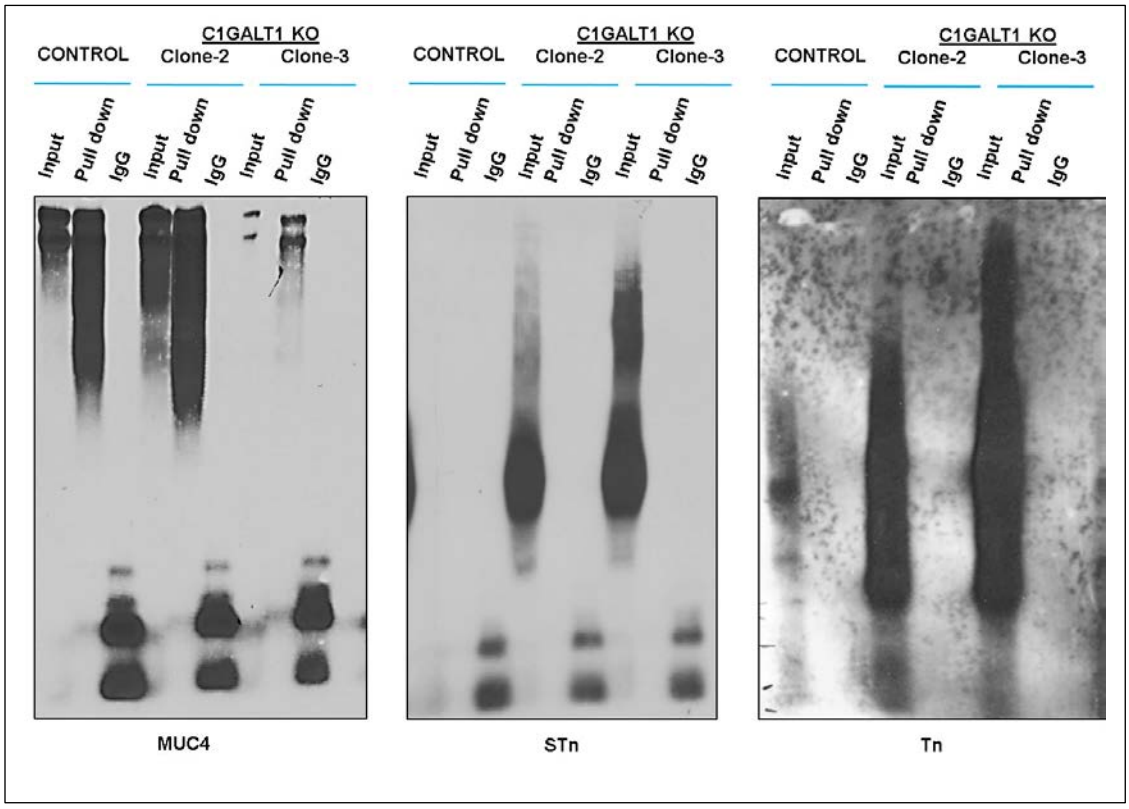
CONTROL
C1GALT1 KO
Clone-2
Clone-3
Input
Pull down
IgG
MUC4
STn
Tn

Figure 4.17 Upregulation of migratory and tumorigenic genes in C1GALT1 KO PDAC cells: Differential gene analysis of RNA-seq data using Cufflinks revealed significant upregulation of genes (marked by arrows) in C1GALT1 KO PDAC cells. IPA analysis using these upregulated genes indicated their involvement in cancer cell migration and tumorigenicity.

Figure 4.17

gene	log2(fold_change)
NGF	3.37257
GAGE1	3.25008
RAB11FIP4	3.13159
CDH11	2.71741
WNT10B	1.95035
RAB36	1.74257
RHOU	1.63805
TWIST2	1.61781
CD44	1.59829
GATA4	1.44596
B4GALNT4	1.41855
MGLL	1.36414
WNT7A	1.30662
GALNT9	1.28388
GCNT2	1.26228
ABCG2	1.16637
B4GALNT1	1.15849
GALNT1	1.08884
TGFB1I1	1.08758
VEGFC	1.00346
RAB3IL1	1.00018
KRT13	-3.38855
KRT7	-2.04229
A4GALT	-1.55817
MGAT4A	-1.48532
GAL3ST2	-1.40035
CLDN1	-1.32659
KRT86	-1.243
GCNT3	-1.23226

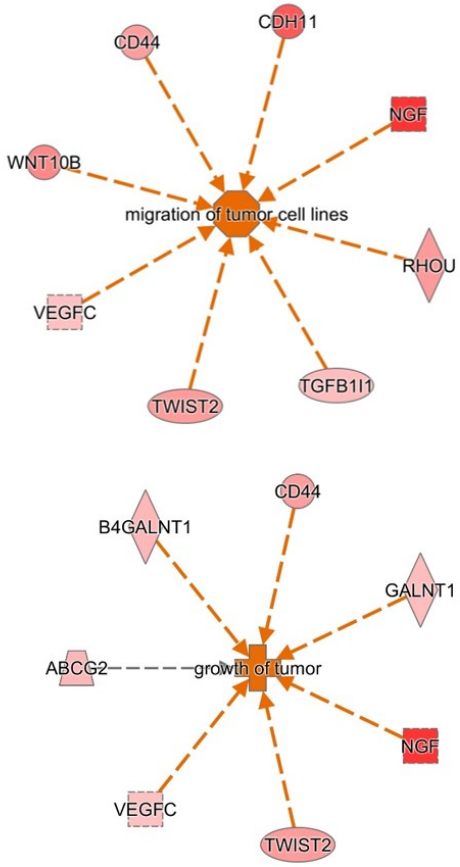

Figure 4.18 Upregulation of PI3K/Akt signaling in C1GALT1 KO PDAC cells: IPA analysis of RNA-seq data from control and C1GALT1 KO PDAC cells indicated upregulation of the PI3K/Akt signaling pathway.

Figure 4.18

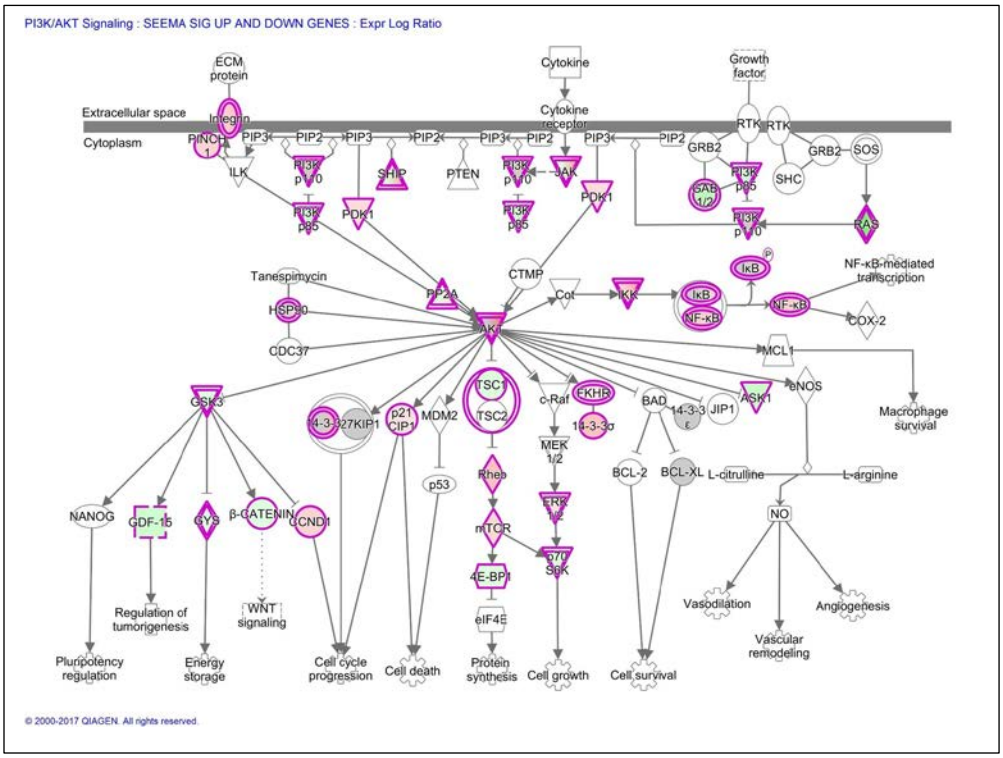
PI3K/AKT Signaling : SEEMA SIG UP AND DOWN GENES : Expr Log Ratio
ECM protein
Cytokine
Growth factor
Extracellular space
Integrin
Cytokine receptor
RTK
Cytoplasm
PINCH 1
ILK
PIP2
PIP3
PI3K p110
PI3K p85
SHIP
PTEN
JAK
PDk1
GRB2
SOS
SHC
SAB 1/2
RAS
Tanespimycin
HSP90
CDC37
PP2A
CTMP
Cot
IKK
IkB
NF-kB
NF-kB-mediated transcription
COX-2
AKT
MCL1
eNOS
Macrophage survival
GSK3
14-3-3
p27KIP1
p21 CIP1
MDM2
TSC1
TSC2
c-Raf
FKHR
14-3-3σ
BAD
14-3-3 ε
JIP1
ASK1
MEK 1/2
ERK 1/2
Rheb
p53
mTOR
S70 S6K
4E-BP1
eIF4E
BCL-2
BCL-XL
L-citrulline
L-arginine
NO
NANOG
GDF-15
CYS
β-CATENIN
CCND1
WNT signaling
Regulation of tumorigenesis
Pluripotency regulation
Energy storage
Cell cycle progression
Cell death
Protein synthesis
Cell growth
Cell survival
Vasodilation
Angiogenesis
Vascular remodeling
© 2000-2017 QIAGEN. All rights reserved.

Figure 4.19 Impact of C1GALT1 KO on EMT markers and signaling proteins: (A) Western blotting demonstrates increased expression of phosphorylated forms of signaling proteins such as EGFR, HER2 and Akt, whereas their total forms were unchanged. **(B)** Western blotting demonstrates increased expression of the mesenchymal protein vimentin, pFAK-Y925, α-4 integrin and decreased expression of epithelial marker ZO-1.

Figure 4.19

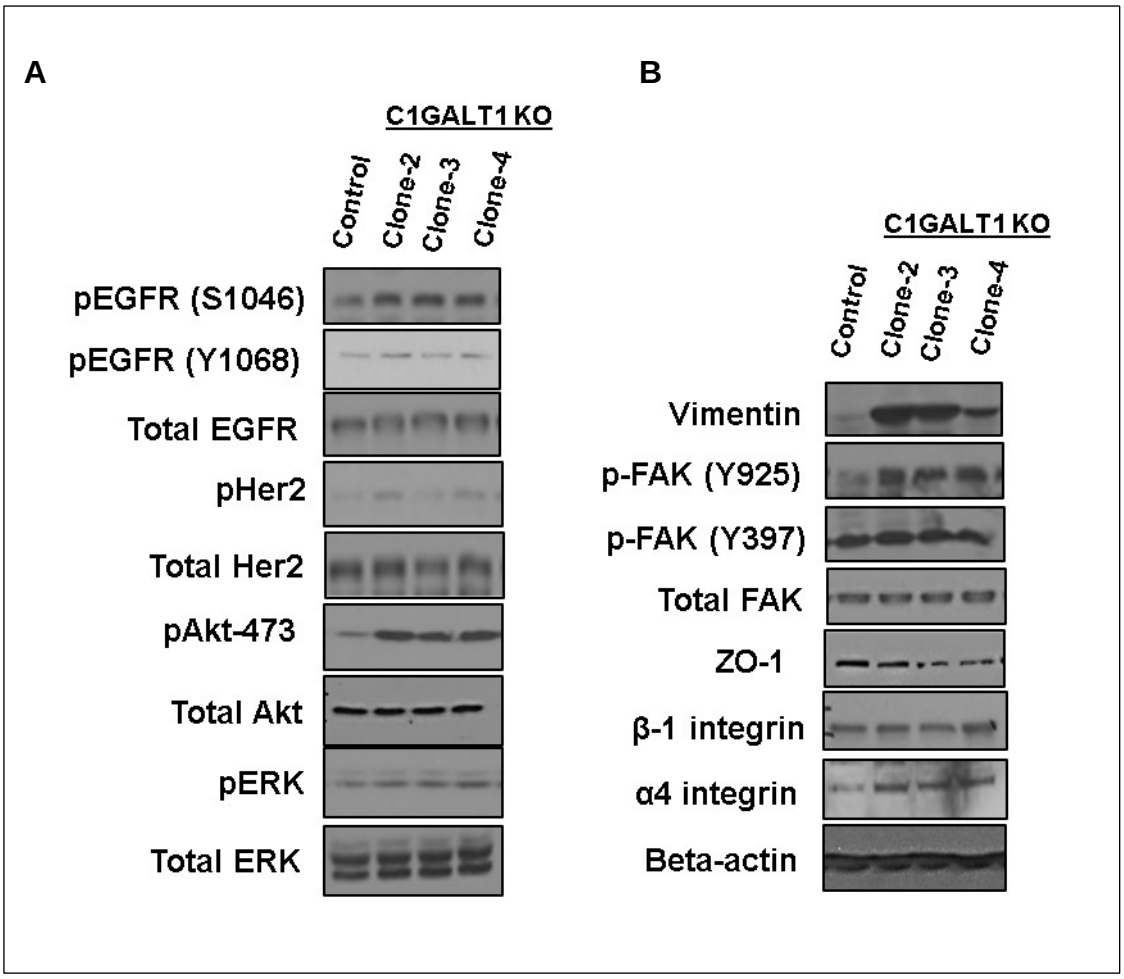
A
C1GALT1 KO
Control
Clone-2
Clone-3
Clone-4
pEGFR (S1046)
pEGFR (Y1068)
Total EGFR
pHer2
Total Her2
pAkt-473
Total Akt
pERK
Total ERK
B
C1GALT1 KO
Control
Clone-2
Clone-3
Clone-4
Vimentin
p-FAK (Y925)
p-FAK (Y397)
Total FAK
ZO-1
β-1 integrin
α4 integrin
Beta-actin

Figure 4.20 Impact of pro-inflammatory cytokines on C1GALT1: Treatment of T3M4 cells with IFN-γ, TNF-α showed slight increase in C1GALT1 expression. On the contrary, treatment of T3M4 PDAC cells with high doses of IL-4 and all doses of IL-6 caused a decrease in C1GALT1 expression.

Figure 4.20

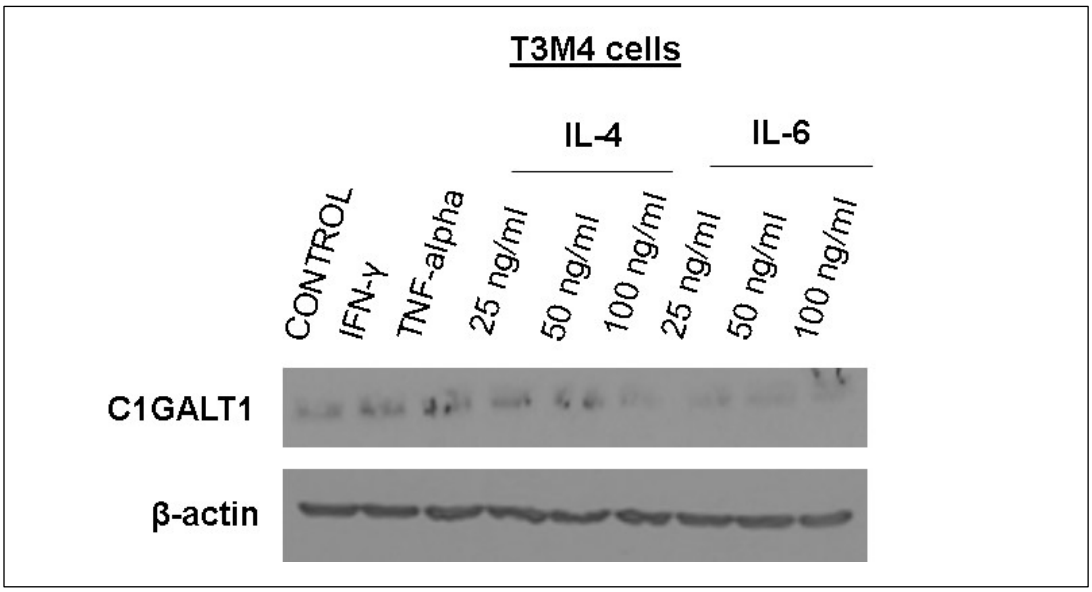
T3M4 cells
IL-4
IL-6
CONTROL
IFN-γ
TNF-alpha
25 ng/ml
50 ng/ml
100 ng/ml
25 ng/ml
50 ng/ml
100 ng/ml
C1GALT1
β-actin

References

[1] S.S. Pinho, C.A. Reis, Glycosylation in cancer: mechanisms and clinical implications, Nature reviews. Cancer, 15 (2015) 540-555.

[2] S. Itzkowitz, T. Kjeldsen, A. Friera, S. Hakomori, U.S. Yang, Y.S. Kim, Expression of Tn, sialosyl Tn, and T antigens in human pancreas, Gastroenterology, 100 (1991) 1691-1700.

[3] N. Remmers, J.M. Anderson, E.M. Linde, D.J. DiMaio, A.J. Lazenby, H.H. Wandall, U. Mandel, H. Clausen, F. Yu, M.A. Hollingsworth, Aberrant expression of mucin core proteins and o-linked glycans associated with progression of pancreatic cancer, Clinical cancer research : an official journal of the American Association for Cancer Research, 19 (2013) 1981-1993.

[4] T. Ju, V.I. Otto, R.D. Cummings, The Tn antigen-structural simplicity and biological complexity, Angew Chem Int Ed Engl, 50 (2011) 1770-1791.

[5] T. Ju, G.S. Lanneau, T. Gautam, Y. Wang, B. Xia, S.R. Stowell, M.T. Willard, W. Wang, J.Y. Xia, R.E. Zuna, Z. Laszik, D.M. Benbrook, M.H. Hanigan, R.D. Cummings, Human tumor antigens Tn and sialyl Tn arise from mutations in Cosmc, Cancer Res, 68 (2008) 1636-1646.

[6] T. Ju, K. Brewer, A. D'Souza, R.D. Cummings, W.M. Canfield, Cloning and expression of human core 1 beta1,3-galactosyltransferase, J Biol Chem, 277 (2002) 178-186.

[7] T. Ju, R.D. Cummings, A unique molecular chaperone Cosmc required for activity of the mammalian core 1 beta 3-galactosyltransferase, Proc Natl Acad Sci U S A, 99 (2002) 16613-16618.

[8] B.T. Hofmann, L. Schluter, P. Lange, B. Mercanoglu, F. Ewald, A. Folster, A.S. Picksak, S. Harder, A.T. El Gammal, K. Grupp, C. Gungor, A. Drenckhan, H. Schluter, C. Wagener, J.R. Izbicki, M. Jucker, M. Bockhorn, G. Wolters-Eisfeld, COSMC knockdown mediated aberrant O-glycosylation promotes oncogenic properties in pancreatic cancer, Molecular cancer, 14 (2015) 109.

[9] P. Radhakrishnan, S. Dabelsteen, F.B. Madsen, C. Francavilla, K.L. Kopp, C. Steentoft, S.Y. Vakhrushev, J.V. Olsen, L. Hansen, E.P. Bennett, A. Woetmann, G. Yin, L. Chen, H. Song, M. Bak, R.A. Hlady, S.L. Peters, R. Opavsky, C. Thode, K. Qvortrup, K.T. Schjoldager, H. Clausen, M.A. Hollingsworth, H.H. Wandall, Immature truncated O-glycophenotype of cancer directly induces oncogenic features, Proc Natl Acad Sci U S A, 111 (2014) E4066-4075.

[10] D.T. Tran, K.G. Ten Hagen, Mucin-type O-glycosylation during development, J Biol Chem, 288 (2013) 6921-6929.

[11] T. Ju, R.D. Cummings, Protein glycosylation: chaperone mutation in Tn syndrome, Nature, 437 (2005) 1252.

[12] T. Terada, Y. Nakanuma, Expression of mucin carbohydrate antigens (T, Tn and sialyl Tn) and MUC-1 gene product in intraductal papillary-mucinous neoplasm of the pancreas, Am J Clin Pathol, 105 (1996) 613-620.

[13] D. Haridas, S. Chakraborty, M.P. Ponnusamy, I. Lakshmanan, S. Rachagani, E. Cruz, S. Kumar, S. Das, S.M. Lele, J.M. Anderson, U.A. Wittel, M.A. Hollingsworth, S.K. Batra, Pathobiological implications of MUC16 expression in pancreatic cancer, PLoS One, 6 (2011) e26839.

[14] D. Haridas, M.P. Ponnusamy, S. Chugh, I. Lakshmanan, P. Seshacharyulu, S.K. Batra, MUC16: molecular analysis and its functional implications in benign and malignant conditions, FASEB J, 28 (2014) 4183-4199.

[15] S. Das, S. Rachagani, M.P. Torres-Gonzalez, I. Lakshmanan, P.D. Majhi, L.M. Smith, K.U. Wagner, S.K. Batra, Carboxyl-terminal domain of MUC16 imparts tumorigenic and metastatic functions through nuclear translocation of JAK2 to pancreatic cancer cells, Oncotarget, 6 (2015) 5772-5787.

[16] S. Muniyan, D. Haridas, S. Chugh, S. Rachagani, I. Lakshmanan, S. Gupta, P. Seshacharyulu, L.M. Smith, M.P. Ponnusamy, S.K. Batra, MUC16 contributes to the metastasis of pancreatic ductal adenocarcinoma through focal adhesion mediated signaling mechanism, Genes Cancer, 7 (2016) 110-124.

[17] S. Chugh, V.S. Gnanapragassam, M. Jain, S. Rachagani, M.P. Ponnusamy, S.K. Batra, Pathobiological implications of mucin glycans in cancer: Sweet poison and novel targets, Biochim Biophys Acta, 1856 (2015) 211-225.

[18] P.M. Campbell, A.L. Groehler, K.M. Lee, M.M. Ouellette, V. Khazak, C.J. Der, K-Ras promotes growth transformation and invasion of immortalized human pancreatic cells by Raf and phosphatidylinositol 3-kinase signaling, Cancer Res, 67 (2007) 2098-2106.

[19] S. Kaur, S. Kumar, N. Momi, A.R. Sasson, S.K. Batra, Mucins in pancreatic cancer and its microenvironment, Nat Rev Gastroenterol Hepatol, 10 (2013) 607-620.

[20] K.A. Maupin, A. Sinha, E. Eugster, J. Miller, J. Ross, V. Paulino, V.G. Keshamouni, N. Tran, M. Berens, C. Webb, B.B. Haab, Glycogene expression alterations associated with pancreatic cancer epithelial-mesenchymal transition in complementary model systems, PLoS One, 5 (2010) e13002.

[21] I. Hauselmann, L. Borsig, Altered tumor-cell glycosylation promotes metastasis, Front Oncol, 4 (2014) 28.

[22] G.F. Springer, T and Tn, general carcinoma autoantigens, Science (New York, N.Y.), 224 (1984) 1198-1206.

[23] H. Ozaki, H. Matsuzaki, H. Ando, H. Kaji, H. Nakanishi, Y. Ikehara, H. Narimatsu, Enhancement of metastatic ability by ectopic expression of ST6GalNAcI on a gastric cancer cell line in a mouse model, Clin Exp Metastasis, 29 (2012) 229-238.

[24] G. Jacquemet, H. Hamidi, J. Ivaska, Filopodia in cell adhesion, 3D migration and cancer cell invasion, Curr Opin Cell Biol, 36 (2015) 23-31.

[25] J.V. Small, T. Stradal, E. Vignal, K. Rottner, The lamellipodium: where motility begins, Trends Cell Biol, 12 (2002) 112-120.

[26] M.J. Schultz, A.F. Swindall, S.L. Bellis, Regulation of the metastatic cell phenotype by sialylated glycans, Cancer Metastasis Rev, 31 (2012) 501-518.

[27] M.G. Mendez, S. Kojima, R.D. Goldman, Vimentin induces changes in cell shape, motility, and adhesion during the epithelial to mesenchymal transition, FASEB J, 24 (2010) 1838-1851.

[28] I. Lakshmanan, P. Seshacharyulu, D. Haridas, S. Rachagani, S. Gupta, S. Joshi, C. Guda, Y. Yan, M. Jain, A.K. Ganti, M.P. Ponnusamy, S.K. Batra, Novel HER3/MUC4 oncogenic signaling aggravates the tumorigenic phenotypes of pancreatic cancer cells, Oncotarget, 6 (2015) 21085-21099.

[29] P. Seshacharyulu, M.P. Ponnusamy, S. Rachagani, I. Lakshmanan, D. Haridas, Y. Yan, A.K. Ganti, S.K. Batra, Targeting EGF-receptor(s) - STAT1 axis attenuates tumor growth and metastasis through downregulation of MUC4 mucin in human pancreatic cancer, Oncotarget, 6 (2015) 5164-5181.

[30] C. Porta, C. Paglino, A. Mosca, Targeting PI3K/Akt/mTOR Signaling in Cancer, Front Oncol, 4 (2014) 64.

[31] S. Rachagani, M.A. Macha, M.P. Ponnusamy, D. Haridas, S. Kaur, M. Jain, S.K. Batra, MUC4 potentiates invasion and metastasis of pancreatic cancer cells through stabilization of fibroblast growth factor receptor 1, Carcinogenesis, 33 (2012) 1953-1964.

[32] Q.S. Zhu, K. Rosenblatt, K.L. Huang, G. Lahat, R. Brobey, S. Bolshakov, T. Nguyen, Z. Ding, R. Belousov, K. Bill, X. Luo, A. Lazar, A. Dicker, G.B. Mills, M.C. Hung, D. Lev, Vimentin is a novel AKT1 target mediating motility and invasion, Oncogene, 30 (2011) 457-470.

CHAPTER 5

Understanding the role of C1GALT1 in pancreatic ductal adenocarcinoma progression and metastasis:

Generation of *Kras^{G12D}; Trp53$^{R172H/+}$; C1galt1$^{loxP/loxP}$; Pdx1-Cre* (KPCC) mice

1. Synopsis

Defective C1GALT1 activity owing to mutations in Cosmc have been reported in pancreatic cancer, but its involvement in PDAC progression and metastasis is not well defined [1, 2]. We aimed to address this question by generating *Kras^{G12D}; Trp53$^{R172H/+}$; C1galt1$^{loxP/loxP}$; Pdx1-Cre* (KPCC) mice that have a pancreas-specific knockout of C1galt1 along with Kras and p53 mutations. These mice were monitored for tumor progression and metastasis at several time points and were compared to KPC mice and their age-matched littermate controls. Our results indicate that knockout of C1galt1 decreases PDAC latency with the appearance of tumors as early as 5 weeks. The majority of 10- and 15-weeks KPCC mice harbors PDAC, whereas pancreatic intraepithelial neoplasia lesions (PanIN) start appearing by 3 weeks. KPCC mice showed a significant decrease in overall survival rate as compared to KPC mice. Knockout mice display significantly increased expression of truncated Tn glycan structure as compared to KPC mice and control littermates. Interestingly, we observed early metastasis in KPCC mice (around 10 weeks) as compared to KPC (around 25-30 weeks) mice. There was a remarkable increase of vimentin, an EMT marker in C1galt1 knockout mice, which could explain early metastatic incidence in these mice. Overall, our findings indicate that genomic depletion of C1galt1 accelerated PDAC progression and metastasis.

2. Background and rationale

Several spontaneous mouse models of PDAC harboring genomic mutations in Kras, p53, and Ink4a and deletions of genes such as Smad4, Shh, and Tgfbr2 have been developed in the past few years [3, 4]. All of these mouse models have significantly contributed to our understanding of PDAC progression and metastasis. In addition to the genetic changes, altered glycosylation also contributes to PDAC growth and metastasis [5]. However, the functional contribution of aberrant glycosylation in PDAC progression and metastasis is not yet addressed. In an attempt to address this, we generated an O-glycosylation-deficient PDAC mouse model. In the previous chapter, we have clearly illustrated the significant impact of knockout of O-glycosyltransferase, C1GALT1, on tumor growth and metastasis. To gain insight into the specific role of C1GALT1 in PDAC progression, we have attempted to develop a C1galt1 knockout PDAC mouse model. Mouse C1galt1 shares 89% homology with human C1GALT1 and is located on chromosome 6 (NCBI BLAST). Therefore, we crossed C1galt1 floxed mice with the KPC (*Kras*^{G12D}*; Trp53*$^{R172H/+}$*: Pdx-Cre*) model of PDAC that resulted in KPCC (*Kras*^{G12D}*; Trp53*$^{R172H/+}$*; C1galt1*$^{loxP/loxP}$*; Pdx1-Cre*) mice, which have pancreas specific knockout of C1galt1 in addition to Kras and p53 mutations.

Disruption of core-1 synthase activity in mice has been associated with embryonic lethality, owing to defective angiogenesis that caused hemorrhages in the brain and spinal cord [6]. The study by Xia *et al.* suggested that angiogenic defects in C1galt$^{-/-}$ mice might be caused by abnormal glycosylation of cellular components constituting vascular network such as endothelial cells and pericytes [6]. Another study from the same group demonstrated that mouse with targeted deletion of C1galt1 in endothelial and hematopoietic cells had improper connections among blood and lymphatic vessels [7].

Disturbance in blood/lymphatics network impaired transport of lipids resulting in fatty liver disease [7]. Further studies using targeted deletion of C1galt1 in spermatogonia and oocytes have established the roles of core-1 glycans in proper embryonic development and spermatogenesis respectively [8, 9]. Interestingly, intestinal knockout of C1galt1 was associated with the spontaneous development of colitis and colitis-associated cancer due to disruption of mucus barrier suggesting the protective role of core-1 glycans in the intestine [10, 11]. Altogether, these studies suggest that loss of C1galt1 is associated with increased expression of truncated Tn carbohydrate glycans and hence the resultant pathology.

Apart from the aforementioned pathological conditions, numerous studies have also reported increased expression of truncated carbohydrate antigens such as Tn, STn in several malignancies including PDAC [12, 13]. Loss of expression of C1GALT1 is one of the mechanisms that results in increased expression of truncated carbohydrate antigens. Loss of C1GALT1 has been linked to mutations in Cosmc, which facilitates its proper folding and thereby prevents its proteasomal degradation [14]. Radhakrishnan *et al.* have demonstrated that epigenetic changes in Cosmc due to promoter hypermethylation is associated with loss of expression of C1GALT1 and increased activation of Tn carbohydrate antigen [2]. Further, the same study, and another study from Hoffman *et al* have demonstrated that knockout of Cosmc in PDAC cells leads to increased expression of truncated carbohydrate antigens and enhanced oncogenicity [1]. Though these studies have revealed an important role of Cosmc in PDAC, the possibility that Cosmc knockdown has other biological effects cannot be excluded. The precise role of C1GALT1 in PDAC progression and metastasis is still unclear.

The objective of our study was to examine the functional impact of core-1 knockout-mediated aberrant O-glycosylation on PDAC progression and metastasis. For this purpose, the study herein involved generation of C1galt1 knockout PDAC model. Detailed characterization of KPCC mice revealed that loss of C1galt1 in KPC mice (KPCC mice) induced truncated glycophenotype and facilitated faster PDAC progression and early metastasis.

3. Results

A. Development of KPCC mouse model

Previous studies have described that genomic instability conferred by endogenous expression of $Trp53^{R172H}$ and $Kras^{G12D}$ in the mouse pancreas leads to spontaneous development of pancreatic ductal adenocarcinoma [15]. To explore the role of C1galt1 in pancreatic cancer, these KPC mice (*$Kras^{G12D}$; $Trp53^{R172H/+}$; Pdx-Cre*) were bred with C1galt1 floxed (*$C1galt1^{loxP/loxP}$*) mice that resulted in KPCC mice (*$Kras^{G12D}$; $Trp53^{R172H/+}$; $C1galt1^{loxP/loxP}$; Pdx-Cre*). C1galt1 floxed mice (*$C1galt1^{loxP/loxP}$*) were a kind gift from Dr. Lijun Xia and have been described in his previous studies [10, 11, 16]. The breeding strategy for the generation of KPCC mice has been outlined in **Figure 5.1**.

B. Deletion of C1galt1 leads to faster PDAC progression and decreased survival

We noted that knockout of core-1 synthase in the context of KPC background accelerated development of PDAC (**Figure 5.2A**). Low-grade PanIN1 and 2 lesions were observed as early as 3 weeks (**Figure 5.2B**). At 5 weeks, 25% of KPCC mice display high-grade PanIN3 lesions, which increased to 60% by 10 weeks. The development of these high-grade lesions was very rapid as compared to KPC mice, which usually develop these

high-grade lesions by 10 weeks. Since these high-grade benign lesions (also known as Carcinoma in situ) eventually leads to PDAC development, KPCC was evaluated at different time points, starting from 3 weeks to 20 weeks, to monitor PDAC progression (**Figure 5.1, Figure 5.2B**). Fully blown pancreatic tumors were apparent as early as 5 weeks (40%) and majority of 15 weeks (60%) and 20 weeks KPCC (80%) animals exhibited PDAC (**Figure 5.3A**). Histopathologic analysis of KPCC tumors revealed poorly differentiated/undifferentiated morphology (sarcomatoid histology, many gigantic cells, and atypical mitotic figures) however, a vast majority of KPC animals showed well to moderately differentiated tumors (**Figure 5.3B**). Notably, the pancreas appeared normal when C1galt1 was deleted ($C1galt1^{loxP/loxP}$; Pdx-Cre) without the background of Kras and p53 gene mutations. This suggests that targeted deletion of C1galt1 in mouse pancreas did not affect its development (**Figure 5.4**). Nevertheless, loss of C1galt1 in conjunction with mutated Kras and p53 significantly accelerated disease progression.

Since knockout of C1galt1 in PDAC induced faster disease progression, we also evaluated its effect on overall survival. Previous studies have reported that the median survival rate of KPC animals is around 200 days. Survival studies were conducted to explore the effect of C1galt1 deficiency in the background of KPC. The mean survival of KPC control littermates was around 205 days (29.2 weeks), whereas KPCC mice have dramatically shortened median survival of 107 days (15.2 weeks) (**Figure 5.5**). Taken together, these findings suggest that knockout of C1galt1 along with Kras and p53 mutations significantly augments PDAC initiation and impacts survival.

C. Fully blown pancreatic tumors in KPCC mice displayed numerous mitotic figures and decreased stroma

To evaluate the effect of C1galt1 knockout on cell proliferation, we counted mitotic figures in KPC and KPCC tumors. KPCC tumors showed numerous mitotic figures as identified by H and E staining. We also observed increased presence of atypical mitotic figures (gigantic nucleus with scarce cytoplasm) in KPCC tumors. Increased presence of these mitotic figures and atypical nuclear structures marks aggressive malignancy and has been used for clinical grading of several tumors (**Figure 5.6**) [17].

We next sought to determine whether loss of C1galt1 has any effect on fibrosis, which is highly observed in PDAC and is frequently observed in tissue histology [18]. We first stained KPC and KPCC tumors with alpha-SMA, which has been widely used to identify cancer-associated fibroblasts in the stroma. C1galt1 lacking tumors showed significantly decreased alpha-SMA expression in comparison to KPC tumors, which showed appreciable levels of alpha-SMA (**Figure 5.7**). Next, to verify changes in the stroma, we analyzed collagen content using Picro-Sirius red staining. Consistent with alpha-SMA staining, the percentage of Sirius red-stained area was also significantly reduced in KPCC tumors as compared to KPC tumors (**Figure 5.8**). Our findings are consistent with recent studies that have described findings showing that targeting stroma renders PDAC more aggressive [19]. Taken together, these results indicate that loss of C1galt1 leads to the formation of aggressive PDAC tumors with a marked decrease in stroma.

D. Truncated glycophenotype of KPCC mice

Next, we investigated whether increased PDAC aggressiveness in KPCC tumors is due to differential glycosylation by the loss of C1galt1. The effect of C1galt1 knockout

on glycosylation was assessed using Alcian blue and lectin staining. Alcian blue staining revealed a marked decrease of sulfated/sialylated (acidic) glycans in KPCC tissues in comparison with KPC tissues (**Figure 5.9**). Since C1galt1 catalyzes the formation of core-1/T carbohydrate antigen, we evaluated its expression in KPC and KPCC tumors (pretreated with neuraminidase) using PNA-Rhodamine [20]. As expected loss of C1galt1 in KPCC tumors led to a significant decrease in T carbohydrate antigen as compared to KPC tumors. This further confirmed effective knockout of C1galt1 in KPCC mice (**Figure 5.10**).

We next stained the KPC and KPCC tumors with VVA lectin, which is used to visualize Tn carbohydrate antigen (**Figure 5.11**). Increased expression of truncated Tn carbohydrate antigen is frequently observed in several malignancies and correlates with their increased aggressiveness [21]. KPCC mice showed a significant increase in Tn carbohydrate antigen as compared to KPC mice (**Figure 5.11**). Taken together, these findings indicate that knockout of C1galt1 in PDAC results in aberrant expression of Tn carbohydrate antigen and loss of core-1 O-glycan structures.

E. Increased metastasis incidence upon loss of C1galt1 in KPC mice

We observed early metastatic lesions in KPCC mice (5 weeks) as compared to KPC mice, which shows late metastasis (**Figure 5.12A**) [15]. We did not observe any metastasis in KPC mice until 20 weeks. **Figure 5.12A** outlines representative pictures showing metastasis to several organs such as liver, peritoneum, and stomach in KPCC mice. Further, we also evaluated RNA collected from KPC and KPCC tumors for EMT markers. We noticed increased expression of the mesenchymal protein vimentin whereas epithelial makers such as keratins (keratin-5 and -7) and claudins (claudin-4 and -6) were decreased (**Figure 5.12B**). To better understand the mechanism involved in early

metastasis, the sections were stained with metastatic marker vimentin. KPCC tumors showed a remarkable increase in vimentin as compared to KPC tumors (**Figure 5.13)**. These results suggest increased metastatic incidence in KPCC mice as compared to KPC mice, which could be explained by increased expression of vimentin in KPCC tumors as compared to KPC tumors.

F. Development of cell lines and organoids from KPC and KPCC tumors

Since mouse model-derived cell lines represent valuable tools to understand PDAC biology and for drug treatment studies, we have developed four cell lines from tumors derived from KPC mouse model (Y846, KCT-3129, KCT-3248, KCT-3266) (**Figure 5.14A**) [22, 23] . Additionally, we have also developed three cell lines from primary tumors (Y543, Y609, Y841) and one cell line from a liver metastasis of KPCC (Y841-LM) mouse model. Representative morphology of some of these cell lines is outlined in **Figure 5.14B**. Preliminary characterization of some of these KPCC cell lines showed increased expression of Tn and STn carbohydrate antigens as compared to the well-characterized Fc-1295 KPC cell line. Expression of CK-19 in all the cell lines suggests their ductal origin. Further, comparison of KPC and KPCC cell lines will unveil the mechanisms underlying increased aggressiveness of C1galt1 knockout tumors.

Along with the cell lines, we have also developed organoids from KPC tumors (Y846, Y3129) [24]. **Figure 5.15** outlines representative pictures of KPC organoids. We are in the process of generating KPCC organoids. Comparative studies with KPC and KPCC organoids will further help us in understanding the role of C1galt1 in PDAC.

4. Discussion

Evidence of increased presence of unusual/aberrant carbohydrate antigens dates back to 1990s. Pioneer studies focused on pancreatic cancer glycobiology have shown the expression of several incomplete/truncated carbohydrate antigens such as Tn, T and STn in intraductal papillary-mucinous neoplasm, chronic pancreatitis and pancreatic cancer tissues [25, 26]. These studies report differential expression of these carbohydrate antigens in all of these pathological states of the pancreas. For instance, Itzkowitz *et al.* have demonstrated marked increase of STn in pancreatic cancer (expressed by 97% of cancer tissues), while it is not expressed by normal pancreas [25]. On the contrary, expression of T carbohydrate structure was observed in normal acinar structures, but only 48% of pancreatic cancer tissues express this carbohydrate antigen [25]. Relatively increased presence of one carbohydrate antigen over the other suggests that expression of glycosyltransferases that synthesize these carbohydrate antigens is modulated with PDAC progression. The notion of aberrant glycosylation in PDAC was further bolstered by a recent study from Dr. Remmers *et al.* that has also demonstrated differential expression of glycans in PDAC [13]. In particular, the study established differential glycosylation of MUC1 and MUC4 during PDAC progression [13].

Though these studies provide insights in to aberrant glycosylation in PDAC, it is really important to understand the underlying mechanism of aberrant glycosylation and how aberrant glycosylation induces PDAC progression. As discussed previously, altered expression of glycosyltransferases could potentially induce expression of aberrant carbohydrate antigens. In this context, study by Radhakrishnan and Hoffman *et al.* have demonstrated that loss of Cosmc, a chaperone for glycosyltransferase C1GALT1 leads to aberrant O-glycosylation and increased aggressiveness [1, 2]. Though these studies have indicated an essential role of C1GALT1 chaperone (Cosmc) in PDAC, precise roles of

C1GALT1 in PDAC need to defined. Another critical aspect that needs to be explored is how aberrant glycosylation impacts PDAC progression and metastasis.

Our study is a maiden attempt to study the aberrant role of glycosylation in PDAC progression using genetically engineered mouse models. Although several animal models of PDAC have been established in the past few years, a genetically engineered mouse model that addresses the specific contribution of truncated O-glycans in PDAC progression is not yet described. In an effort to explore the role of truncated O-glycans in PDAC, we attempted to develop an animal model of PDAC that has truncated O-glycans. As discussed previously in Chapter 4 that loss of C1galt1 in PDAC cancer cells leads to truncated glycans, we developed the KPCC model that has pancreas-specific C1galt1 depletion along with Kras and p53 mutations. We observed that loss of C1galt1 in the context of already established tumor setting (Kras and p53 mutations) significantly affected PDAC latency. PanIN (pancreatic intraepithelial neoplasia) lesions were noticed in 3-weeks-old KPCC mice. This finding was quite intriguing, as this early lesion development has not been observed with KPC mice. PanIN initiation was observed at around 5-weeks in KPC mouse model. Strikingly, loss of C1galt1 along with Kras and p53 mutations in mouse pancreas significantly reduced survival of mice in comparison with mice that have only Kras and p53 mutations. The median survival of KPCC mice was around 15 weeks as compared to 28 weeks for KPC mice.

Tissue histology revealed poorly differentiated/undifferentiated morphology of these tumors as compared to KPC tumors that are more differentiated. KPCC tumors were highly proliferative as assessed by mitotic figure count. We assessed desmoplasia in KPCC and KPC tumors using alpha-SMA and Sirius red staining. Increased desmoplasia is one of the characteristic features of pancreatic tumors and adversely affects PDAC outcome [27]. We noticed that there is diminished fibrosis in KPCC tumors as compared

to KPC tumors. This contradictory finding is in agreement with a previous study by Rhim *et al.* that demonstrates increased aggressiveness of PDAC with less stroma [19]. The study targeting Shh signaling (important in fibrosis) points to the extensive proliferation of tumor cells in the absence of stroma [19]. We observed a similar tumor phenotype with C1galt1 knockout in KPCC mice. Two possibilities may account for this aggressive phenotype. First, loss of C1galt1 leads to significant increase in proliferation of tumor cells that overnumbers the stromal component. Another is loss of C1galt1 decreases growth of stromal population and hence gives a chance to tumor cells to expand. Our results from CRISPR/Cas9-based knockout of C1GALT1 in human PDAC cells (Chapter-4 of dissertation) support the first possibility as we observed increased tumorigenicity of C1GALT1 KO PDAC cells. However, specific experiments need to be performed to test this paradoxical finding.

Interestingly, we observed early metastasis in KPCC tumors (5 weeks) as compared to KPC tumors, which develops late metastasis (20-25 weeks). KPCC is the first PDAC model to show very early metastasis (5 weeks), compared to other PDAC animal models developed so far. To understand the molecular mechanism involved in increased metastasis, we analyzed EMT markers in KPC and KPCC models, due to the spindled morphology of tumor cells in the KPCC model. It is well known that EMT is the initial step for the metastatic cascade [28]. The assessment of EMT markers in KPC and KPCC tumors revealed increased expression of a mesenchymal marker, vimentin and decreased expression of several epithelial markers such as claudins and keratins [29]. Further, we stained KPC and KPCC tumors for the mesenchymal protein vimentin [30]. Increased vimentin expression allows cells to gain mesenchymal phenotype and hence increased migration and metastasis [31]. There was a remarkable increase in vimentin expression

in KPCC tumors as compared to KPC tumors. Overall, this result suggests that increased expression of vimentin with depletion of C1galt1 may lead to early metastasis of PDAC.

To investigate if the observed aggressive phenotype is linked to altered glycosylation, we stained KPC and KPCC tumors with alcian-blue, PNA-Rhodamine and VVA-Fluorescein. Assessment of O-glycans via these carbohydrate specific stains demonstrated significantly altered glycosylation in KPCC pancreatic tumors as compared to KPC. In particular, we have observed increased expression of truncated Tn carbohydrate antigen. Truncated glycosylation on proteins has been shown to activate signaling molecules, possibly via relief of steric hindrance imparted by extended glycan structures. Further, the increased expression of truncated glycans has been shown to facilitate disease progression and metastasis by interacting with lectins such as galectins and Siglecs [32]. However, the possible involvement of such carbohydrate interactions in aggressiveness of KPCC tumors needs to be explored. Collectively, our study highlights the significant involvement of loss of C1galt1 expression in PDAC progression and metastasis. Since increased expression of Tn carbohydrate antigen in KPCC mouse models aggravates PDAC progression, our study holds potential clinical implications. Assessment of C1GALT1/Tn carbohydrate antigen in PDAC patients can predict disease severity. So far, CA-19.9 is one of the prognostic tests for PDAC [33, 34]. However, sensitivity and specificity of this serological assay needs to be improved. Further, a subset of patients does not express CA19.9 [35]. We speculate that assessing C1GALT1/Tn carbohydrate antigen in PDAC patients, especially for this subset of patients, can be of great benefit. Additionally, since the KPCC model represents faster PDAC progression model, we believe that this model could be used in pre-clinical studies to test the effect of several therapeutic agents on PDAC growth and metastasis. Together, the findings from our study indicate that knockout of C1galt1 in already established tumor setting (Kras and

p53 mutations) caused aberrant glycosylation that decreased PDAC latency and increased tumor progression and metastasis .

Figure legends

Figure 5.1: Schematic representation of the breeding strategy for the development of *Kras^{G12D}; Trp53$^{R172H/+}$; C1galt1$^{loxP/loxP}$; Pdx1-Cre* (KPCC) mouse model to investigate the role of C1galt1 in PDAC progression and metastasis: *Kras^{G12D}; Pdx1-Cre* and *LSLTrp53$^{R172H/+}$* were crossed with *C1galt1$^{loxP/ loxP}$* mice separately to obtain the F1 progeny with *Kras^{G12D}; Pdx1-Cre; C1galt1$^{+/loxP}$* and *LSLTrp53$^{R172H/+}$; C1galt1$^{+/loxP}$* genotype. Intercrossing of F1 progeny resulted in *Kras^{G12D}; Trp53$^{R172H/+}$; C1galt1$^{loxP/loxP}$; Pdx1-Cre* (KPCC) mouse model. Following birth, the F2 progeny was then euthanized at 3, 5, 10, 15 and 20 weeks of age to analyze pancreatic cancer progression in the absence of C1galt1.

Figure 5.1

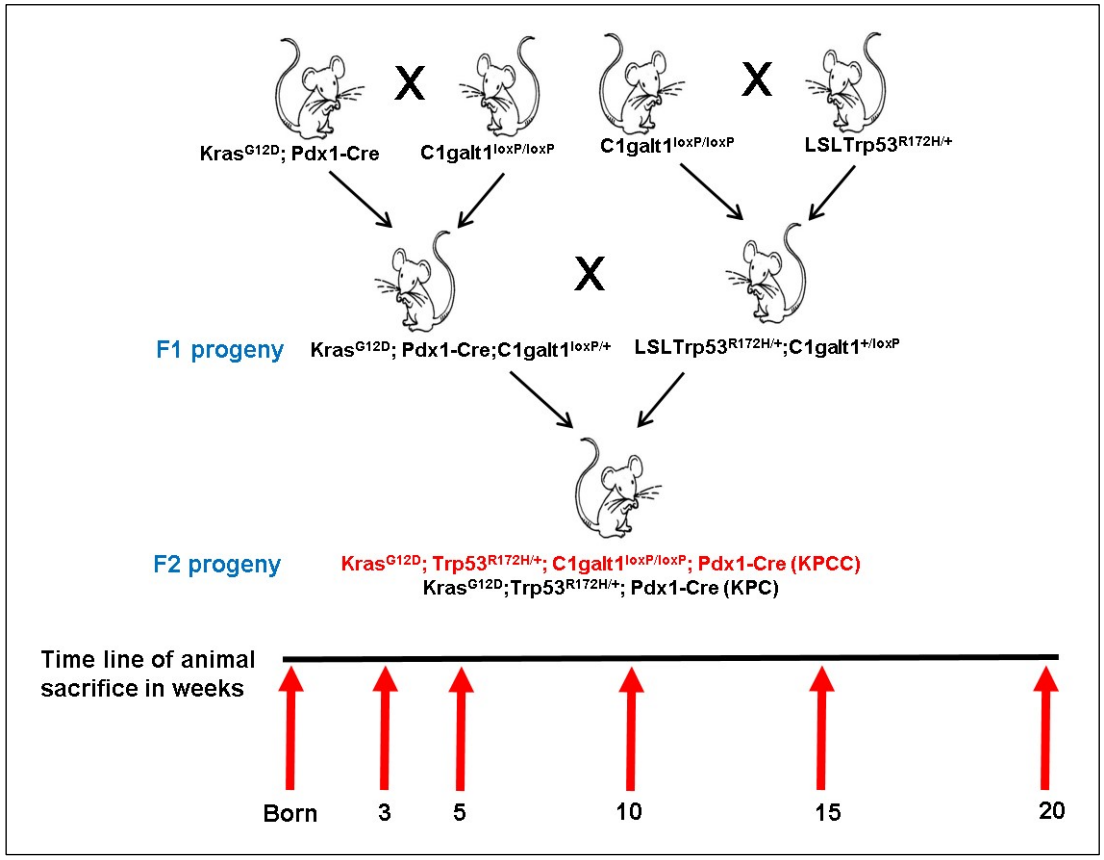
Kras^{G12D}; Pdx1-Cre
X
C1galt1$^{loxP/loxP}$
C1galt1$^{loxP/loxP}$
X
LSLTrp53$^{R172H/+}$
X
F1 progeny
Kras^{G12D}; Pdx1-Cre;C1galt1$^{loxP/+}$
LSLTrp53$^{R172H/+}$;C1galt1$^{+/loxP}$
F2 progeny
Kras^{G12D}; Trp53$^{R172H/+}$; C1galt1$^{loxP/loxP}$; Pdx1-Cre (KPCC)
Kras^{G12D};Trp53$^{R172H/+}$; Pdx1-Cre (KPC)
Time line of animal sacrifice in weeks
Born
3
5
10
15
20

Figure 5.2: Loss of C1galt1 resulted in faster PDAC progression: (A) Gross appearance of pancreatic tumors in KPC and KPCC mice. Large pancreatic tumor was seen for KPCC mice at around 10 weeks as compared to 28 weeks KPC mice with a small tumor. **(B)** Representative histological pictures of the pancreas from age-matched control, KPC and KPCC mice at 3, 5, 10, 15 and 20 weeks. (n=5 for control, KPC and KPCC mice). H and E stained pictures reveal the appearance of neoplastic lesions at around 3 weeks in KPCC mice as compared to KPC mice, which has a normal pancreas. Tumors were seen in 10-, 15 and 20-weeks old KPCC mice. However, KPC mice showed late tumor development at around 20 weeks. All the pictures were taken at 20X magnification.

Figure 5.2

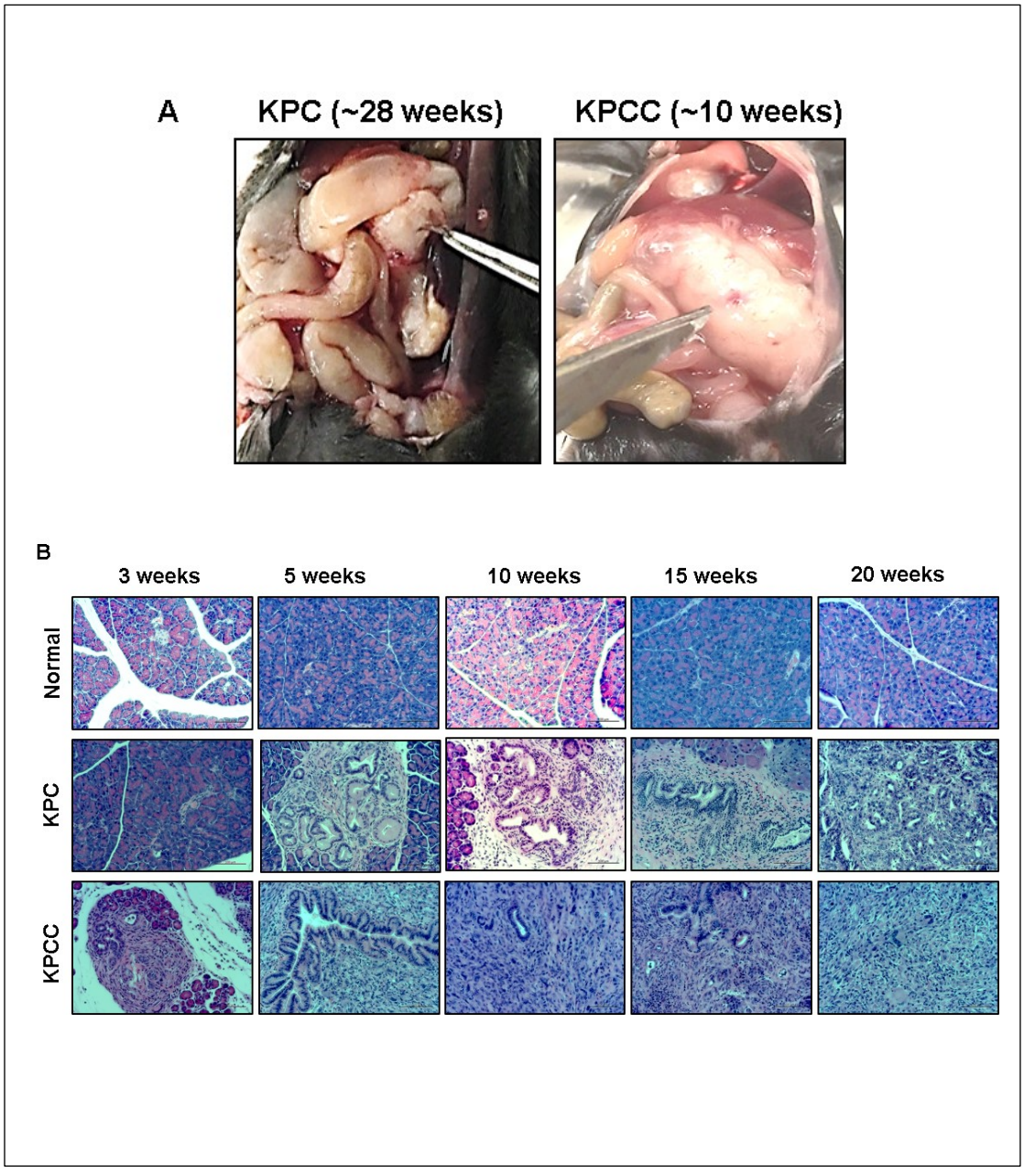
A
KPC (~28 weeks)
KPCC (~10 weeks)
B
3 weeks
5 weeks
10 weeks
15 weeks
20 weeks
Normal
KPC
KPCC

Figure 5.3: Early tumor development in KPCC mice: (A) Increased percentage of tumor-bearing animals was observed in KPCC cohort as compared to KPC cohort at 5, 10, 15 and 20 weeks. **(B)** Representative H and E stained picture of pancreatic tumors from 30-week old KPC and 10-week old KPCC mice. KPC mice pancreatic tumors displayed well-differentiated pancreatic tumor histology, whereas poorly differentiated/undifferentiated tumor histology was observed for KPCC tumors. Whole slides containing pancreatic sections were scanned at TSF and the enlarged pictures represent 40X magnification.

Figure 5.3

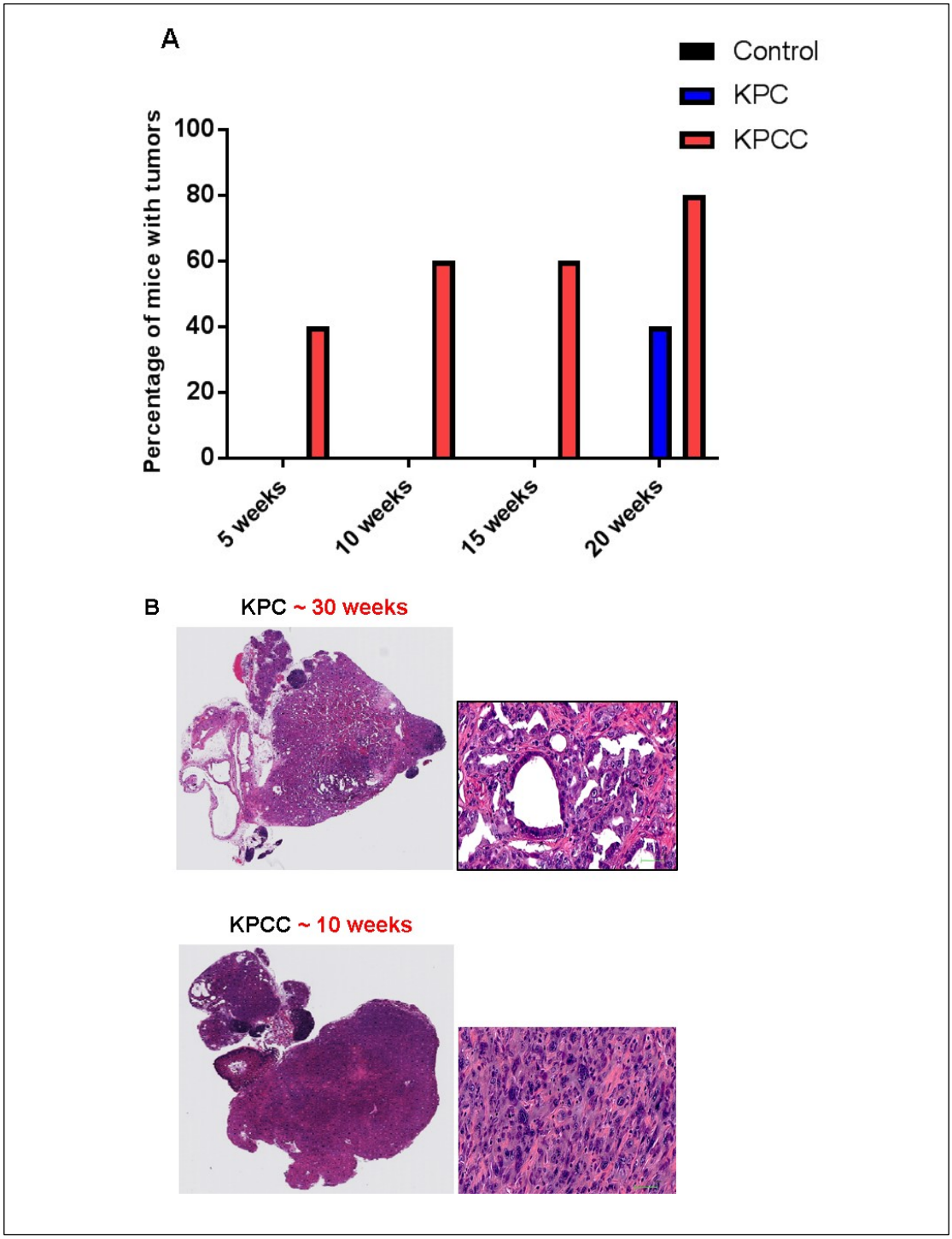
A
Control
KPC
KPCC
Percentage of mice with tumors
100
80
60
40
20
0
5 weeks
10 weeks
15 weeks
20 weeks
B
KPC ~ 30 weeks
KPCC ~ 10 weeks

Figure 5.4 C1galt1 depletion in mouse pancreas did not affect pancreatic development: H and E stained pictures from two 4-weeks old *C1galt1* $^{loxP\ /loxP}$; Pdx1-Cre mice demonstrates that C1galt1 deletion in mouse pancreas have no effect on its development. Pancreas from *C1galt1* $^{loxP\ /loxP}$; Pdx1-Cre mice showed normal islets and acinar structures.

Figure 5.4

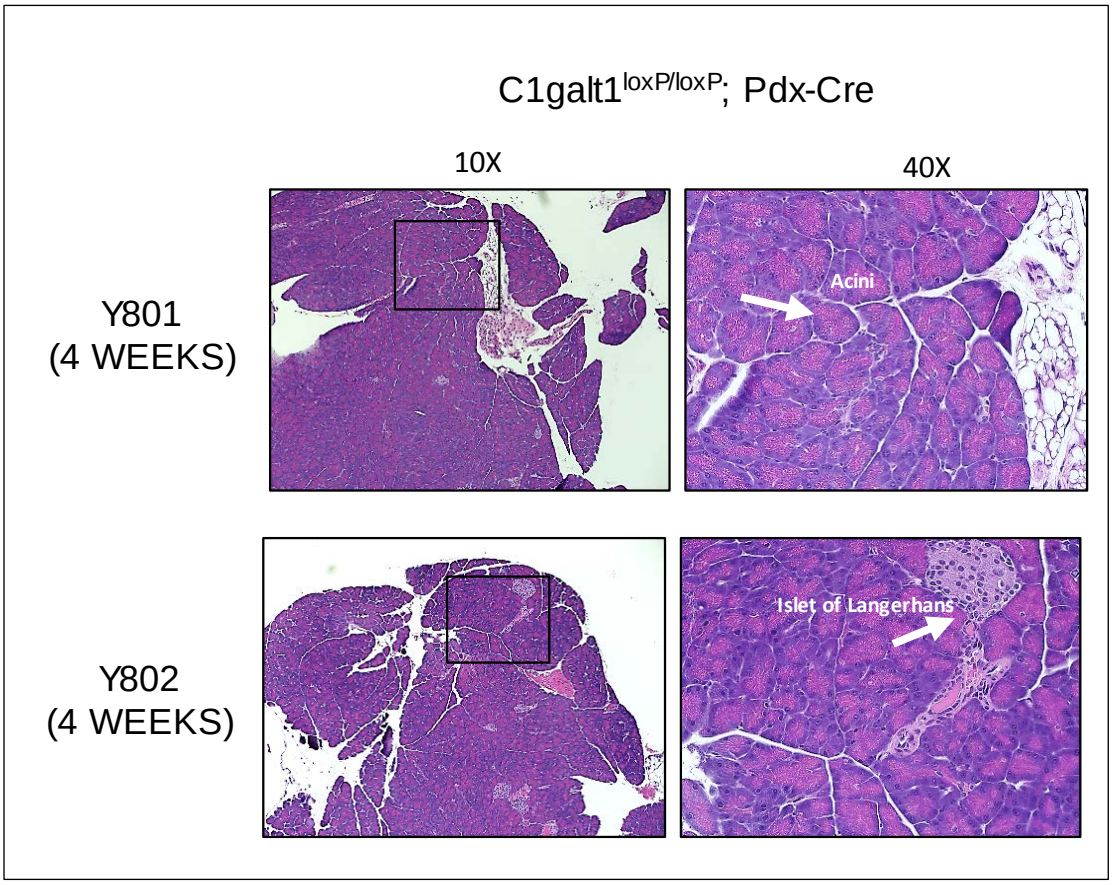
C1galt1loxP/loxP; Pdx-Cre
10X
40X
Y801
(4 WEEKS)
Acini
Y802
(4 WEEKS)
Islet of Langerhans

Figure 5.5: Knockout of C1galt1 significantly decreased overall Survival: Survival analysis of KPC and KPCC mice using Kaplan-Meier approach shows that genomic depletion of C1galt1 in KPCC mice significantly decreased median survival as compared to KPC mice. (n=11 for KPC and n=8 for KPCC). KPCC mice has significantly decreased median survival (107 days) as compared to KPC mice (205 days)

Figure 5.5

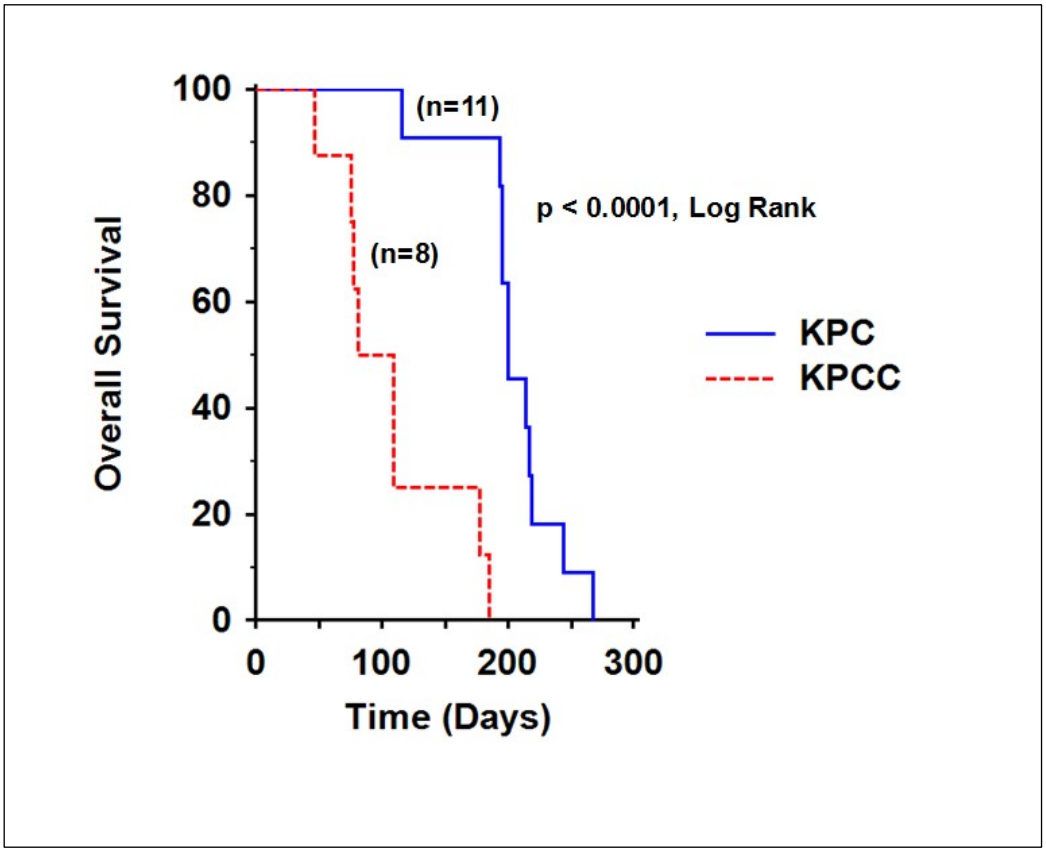
100
80
60
40
20
0
Overall Survival
0
100
200
300
Time (Days)
(n=11)
(n=8)
p < 0.0001, Log Rank
KPC
KPCC

Figure 5.6: Increased proliferation of KPCC tumors as compared to KPC tumors: ***Top panel:*** Proliferation of KPC and KPCC tumors was assessed by counting mitotic figures (cells undergoing mitosis). Bar diagram demonstrates significant increase of mitotic figures in KPCC tumors as compared to KPC tumors (n=3 for KPC and KPCC mice); ***Bottom panel:*** Representative histologic pictures showing increased presence of typical and atypical mitotic figures in KPCC mice as compared to KPC mice. Enlarged pictures represent abnormal/dividing nuclear structures. Representative pictures were taken at 20X magnification. Error bars represent mean ± s.e.m. *P<0.05; by unpaired two-sided Student's t-test.

Figure 5.6

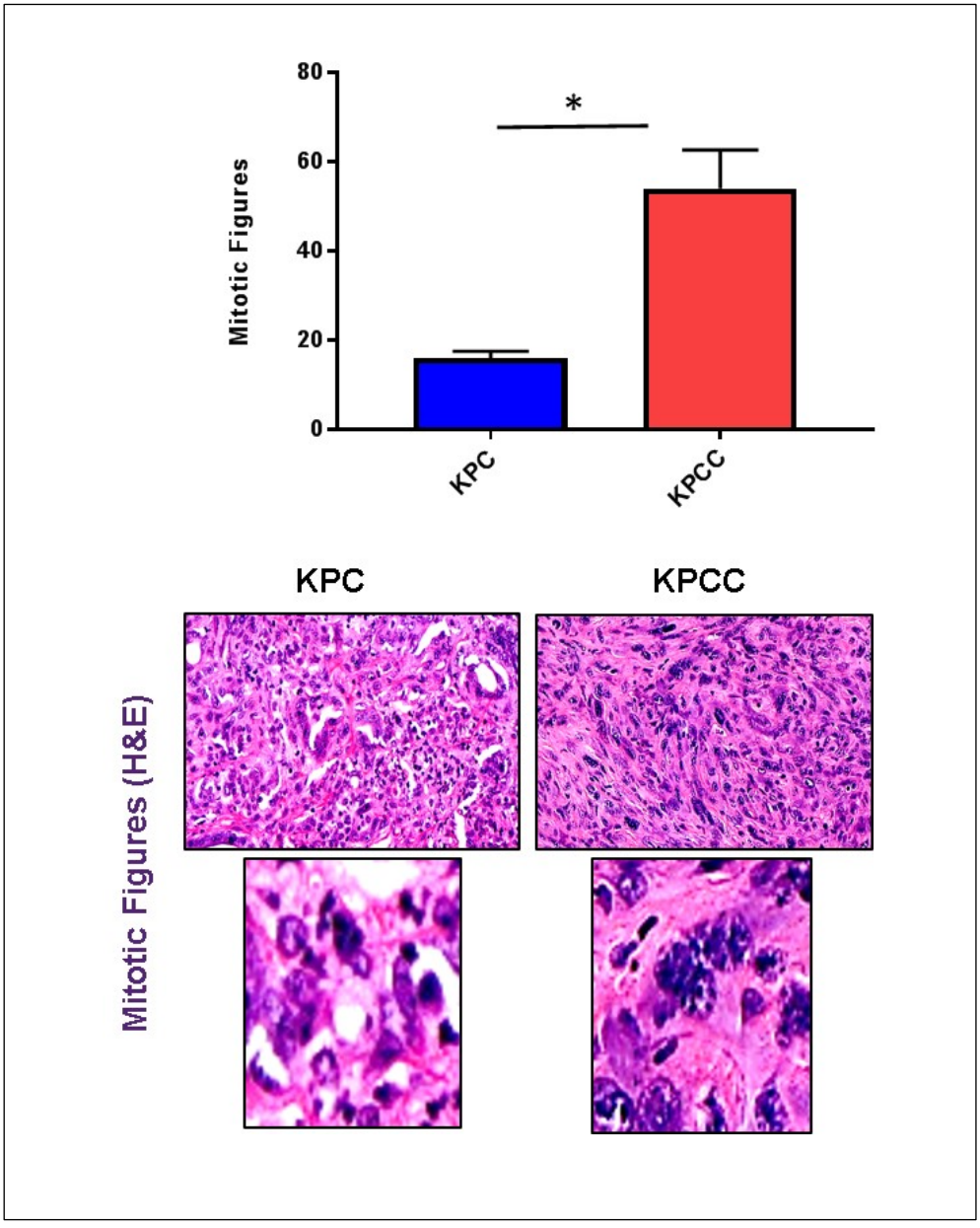
Mitotic Figures
80
60
40
20
0
*
KPC
KPCC
KPC
KPCC
Mitotic Figures (H&E)

Figure 5.7: Decreased alpha-SMA in KPCC tumors: ***Top panel:*** Cancer-associated fibroblasts in KPC and KPCC pancreatic tumors were examined using alpha-SMA staining. Scatter dot plot demonstrates significant decrease of alpha-SMA composite score in KPCC tumors as compared to KPC tumors (n=6 for KPC and KPCC mice); ***Bottom panel:*** Representative histologic pictures showing decreased alpha-SMA staining in KPCC tumors as compared to KPC tumors. Error bars represent mean ± s.e.m. *P<0.05; by Wilcoxon Signed Rank Test. **(B)** ***Top panel:*** Significant decrease in mean fluorescent intensity of alpha-SMA in KPCC pancreatic tumors as compared to KPC tumors. ***Bottom panel:*** Representative immunofluorescent pictures showing decreased alpha-SMA staining in KPCC pancreatic tumors as compared to KPC pancreatic tumors (n=5 for KPC and KPCC mice). Error bars represent mean ± s.e.m. **P<0.005; by Mann Whitney test.

Figure 5.7

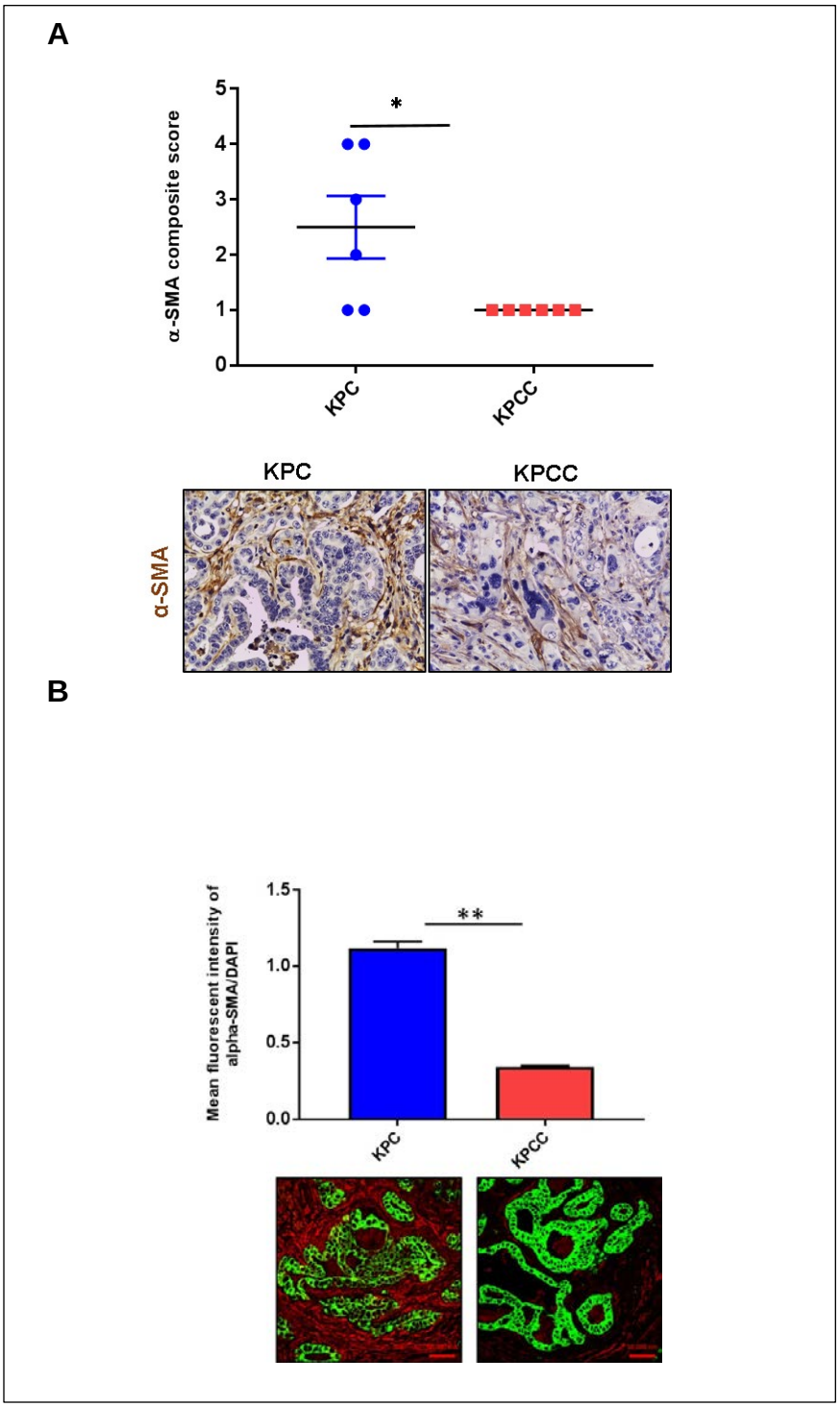
A
α-SMA composite score
5
4
3
2
1
0
*
KPC
KPCC
KPC
KPCC
α-SMA
B
Mean fluorescent intensity of alpha-SMA/DAPI
1.5
1.0
0.5
0.0
**
KPC
KPCC

Figure 5.8: Decreased fibrosis in KPCC tumors: ***Top panel:*** Fibrosis in KPC and KPCC pancreatic tumors was asessed using Picro-Sirius red staining. Sirius red-stained area in KPC and KPCC tumor nodules was quantified using Definiens software (Tissue Science Facility, UNMC). Bar diagram demonstrates significant decrease of percentage of Sirius red-positive area in KPCC tumors as compared to KPC tumors. (n=5 for KPC and KPCC mice); ***Bottom panel:*** Representative histologic pictures showing decreased percentage of Sirius red-stained area in KPCC mice as compared to KPC mice. Whole slides containing pancreatic sections were scanned at TSF and the enlarged pictures represent 40X magnification. Error bars represent mean ± s.e.m. *P<0.05; by unpaired two-sided Student's t-test.

Figure 5.8

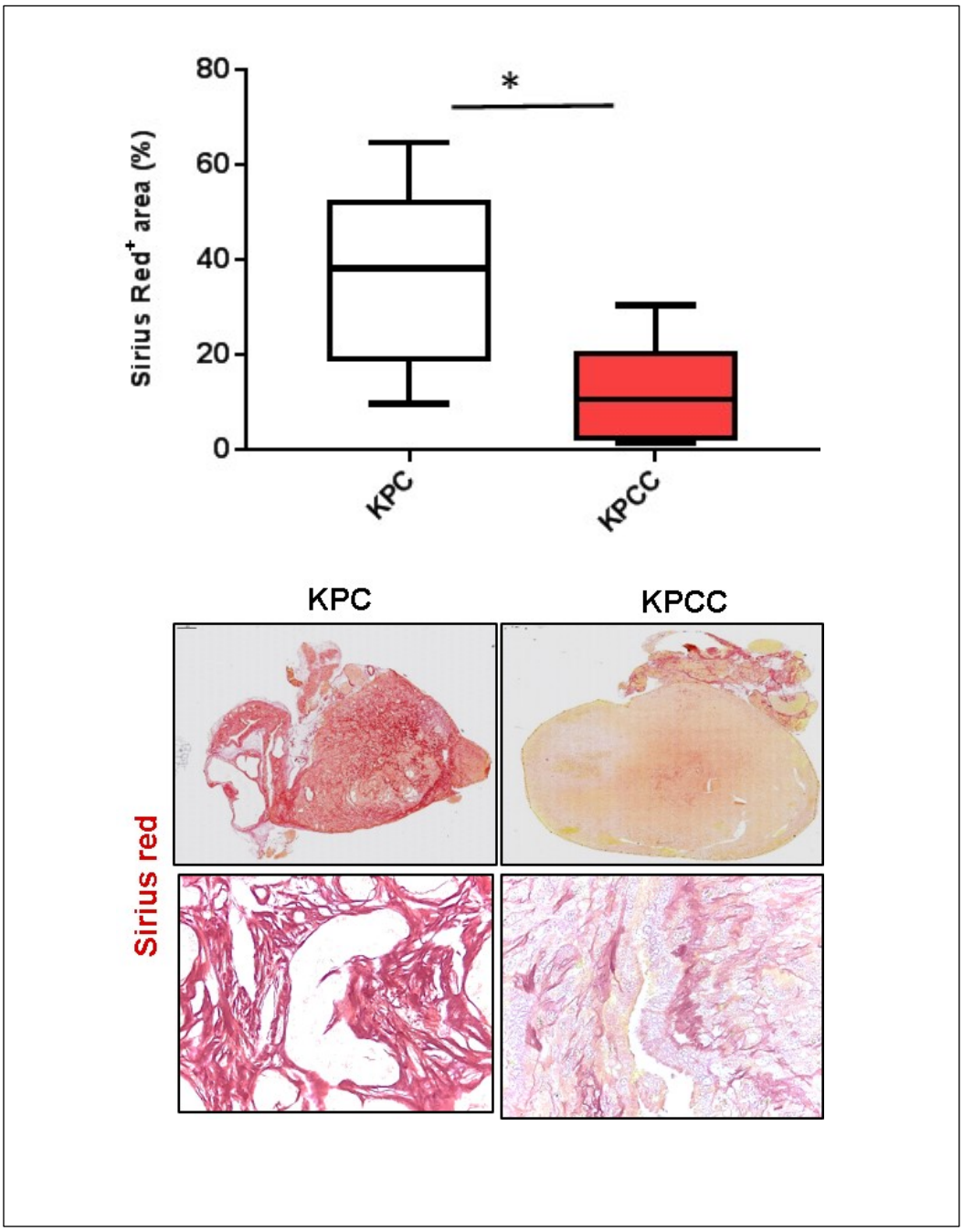

Figure 5.9: Decreased Alcian blue staining in KPCC tumors: KPC and KPCC tissue sections collected at different time points were stained with Alcian blue to assess the impact of C1galt1 knockout on O-glycans. Alcian blue is commonly used to visualize acidic (sulfated/sialylated) glycans. ***Top panel:*** Box and whiskers plot showing significant decrease of Alcian blue composite score in KPCC tumors, as compared to KPC tumors, at different time points; ***Bottom panel:*** Representative histologic pictures showing strong Alcian blue positivity in mucinous neoplastic pancreatic ducts of KPC mice, whereas trace to weak positivity was seen for KPCC pancreatic ducts. (n=4-5 for KPC and KPCC mice; *p<0.05; **p<0.05). Representative pictures were taken at 20X magnification. *P<0.05; by Mann Whitney test.

Figure 5.9

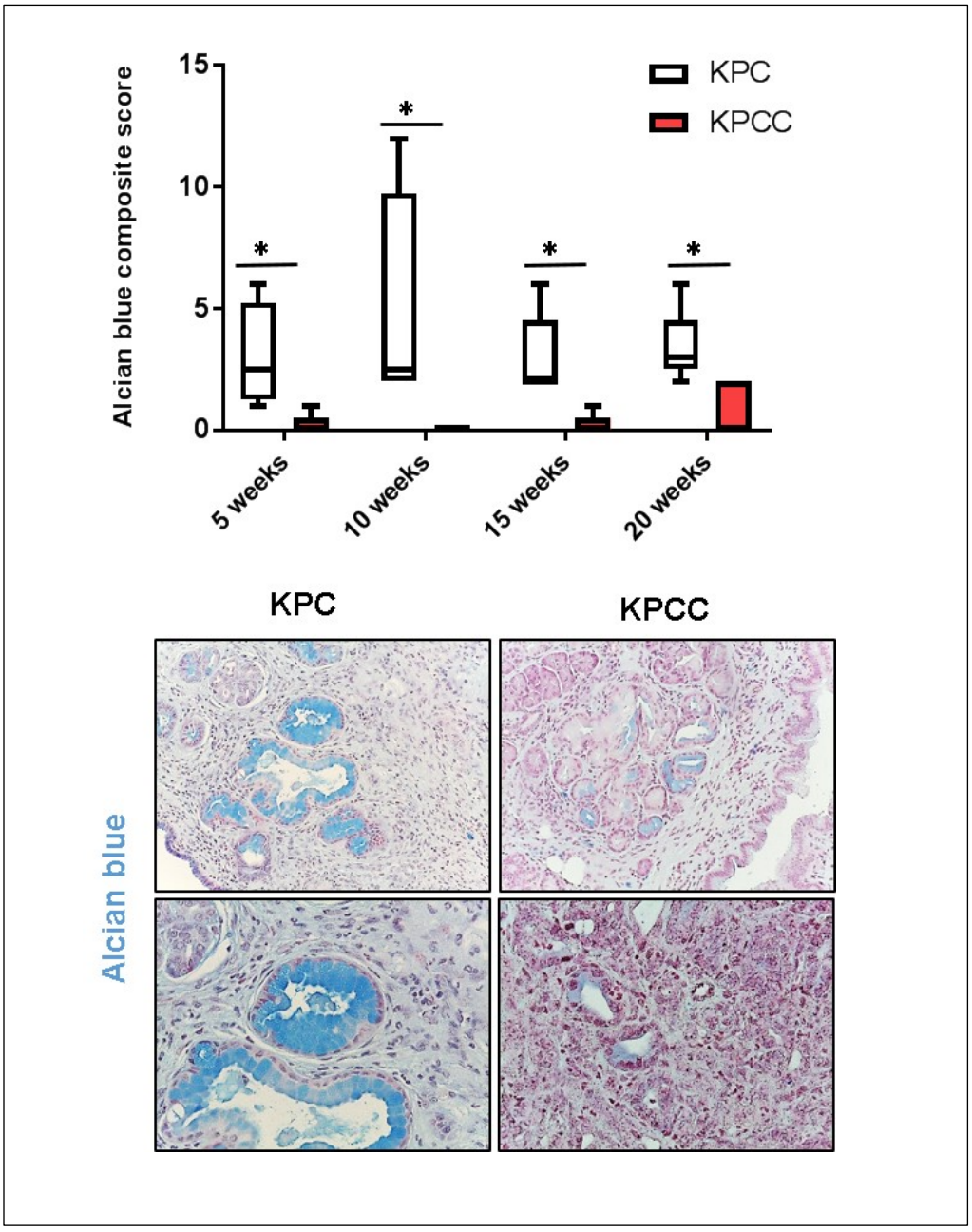
Alcian blue composite score
15
10
5
0
KPC
KPCC
*
*
*
*
5 weeks
10 weeks
15 weeks
20 weeks
KPC
KPCC
Alcian blue

Figure 5.10: Loss of T carbohydrate antigen with knockout of C1galt1 in KPCC mice: KPC and KPCC tumor sections were stained with PNA-Rhodamine to evaluate the impact of C1galt1 knockout on the T carbohydrate antigen synthesis (catalyzed by C1galt1). (**A)** Treatment of PDAC tissue with neuraminidase that cleaves sialic-acids resulted in exposure of T-carbohydrate antigen and hence increased binding of PNA-Rhodamine to T carbohydrate antigen in the neoplastic ducts. (n=4 for KPC and KPCC mice **(B)** ***Top panel:*** Bar diagram depicts significant decrease of mean fluorescent intensity of T carbohydrate antigen in KPCC tumors as compared to KPC tumors; ***Bottom panel:*** Representative fluorescent pictures and histograms showing decreased T carbohydrate antigen staining in neoplastic pancreatic ducts of KPCC mice as compared to KPC mice. Error bars represent mean ± s.e.m. *P<0.05; by Mann Whitney test.

Figure 5.10

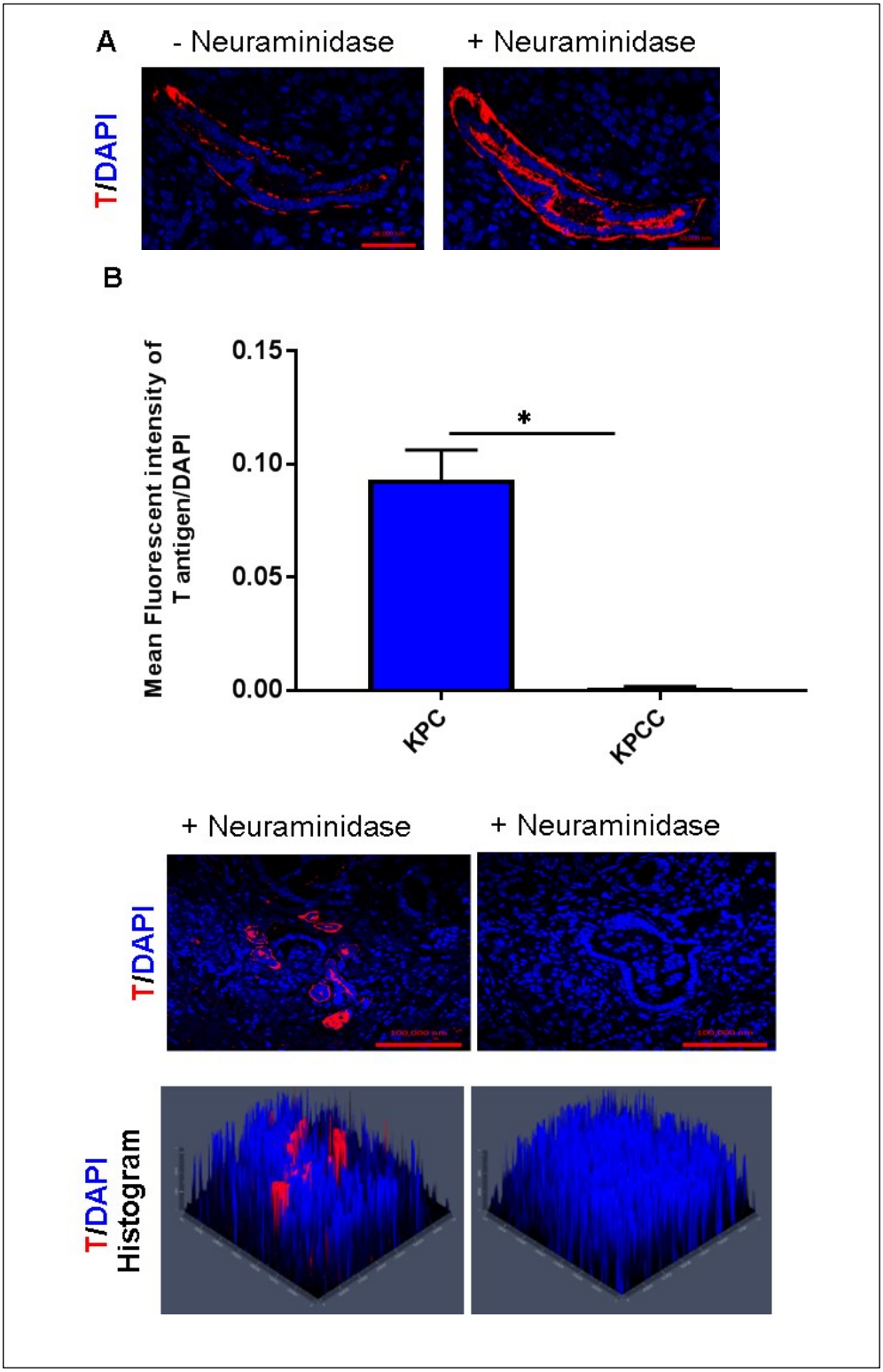
A
- Neuraminidase
+ Neuraminidase
T/DAPI
B
Mean Fluorescent intensity of T antigen/DAPI
0.15
0.10
0.05
0.00
*
KPC
KPCC
+ Neuraminidase
+ Neuraminidase
T/DAPI
T/DAPI Histogram

Figure 5.11: Aberrant expression of truncated Tn carbohydrate antigen in KPCC mice: KPC and KPCC tumors were probed with VVA-Fluorescein to evaluate the impact of C1galt1 knockout on Tn carbohydrate antigen (catalytic substrate for C1galt1). ***Top panel:*** Bar diagram depicts significant increase of mean fluorescent intensity of Tn carbohydrate antigen in KPCC tumors as compared to KPC tumors (n=6 for KPC and KPCC). ***Bottom panel:*** Representative fluorescent pictures and histograms showing increased Tn carbohydrate antigen staining in KPCC mice as compared to KPC mice. Error bars represent mean ± s.e.m. **P<0.005; by Mann Whitney test.

Figure 5.11

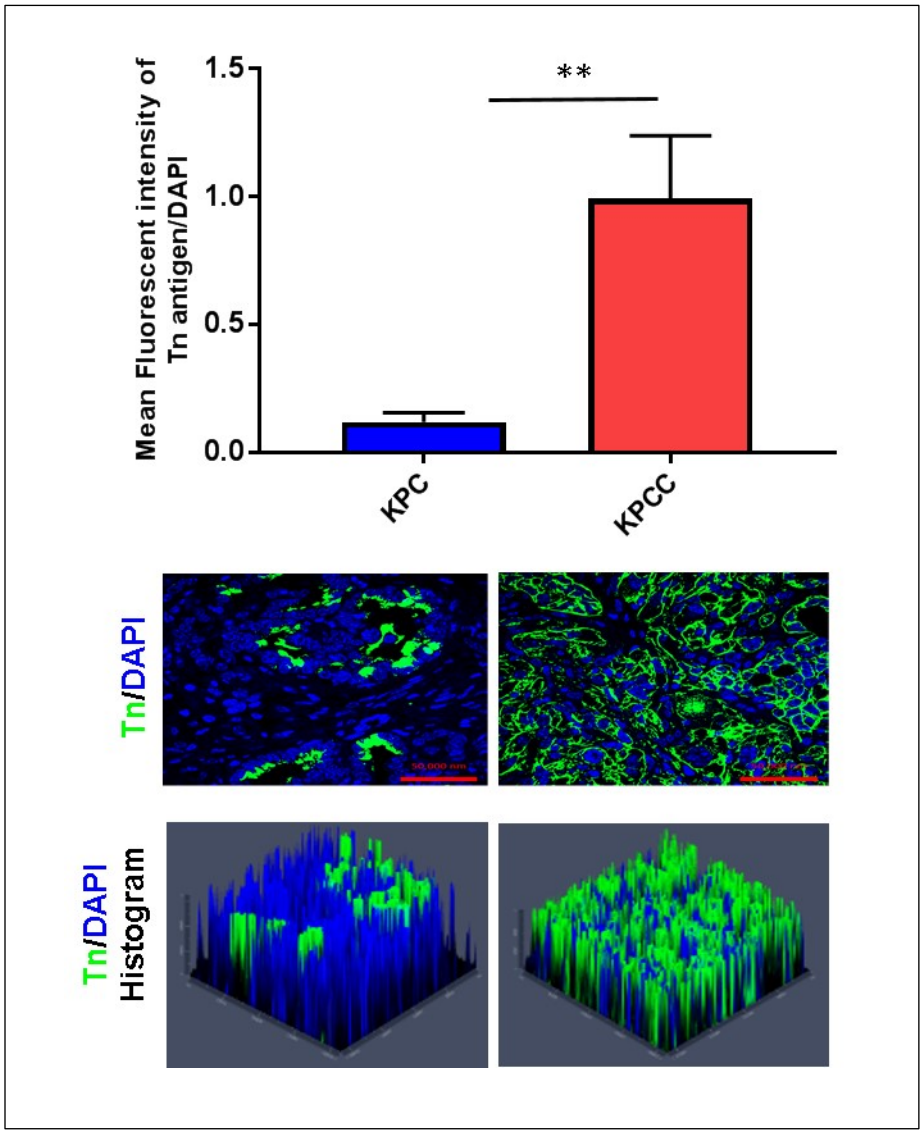
Mean Fluorescent intensity of Tn antigen/DAPI
1.5
1.0
0.5
0.0
**
KPC
KPCC
Tn/DAPI
Tn/DAPI Histogram

Figure 5.12 Loss of C1galt1 resulted in enhanced metastasis: (A) ***Left panel:*** Bar diagram demonstrates increased percentage of animals with metastasis in KPCC mice as compared to KPC mice at different time points (n=5 for KPC and KPCC mice) ***Right panel:*** Representative H & E pictures showing metastatic lesions in peritoneum, oviduct, liver and stomach in KPCC mice. **(B)** RT-PCR analysis of several EMT genes shows significant increase of mesenchymal marker vimentin and significant decrease of epithelial markers, keratin-5, keratin-7, claudin-4 and claudin-6. Error bars represent mean ± s.e.m. * $P<0.05$, **$P<0.005$; by unpaired two-sided Student's t-test.

Figure 5.12

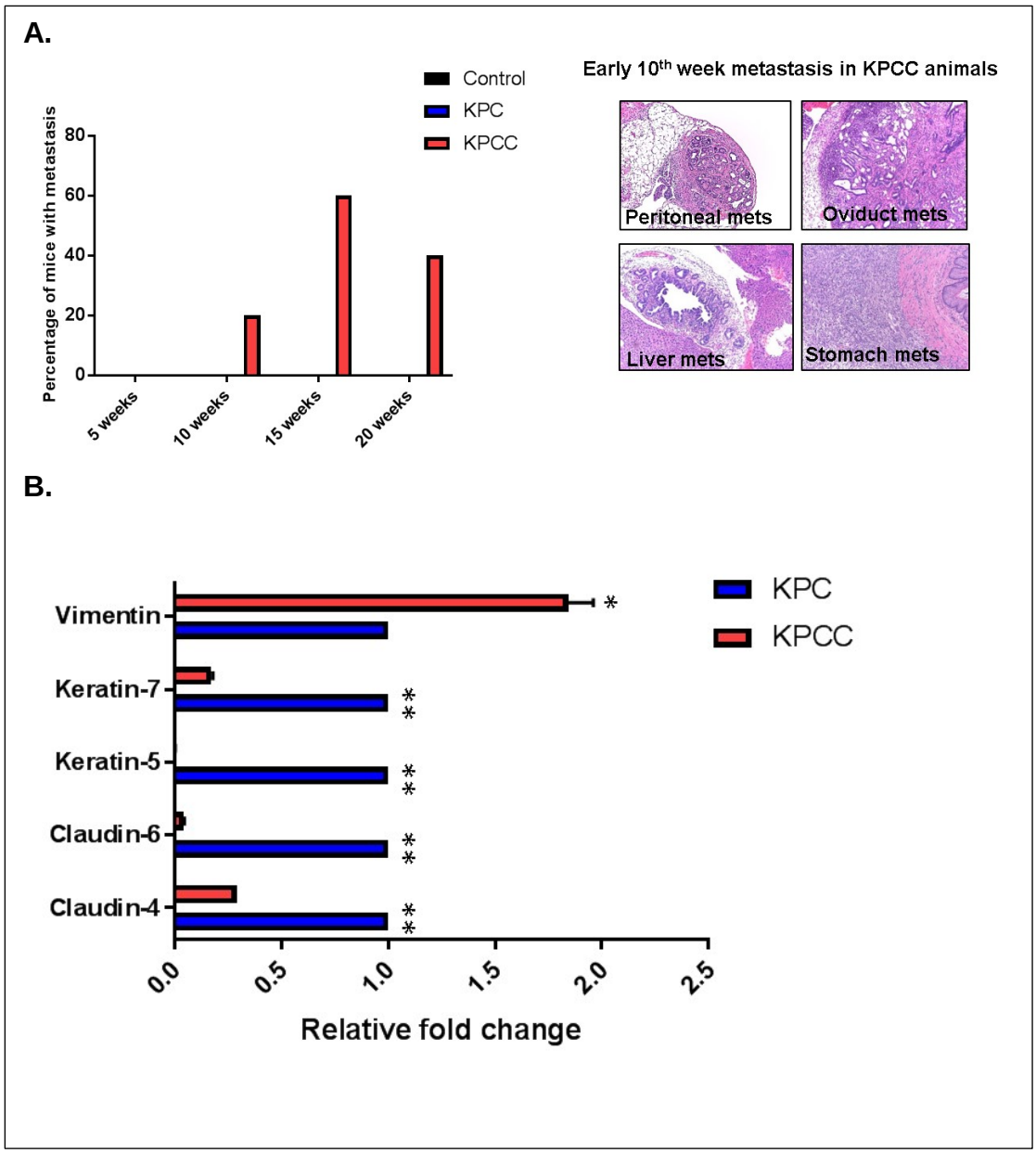
A.
Control
KPC
KPCC
Percentage of mice with metastasis
80
60
40
20
0
5 weeks
10 weeks
15 weeks
20 weeks
Early 10th week metastasis in KPCC animals
Peritoneal mets
Oviduct mets
Liver mets
Stomach mets
B.
KPC
KPCC
Vimentin
Keratin-7
Keratin-5
Claudin-6
Claudin-4
0.0
0.5
1.0
1.5
2.0
2.5
Relative fold change

Figure 5.13 Remarkable increase of vimentin expression in KPCC pancreatic tumors: (A) ***Top panel:*** Significant increase in mean fluorescent intensity of vimentin in KPCC pancreatic tumors as compared to KPC tumors. ***Bottom panel:*** Representative immunofluorescent pictures showing increased vimentin staining in KPCC pancreatic tumors as compared to KPC pancreatic tumors (n=6 for KPC and KPCC mice). **(B)** ***Top panel:*** Asessment of vimentin staining in pancreatic tumor cells of KPC and KPCC mice reveals significant increase of vimentin composite score in KPCC pancreatic tumors as compared to KPC (n=7 for KPC and KPCC mice). ***Bottom panel:*** Representative immunohistochemical pictures showing increased vimentin staining in KPCC pancreatic tumors as compared to KPC pancreatic tumors. Error bars represent mean ± s.e.m. **P<0.005; by Mann Whitney test.

Figure 5.13

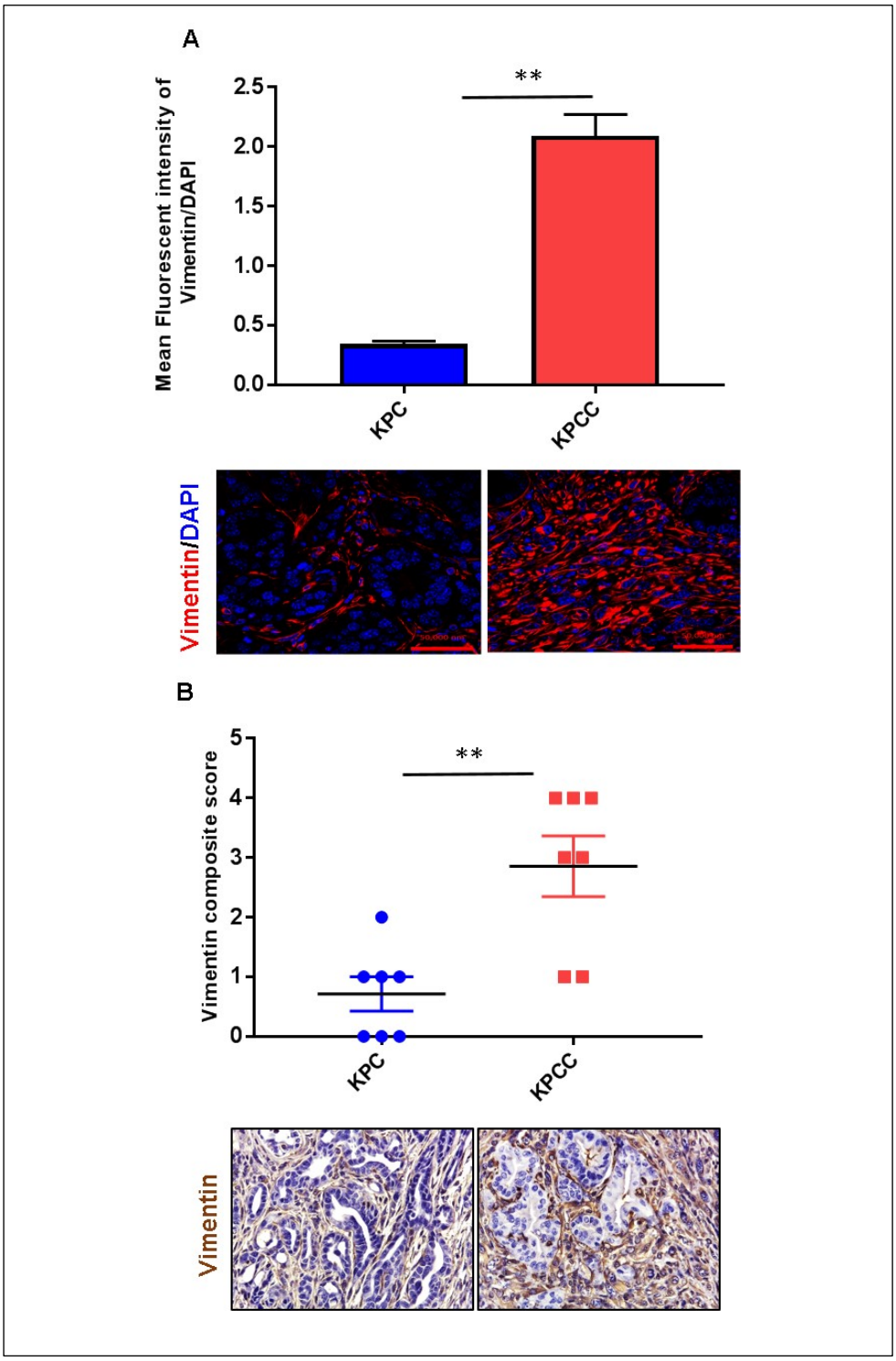
A
Mean Fluorescent intensity of Vimentin/DAPI
2.5
2.0
1.5
1.0
0.5
0.0
**
KPC
KPCC
Vimentin/DAPI
B
Vimentin composite score
5
4
3
2
1
0
**
KPC
KPCC
Vimentin

Figure 5.14: Characterization of murine cell lines derived from KPC and KPCC tumors: The role of C1galt1 in PDAC was studied by development of cancer cell lines from KPC and KPCC tumors. **(A)** Representative morphology of KPC (top panel) and KPCC (bottom panel) pancreatic tumor cell lines. **(B)** Left panel depicts DNA gel picture showing knockout of C1galt1 in KPCC cell lines as compared to KPC cell line. Right panel demonstrates increased expression of Tn and STn truncated carbohydrate antigens in KPCC cell lines as compared to the KPC cell line. All the cell lines express CK-19, however the expression of CK-19 was decreased in one of the KPCC cell line (Y609) as compared to Y543 and Fc-1295.

Figure 5.14

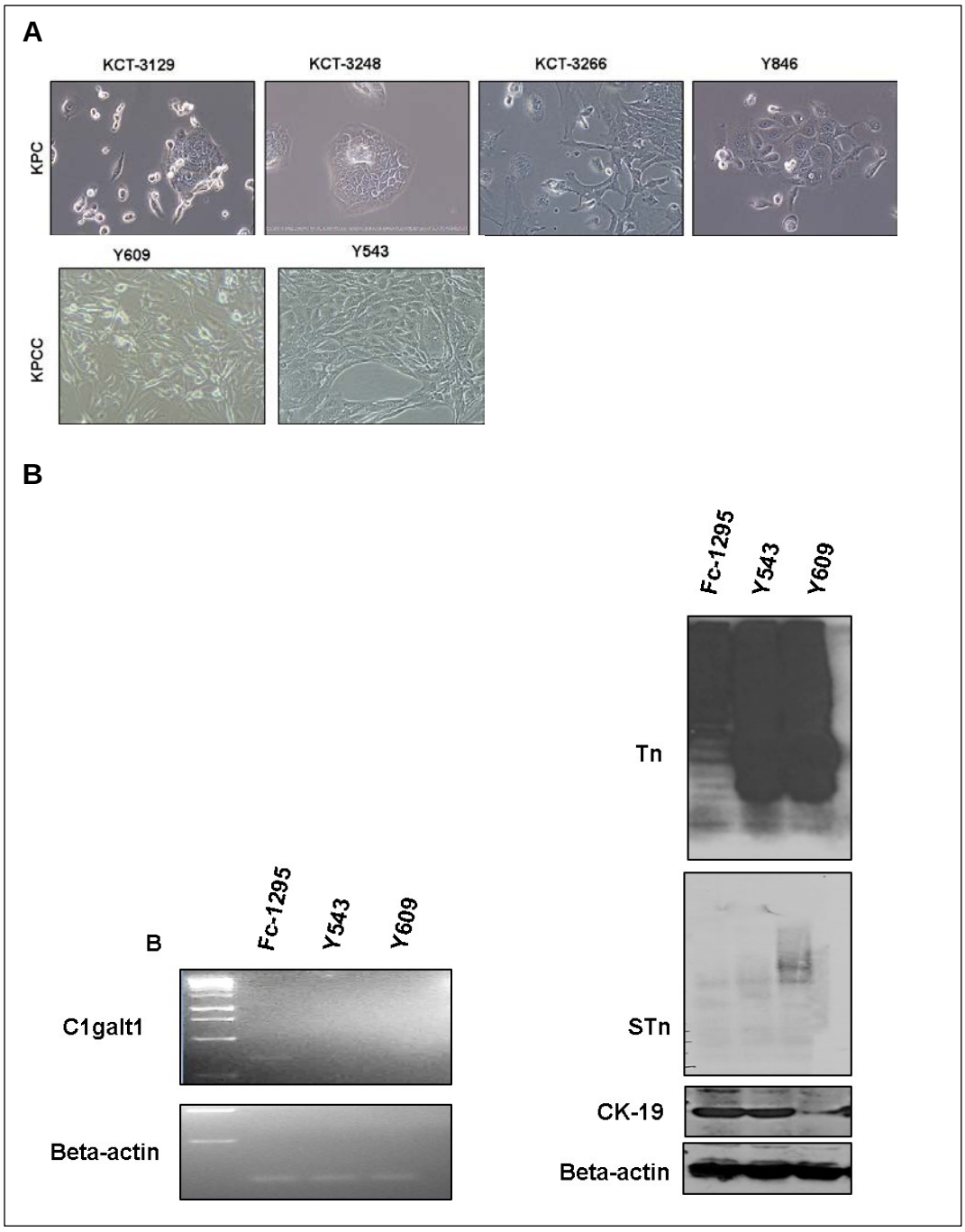
A
KCT-3129
KCT-3248
KCT-3266
Y846
KPC
Y609
Y543
KPCC
B
Fc-1295
Y543
Y609
Tn
STn
CK-19
Beta-actin
B
Fc-1295
Y543
Y609
C1galt1
Beta-actin

Figure 5.15: Development of KPC tumor organoids: 3-D organoid system was developed from KPC mice that recapitulates *in vivo* PDAC histology. (A) Representative microscopic pictures of organoids developed from KPC tumors shows ductal structures. Fibroblast like structures (marked by arrow) were also noticed among organoids, indicating the presence of tumor microenvironment components in 3-D organoid cultures. **(B)** Representative H and E stained pictures of organoids sections showing ductal structures.

Figure 5.15

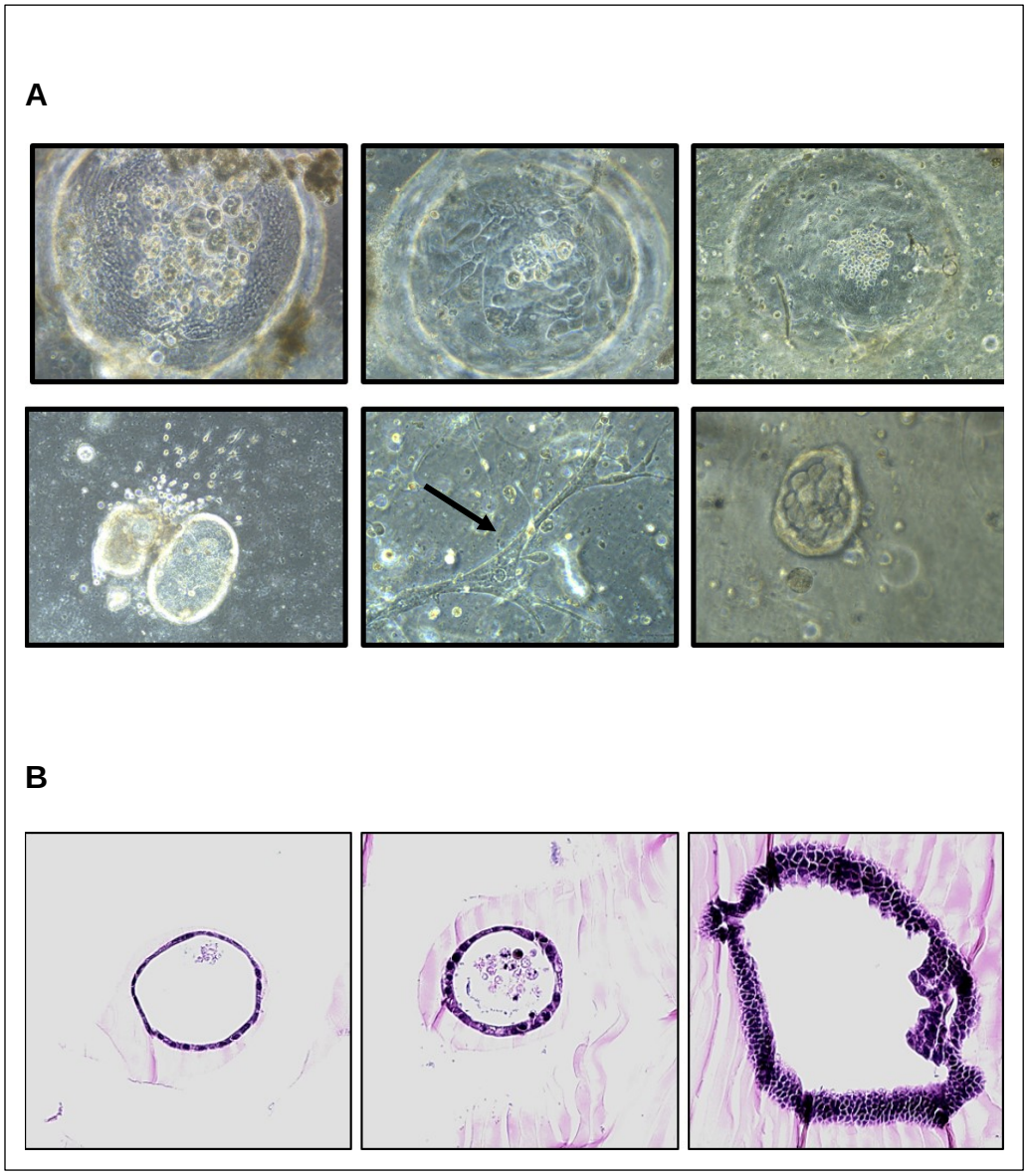

References

[1] B.T. Hofmann, L. Schluter, P. Lange, B. Mercanoglu, F. Ewald, A. Folster, A.S. Picksak, S. Harder, A.T. El Gammal, K. Grupp, C. Gungor, A. Drenckhan, H. Schluter, C. Wagener, J.R. Izbicki, M. Jucker, M. Bockhorn, G. Wolters-Eisfeld, COSMC knockdown mediated aberrant O-glycosylation promotes oncogenic properties in pancreatic cancer, Molecular cancer, 14 (2015) 109.

[2] P. Radhakrishnan, S. Dabelsteen, F.B. Madsen, C. Francavilla, K.L. Kopp, C. Steentoft, S.Y. Vakhrushev, J.V. Olsen, L. Hansen, E.P. Bennett, A. Woetmann, G. Yin, L. Chen, H. Song, M. Bak, R.A. Hlady, S.L. Peters, R. Opavsky, C. Thode, K. Qvortrup, K.T. Schjoldager, H. Clausen, M.A. Hollingsworth, H.H. Wandall, Immature truncated O-glycophenotype of cancer directly induces oncogenic features, Proc Natl Acad Sci U S A, 111 (2014) E4066-4075.

[3] S.D. Leach, Mouse models of pancreatic cancer: the fur is finally flying!, Cancer Cell, 5 (2004) 7-11.

[4] P.K. Mazur, J.T. Siveke, Genetically engineered mouse models of pancreatic cancer: unravelling tumour biology and progressing translational oncology, Gut, 61 (2012) 1488-1500.

[5] S.R. Stowell, T. Ju, R.D. Cummings, Protein glycosylation in cancer, Annu Rev Pathol, 10 (2015) 473-510.

[6] L. Xia, R.P. McEver, Targeted disruption of the gene encoding core 1 beta1-3-galactosyltransferase (T-synthase) causes embryonic lethality and defective angiogenesis in mice, Methods Enzymol, 416 (2006) 314-331.

[7] J. Fu, H. Gerhardt, J.M. McDaniel, B. Xia, X. Liu, L. Ivanciu, A. Ny, K. Hermans, R. Silasi-Mansat, S. McGee, E. Nye, T. Ju, M.I. Ramirez, P. Carmeliet, R.D. Cummings, F. Lupu, L. Xia, Endothelial cell O-glycan deficiency causes blood/lymphatic misconnections and consequent fatty liver disease in mice, J Clin Invest, 118 (2008) 3725-3737.

[8] F. Batista, L. Lu, S.A. Williams, P. Stanley, Complex N-glycans are essential, but core 1 and 2 mucin O-glycans, O-fucose glycans, and NOTCH1 are dispensable, for mammalian spermatogenesis, Biol Reprod, 86 (2012) 179.

[9] P. Grasa, H. Kaune, S.A. Williams, Embryos generated from oocytes lacking complex N- and O-glycans have compromised development and implantation, Reproduction, 144 (2012) 455-465.

[10] J. Fu, B. Wei, T. Wen, M.E. Johansson, X. Liu, E. Bradford, K.A. Thomsson, S. McGee, L. Mansour, M. Tong, J.M. McDaniel, T.J. Sferra, J.R. Turner, H. Chen, G.C. Hansson, J. Braun, L. Xia, Loss of intestinal core 1-derived O-glycans causes spontaneous colitis in mice, J Clin Invest, 121 (2011) 1657-1666.

[11] K. Bergstrom, X. Liu, Y. Zhao, N. Gao, Q. Wu, K. Song, Y. Cui, Y. Li, J.M. McDaniel, S. McGee, W. Chen, M.M. Huycke, C.W. Houchen, L.A. Zenewicz, C.M. West, H. Chen,

J. Braun, J. Fu, L. Xia, Defective Intestinal Mucin-Type O-Glycosylation Causes Spontaneous Colitis-Associated Cancer in Mice, Gastroenterology, 151 (2016) 152-164.e111.

[12] G.F. Springer, T and Tn, general carcinoma autoantigens, Science (New York, N.Y.), 224 (1984) 1198-1206.

[13] N. Remmers, J.M. Anderson, E.M. Linde, D.J. DiMaio, A.J. Lazenby, H.H. Wandall, U. Mandel, H. Clausen, F. Yu, M.A. Hollingsworth, Aberrant expression of mucin core proteins and o-linked glycans associated with progression of pancreatic cancer, Clinical cancer research : an official journal of the American Association for Cancer Research, 19 (2013) 1981-1993.

[14] R.P. Aryal, T. Ju, R.D. Cummings, The endoplasmic reticulum chaperone Cosmc directly promotes in vitro folding of T-synthase, J Biol Chem, 285 (2010) 2456-2462.

[15] S.R. Hingorani, L. Wang, A.S. Multani, C. Combs, T.B. Deramaudt, R.H. Hruban, A.K. Rustgi, S. Chang, D.A. Tuveson, Trp53R172H and KrasG12D cooperate to promote chromosomal instability and widely metastatic pancreatic ductal adenocarcinoma in mice, Cancer Cell, 7 (2005) 469-483.

[16] K. Bergstrom, J. Fu, M.E. Johansson, X. Liu, N. Gao, Q. Wu, J. Song, J.M. McDaniel, S. McGee, W. Chen, J. Braun, G.C. Hansson, L. Xia, Core 1- and 3-derived O-glycans collectively maintain the colonic mucus barrier and protect against spontaneous colitis in mice, Mucosal Immunol, 10 (2017) 91-103.

[17] R.H. Hruban, N. Fukushima, Pancreatic adenocarcinoma: update on the surgical pathology of carcinomas of ductal origin and PanINs, Modern pathology : an official journal of the United States and Canadian Academy of Pathology, Inc, 20 Suppl 1 (2007) S61-70.

[18] H. Laklai, Y.A. Miroshnikova, M.W. Pickup, E.A. Collisson, G.E. Kim, A.S. Barrett, R.C. Hill, J.N. Lakins, D.D. Schlaepfer, J.K. Mouw, V.S. LeBleu, N. Roy, S.V. Novitskiy, J.S. Johansen, V. Poli, R. Kalluri, C.A. Iacobuzio-Donahue, L.D. Wood, M. Hebrok, K. Hansen, H.L. Moses, V.M. Weaver, Genotype tunes pancreatic ductal adenocarcinoma tissue tension to induce matricellular fibrosis and tumor progression, Nat Med, 22 (2016) 497-505.

[19] A.D. Rhim, P.E. Oberstein, D.H. Thomas, E.T. Mirek, C.F. Palermo, S.A. Sastra, E.N. Dekleva, T. Saunders, C.P. Becerra, I.W. Tattersall, C.B. Westphalen, J. Kitajewski, M.G. Fernandez-Barrena, M.E. Fernandez-Zapico, C. Iacobuzio-Donahue, K.P. Olive, B.Z. Stanger, Stromal elements act to restrain, rather than support, pancreatic ductal adenocarcinoma, Cancer Cell, 25 (2014) 735-747.

[20] T. Ju, K. Brewer, A. D'Souza, R.D. Cummings, W.M. Canfield, Cloning and expression of human core 1 beta1,3-galactosyltransferase, J Biol Chem, 277 (2002) 178-186.

[21] T. Ju, V.I. Otto, R.D. Cummings, The Tn antigen-structural simplicity and biological complexity, Angew Chem Int Ed Engl, 50 (2011) 1770-1791.

[22] A. Goodspeed, L.M. Heiser, J.W. Gray, J.C. Costello, Tumor-Derived Cell Lines as Molecular Models of Cancer Pharmacogenomics, Mol Cancer Res, 14 (2016) 3-13.

[23] M.P. Torres, S. Rachagani, J.J. Souchek, K. Mallya, S.L. Johansson, S.K. Batra, Novel pancreatic cancer cell lines derived from genetically engineered mouse models of spontaneous pancreatic adenocarcinoma: applications in diagnosis and therapy, PLoS One, 8 (2013) e80580.

[24] S.F. Boj, C.I. Hwang, L.A. Baker, Chio, II, D.D. Engle, V. Corbo, M. Jager, M. Ponz-Sarvise, H. Tiriac, M.S. Spector, A. Gracanin, T. Oni, K.H. Yu, R. van Boxtel, M. Huch, K.D. Rivera, J.P. Wilson, M.E. Feigin, D. Ohlund, A. Handly-Santana, C.M. Ardito-Abraham, M. Ludwig, E. Elyada, B. Alagesan, G. Biffi, G.N. Yordanov, B. Delcuze, B. Creighton, K. Wright, Y. Park, F.H. Morsink, I.Q. Molenaar, I.H. Borel Rinkes, E. Cuppen, Y. Hao, Y. Jin, I.J. Nijman, C. Iacobuzio-Donahue, S.D. Leach, D.J. Pappin, M. Hammell, D.S. Klimstra, O. Basturk, R.H. Hruban, G.J. Offerhaus, R.G. Vries, H. Clevers, D.A. Tuveson, Organoid models of human and mouse ductal pancreatic cancer, Cell, 160 (2015) 324-338.

[25] S. Itzkowitz, T. Kjeldsen, A. Friera, S. Hakomori, U.S. Yang, Y.S. Kim, Expression of Tn, sialosyl Tn, and T antigens in human pancreas, Gastroenterology, 100 (1991) 1691-1700.

[26] T. Terada, Y. Nakanuma, Expression of mucin carbohydrate antigens (T, Tn and sialyl Tn) and MUC-1 gene product in intraductal papillary-mucinous neoplasm of the pancreas, Am J Clin Pathol, 105 (1996) 613-620.

[27] S. Pandol, M. Edderkaoui, I. Gukovsky, A. Lugea, A. Gukovskaya, Desmoplasia of pancreatic ductal adenocarcinoma, Clin Gastroenterol Hepatol, 7 (2009) S44-47.

[28] R. Kalluri, R.A. Weinberg, The basics of epithelial-mesenchymal transition, J Clin Invest, 119 (2009) 1420-1428.

[29] S. Lamouille, J. Xu, R. Derynck, Molecular mechanisms of epithelial-mesenchymal transition, Nat Rev Mol Cell Biol, 15 (2014) 178-196.

[30] C.Y. Liu, H.H. Lin, M.J. Tang, Y.K. Wang, Vimentin contributes to epithelial-mesenchymal transition cancer cell mechanics by mediating cytoskeletal organization and focal adhesion maturation, Oncotarget, 6 (2015) 15966-15983.

[31] M.G. Mendez, S. Kojima, R.D. Goldman, Vimentin induces changes in cell shape, motility, and adhesion during the epithelial to mesenchymal transition, FASEB J, 24 (2010) 1838-1851.

[32] S. Chugh, V.S. Gnanapragassam, M. Jain, S. Rachagani, M.P. Ponnusamy, S.K. Batra, Pathobiological implications of mucin glycans in cancer: Sweet poison and novel targets, Biochim Biophys Acta, 1856 (2015) 211-225.

[33] D.A. Parikh, B. Durbin-Johnson, S. Urayama, Utility of serum CA19-9 levels in the diagnosis of pancreatic ductal adenocarcinoma in an endoscopic ultrasound referral population, J Gastrointest Cancer, 45 (2014) 74-79.

[34] K.E. Poruk, D.Z. Gay, K. Brown, J.D. Mulvihill, K.M. Boucher, C.L. Scaife, M.A. Firpo, S.J. Mulvihill, The clinical utility of CA 19-9 in pancreatic adenocarcinoma: diagnostic and prognostic updates, Curr Mol Med, 13 (2013) 340-351.

[35] K.S. Goonetilleke, A.K. Siriwardena, Systematic review of carbohydrate antigen (CA 19-9) as a biochemical marker in the diagnosis of pancreatic cancer, Eur J Surg Oncol, 33 (2007) 266-270.

CHAPTER 6

Summary, Conclusions and Future directions

1. Summary

Aberrant O-glycosylation is one of the hallmarks of pancreatic cancer [1, 2]. Mucin-type O-glycosylation involves a plethora of glycosyltransferases [3]. Alterations in the expression/activity of O-glycosyltransferases results in aberrant O-glycosylation, which has been shown to play an important role in cancer progression and metastasis [2].

Aberrant O-glycan structures include truncated carbohydrate structures such as Tn, STn, T, ST. These have been named as tumor-associated carbohydrate antigens (TACA) because these are not observed under normal conditions, as they are masked by addition of several carbohydrate moieties [4]. However, under malignant conditions, these cryptic glycan structures are exposed because of altered activity of glycosyltransferases. Differential expression of these truncated carbohydrate antigens has been reported in several malignancies including PDAC [5, 6]. However, several aspects of aberrant glycosylation remain unanswered. For instance, what are the specific roles played by these truncated glycans in PDAC progression and metastasis? In this context, how does differential expression of glycosyltransferases contribute to PDAC progression and metastasis? We have attempted to address parts of these questions through the studies presented in this thesis.

The major focus of the studies presented in this thesis is to examine the role of aberrant glycosylation in PDAC progression. Briefly, we have examined the role of two glycosyltransferases in this aspect. To achieve this, we have designed three major goals. First, we investigated the role of one of the members of the O-glycosylation-initiating enzyme family, GALNT3, in PDAC aggressiveness. Secondly, we explored the functional implications of the loss of C1GALT1 (the second enzyme of the mucin-type O-glycosylation pathway) in PDAC. Finally, to understand the role of C1GALT1 in PDAC

progression and metastasis, we generated a mouse model of PDAC that has loss of C1galt1.

Concisely, we have observed that loss of both of the O-glycosyltransferases leads to altered glycosylation and increased aggressiveness. Further, loss of C1galt1 in a PDAC mouse model resulted in reduced overall survival, faster PDAC progression and increased metastasis. Loss of GALNT3 induced aberrant glycosylation on EGFR and Her2, whereas loss of C1GALT1 induced aberrant MUC16 glycosylation. Aberrant glycosylation of these proteins could be the plausible mechanism by which PDAC cells acquire increased aggressiveness. The summary of all the three projects is described below:

A. Loss of GALNT3 in poorly differentiated cancer leads to increased aggressiveness

The rationale of this study is based on previous studies in lung, gastric and colon adenocarcinoma, where patients with decreased expression of GALNT3 showed poor survival [7-10]. Further, prior studies have also shown decreased expression of GALNT3 expression in poorly differentiated PDAC [11, 12]. However, limited information is available on the role of GALNT3 in PDAC. First, we examined the expression of GALNT3 in a panel of pancreatic cancer cell lines and tissues derived from different grades of cancer (ranging from well differentiated to poorly differentiated). We did not observe GALNT3 expression in poorly differentiated PDAC cells. However, well/moderately differentiated PDAC cells were found to express GALNT3. Similarly, poorly differentiated PDAC tissues showed weak and less staining of GALNT3 as compared to well/moderately differentiated PDAC.

Having established that there is no/reduced GALNT3 expression in a poorly differentiated subtype of PDAC, we wanted to understand the impact of its loss on disease aggressiveness. Therefore, we performed stable knockdown of GALNT3 in four different

PDAC cell lines. Knockdown of GALNT3 resulted in slightly decreased expression of Tn carbohydrate antigen. Further, there was altered expression of poorly differentiated PDAC markers. Increased expression of Sox-2 and decreased expression of CA19.9 was seen in GALNT3-knockdown PDAC cells as compared to control cells.

We next examined the impact of GALNT3 loss on PDAC by performing *in vitro* growth and migration assays in control and GALNT3 knockdown PDAC cells. *In vitro* functional studies revealed increased growth and migration of GALNT3-knockdown in PDAC cells. Some of the proteins involved in increased growth and motility were also evaluated in control and GALNT3-knockdown cells. GALNT3 knockdown showed increased expression of cyclin A, ZEB-1, N-cadherin and vimentin and decreased expression of E-cadherin. We observed increased expression of carbohydrate antigen SLe^x in GALNT3 knockdown PDAC cells. Since SLe^x have been implicated in extravasation by mediating attachment of tumor cells with the endothelial cells, we conducted tumor-endothelium adhesion assay [13]. GALNT3-knockdown cells showed significantly increased adhesion to endothelial cells monolayer as compared to control cells.

Mechanistic insights were provided by protein expression studies, where we observed increased phosphorylation of ErbB receptors such as EGFR, Her2, and Her3. To specifically understand how the loss of a glycosyltransferase is causing increased activation of ErbB receptors, we examined glycosylation alterations on these receptors. Recent studies have established the link between glycosylation and activation of EGFR [14, 15]. Therefore, we carried out lectin-pull down assay using VVA and PNA lectin that pulls down Tn and T carbohydrate antigen, respectively. Lectin-pull down study demonstrated increased expression of Tn and T carbohydrate antigen on EGFR and Her2. This increase in truncated carbohydrate antigens on EGFR and Her2 could be explained

by the compensatory increase of other GALNTs such as GALNT2. Our conclusion from the first part of the study is that expression of GALNT3 is reduced in poorly differentiated PDAC and loss of this glycosyltransferase is associated with increased aggressiveness and altered glycosylation on ErbB receptors.

B. C1GALT1 knockout in PDAC cells leads to increased tumor growth and metastasis

Given the fact that loss of C1GALT1 leads to the formation of truncated glycans in cancer, and the recent studies that indicate loss of C1GALT1 activity in PDAC patients; we decided to investigate whether loss of C1GALT1 in PDAC is associated with aberrant glycosylation and increased aggressiveness [5, 16].

As a part of this project, RNA and tissues collected from a panel of pancreatic cancer patients were profiled for C1GALT1 expression. C1GALT1 was not expressed in the majority of PDAC cases examined. We further observed decreased C1GALT1 expression in fully transformed HPNE cells as compared to untransformed HPNE cells. All of these studies suggests that loss of C1GALT1 might mediate increased aggressiveness.

The specific role of C1GALT1 in PDAC was studied by CRISPR/Cas9-mediated knockout of C1GALT1 in three different PDAC cancer cells. As expected, all the C1GALT1 knockout cells showed truncated glycophenotype. Functional studies showed increased migration of C1GALT1-knockout PDAC cells. We also developed a migratory model of PDAC to evaluate if highly migratory cells modulate C1GALT1 expression. Highly migratory sublines showed decreased expression of C1GALT1 as compared to parental cells. Our *in vitro* results instigated examination of the impact of C1GALT1 knockout on tumorigenicity and metastasis. Orthotopic implantation of two different C1GALT1 knockout

clones yielded significantly increased tumor weights and metastatic lesions as compared to control cells.

Our next focus was to understand the molecular mechanism by which loss of an O-glycosyltransferase leads to increased tumorigenicity and metastasis. We evaluated the expression of mucins, which are amongst the heavily glycosylated proteins and play pivotal role in PDAC growth and metastasis. C1GALT1-knockout cells showed decreased expression of mucins such as MUC1 and MUC4. Interestingly, we observed molecular weight shift of MUC16 but not MUC4 and MUC1. Lectin pull down assay and glycan cleaving enzymatic assays demonstrated that altered glycosylation accounts for observed shifts in molecular weight. Tn was remarkably increased on MUC16 in C1GALT1 knockout cells as compared to control cells. Further, RNA-seq data provided detailed insights in to the molecular mechanism by which altered glycosylation is causing increased aggressiveness. We observed differential expression of several tumorigenic and migratory genes in C1GALT1 KO PDAC cells. In line with these findings, we also observed increased activation (phosphorylation) of oncogenic signaling proteins such as EGFR and Her2, and mesenchymal markers, vimentin and pFAK-Y925, whereas expression of the epithelial marker, ZO-1 was decreased in C1GALT1 knockout-PDAC cells.

Our conclusion from this part of the study is that knockout of C1galt1 in PDAC leads to increased tumorigenicity and metastasis possibly via aberrant MUC16 glycosylation.

C. Genomic depletion of C1galt1 accelerates PDAC progression and metastasis

Our *in vitro* studies with human PDAC cells indicated the significant impact of the loss of O-glycosyltransferase C1GALT1 on tumor growth and metastasis. In this part of the project, we sought to study the role of C1GALT1 in PDAC progression and metastasis.

Conventional KPC *(Kras^{G12D}; Trp53$^{R172H/+}$; Pdx1-Cre)* model of PDAC progression was crossed with *C1galt1$^{loxP/loxP}$* mice, resulting in the KPCC *(Kras^{G12D}; Trp53$^{R172H/+}$; C1galt1$^{loxP/loxP}$; Pdx1-Cre)* model. KPC mice and age-matched control littermates were used as controls in our study. PDAC progression in KPCC mice was compared to KPC mice. Knockout of C1galt1 specifically in the pancreas with the background of Kras and p53 mutations lead to decrease tumor latency. KPCC mice developed tumors as early as 5 weeks, whereas tumors are generally seen by 20-25 weeks in KPC mice. Low-grade PanIN lesions appear by 3 weeks in KPCC mice, which might explain early development of tumors. Survival analysis indicated significantly reduced survival rate of KPCC mice as compared to KPC mice.

Most KPCC tumors displayed poorly differentiated/undifferentiated histology. Quantification of atypical mitotic figures demonstrated increased proliferation of KPCC tumors as compared to KPC tumors. Also, IHC staining with alpha-SMA and Sirius red indicated decreased stroma in full-blown cancerous regions of KPCC mice as compared to KPC mice. Decreased stroma might account for increased aggressiveness of KPCC tumors.

Early formation of metastatic lesions was seen for KPCC tumors as compared to KPC tumors. Tumor metastasis was seen in several organs such as peritoneum and liver. KPCC mice showed a remarkable increase in vimentin expression as compared to KPC mice, which may account for increased metastasis.

We next want to determine if observed tumor growth and metastasis is linked to altered glycosylation. Glycan analysis showed decreased expression of T carbohydrate antigen in tumors of KPCC mice in comparison to KPC mice. On the contrary, expression of Tn carbohydrate antigen was significantly increased in KPCC mice as compared to KPC

mice. Altogether, this part of the project demonstrates that loss of C1galt1 in PDAC leads to truncated glycophenotype and faster PDAC progression and metastasis.

2. Future Directions

A. Loss of GALNT3 in poorly differentiated cancer leads to increased aggressiveness

(i) Does loss of GALNT3 expression lead to poorly differentiated PDAC or is it a consequence of poorly differentiated PDAC?

Considering that the loss of GALNT3 in well/moderately differentiated PDAC cells leads to altered expression of poorly differentiated markers, we questioned if GALNT3 expression governs PDAC differentiation status. Previous research in thyroid cancer and several malignancies have indicated the potential loss of GALNT3 in poorly differentiated cancer [17]. Further, we have observed that treatment with IFN-γ and differentiation-inducing factor, retinoic acid, induced expression of GALNT3 as compared to untreated PDAC cells (**Figure 6.1**). To explore the role of GALNT3 in PDAC differentiation, GALNT3 over-expression in poorly differentiated PDAC cells such as Panc-1 and MIA PaCa-2 and normal pancreatic epithelial cells (HPNE) needs to be performed. Further, generation of a KPC mouse model with an inducible knockout of GALNT3 can effectively address its role in PDAC.

(ii) Does EGFR O-glycosylation impact its function?

Our results have shown that knockdown of GALNT3 resulted in increased expression of truncated glycans on EGFR and Her2, which might account for their increased phosphorylation/activation. Using NetOGlyc 4.0 Server, which is a bioinformatics-based tool used to predict O-GalNAc sites in mammalian proteins, we identified a few O-glycosylation sites on Her2. Experimental detection of exact sites of O-glycosylation is a

challenging task and needs to be done using comprehensive tools such as a mass spectrometry-based glycoproteomic approach. Another unexplored aspect of our study is the relative contribution of aberrant glycosylation on the function of these receptors. Truncated glycans may relieve steric hindrance posed by extended glycans and thus facilitate increased interaction of ErbB receptors among themselves or with other signaling proteins. To better understand this, co-immunoprecipitation and reciprocal IP studies with known EGFR and Her2 interacting partners need to be performed.

B. C1GALT1 knockout in PDAC cells leads to increased tumor growth and metastasis

(i) What is the clinical relevance of C1GALT1?

Though we do not have any conclusive results for the clinical significance of C1GALT1 expression in PDAC, C1GALT1 expression studies in RNA and tissue samples from PDAC patients suggest that C1GALT1 expression is lost in a subset of PDAC patients. Further, our *in vitro* and *in vivo* studies have highlighted the significant impact of loss of C1GALT1 on PDAC aggressiveness and survival. These findings suggest that evaluating C1GALT1 expression in PDAC patients could predict disease severity and can potentially help in better management of patients with PDAC.

(ii) What is the role of C1GALT1 in pancreatic cancer stem cells?

Our *in vitro* and *in vivo* studies have established that knockout of C1GALT1 induces PDAC growth and metastasis. In line with these findings, we also observed increased expression of CD44 in C1GALT1-knockout PDAC cells. Interestingly, the increased expression of C1GALT1 was observed at several molecular weights that may correspond to different splice variants/glycoforms of CD44 (**Figure 6.2**). Since increased expression of CD44 is one of the characteristic features of PDAC cancer stem cells, it will

be interesting to investigate if C1GALT1 knockout in PDAC induces altered glycosylation on cancer stem cells markers [18, 19]. The importance of cancer stem cells in tumor growth and several steps of metastasis has been well described in several studies [20]. Analysis of cancer stem cells in control and C1GALT1 knockout PDAC cells could potentially unveil the involvement of C1GALT1-mediated truncated glycosylation in cancer stem cells and metastasis.

C. Genomic depletion of C1galt1 accelerates PDAC progression and metastasis

(i) Do pancreatic cells modulate expression of C1GALT1 during PDAC progression?

Since differential expression of O-glycans has been reported during PDAC progression, it can be possible that pancreatic cells modulate expression of glycosyltransferases during the course of disease development in order to gain differential glycophenotype and hence aggressiveness [6]. Our preliminary results demonstrate that treatment of T3M4 PDAC cells with inflammatory cytokines such as IL-4 and IL-6 decrease C1GALT1 expression (CHAPTER 4-Figure 17). Another study focused on IgA nephropathy have shown that treatment of B cells with TGF-β1 decreases C1GALT1 expression that causes aberrant glycosylation of IgA [21]. TGF-beta has been widely used *in vitro* to induce EMT, whereas Inflammatory cytokines such as IL-4 and IL-6 have been shown to play an important role in tumor growth.[22-24] Based on these findings, we anticipate that several cues from microenvironment modulate C1GALT1 expression during PDAC progression.

To test this, we could begin with RNA-seq analysis of pancreatic tissues procured from KPC progression model at several time points representing low-grade PanINs, high-grade PanINs, cancer, and metastasis. Our group has identified several differentially expressed cytokines and chemokines in PDAC progression. This can be used further to check the regulation of C1GALT1 by secretory cues from tumor microenvironment.

(ii) Role of C1GALT1 in acinar to ductal metaplasia (ADM)

Several studies have proposed acinar to ductal metaplasia (ADM) as a key event in PDAC initiation [25]. While we haven't yet performed definite experiments to test the possibility of C1GALT1-knockout mediated altered glycosylation on ADM, preliminary IHC studies depict expression of amylase (acinar cell marker) in metaplastic ducts from KPCC tissues (**Figure 6.3**). These findings give us a reason to believe that C1GALT1 knockout may drive ADM and results in increased cancer aggressiveness.

Therefore, to explore the prospective involvement of C1GALT1 loss on ADM, we could use an *in vivo* model of ADM well characterized in our lab. Prior studies from our lab have very well established that caerulein treatment in KPC mice induces ADM-like histology, which eventually progresses to PDAC [26]. Evaluation of C1GALT1 in the RNA and tissues samples from control and caerulein-treated KPC mice could ascertain the plausible involvement of C1GALT1 role in ADM.

(iii) Therapeutic studies with KPCC mouse model

Since the KPCC mouse model represents faster PDAC progression model, it can possibly be utilized for therapeutic studies. Knockout of C1GALT1 in PDAC cells resulted in increased activation of ErbB receptors, FAK and Akt. All of these signaling proteins have been implicated in growth and metastasis of PDAC. Some of the drugs targeting these proteins are FDA approved and are in clinical trials for several pathological conditions and cancers, including PDAC. For instance, VS-4718 is a clinically available FAK inhibitor and has been shown effective for targeting PDAC [27]. Afatinib/Gilotrif is an another FDA approved drug for non-small cell lung cancer and several studies from various other groups and our lab also supports its use in PDAC [28, 29]. Efficacy of these drugs to control PDAC progression and metastasis can be tested in this animal model.

These preclinical studies on mice models could pave the way of targeting PDAC in patient samples. We believe that personalized approach should be used for therapeutic targeting in PDAC patients.

Figure legends

Figure 6.1 Regulation of GALNT3 expression: Western blot demonstrates that pro-inflammatory cytokine-IFN-γ and differentiation inducing factor-retinoic acid upregulates GALNT3 expression in CD18/HPAF PDAC cells

Figure 6.1

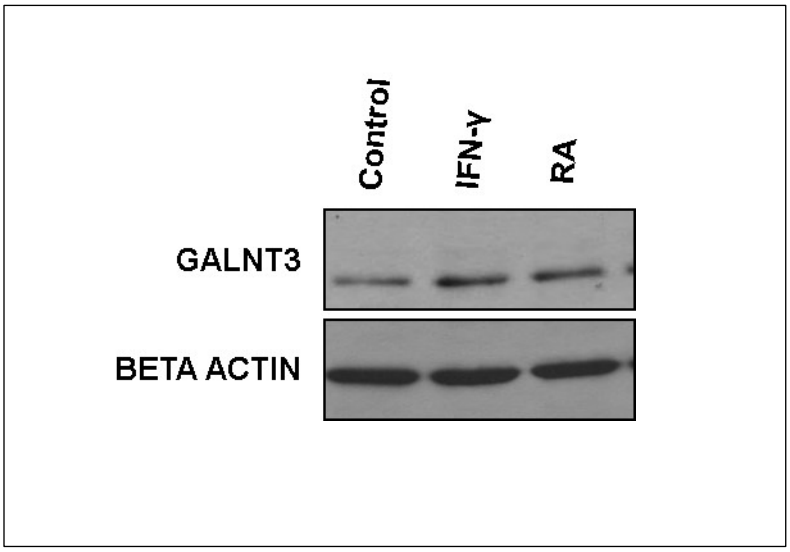

Figure 6.2 Differential expression of CD44 in C1GALT1 KO PDAC cells: Western blotting demonstrates increased CD44 expression in KO clones as compared to wild-type control cells. Further, a number of CD44 bands were seen in C1GALT1 KO cells, which might correspond to CD44 glycoforms.

Figure 6.2

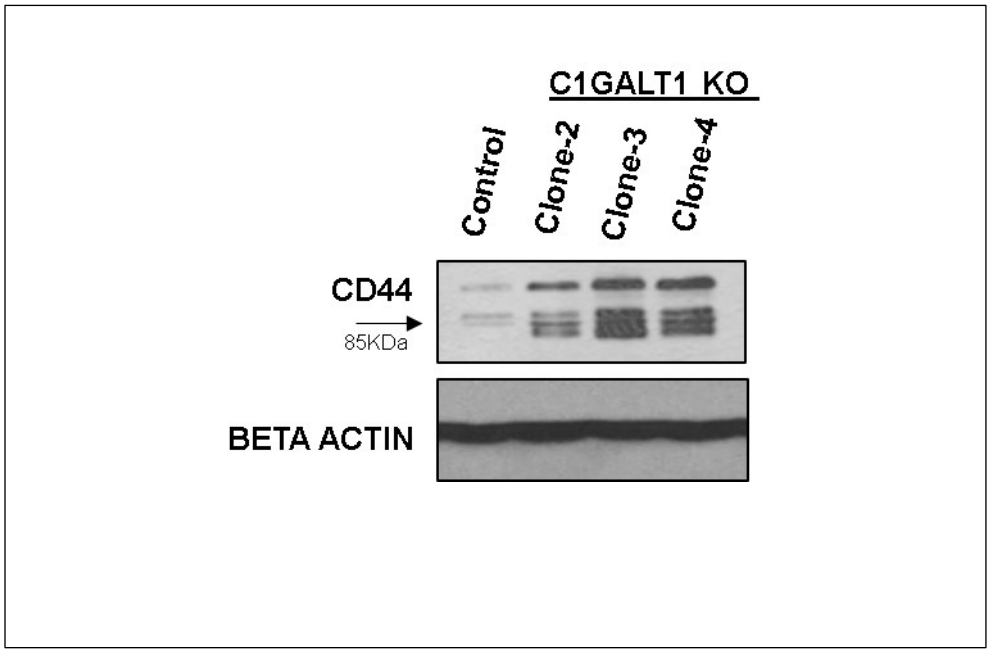
C1GALT1 KO
Control
Clone-2
Clone-3
Clone-4
CD44
85KDa
BETA ACTIN

Figure 6.3: Amylase expression in KPCC neoplastic ducts: Immunofluorescence staining with amylase (acinar cell marker) demonstrates positive staining in KPCC ducts.

Figure 6.3

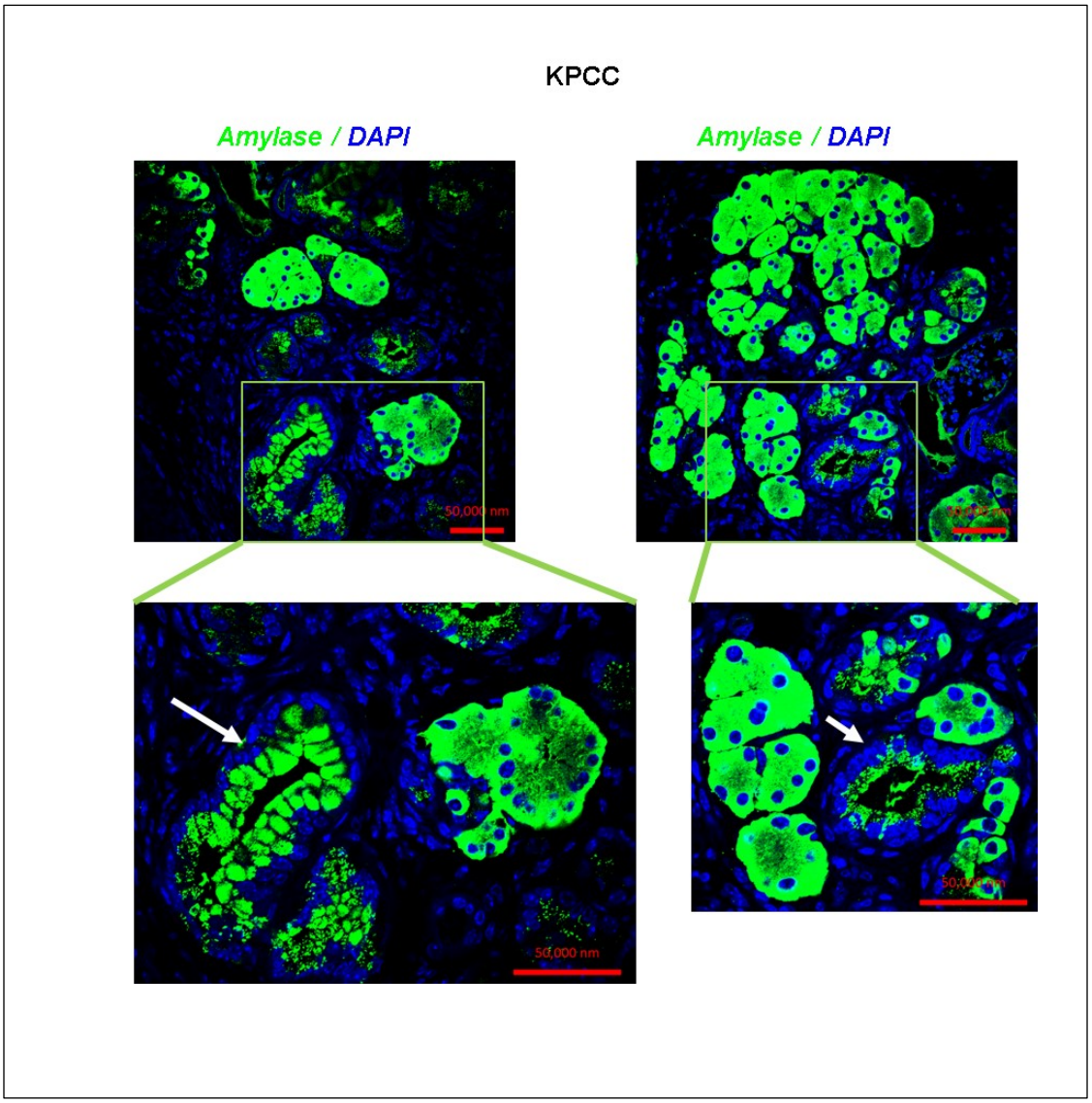

References

[1] S. Itzkowitz, T. Kjeldsen, A. Friera, S. Hakomori, U.S. Yang, Y.S. Kim, Expression of Tn, sialosyl Tn, and T antigens in human pancreas, Gastroenterology, 100 (1991) 1691-1700.

[2] S.S. Pinho, C.A. Reis, Glycosylation in cancer: mechanisms and clinical implications, Nature reviews. Cancer, 15 (2015) 540-555.

[3] D.T. Tran, K.G. Ten Hagen, Mucin-type O-glycosylation during development, J Biol Chem, 288 (2013) 6921-6929.

[4] S. Hakomori, Aberrant glycosylation in tumors and tumor-associated carbohydrate antigens, Adv Cancer Res, 52 (1989) 257-331.

[5] P. Radhakrishnan, S. Dabelsteen, F.B. Madsen, C. Francavilla, K.L. Kopp, C. Steentoft, S.Y. Vakhrushev, J.V. Olsen, L. Hansen, E.P. Bennett, A. Woetmann, G. Yin, L. Chen, H. Song, M. Bak, R.A. Hlady, S.L. Peters, R. Opavsky, C. Thode, K. Qvortrup, K.T. Schjoldager, H. Clausen, M.A. Hollingsworth, H.H. Wandall, Immature truncated O-glycophenotype of cancer directly induces oncogenic features, Proc Natl Acad Sci U S A, 111 (2014) E4066-4075.

[6] N. Remmers, J.M. Anderson, E.M. Linde, D.J. DiMaio, A.J. Lazenby, H.H. Wandall, U. Mandel, H. Clausen, F. Yu, M.A. Hollingsworth, Aberrant expression of mucin core proteins and o-linked glycans associated with progression of pancreatic cancer, Clinical cancer research : an official journal of the American Association for Cancer Research, 19 (2013) 1981-1993.

[7] H. Dosaka-Akita, I. Kinoshita, K. Yamazaki, H. Izumi, T. Itoh, H. Katoh, M. Nishimura, K. Matsuo, Y. Yamada, K. Kohno, N-acetylgalactosaminyl transferase-3 is a potential new marker for non-small cell lung cancers, British journal of cancer, 87 (2002) 751-755.

[8] C. Gu, T. Oyama, T. Osaki, J. Li, M. Takenoyama, H. Izumi, K. Sugio, K. Kohno, K. Yasumoto, Low expression of polypeptide GalNAc N-acetylgalactosaminyl transferase-3 in lung adenocarcinoma: impact on poor prognosis and early recurrence, British journal of cancer, 90 (2004) 436-442.

[9] K. Onitsuka, K. Shibao, Y. Nakayama, N. Minagawa, K. Hirata, H. Izumi, K. Matsuo, N. Nagata, K. Kitazato, K. Kohno, H. Itoh, Prognostic significance of UDP-N-acetyl-alpha-D-galactosamine:polypeptide N-acetylgalactosaminyltransferase-3 (GalNAc-T3) expression in patients with gastric carcinoma, Cancer Sci, 94 (2003) 32-36.

[10] K. Shibao, H. Izumi, Y. Nakayama, R. Ohta, N. Nagata, M. Nomoto, K. Matsuo, Y. Yamada, K. Kitazato, H. Itoh, K. Kohno, Expression of UDP-N-acetyl-alpha-D-galactosamine-polypeptide galNAc N-acetylgalactosaminyl transferase-3 in relation to differentiation and prognosis in patients with colorectal carcinoma, Cancer, 94 (2002) 1939-1946.

[11] Z. Li, S. Yamada, S. Inenaga, T. Imamura, Y. Wu, K.Y. Wang, S. Shimajiri, R. Nakano, H. Izumi, K. Kohno, Y. Sasaguri, Polypeptide N-acetylgalactosaminyltransferase 6 expression in pancreatic cancer is an independent prognostic factor indicating better overall survival, British journal of cancer, 104 (2011) 1882-1889.

[12] S. Yamamoto, S. Nakamori, M. Tsujie, Y. Takahashi, H. Nagano, K. Dono, K. Umeshita, M. Sakon, Y. Tomita, Y. Hoshida, K. Aozasa, K. Kohno, M. Monden, Expression of uridine diphosphate N-acetyl-alpha-D-galactosamine: polypeptide N-acetylgalactosaminyl transferase 3 in adenocarcinoma of the pancreas, Pathobiology, 71 (2004) 12-18.

[13] Y. Kawarada, H. Ishikura, T. Kishimoto, H. Kato, T. Yano, H. Kato, T. Yoshiki, The role of sialylated Lewis antigens on hematogenous metastases of human pancreas carcinoma cell lines in vivo, Pathol Res Pract, 196 (2000) 259-263.

[14] M.J. Huang, R.H. Hu, C.H. Chou, C.L. Hsu, Y.W. Liu, J. Huang, J.S. Hung, I.R. Lai, H.F. Juan, S.L. Yu, Y.M. Wu, M.C. Huang, Knockdown of GALNT1 suppresses malignant phenotype of hepatocellular carcinoma by suppressing EGFR signaling, Oncotarget, 6 (2015) 5650-5665.

[15] M.C. Lin, M.J. Huang, C.H. Liu, T.L. Yang, M.C. Huang, GALNT2 enhances migration and invasion of oral squamous cell carcinoma by regulating EGFR glycosylation and activity, Oral Oncol, 50 (2014) 478-484.

[16] B.T. Hofmann, L. Schluter, P. Lange, B. Mercanoglu, F. Ewald, A. Folster, A.S. Picksak, S. Harder, A.T. El Gammal, K. Grupp, C. Gungor, A. Drenckhan, H. Schluter, C. Wagener, J.R. Izbicki, M. Jucker, M. Bockhorn, G. Wolters-Eisfeld, COSMC knockdown mediated aberrant O-glycosylation promotes oncogenic properties in pancreatic cancer, Molecular cancer, 14 (2015) 109.

[17] Y. Mochizuki, K. Ito, H. Izumi, K. Kohno, J. Amano, Expression of polypeptide N-acetylgalactosaminyl transferase-3 and its association with clinicopathological factors in thyroid carcinomas, Thyroid, 23 (2013) 1553-1560.

[18] Y. Yan, X. Zuo, D. Wei, Concise Review: Emerging Role of CD44 in Cancer Stem Cells: A Promising Biomarker and Therapeutic Target, Stem Cells Transl Med, 4 (2015) 1033-1043.

[19] C. Li, C.J. Lee, D.M. Simeone, Identification of human pancreatic cancer stem cells, Methods Mol Biol, 568 (2009) 161-173.

[20] F. Li, B. Tiede, J. Massague, Y. Kang, Beyond tumorigenesis: cancer stem cells in metastasis, Cell Res, 17 (2007) 3-14.

[21] J. Xiao, M. Wang, D. Xiong, Y. Wang, Q. Li, J. Zhou, Q. Chen, TGF-beta1 mimics the effect of IL-4 on the glycosylation of IgA1 by downregulating core 1 beta1, 3-galactosyltransferase and Cosmc, Mol Med Rep, 15 (2017) 969-974.

[22] J. Xu, S. Lamouille, R. Derynck, TGF-beta-induced epithelial to mesenchymal transition, Cell Res, 19 (2009) 156-172.

[23] O. Prokopchuk, Y. Liu, D. Henne-Bruns, M. Kornmann, Interleukin-4 enhances proliferation of human pancreatic cancer cells: evidence for autocrine and paracrine actions, British journal of cancer, 92 (2005) 921-928.

[24] R. Holmer, F.A. Goumas, G.H. Waetzig, S. Rose-John, H. Kalthoff, Interleukin-6: a villain in the drama of pancreatic cancer development and progression, Hepatobiliary Pancreat Dis Int, 13 (2014) 371-380.

[25] L.C. Murtaugh, S.D. Leach, A case of mistaken identity? Nonductal origins of pancreatic "ductal" cancers, Cancer Cell, 11 (2007) 211-213.

[26] P. Dey, S. Rachagani, A.P. Vaz, M.P. Ponnusamy, S.K. Batra, PD2/Paf1 depletion in pancreatic acinar cells promotes acinar-to-ductal metaplasia, Oncotarget, 5 (2014) 4480-4491.

[27] H. Jiang, S. Hegde, B.L. Knolhoff, Y. Zhu, J.M. Herndon, M.A. Meyer, T.M. Nywening, W.G. Hawkins, I.M. Shapiro, D.T. Weaver, J.A. Pachter, A. Wang-Gillam, D.G. DeNardo, Targeting focal adhesion kinase renders pancreatic cancers responsive to checkpoint immunotherapy, Nat Med, 22 (2016) 851-860.

[28] G.M. Keating, Afatinib: a review of its use in the treatment of advanced non-small cell lung cancer, Drugs, 74 (2014) 207-221.

[29] P. Seshacharyulu, M.P. Ponnusamy, S. Rachagani, I. Lakshmanan, D. Haridas, Y. Yan, A.K. Ganti, S.K. Batra, Targeting EGF-receptor(s) - STAT1 axis attenuates tumor growth and metastasis through downregulation of MUC4 mucin in human pancreatic cancer, Oncotarget, 6 (2015) 5164-5181.

Bibliography of Seema Chugh

Published Manuscripts

1. Karmakar S, Seshacharyulu P, Lakshmanan I, Vaz AP, **Chugh S**, Sheinin YM, Mahapatra S, Batra SK, Ponnusamy MP. *hPaf1/PD2 interacts with OCT3/4 to promote self-renewal of ovarian cancer stem cells*. **Oncotarget**. 2017. doi: 10.18632

2. Pai P, Rachagani S, Dhawan P, Sheinin YM, Macha MA, Qazi AK, **Chugh S**, Ponnusamy MP, Mallya K, Pothuraju R, Batra SK. *MUC4 is negatively regulated through the Wnt/β-catenin pathway via the Notch effector Hath1 in colorectal cancer.* **Genes Cancer.** 2016; 7(5-6):154-68.

3. Muniyan S, Haridas D, **Chugh S**, Rachagani S, Lakshmanan I, Gupta S, Seshacharyulu P, Smith LM, Ponnusamy MP, Batra SK. *MUC16 contributes to the metastasis of pancreatic ductal adenocarcinoma through focal adhesion mediated signaling mechanism*. **Genes Cancer.** 2016; 7(3-4):110-24.

4. Chugh S, Meza J, Sheinin YM, Ponnusamy MP, Batra SK. *Loss of N acetylgalactosaminyltransferase 3 in poorly differentiated pancreatic cancer: augmented aggressiveness and aberrant ErbB family glycosylation.* **Br J Cancer.** 2016; 114(12):1376-86.

5. Chugh S, Gnanapragassam VS, Jain M, Rachagani S, Ponnusamy MP, Batra SK. *Pathobiological implications of mucin glycans in cancer: Sweet poison and novel targets.* **Biochim Biophys Acta**. 2015; 1856(2):211-25.

6. Rachagani S, Macha MA, Heimann N, Seshacharyulu P, Haridas D, **Chugh S**, Batra SK. *Clinical implications of miRNAs in the pathogenesis, diagnosis and therapy of pancreatic cancer.* **Adv Drug Deliv Rev.** 2015; 81:16-33

7. Haridas D, Ponnusamy MP, **Chugh S**, Lakshmanan I, Seshacharyulu P, Batra SK. *MUC16: molecular analysis and its functional implications in benign and malignant conditions.* **FASEB J.** 2014; 28(10):4183-99.

8. Ponnusamy MP, Seshacharyulu P, Lakshmanan I, Vaz AP, **Chugh S**, Batra SK. *Emerging role of mucins in epithelial to mesenchymal transition.* **Curr Cancer Drug Targets.** 2013; 13(9):945-56.

Manuscripts near Submission

1. Chugh S, Barkeer S*, Rachagani S*, Nimmakayala RK, Pothuraju R, Yu X, Neelamegham S, Xia L, Sheinin YM, Talmon GA, Smith LM, Ponnusamy MP, Batra SK. *Genomic depletion of core 1 β1,3- galactosyltransferase (C1galt1) in pancreatic cancer leads to increased tumor progression and metastasis.* (Near submission)

2. Chugh S, Barkeer S, Rachagani S, Ponnusamy MP, Batra SK. *Differential expression of glycans in pancreatic cancer progression (KC- KrasG12D/+; Pdx1-Cre and KPC -*

KrasG12D/+; Trp53R172H/+; Pdx1-Cre) and its implication in aggressiveness of pancreatic cancer. (Near submission)

3. Chugh S, Nimmakayala RK, Ponnusamy MP, Batra SK. *Characterization of migratory sublines with differential metastatic potential and organ specific metastasis.* (Near submission)

4. Nimmakayala RK, Seshacharyulu P, Lakshmanan I; **Chugh S**; Rachagani S; Batra SK and Ponnusamy MP. *Cigarette smoke activates PD2/Paf1 through ERK-FRA1 (FOSL1)/c-JUN signaling axis resulting in the enrichment of pancreatic cancer stem cells.* (Near submission)

5. Barkeer S, **Chugh S**, Ponnusamy MP, Batra SK. *Recent advances in glycosylation variation in stem cells and cancer stem cells.* (Near submission)